The Expedition Antarktis VII/3 (EPOS LEG 2) of RV "Polarstern" in 1988/89

Contributions of the participants

edited by

I. Hempel, P. H. Schalk and V. Smetacek

Ber. Polarforsch. 65 (1989)
ISSN 0176-5027

Dr. Irmtraut Hempel
Universität Kiel
Institut für Polarökologie
Olshausenstraße 40–60
D-2300 Kiel

Dr. P. H. Schalk
Institut voor Taxonomische Zoologie
P.O.Box 4766
NL-1009 AT Amsterdam

Prof. Dr. V. Smetacek
Alfred-Wegener-Institut für Polar- und Meeresforschung
D-2850 Bremerhaven 1

In memoriam Jenne J. Zijlstra

This report on the second part of the European Polarstern Study is dedicated to the memory of Professor Jenne J. Zijlstra, who died on 2 August 1989 in his home in Schargen/Holland. His illness had been detected in October of last year when he was about to take off for the second leg of EPOS. So he had to stay behind. He recommended his colleague and friend Dr. K. Veth to replace him as the international Scientific Advisor on board the vessel.

Jenne has largely determined the scientific concept of EPOS as an entity, where the three legs had at least partly common goals. He contributed his ideas and experience gathered during expeditions to the tropical Atlantic and to Indonesian waters. Everyone was looking forward to have him on board "Polarstern" and to enjoy his scientific leadership, his organizational skill and above all his delightful personality. Once again we will miss Jenne when we meet in November 1989 in his home institute for the EPOS evaluation meeting.

For the last two years Jenne had put his heart in the EPOS venture, in which he saw a great opportunity to stimulate European cooperation in marine science. He strongly believed that the cooperation of various disciplines and nations on a vessel is the source of new ideas and approaches in oceanic research. With that view he had always pushed for the combination of different fields of research and for the application of new techniques in the Netherlands Institute for Sea Research, of which he was director for many years. He conveyed the same line of thinking in his capacity as member of the advisory board of the Alfred Wegener Institute.

Jenne promoted international cooperation at many conferences and working groups he took part of. His last major international event was the 5th Conference on Antarctic Biology and the SCAR meeting in Hobart/Tasmania in August/September 1988 where he offered the integration of Dutch Antarctic research into modern cooperative programmes.

For 35 years the European and world-wide cooperation in marine science has greatly benefitted from Jenne Zijlstra's broad scientific knowledge, bright ideas, eager efforts and fine comradeship.

CONTENTS

1. INTRODUCTION

V. Smetacek, C. Veth

1.1 Scientific Objectives of EPOS Leg 2

The second leg of EPOS was devoted primarily to the study of the pelagic system. It is well known that biological processes are constrained by the physico-chemical environment but the relationship is not a simple one as demonstrated by the situation prevailing in Antarctic waters. Here, macronutrients such as nitrate, phosphate and silicate are not exhausted by plant growth and it is not clear why this is so. The factors most often invoked to explain this phenomenon are:
a) light limitation of photosynthesis due to deep mixing;
b) limitation by a trace nutrient such as iron;
c) control of phytoplankton biomass by heavy grazing pressure.
Obviously, the relative role of each of these factors will vary both regionally and seasonally and none of them can be invoked singly to explain the general phenomenon of excess macronutrients in Antarctic waters. Thus, factor a) will not apply at the border of the retreating ice edge where meltwater stabilises a shallow surface layer. Similarly, factor b) may well be important in open ocean water but not over a shelf region where vertical mixing reaches down to the iron-rich sediments. Further, it is hard to envision that grazing pressure throughout the length and breadth of the Antarctic will always be high enough to control phytoplankton stocks from entering the explosive growth phase so characteristic of other oceanic and neritic regions. Hence, one of the objectives of Leg 2 was to study phytoplankton distribution and growth performance in relation to each of the factors listed above.

In recent years, it has become increasingly apparent that Antarctic pelagic systems undergo the same pattern of seasonal succession from a diatom dominated spring community to a flagellate dominated summer one. The transition is obviously not mediated by exhaustion of macronutrients as appears to be the case elsewhere. As comprehensive studies of all components of the pelagic system in relation to seasonal changes of the physico-chemical environment were lacking to date, the EPOS cruise provided an ideal opportunity to fill this gap. The expertise assembled on board RV "Polarstern" permitted a detailed assessment of algal, bacterial, protozoan and metazoan compartments of pelagic communities both in terms of abundance as well as activity parameters. In conjunction with groups studying physical and chemical properties of the system we hoped to elucidate the mechanisms of transition between the two types of pelagic community.

The distribution patterns of various elements (such as Barium and rare earths) and compounds (such as hydrogen peroxide) seem to be influenced by biological activity although the mechanisms are not clear. The comprehensive biological programme of Leg 2 provided an ideal background to gain a better understanding of the behaviour of these elements. Thus, one of the objectives of Leg 2 was to study their distribution in relation to biological processes.

Apart from these more general objectives, each of the groups participating in the cruise addressed specific questions too numerous to list here. They will, however, become evident from a perusal of the individual reports.

It was our intention to combine field observations with experiments to address the objectives mentioned above. The investigation area chosen for Leg 2 is located between the tip of the Antarctic Peninsula and the South Orkney islands, along the 49° and 47° W meridians and between 57° and 62° S. In this area, the open water of the Circumpolar Current (Scotia Sea) contacts the northern rim of the Weddell Gyre along a broad frontal zone, the Weddell-Scotia Confluence. Thus, water masses with different histories lie within a short distance of each other rendering comparative studies of seasonal development convenient. To this end, we planned a series of three transects extending from the open waters of the Scotia Sea, that were ice-free for several weeks, to deep within the ice-covered Weddell Sea. At least one of the transects was to cross the shelf of the South Orkney islands. Between each transect we intended occupying three time stations of 2.5 day duration in each of the characteristic water masses of the area in order to follow ambient processes. A free-floating sediment trap array was to be used as a drogue to follow the same water mass during each time station.

1.2 Summary Review of EPOS Leg 2

RV "Polarstern" left Punta Arenas, Chile, on 22 November 1988 and, after conducting a test station on 25 November, the first transect along the 49°W meridian was commenced with a "mesostation" (Sta. 143) at 57°S, followed by a "microstation" at 57°30´S. This sequence of meso- and microstations at half degree intervals (30 naut. miles, nm) was extended down to 62°S. The cruise track is depicted in Fig.1. A list of the stations is given in the annex.

The following gear were deployed at the mesostations:
- Optical probes at stations occupied during full daylight.
- CTD rosette with an oxygen probe and a combination of Niskin and Go-Flo (for ultraclean trace metal analyses) bottles down to 1500 m depth.
- A series of twelve 30 l Niskin bottles for Barium analyses.
- An extra long (2.5 m) 50 µm mesh net with a mouth opening of 0.07 m^2 ("Fransz net") for quantitative collection of micro- and mesozooplankton.
- Multinet for collection of mesozooplankton from different depth ranges down to 1,000 m.
- Omori net (500 µm, 2 m diameter) was hauled vertically to sample macrozooplankton This net was lost on 21 December and was replaced thereafter with a vertically hauled Bongo net (500 µm).
- In the absence of ice cover an open Rectangular Midwater Trawl (RMT) was employed for sampling macrozooplankton.

The microstations comprised one cast of the CTD rosette equipped only with Niskin bottles down to 1,500 m depth.

The first scattered pack ice floes were encountered at approx 60°S with coverage increasing further south. This transect was completed on 29 November with Sta. 153. The CTD section clearly showed the presence of a marked front, extending down to >1,500 m depth and most evident in the isotherms, between 57° 30´ and 58° S, i.e between stations 144 and 145;

this front was followed by a sequence of cold and warm water columns till homogeneous cold Weddell Sea water was reached south of 60°S. The broad belt of the transect characterized by vertically inclined isopleths is referred to as the Weddell-Scotia Confluence (WSC) as distinct from Weddell Sea Water (WSW) and Scotia Sea Water (SSW) to the south and north of the WSC respectively. This distinction is based on isopleths below 200 m depth, the front was not clearly discernible in the isotherms and isohalines of surface water; however, there were clear south to north differences in the biology of this layer manifested in biomass and species composition of phyto- and zooplankton. Thus a fairly advanced community with phytoplankton cells in poor condition albeit at low biomass, was present in the two stations at 57°00´and 57°30´. At 58°30´ the maximum chlorophyll concentrations (>3 $\mu g\ l^{-1}$) of the cruise were encountered: the community consisted of a healthy mixed population of large diatoms. Further south, biomass dropped continuously to low values (<0.5 $\mu g\ l^{-1}$) under closed ice cover.

The scientific programme was interrupted briefly in order to carry personnel from the disabled RV "John Biscoe" to the British station at nearby Signy Island (South Orkneys). The first time station (Sta. 156) was occupied at 61°S for a period of 2.5 days. A free-floating sediment trap served as a drogue and was followed by the ship till its recovery 24 h later. During its second deployment, the surface buoy of the trap disappeared under an ice floe and could not be recovered even though the particular floe was marked by signal dye. Thereafter, sediment traps were only deployed under ideal conditions. In some areas, an algal-rich infiltration layer (the zone between ice and snow cover) was evident in many floes broken by the ship. However, ice cores collected from promising floes yielded only low biomass of ice algae. In order to satisfy the demands of the various groups for algal biomass, ice stained brown by algae was collected from the sides rather than the interior of a floe. Juvenile Krill were fairly abundant on the undersurface of ice floes.

The second time station (157) was to be located in the Confluence at a site with a large diatom biomass. On our return to the position of the biomass maximum encountered on the southgoing transect, a comparable population could no longer be located. The time station was hence sited at 59°S in an area where chlorophyll concentrations were the highest in the locality. Within six hours after the first CTD cast, biomass values were found to have dropped significantly accompanied by the appearance of a Krill swarm. This station hence provided an unexpected opportunity to study the effect of heavy Krill grazing on the pelagic system. After completion of this station, it was decided to occupy another time station in the area on an ungrazed diatom population. A zig-zag course (not indicated in fig.1) was accordingly followed in search of such a population. During this search, a negative correlation between Krill occurrence on the echo-sounder and surface chlorophyll concentrations seemed to exist. The highest chlorophyll concentrations were located close to the edge of the melting pack-ice border and were contributed largely by a population of small pennate diatoms that seemed to emanate from the infiltration layer of the pack ice. The third time station (158) was occupied at this site.

The fourth time station (159) was occupied in Scotia Sea water at 57° S. Chlorophyll concentrations in the well-defined mixed layer were below 0.4 µg l^{-1} but varied considerably with depth and time. This was a surprising finding as we had assumed Scotia Sea water to be reasonably homogeneous. An evaluation of all time station data indicated significant temporal variability that could not be related to ongoing processes in the same water mass (with the exception of the Krill grazing event at Sta. 157) but seemed rather to be due to small-scale patchiness. The wisdom of continuing with time stations was questioned and it was decided to conduct smaller transects instead.

The second major transect with alternating meso- and microstations was conducted along the 47° W meridian which crosses the western shelf of the South Orkney islands. Heavy ice cover precluded its extension down to 62° S as planned and it was hence terminated at 61° 30´S (Sta. 169). The distribution of chlorophyll in relation to the hydrography along this transect was essentially similar to that recorded along 49° W although the biomass maximum in the Confluence zone was much less pronounced. Apparently, the transition to a low-biomass, a flagellate dominated system was well underway.

A brief respite from scientific work was provided by a day´s visit to the British base on Signy Island. The next station (171), equivalent to a prolonged mesostation, was occupied on the broad southern shelf of the South Orkney islands on 19 December. With the exception of the presence of some neritic zooplankters, the pelagic system prevailing here did not differ markedly from that encountered over deep water from the same latitude.

It was apparent from the two transects that phytoplankton biomass distribution was not related to the depth of the mixed layer. Indeed, a mixed layer marked by a sharp pycnocline was encountered only in Scotia Sea water. Everywhere further south, the density gradient sloped gently downward, evidently a result of the admixture of melt water in the absence of strong winds. This environment should have provided ideal conditions for rapid algal growth, particularly as these favourable growth conditions had prevailed for well over two weeks. This conclusion was fortified by the results of experiments with natural populations maintained under ultraclean conditions, where nitrate exhaustion occurred within 10 - 14 days, even in the absence of additives such as iron. We tentatively concluded that Krill grazing pressure, exerted by individuals leaving their winter ice habitat, was the foremost reason for the absence of sizeable phytoplankton stocks in the melt water stabilized areas. Furthermore, the phytoplankton was now dominated by a small, pear-shaped cryptomonad, a species which also dominated natural populations maintained in culture that were subjected to Krill grazing. In controls not exposed to Krill, diatoms tended to dominate.

In order to study the situation prevailing in the marginal ice zone (MIZ) more closely, we decided to conduct a transect again along the 49°W meridian with closely spaced (30 nm) mesostations extending from the Confluence at 59°S (Sta. 172) deep into the pack ice at 62° S (Sta. 179). This MIZ transect was completed on Christmas day. Chlorophyll concentrations throughout this transect were monotonously low, indicating that even the pronounced melt water stabilization that we encountered did not necessarily induce

blooms, again, in spite of input of substantial seeding populations from the melting ice. Low rate of photosynthesis was not a reason for this paucity of phytoplankton as up to 1 g C m^{-2} d^{-1} was recorded at these stations. Krill was less abundant under the ice than during our previous visit some 3-4 weeks earlier as were also the main Krill predators (penguins and seals). It could therefore not be established whether heavy grazing pressure was responsible for the low accumulation rate of phytoplankton biomass.

Following the MIZ transect, our attention shifted to the northern rim of the Confluence as the locality most likely to harbour large phytoplankton stocks. Another point of interest was the mechanisms of water exchange across the northern front of the Confluence. The third and last long transect along the 49° W meridian was conducted from 27 - 30 December. In addition to the usual sequence of meso- and microstations, we placed 2 additional CTD-stations without tripping bottles (picostations) on the northern front in order to gain a higher resolution picture of water mass distribution. The results indicated that the front had moved northward and the sharp delineation of warm and cold water columns recorded during the first transect was no longer evident. Diatom dominated populations were not encountered and the small cryptomonad flagellate seemed to be the dominant phytoplankter south of the front. The pack ice south of 60° S differed considerably from that present during the MIZ study of the previous week. The floes were much larger and had not been subjected to extensive melting. Following completion of this transect (Sta. 182 to 195) we returned to the Confluence at 59° S.

We had decided to lay a grid across the northern half of the Confluence in order to obtain a three-dimensional picture of the water masses and relate these to plankton distribution. The grid was to be completed as fast as possible and biological sampling was restricted to a minimum. Our intention was to return to interesting sites following completion of the grid. The grid was accomplished by means of a zig-zag course across the Confluence and phytoplankton biomass distribution was monitored by continuous underway measurement of chlorophyll fluorescence in surface water.

The data from the grid could not be adequately processed before the end of the cruise but a preliminary impression was that the front had broadened considerably. Phytoplankton concentrations were patchily distributed and maximum values were recorded in a patch located just north of the front. The phytoplankton community at this station was quite different to those found further south. The species composition was very diverse and large diatoms were again prominent. However, large dinoflagellates and many small forms were also abundant. Following completion of this 24 h time station, 3 mesostations were occupied along a minitransect going from plankton-rich to impoverished water. An interdisciplinary exercise measuring phytoplankton growth parameters by various methods in this diatom rich patch was conducted next. A detailed assessment of zooplankton distribution in relation to the front that was planned as the last undertaking of the cruise had to be cancelled due to the onset of bad weather. RV "Polarstern" left the now stormy investigation area a day in advance and arrived in Punta Arenas on January 9, 1989.

Preliminary Conclusions

Some of the major conclusions of EPOS Leg 2 are listed next. These might well have to be modified following analyses of the many samples collected, however, their substance appears to be well established at the time of writing.

1) No deep mixed layer was encountered anywhere in the investigation area. Even in the Scotia Sea, the maximum depth of a distinct pycnocline was 60 m and the depths were generally much shallower. South of 58° S, the surface layer was strongly stratified without a sharp density gradient. This salinity stabilization - evidently the result of ice melt - was present in the form of wind-driven lenses that occurred more than 100 km north of the northernmost ice floe fields. On occasion, the salinity gradient ranged from 33.8 to 34.3 ‰ within the upper 50 m. Phytoplankton biomass distribution was not related to the stratification pattern. We conclude that a shallow stratified water column may well be a prerequisite but does not necessarily result in accumulation of phytoplankton biomass. This conclusion is contrary to general opinion that mixed layer depth is the single most important factor in controlling the occurrence of blooms. Hence, there must be other factors operating in this region that control algal biomass build-up.

2) Another potential factor controlling algal growth rates that has recently gained much attention is the availability of iron. Our results show that iron addition stimulates algal growth and increases chlorophyll yield in the cultures; however, it is obviously not the limiting factor as shown by algal growth performance in the controls without iron. Horizontal patchiness in iron distribution, such as in the wake of ice bergs or in meltwater lenses may well be a factor inducing small scale patchiness in chlorophyll biomass.

3) Maximum algal biomass was invariably present along the northern rim of the Weddell-Scotia Confluence (WSC). Whereas this bloom might well have been induced by meltwater from the receding ice edge, the same effect was not achieved further south. Chlorophyll concentrations above 2 $\mu g\ l^{-1}$ were, with one exception, contributed by large diatoms. It is yet unclear why diatom blooms were restricted to this region. A further indication of higher productivity in the Confluence was the development of a subsurface ammonia maximum in the course of the study. The high values (up to 3 µM) recorded are an indication of intense heterotrophic activity evidently induced by the high productivity in the upper layer.

4) South of 58°S a transition from a diatom-dominated plankton to a flagellate-dominated, regenerating community occurred during the course of Leg 2. Krill grazing pressure was found to be a decisive factor in this development. At one particular station this transition was achieved by a Krill swarm within a few hours. Following the feeding event, heterotrophic activity increased abruptly and a cryptophyceaen flagellate became the dominant autotroph. This shift in community composition was confirmed by results of grazing experiments.

5) The photosynthesis: light relationship measured on various phytoplankton communities revealed interesting differences but one universal feature: light inhibition at intensities prevailing in the uppermost

metres, even on sunny days, could not be severe. This finding hence rules out another possible explanation for the absence of ice algal blooms in meltwater masses; it has been argued that ice algae are shade adapted and would hence suffer upon release from the ice habitat.

6) Although no phytoplankton biomass accumulation was observed in the water lenses, zooplankton biomass and ETS-respiratory activity were evidently higher in the ice edge zone than southward under the ice or northward in open water. Birds and mammal biomass was also much higher at the ice edge than further north. Krill was sexually maturing during the two months of study. Juveniles and subadults were caught in ice covered waters and showed considerably lower respiratory activities than mature adults which occurred in open water.

6) Krill grazing seems to be the most important factor preventing development of ice edge blooms. Krill were apparently abandoning the winter ice habitat in the course of the investigation. The ice algae released from the inaccessible infiltration layer - where they build-up a large biomass - are grazed down effectively by the Krill. This is likely to be an important food source in the seasonal cycle of Krill.

7) An interesting finding was the transient occurrence of a heterotrophic community that had a net oxygen consumption in the light, with the rate of O_2 consumption increasing with light intensity. Bacterial thymidine uptake was unusually high. Ammonia concentration was also relatively high.

Acknowledgements

We take this opportunity to thank the captain and crew of RV "Polarstern" for the magnificent treatment on board and for their tireless, able assistance during work. They provided the ideal climate for a successful cruise.

The logistics department of the Alfred-Wegener-Institute deserve special mention for the excellent organisation of the preparatory and final phase of the cruise.

Last but not least, we extend our thanks to Ingrid Lukait for her constant efforts throughout to ensure that everything ran smoothly.

Figure 1: Cruise Track - EPOS Leg 2

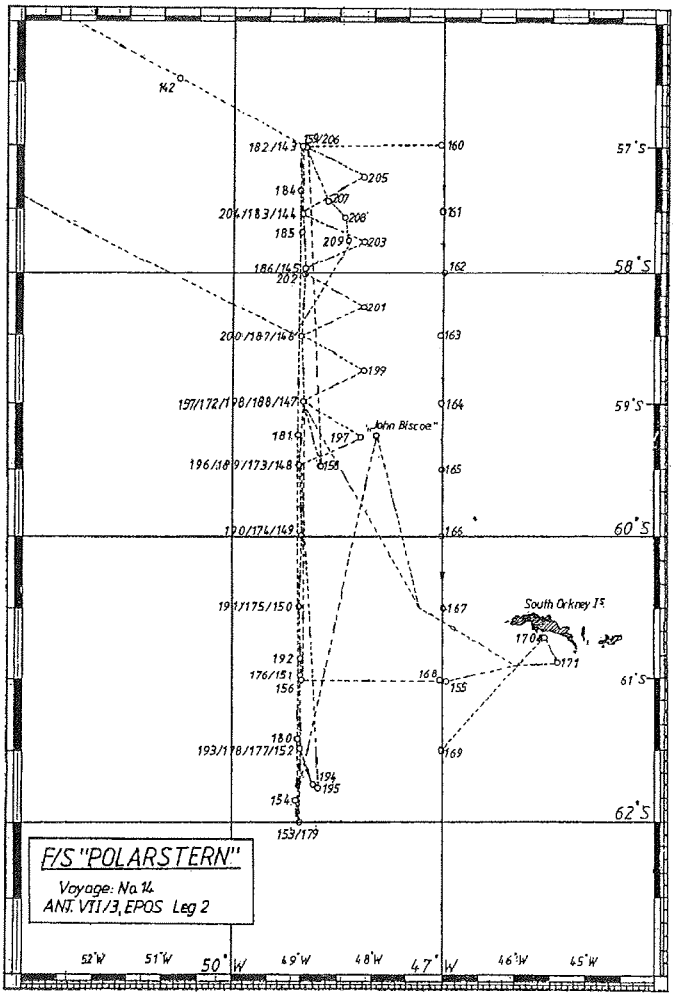

2. EPOS Leg 2 - Meteorological Situation

M. Gebauer

While leaving Punta Arenas on 23 November 1988, the weather was mainly dominated by storm cyclones, moving rather fast from the South Pacific through Drake Passage in the direction of South Georgia. Due to orographic effects induced by coastal mountain chains,westerly winds of Bft. 7-9 prevailed. But as the ship sailed eastsoutheast, disturbances disappeared.

A small cyclone that originated from a rather old low pressure system east of Cape Horn developed into a storm with its centre near the "Polarstern". The ship had to steam to the first station against Bft. 8. The frontal area soon moved to the north, because an intensive and nearly stationary low pressure system west of the Antarctic Peninsula induced a rather meridional streaming in higher layers of the troposphere. Due to the ship´s simultaneous sailing into the ice southward, wind-speed and swell decreased markedly from Bft. 6-7 down to 3-4. Rather warm and humid air over cold ice water induced widespread fog and poor visibility.

Later on, cyclones passed close to the ship resulting in rather low wind velocity with Bft. 4, but with frequent changes in wind direction and also frequent occurrence of fog. In the beginning of December, a nearly stationary and complex low pressure system over the eastern Weddell Sea conducted rather cold and dry air to the ship´s area. Only occasional snow decreased visibility for short periods and Bft. 3-5 was maintained. After the first ten days of December, an intense low approached from the Drake Passage, conducting rather mild and humid air to the ship. Again fog set in, but the "Polarstern" sailed northward to the Scotia Sea, and due to increasing water temperature the visibility increased also. Again the ship was in the frontal area with Bft. 5-7.

During the middle of the month the ship sailed southward accompanied by Bft. 5-7. But due to the ice and despite wind velocity up to Bft. 7-8 there were not any disturbances. In a low pressure area along the 60th latitude the wind velocity decreased substantially. Christmas was accompanied by high pressure influence over the western Weddell Sea and by Bft. 2-4.

Afterwards, an intense cyclone developed over the Bellingshausen Sea. It moved very slowly via the Antarctic Peninsula to the Weddell Sea, reaching this area at the year´s end. In front of the cyclone, warm and humid air repeatedly caused widespread fog and the wind velocity increased slowly up to Bft. 5-6.

Leaving the ice in the new year there was a marked westerly swell. Small cyclones moving from Tierra del Fuego eastward caused wind Bft. 6-7. Scientific work was done from now on in an area around 58°S / 49°W.

The intense cyclone that moved from Bellingshausen Sea to the eastern Weddell Sea became stationary and between this cyclone and high pressure influence east of Argentina there were westerly winds Bft. 6-7, sometimes 8, and the height of the swell was round about 3 m, thus hindering the ship´s progress.

3. Sea Ice Conditions

J.A. van Franeker

Occurrence and characteristics of sea ice during the second leg of EPOS were monitored in connection with observations of birds and mammals. Since distribution of sea ice is of evident importance to all EPOS investigations, some basic data are summarized in this report

When sailing between stations, ice conditions were noted for each 10 minute observation period (see § 4.4: Seabirds, seals and whales). Ice coverage (in percent), floe size, approximate thickness, and an estimate of the number of icebergs in the area were monitored. In this preliminary report only the most important factor, ice coverage, will be discussed. Additional data will be available at a later date. Ice coverage was noted as the estimated percentage of the surface covered with ice, within the transect of 150 meters on both sides of the ship, during the distance covered in 10 minutes. Judging ice coverage over greater distances was considered inappropriate as this is very difficult to do, and would also obscure small scale variations of importance to distribution patterns of birds and seals. A generalized view of ice conditions over larger areas is probably better obtained by comparing results of consecutive 10 minute observations. Ice coverage was generally described in a scale with steps of 10 percent, but close to the ends of the scale (open water / permanent ice) these steps were reduced as appropriate. A strongly summarized impression of ice conditions during the four consecutive transects of EPOS Leg 2 is given in Tab. 1. However, as most studies will require more detailed information on ice distribution, all ice observations have been plotted in graphs for separate transects (Fig. 2 to 5). Tab. 1 and graphs are based on both south- and northward leg of each transect which usually showed little difference. Graphs clearly show the often erratic distribution of the ice at short distances, but at the same time they reveal the overall trends.

Most EPOS investigations were concentrated at stations at intercepts of half a degree latitude. General ice conditions at the latitude of different stations can be deduced from Fig. 2 to 5. A more local judgement of ice conditions around stations can be found in Tab. 2, which lists ice coverages during bird observations at stations. It has to be kept in mind however, that icecover is very variable in both time and space. Even the ship itself may cause considerable changes in icecover in its surroundings, especially at stations of longer duration. To reduce such artifacts, ice coverage at stations was judged over a much larger area than during 10 minute counts, and averaged for multiple observations at the same station.

Figures 2 + 3: Icecover at the First and Second Transect

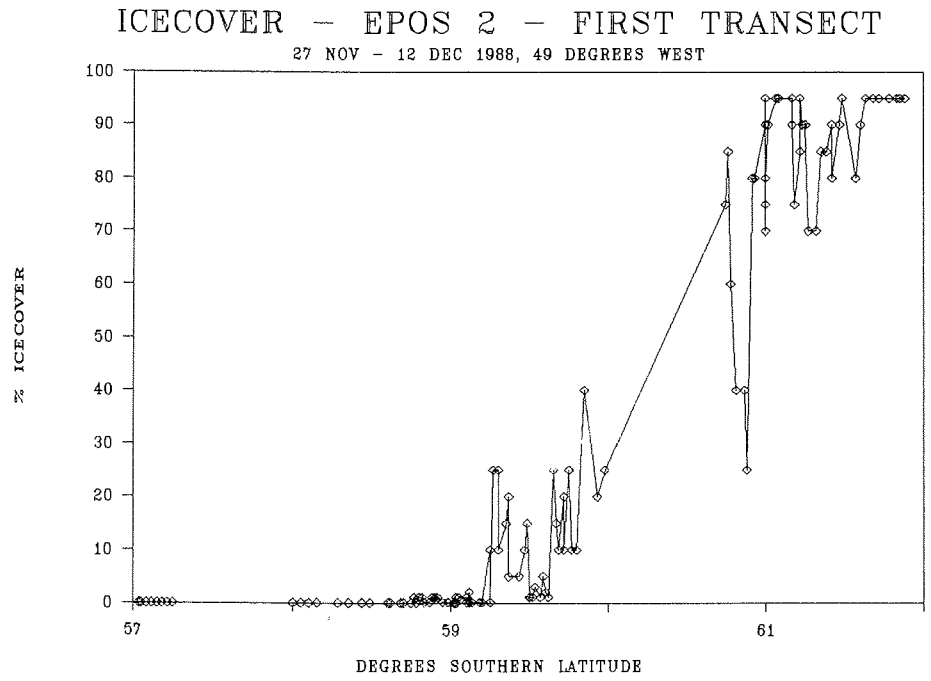

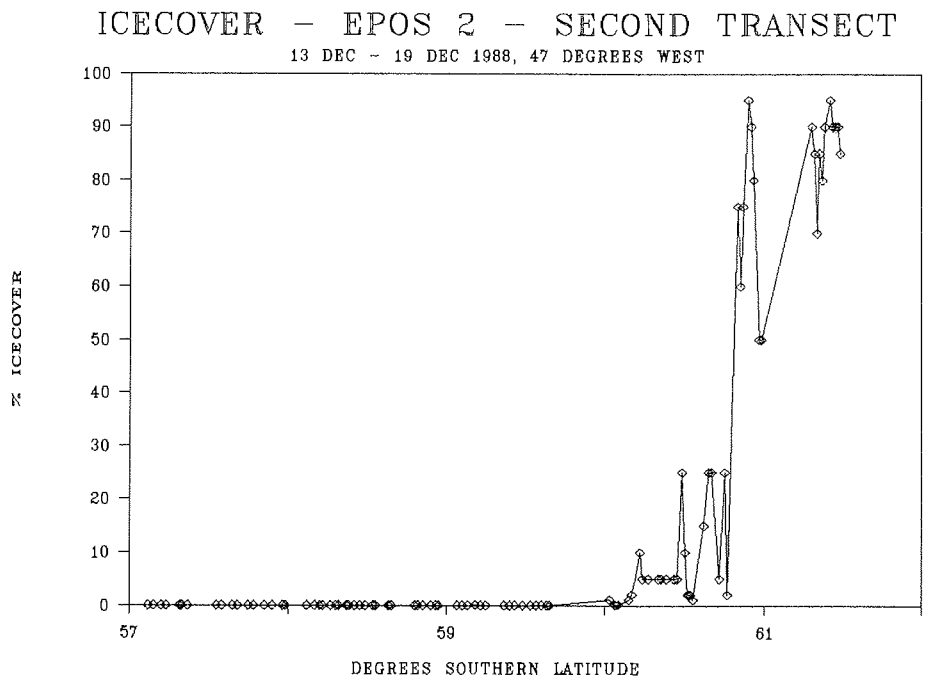

Figures 4 + 5: Icecover at the Third and Fourth Transect

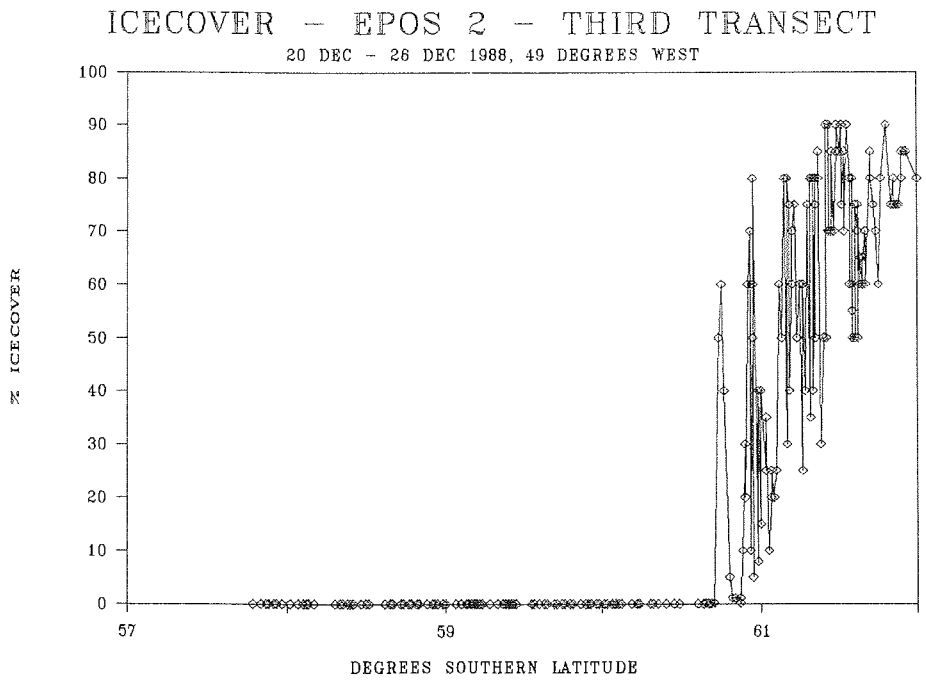

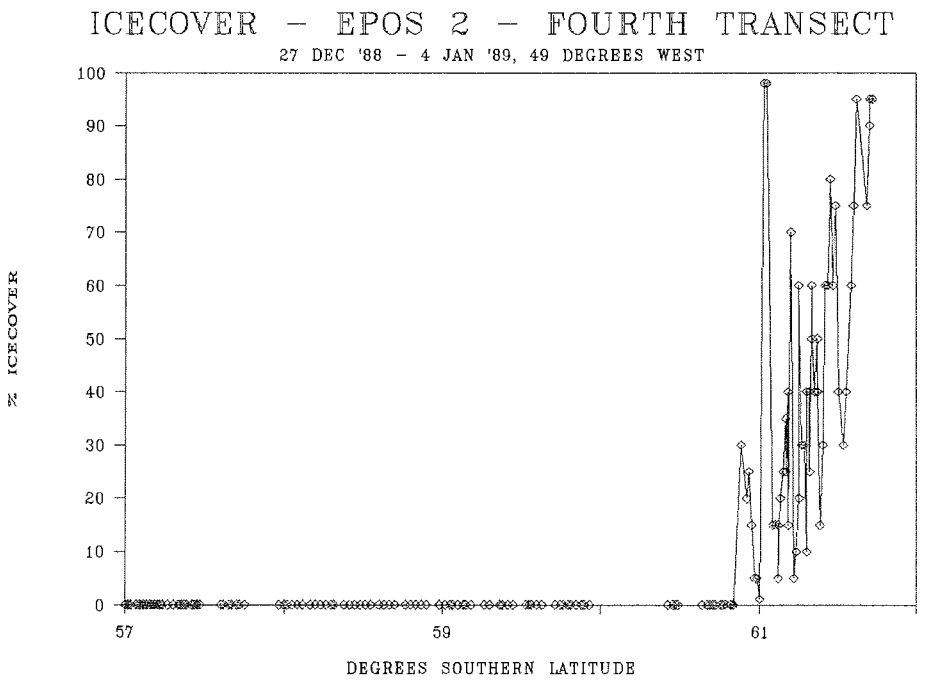

Table 1: Summary of Ice Data - EPOS Leg 2

Transect	I	II	III	IV
start date	27 Nov	13 Dec	20 Dec	27 Dec
end date	12 Dec	16 Dec	26 Dec	04 Jan
first ice	58°50'S	60°02'S	60°39'S	60°47'S
50 % ice	60°30'S	60°50'S	60°55'S	61°12'S
cont. ice	61°00'S	61°00'S	61°30'S	61°36'S

Table 2: Icecover Percentage at Stations During EPOS Leg 2

Transect I		Transect II		Transect III		Transect IV	
StaNo	Icecover	StaNo.	Icecover	StaNo	Icecover	StaNo.	Icecover
142	0	160	0	172	0	182	0
143	0	161	0	173	0	183	0
144	0	162	0	174	0	184	0
145	0	163	0	175	0	185	0
146	0	164	0	176	50	186	0
147	0	165	0	177	80	187	0
148	1	166	1	178	90	188	0
149	35	TEST	2	179	70	189	0
150		167	20	180	30	190	0
151	75	168	50	181	0	191	0
152	95	169	85			192	2
153	98	170	+			193	70
154	95	171	1			194	90
155	+					195	90
156	50					196-205	-
157	1					206	0
158	5					207	0
159	0					208	0
						209	0

4. SCIENTIFIC REPORTS

4.1. PHYSICS AND CHEMISTRY

4.1.1 Hydrography

U. Cederlöf, S. Ober, R. Schmidt, A. Svansson, C. Veth

The Weddell-Scotia Confluence is the frontal system separating the eastward flowing waters of the Circumpolar Current and the northern branch of the Weddell Gyre. The hydrographical structure of the Confluence area is dominated by the sharp temperature gradient at the northern edge (the Scotia front), extending from about 200 to 2500 meters. South of the Scotia front is a dynamic hence highly variable transition zone consisting of mesoscale water masses and eddies of intermediate characteristics. These eddies seem to originate from occasional transfer of warm deep Circumpolar Water through the Scotia front. The waters of the Bransfield Strait are far too low in temperature and salinity (Gordon & Nowlin, 1978) to be the origin of these structures.

The surface hydrography is dominated by the winter water, a remnant of the convection during winter freezing. This cold northward flowing watermass with temperature minimum around 100 meters, extends across the Scotia front to the polar front, where it descends and becomes part of the Antarctic Intermediate Water.

The stability of the surface water develops in the spring when low saline water spreads from the melting ice and appears in wind driven patches in the vicinity of the ice margin. Later, the stabilizing effect of surface heating adds to that of salinity and a shallow, wind-mixed layer develops.

Objectives

The physical environment, in particular the depth of the mixed layer, is widely considered to be the most important factor controlling productivity and biomass accumulation of phytoplankton in Antarctic waters. One of the objectives of our group was to study the structure and dynamics of the surface layer in order to acquire the data necessary for interpretation of chemical and biological properties.

Surface layer processes cannot be understood without paying attention to the structure and dynamics of underlying water masses This applies particularly to the investigation area where large-scale exchange of water between Scotia and Weddell Seas occurs at depth and is likely to disrupt the surface layer. Further, overwintering organisms such as copepods do so at depths below 1,000 m; therefore, the CTD casts were extended to 1,500 m depth in most cases

Another task of our group was to provide water samples according to the wishes of the chemists and biologists on board.

Work at Sea

During EPOS Leg 2 the CTD/ROSETTE - system belonging to the Netherlands Institute of Sea Research was employed which mainly consists of:

In situ unit:
- Neil Brown Mark III B - probe
- Beckmann Oxygen probe
- General Oceanic rosette sampler (24 positions)
- Niskin and Go-Flo bottles (12 l)
- A frame with a special coating to avoid heavy metal contamination

Deck unit:
- EG&G 1401 deck-unit with power supply
- General Oceanic Rosette deck unit
- IBM - AT computer with peripherals (industrial version)
- EG&G - software for data acquisition and post-processing

The CTD-system worked reliably throughout EPOS Leg 2. Occasional problems were solved without programme delay. This was made possible by the modular design of the system and the availability of spare modules. The combination of Go-Flo bottles with the 24-position rosette was unfortunate and required extreme care because the Go-Flo bottles seem to overstrain the fine mechanics of the rosette.

A total of 157 casts were carried out with this system. As part of the post-processing on board, isoplots of the transects were made available for the relevant parameters. In addition to this, about 3600 bottles with a total of 40,000 litres of precious seawater were brought on deck to meet the demands of 44 craving scientists.

Temperature calibrations were carried out with both mercury and electronic reversing thermometers. Salinity calibrations were made on board with a Guildline Autosal Salinometer. Oxygen calibrations were done by means of Winkler titrations (Special thanks to Mario Pamatmat and Anita Buma). An intercalibration cast was made with the Neil-Brown Mark III CTD-probe contributed by the Institute of Oceanography, Gothenburg which had been used during EPOS Leg 1.

At the end of the cruise a CTD data report was made available to all participating institutes. This report contains for each water sample: Pressure, temperature, conductivity and salinity, and in addition the position, time and date of the cast.

Preliminary Results

The hydrographical data from the EPOS Leg 2 transects all conform to the given general description of the Confluence area. In transect I, the Scotia front was found between Stat 144 and 145. The temperature (Fig 6) drops from 2° to 0.4° in a distance of less than 60 km. Warm structures were found at Stat 146 and 148 with temperature and salinity maxima at about 1.4° and 34.70‰. Also, a remarkably deep penetration of winter water was found at Stat 145. The salinity structure (Fig 7) shows the typical maximum of 34.70 in the circumpolar water, just north of the front and a slight southward decrease across the front. Almost every structure in the temperature field is counteracted by a corresponding variation in salinity, such that the density field (Fig 8) shows isopycnals, smoothly ascending southward through the front. This suggests that exchange of water between the Scotia and Weddell Seas takes place as occasional transfer of large water volumes, that more or less retain their characteristics and move vertically by buoyancy force to the equilibrium level. This means that southgoing warm water would rise and compress vertically, thereby acquiring anti-cyclonic rotation. Northgoing water would experience the opposite effect. Transect II at 47°W, shows a similar picture, except that the Scotia front was encountered about 100 km further to the south. The hydrographical structure found in transects I and II, seem to constitute a basic state of the Confluence. Reports from earlier studies from the same area (e.g. Patterson & Sievers 1980, Foster & Middleton 1984) do not differ in any essential way from this description.

In the last two transects IV and V, along 49°W, the picture is quite different. The Scotia front is expanded southward, apparently due to ongoing dramatic exchange of water. The sections for temperature (Fig.9) and salinity (Fig 10) from transect V (the grid), shows a somewhat confusing picture with huge water blobs, disrupting the front. However, in spite of the irregular temperature and salinity fields, the density structure (Fig 11) is still strikingly smooth and similar to the first transects.

The discussion so far only concerns the region below the winter-water which is present in all the transects with its cold core at some 100 meters. It appears as if this water layer acts to disconnect the surface layer from the underlying structures and even prevents the Scotia front from reaching the surface. The thickness of the wind-mixed layer varied during the cruise between 20 and 40 meters. In the first transects, the surface stratification was due mainly to melt water. The summer thermocline, adding to the stability, gradually developed and the last transects show a warm, low salinity mixed layer with a sharp pycnocline.

Literature Cited

Patterson, S.L.& H.A. Sievers (1980). The Weddell-Scotia-Confluence., J. Phys..Oceanogr. 10: 1584-1610.

Gordon, A.L. & W.D. Nowlin Jr. (1978). The Basin Waters of the Bransfield Strait. J.Phys. Oceanogr 8: 258-264.

Foster, T.D. & J.H. Middleton (1984). The oceanographic structure of the eastern Scotia Sea - I. Physical oceanography. Deep-Sea Res. 31: 529-550.

Figure 6: Temperature Section from Stations 143 (57°S, 49°W) to 153 (62°S, 49°W)

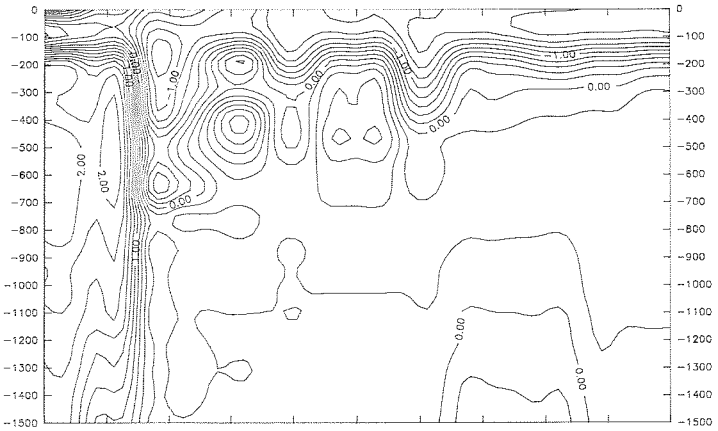

Figure 9: Temperature Section from Grid Section between Station 196 and 206

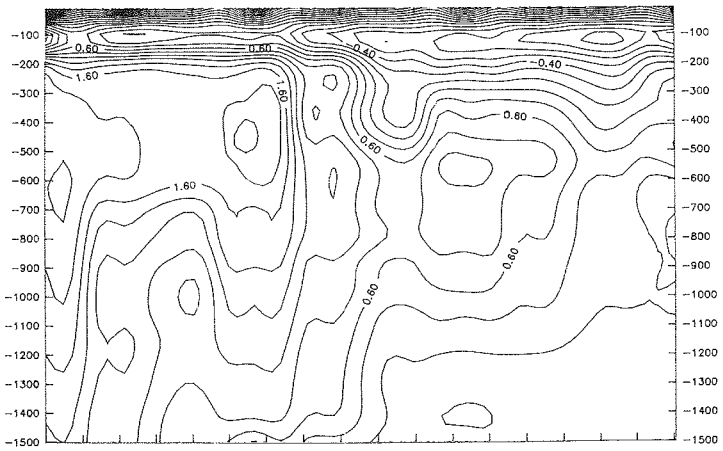

Figure 7: Salinity Section from Stations 143 (57°S, 49°W) to 153 (62°S, 49°W)

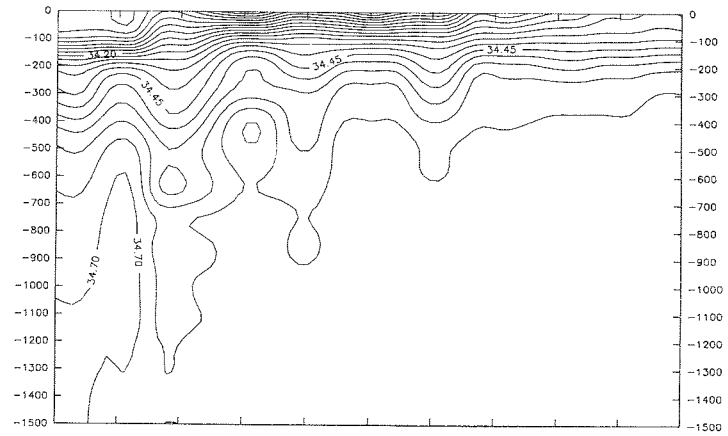

Figure 10: Salinity Section from Grid Section between Station 196 and 206

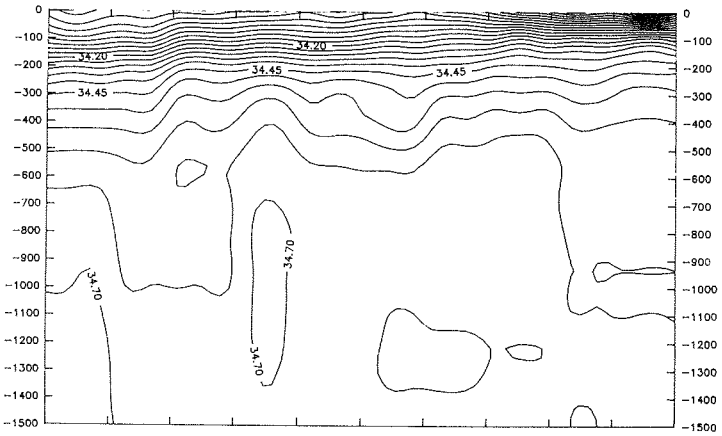

Figure 8: Density Section from Stations 143 (57°S, 49°W) to 153 (62°S, 49°W)

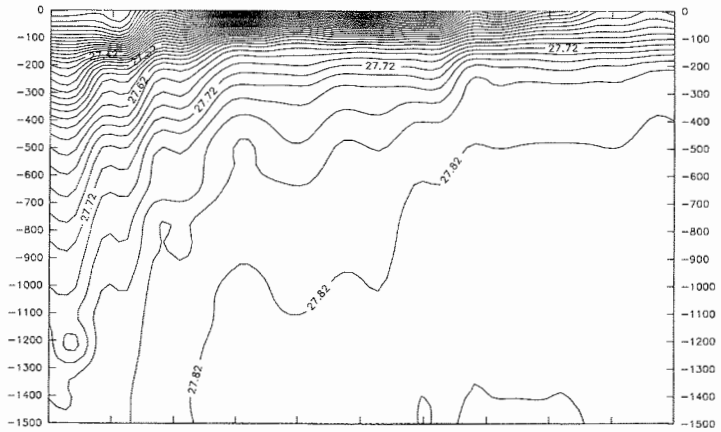

Figure 11: Density Section from Grid Section between Station 196 and 206

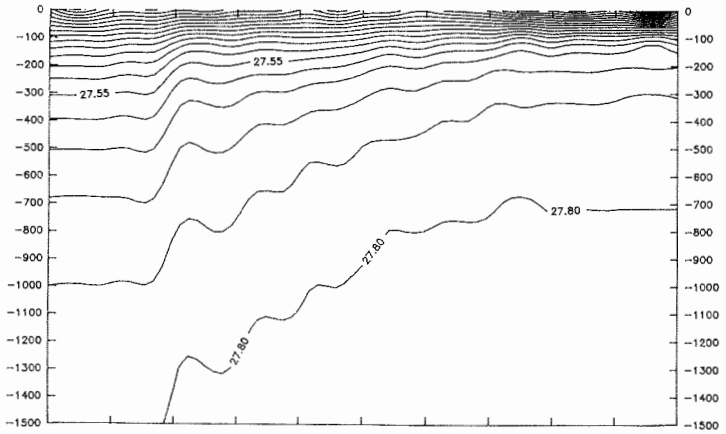

4.1.2 Optics

B. Magas, A. Svansson

Objectives

The light regime in the sea determines the rate of photosynthesis and its measurement is hence of great importance for productivity studies. However, there is no consensus yet on an optimum method for doing so, simply and effectively. It was our aim to compare different methods and relate the results to ambient conditions. The instruments employed were a Quanta Meter, a Colour Index Meter and the venerable Secchi disc.

Work at Sea

The Quanta Meter and the Colour Index Meter used are described by Jerlov (1976) and Højerslev (1980) respectively. The Secchi disc was a little larger than usual, i.e., 1 m in diameter. All the sensors, the Secchi disc included, were lowered by the same winch using a 0.5 inch steel cable. Wire angles were rare. The Quanta Meter is equipped with a depth meter. Instruments at the sea surface were situated 3 m from the ship´s side and 4 m from the working deck; thus, Secchi judgements were made at about 6 m distance from the sea surface. The draught of the ship is nearly 11 m (and the length and the max-width 118 m and 25 m respectively). Most of the measurements were carried out on the sunny side as far as this could be judged.

Preliminary Results

Mean values of some 10 measurements without sea surface waves present gave 33 m, 48 m and 56 m as the 1% quanta levels derived from Secchi (Højerslev 1984), Colour Index (Højerslev 1980) and Quanta Meter, respectively. The discrepancy between the 3 methods has so far not been explained as each one has its limitations.

Secchi depth judgements vary somewhat from observer to observer. Wave height is also a factor accounted for by Højerslev´s expression:

$$Z_S \text{ (true)} = Z_S \text{ (observed)} \times (1 + 0.4\ H).$$

where Z_S is Secchi depth and H is wave height. As wave heights are difficult to judge, "wave" Secchis have not been transformed to 1% quanta levels in Tab. 3. Another problem is the sun condition. If Z_S is e.g. 10 m, Højerslev´s (1984) tables indicate 13 m for high sun and blue sky, but 17 m for low sun or overcast, as the 1% quanta level. In Tab. 1 the latter alternative has nearly always been chosen. Note that Hojerslev´s 1 % levels computed from Z_s are smaller, mostly $2 \times Z_s$, than the more "classical" $2.7 \times Z_s$.

Quanta Meter measurements can also be of different quality hence problematical. The best data are derived on sunny days when clouds are completely absent. In the present data file there is only one such case (Sta. 179); usually the conditions were more or less overcast. As pointed out by Jerlov (1976), ship shadowing is more pronounced under these conditions than in clear sun. Usually the deck irradiance was varying; data from the

deck quanta meter, mounted on the mast, were used to correct the Quanta Meter readings. Such a procedure is, however, not always effective. A cloud shadow at some distance from the ship may affect the underwater unit whereas the deck meter receives full sunlight (Jerlov, 1976.).

To overcome some of the problems mentioned above, Jerlov (1979) and Højerslev and Jerlov (1977) introduced the Colour Index Meter. It contains two photo-cells equipped with interference filters of 450 nm and 520 nm respectively that face downward to record nadir radiances. Jerlov (1979) mentions that the Colour Index (CI = L(450)/L(520)) is independent of solar elevation above 15° and little dependent on cloudiness. Its use in determining the 1% quanta levels depends upon very good simultaneous Quanta Meter determinations to construct e.g. the table in Højerslev (1980).

There is at least one more complication: the ice cover in connection with many of our measurements. A thorough data processing is difficult because the special influence of this parameter is not known.

The correlation coefficient between the 1% quanta levels Z_1 from the Quanta Meter, Z_1 QM, and the Colour Index Meter, Z_1 CI, is 0.91 with the regression line being

$$Z_1 \text{ QM} = 5 + 1.15 \times Z_1 \text{ CI}$$

For a relation between Secchi Z_1, Z_1 Se, and Z, CI, only calm sea Secchi readings have been used. The correlation is 0.81 and the regression line is

$$Z_1 \text{ Se} = 0.75 \times Z_1 \text{ CI}.$$

At some 40 stations Colour Index and Secchi depths were measured. At about 30 of these stations, Quanta Meter readings were also done at 5, 10, 20, 30, 40, 50, 60, 70, and 75 m. The above-sea-surface figure divided by 1.3 (Højerslev,1980) was used as the sea surface value (=100%).

Only Z_1 CI as determined by the table in Højerslev (1980) from Colour Index data, will be referred to below.

The variations in Z_1 are highly dependent upon the particle content in ocean waters, less upon dissolved (yellow) substances. The particles in the "clean" Antarctic waters are probably mostly of biological origin. Fig. 12 shows the relation between Z_1 and the Chlorophyll-a mean content between surface and 75 m. A logarithmic transformation yields the following relationship:

$$Z_1 = 31 - 21 \times \ln(\text{Chl})$$

with a correlation coefficient of 0.81.

Fig. 13 shows Z_1 data from stations 143 - 182 plotted as a function of latitude. The line shows the general tendency of two end maxima at 57° and 62° respectively, and a minimum at about 59°. The clarity of the water in the South is partly due to the presence of ice = small subsurface irradiances. The rather steep events in the North are probably coupled to the existence of the front at the northern rim of the Confluence. The measurements from

Sta. 183 onwards seem to have made the pattern in the northern part of the area look more diffuse than in Fig. 13

We thank Niels Højerslev, University of Copenhagen for lending us the Quanta Meter, the Colour Index Meter and the Secchi Disk.

Literature Cited

Højerslev, N.K. (1980): Water colour and its relation to primary production. Boundary-Layer Meteorology 18: 203-220

Højerslev (1984). Optical properties of sea water In: Landolt-Brönstein., chapter 3.3.

Højerslev & Jerlov (1977).The use of the colour index for determining quanta irradiance in the sea. Rep. Inst. Phys. Oceanogr. Univ. Copenhagen, Nr. 35.12 pp.

Jerlov (1976). Marine optics. Elsevier Oc.Ser. No. 14, 231 pp.

Figure 12 : Relation between Z_1 and Chlorophyll-a concentration

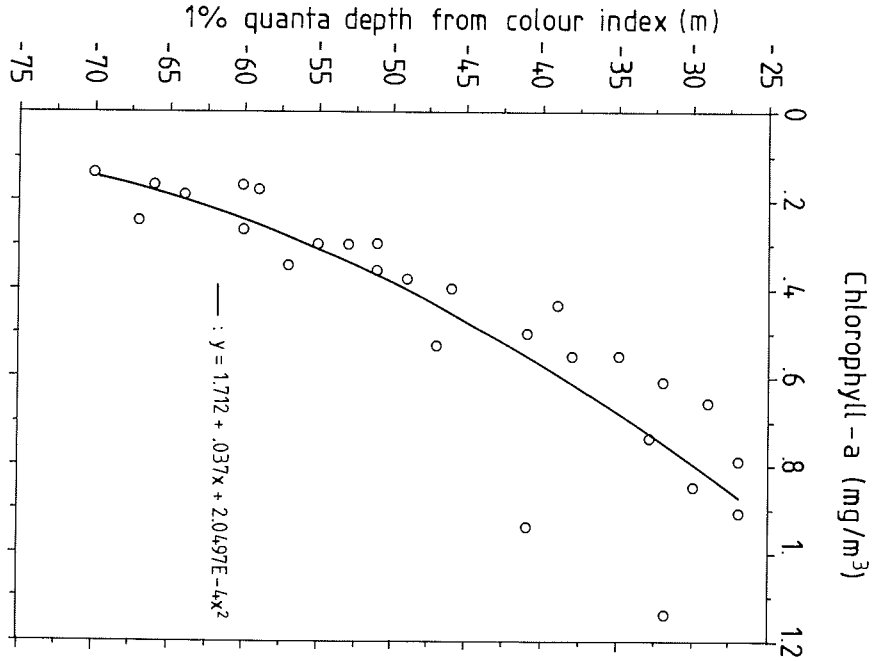

Figure 13: Relation between Z_1 and geographical position

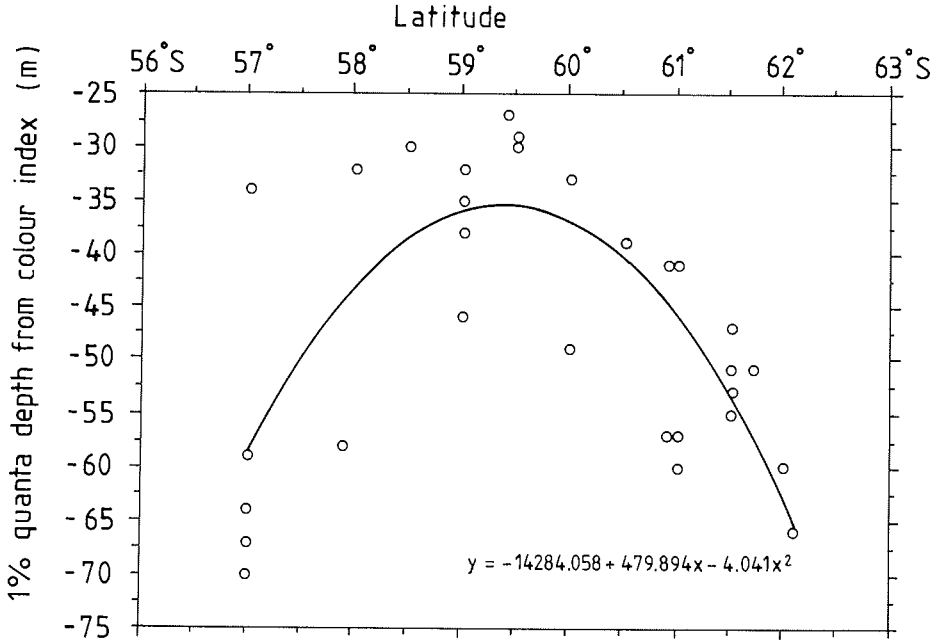

Table 3: Preliminary optical data

Date 88/89	GMT	Station No.	South	West	Clouds	Wave Height m	Ice Coverage	Secchi Depth m	Colour Index C1	1% quanta depth (m) computed from: Secchi m	Colour Index	Quanta Meter
27.11	14	145	58.0	49.0	8/ 8	2.50	0%	-	0.88	-	32	40
28.11	13	148	59.5	49.0	8/ 8	0.00	0%	15	0.79	28	30	40
29.11	16	151	61.0	49.0	8/ 8	0.00	90%	25	2.03	52	60	75
30.11	13	153	62.0	49.0	8/ 8	0.00	99%	32	2.23	75	66	65
03.12	15	156a	61.0	49.2	7to8/ 8	0.10	70%	25	1.88	52	57	80
04.12	15	156b	60.9	49.2	8/ 8	0.05	80%	22	1.85	45	57	70
05.12	17	157a	59.0	49.0	8/ 8	0.10	5%	16	0.90	30	32	35(40)
06.12	15	157b	59.0	48.9	8/ 8	0.20	5%	19	1.44	36	46	55
07.12	15	157c	59.0	48.7	8/ 8	0.75	1%	18	1.44	-	46	50
08.12	16	158a	59.4	48.8	8/ 8	1.0+swell	20%	9	0.70	-	27	35
09.12	15	158B	59.4	48.8	8/ 8	0.1+swell	25%	11	0.68	20	27	30
10.12	16	159a	57.0	48.9	8/ 8	2.00	0%	20	2.25	-	67	85
11.12	15	159b	57.0	48.8	5/ 8	2.50	0%	22	1.95	-	59	75
12.12	15	159c	57.0	48.4	3to5/ 8	1.00	0%	25	2.39	-	70	90
13.12	14	160	57.0	47.0	3to5/ 8	1.50	0%	23	2.14	-	64	80
14.12	15	164	59.0	47.0	8/ 8	0.40	0%	15	1.11	27	38	50
15.12	13	166	60.0	47.0	7to8/ 8	0.25	0.50%	21	1.57	42	49	60
16.12	15	169a	61.5	46.9	8/ 8	0.05	90%	16	1.46	30	47	65
17.12	15	169b	61.7	46.6	8/ 8	0.25	95%	17	1.64	32	51	65
19.12	15	171	60.9	46.4	8/ 8	0.60	5%	15	1.23	27	41	55
20.12	09	172	59.0	49.0	5/ 8	0.5+swell	0%	-	1.00	-	35	-
20.12	17	173	59.5	49.0	8/ 8	0.3+swell	0%	9	0.76	16	29	28
21.12	09	174	60.0	49.0	8/ 8	0.20	0%	12	0.94	22	33	-
21.12	18	175	60.5	49.0	7/ 8	0.25	0%	11	1.15	20	39	50
22.12	09	176	61.0	49.0	7/ 8	0.05	75%	12	1.27	22	41	-
22.12	19	177	61.5	49.0	7/ 8	0.00	95%	18	1.77	34	55	70
23.12	10	178a	61.5	49.0	7to8/ 8	0.00	95%	16	1.72	30	53	-
23.12	14	178b	61.5	49.0	3/ 8	0.05	95%	21	1.60	42	51	65
24.12	15	179	62.1	49.0	3/ 8	0.01	95%	30	2.22	46	66	?
27.12	15	182	57.0	49.0	8/ 8	0.50	0%	14	0.97	28	34	45
28.12	14	186	57.9	49.0	6/ 8	1.50	0%	22	1.93	-	58	75
28.12	20	187	58.5	49.0	7to8/ 8	1.50	0%	12	0.79	22	30	-
29.12	09	188	59.0	49.0	8/ 8	0.25	0%	13	1.03	23	35	-
29.12	15	189	59.3	49.0	8/ 8	0.25	0%	14	0.88	25	32	55
30.12	10	191	60.5	49.0	8/ 8	0.10	0%	13	0.75	24	29	-
30.12	14	192	61.0	49.0	8/ 8	0.05	80%	14	1.26	25	41	55
31.12	15	194	61.8	48.8	8/ 8	0.00	99%	21	1.87	42	57	50
03.01	11	205	59.3	48.2	8/ 8	0.50	0%	11	0.99	20	35	-
03.01	21	207	57.4	48.6	8/ 8	2.00	0%	9	0.55	-	23	
04.01	13	208	57.6	48.4	8/ 8	1.00	0%	11	1.00	-	35	
04.01	16	209	57.8	48.4	8/ 8	0.75	0%	17	1.95	-	59	

4.1.3 Oxygen Production and Uptake; Hydrogen Peroxide

M. Pamatmat

Objectives

The rates of oxygen production and consumption were measured especially for comparison with other measures of biological activity (^{14}C uptake measured by Estrada, Lancelot and Mathot, ETS activity measured by Estrada, ^{3}H-thymidine uptake measured by Becquevort, nutrient regeneration measured by Treguer and Goeyens) in order to gain some insight into these processes at the ecosystem level and their rates in low-temperature waters. Such comparisons for different ecosystems were expected to demonstrate important differences in the meaning of the results obtained by different methods that are often presumed to be equivalent, analogous, or comparable, e.g. ^{14}C uptake and oxygen production as measures of primary production; oxygen consumption and ETS activity as measures of metabolic rates; oxygen consumption and nutrient regeneration as measures of mineralization rates.

Hydrogen peroxide is of interest as a metabolic by-product of a vast majority of organisms, perhaps of all aerobic organisms, as a by-product of photo-activated reduction of oxygen in surface waters, and as a by-product of photochemical reactions in the atmosphere. Being more reactive than oxygen, it may be important in redox reactions with many organic and inorganic substances that would otherwise be much more stable in solution. As such it could play a significant intermediary role in biological and chemical processes other than those directly involved in its production. An early step in assessing this role is to map its distribution, experimentally identify the factors that affect it, and determine their quantitative relation.

Work at Sea

Dissolved oxygen was measured by a Winkler method employing a potentiometric dead-stop end-point determination with a double-platinum electrode. In connection with light and dark incubation experiments, initial and final oxygen values were measured with a Radiometer Acid-Base Analyzer equipped with an E-5046 electrode. The latter was preferred over the Winkler method in order to avoid interference from various dissolved substances including nitrite and hydrogen peroxide. Both methods have about the same coefficient of variation of less than 0.1% to as good as 0.01%, but with different underlying reasons for their respective variability. The pO_2 electrode was calibrated with equilibrated water at 20°C and pO_2 readings were converted to oxygen concentrations from known temperature and pressure according to the equation of Weiss (1970). All incubations were done at or close to in situ temperatures.

Hydrogen peroxide was measured in terms of fluorescence resulting from peroxidase-catalyzed oxidation of hydroxyphenylpropionic acid (Palenik & Morel, 1988). Water samples were tapped from Niskin samplers into linear polyethylene bottles and kept refrigerated at 6°C in the dark until analyzed, usually within several hours. Surface samples were scooped with a bucket. It was not necessary to warm the sample to room temperature before

transferring an aliquot into a 1-cm quartz cuvet in the spectrofluorometer. Samples were usually stable overnight although some samples were much less stable than others. In determining hydrogen peroxide in snow and sea ice these were melted slowly inside the refrigerator and analyzed as soon as they were completely melted.

Preliminary Results

Light-bottle incubations.

Oxygen was produced in light bottles as expected (Fig. 14). However, in contrast to findings with the ^{14}C method (see § 4.2.6), the rate of oxygen production decreased with increasing light intensity above 96 $\mu E\ m^{-2}\ s^{-1}$. Carbon-14 (parallel measurements by Estrada of water samples from the same cast though different water bottle) was taken up at increasing rates up to the highest light level without showing light saturation. Furthermore, the quantitative relation between oxygen production and ^{14}C uptake changed with increasing light intensity (Fig. 15). PQ's (moles of oxygen produced to moles of carbon dioxide taken up) ranged from 2.9 to 0.7 depending on light level and location (Fig. 16).

One experiment at Time Station 157 produced an unusual and unexpected result: all samples showed a loss of oxygen during light incubation, the rates of uptake increasing with increasing light intensity (Fig. 17). This result could have been produced only if heterotrophic exceeded autotrophic activity in a mixed community. Since parallel samples showed photosynthetic ^{14}C uptake, the oxygen uptake in the light clearly shows that the two methods did not measure one and the same process in the light; rather their results represent two different parameters about a mixed community.

Effect of Light on Oxygen Consumption.

The increase in oxygen consumption with increasing light intensity, rarely observed (in fact, I am aware of only one other reported observation, namely by Hutchinson in Linsley Pond, Connecticut), has significant implications. It means that the general assumption made in doing light-dark bottle incubations, that respiration in the dark is the same as respiration in the light, is not always true. When it is not true, adding dark oxygen uptake to light oxygen production underestimates gross primary production, and, from the results obtained during this cruise, sometimes greatly do.

The observed oxygen consumption in light bottles provides an explanation for the apparent inhibition of light-bottle oxygen production but not of ^{14}C uptake in station 156 and 158. That is, photosynthetic oxygen production must not have been inhibited either, but rather in a mixture of autotrophs and heterotrophs the decreased rate above light saturation level was the effect of increased heterotrophic metabolism.

Photosynthetic Quotients.

The decrease in PQ's (Fig. 16) with increasing light clearly shows that ^{14}C uptake and oxygen production for communities of mixed auto- and heterotrophs are not related in the same way as in a plant organism or a pure phytoplankton population. ^{14}C uptake more nearly measures net primary production while oxygen change actually represents the balance between autotrophic and heterotrophic activity. The photosynthetic quotient of a plant is something quite different from calculated community PQ's. This casts doubt on the liberal use of PQ's gleaned from the literature when interconverting carbon and oxygen. In addition to the usual nitrate versus ammonia metabolism to explain the range of PQ's, the changing proportions of heterotrophs and autotrophs also have a considerable influence on mixed-community PQ and RQ (respiratory quotient, the reverse of PQ).

A Time Series of Events Recorded by Different Measurements.

Oxygen consumption in light bottles at Time Station 157 was corroborated by many other independent measurements. From a web of circumstantial evidence, it has become evident that over the course of this 3-day station the entire team of collaborating scientists had by chance gathered a variety of results pointing to an impressively rapid transformation of a diatom-dominated autotrophic community into a heterotrophic community. On day 1 we started sampling a water mass with a diatom bloom. Direct and indirect observations (echo soundings, net catches, light transmission; see § 4.3.3 and § 4.1.2) showed a swarm of Krill grazing down the bloom (see § 4.2.1). On day 2 the water sample from 10 m depth showed high heterotrophic activity (see §4.2.9 for ^{3}H-thymidine uptake, indicating high bacterial production, and § 4.2.6 for ETS activity). Station 157 had the highest ratio of ETS to chlorophyll values, which is also indicative of a heterotrophic community. On day 2 there was also an increase in ammonia concentration (see § 4.2.1). It appears that the team of EPOS Leg 2 had witnessed, without fully realizing it at the time, the transformation of a diatom-dominated autotrophic community (with net oxygen production in the light) into a microheterotrophic-dominated community (with net oxygen consumption in the light).

A General Hypothesis.

The coherent set of evidence leads to the following hypothesis: when Krill swarms graze down the diatom blooms they excrete, and/or liberate as a consequence of their feeding, ammonia and various dissolved organic substances. Moulting must also liberate considerable amounts of metabolizable substrate for bacteria. Hence, the passage of Krill swarms enhances bacterial production. Microautotrophs that are by-passed by the grazing Krill grow as fast or faster than before but they are always kept in check by microheterotrophs. Total biomass remains low after a diatom bloom, but the level of biological activity and the turnover rate of living matter and nutrients are high, in spite of the low temperature. Blooms resulting from "new" production are replaced by "regenerating" microbial loops or networks. A heterotrophic state in the euphotic zone is transitional, lasting in Antarctic waters not more than a few days at most, giving way to a longer-lasting more balanced community with little net community production.

System-level theories have been generally untestable in that the results always turned out to be ambiguous and not totally convincing in the end. The foregoing hypothesis, on the other hand, seems to be verifiable in the field if a diatom bloom about to be grazed by a swarm of Krill can be located ahead of time by a team of scientists prepared to measure all the necessary variables, states and processes. Or it can be tested in a laboratory by Krill-grazing on a diatom bloom within a mixed natural community. In either case, our ability to perform the test would be a demonstration of a deeper understanding of the natural ecosystem.

Hydrogen Peroxide and Oxygen Distribution

In the Water column.

Fig. 18 shows some typical profiles of H_2O_2 and O_2 in the upper few hundred meters. Fig. 19 shows a vertical section along a transect at 47° W longitude. The similarity between H_2O_2 and O_2 in the upper layer is evident. In mid-depths of 400 to 700 m depending on location, where oxygen shows a consistent minimum, H_2O_2 does not show a comparable minimum. Rather H_2O_2 shows a more uniformly low concentration of 0.6 to 0.9 fluorescence units below 200 m, with only occasional values above 1. The range of values measured during the cruise was 0.1 to 30.0 in the water. Each fluorescence unit is approximately equal to 2×10^{-8} M, the exact concentration is still to be calculated for each sample.

Higher values of H_2O_2 in near-surface layers are evidently related to light level. Water samples incubated in a light (halogen lamp) gradient in an incubator maintained at sea-surface temperature showed the highest H_2O_2 increase at the highest light level (709 $\mu E\ m^{-2}\ s^{-1}$). The amount of H_2O_2 production decreased exponentially and levelled off at about 160 $\mu E\ m^{-2}\ s^{-1}$. Seawater incubated at the highest light intensity showed an exponential increase in H_2O_2 with time. H_2O_2 production during light incubation is significantly higher in polystyrene flasks than in glass vials. Deck incubations in a flowing seawater-bath under natural sunlight resulted in higher H_2O_2 production rates than under halogen light.

DCMU, a commonly used inhibitor of photosynthetic activity, was added to seawater and Milli-Q water to try to differentiate photorespiratory source of H_2O_2 from purely photochemical process. In the dark, the presence of DCMU did not change H_2O_2 concentration. In the light, however, DCMU increased H_2O_2 in both Milli-Q and natural seawater, although the increase was greater in the latter. The greater increase in seawater could be due in part to photorespiration.

To be sure, the spatial and temporal distribution of H_2O_2 is the balance between the rates of formation, decomposition, and mixing of water masses, none of which is known. Until then, not much more can be said about distribution patterns.

In Sea ice, snow and rain.

Sea ice, snow and rain had often higher concentrations of H_2O_2 than sea water, ranging from the same values as surface water and up to two orders of magnitude higher. Fresh snow and rainwater had 40-50 fluorescence units. The very different concentrations in frozen and liquid water suggest different sources or mechanisms of formation and accumulation in the two states. Since seawater has lower H_2O_2 content than sea ice, the H_2O_2 in frozen seawater must have come from elsewhere, e.g. from atmospheric precipitation. If this is so, the amount of H_2O_2 in sea ice must be in agreement with the amount of precipitation and its content of H_2O_2.

The curious profiles in ice and snow cores could be evidence of their past history, mode of growth or accumulation, and the conditions during precipitation and freezing. When seawater containing hydrogen peroxide freezes, the liquid brine is not only more saline but is also enriched in H_2O_2. The situation becomes more complex with the growth of ice algae, which produce catalase enzyme that decompose hydrogen peroxide. Thus some layers of "brown ice" contained little or no hydrogen peroxide while the layer above them contained high concentrations. Some samples of brown ice, however, also contained high concentrations of H_2O_2. It would be of interest to know how or whether H_2O_2 diffuses through ice and snow.

Dissolved oxygen was measured with Anita Buma´s cooperation to calibrate the CTD oxygen probe about once per day.

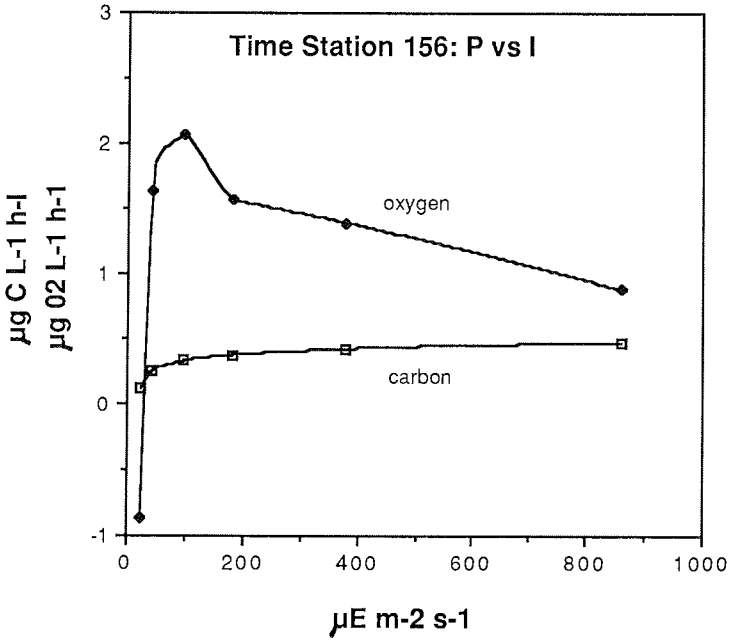

Figure 14: Rates of oxygen production and carbon-14 uptake in relation to light intensity

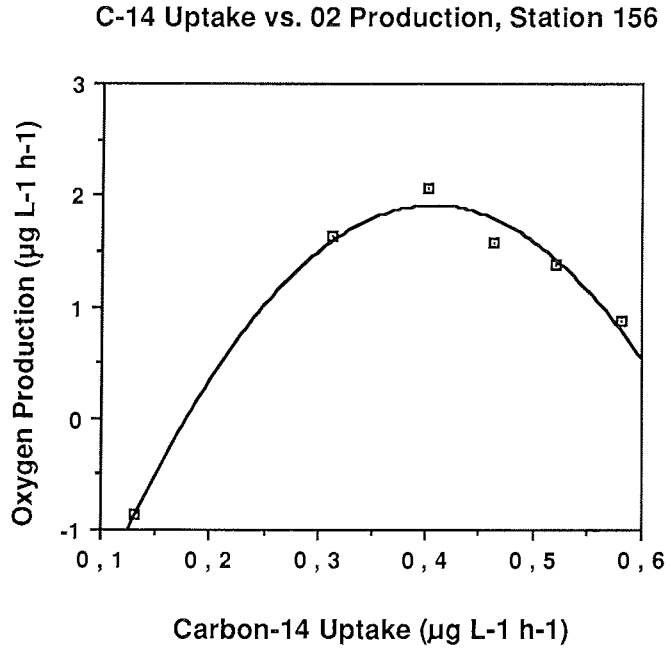

Figure 15: The changing relation between oxygen production and carbon-14 uptake with increasing light intensity

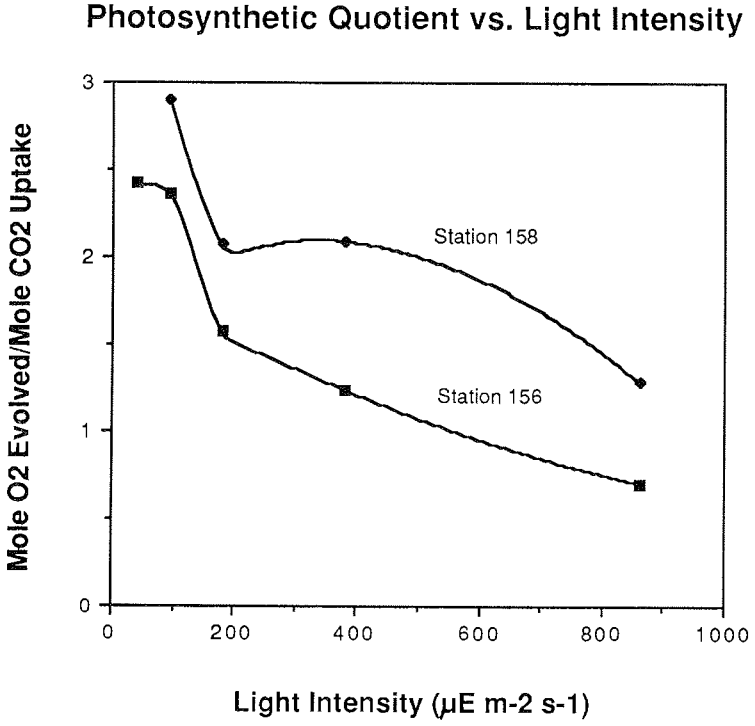

Figures 16: The change in photosynthetic quotient with increasing light intensity

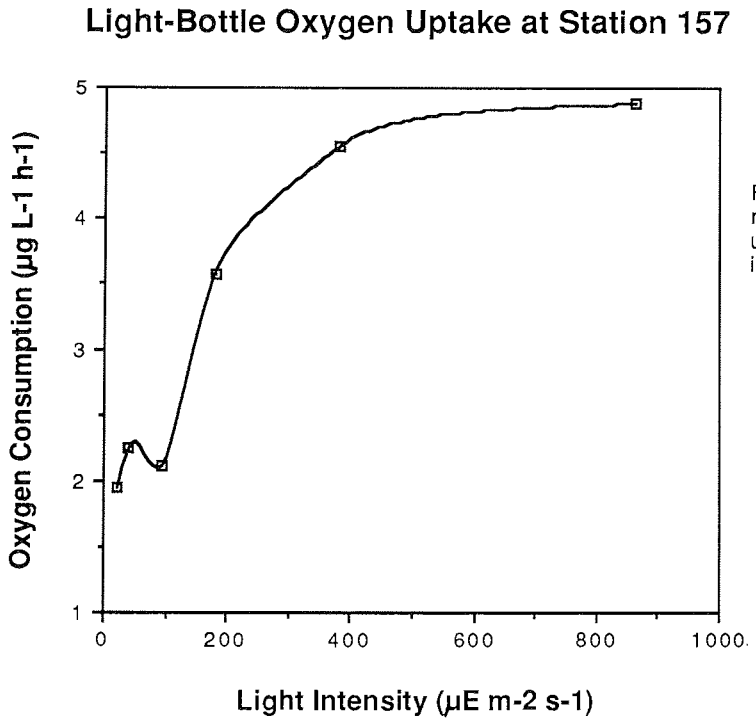

Figure 17: Increasing rates of oxygen uptake with light intensity

Figure 18: Profiles of hydrogen peroxide and oxygen at a shelf station showing bottom effect on both distributions.

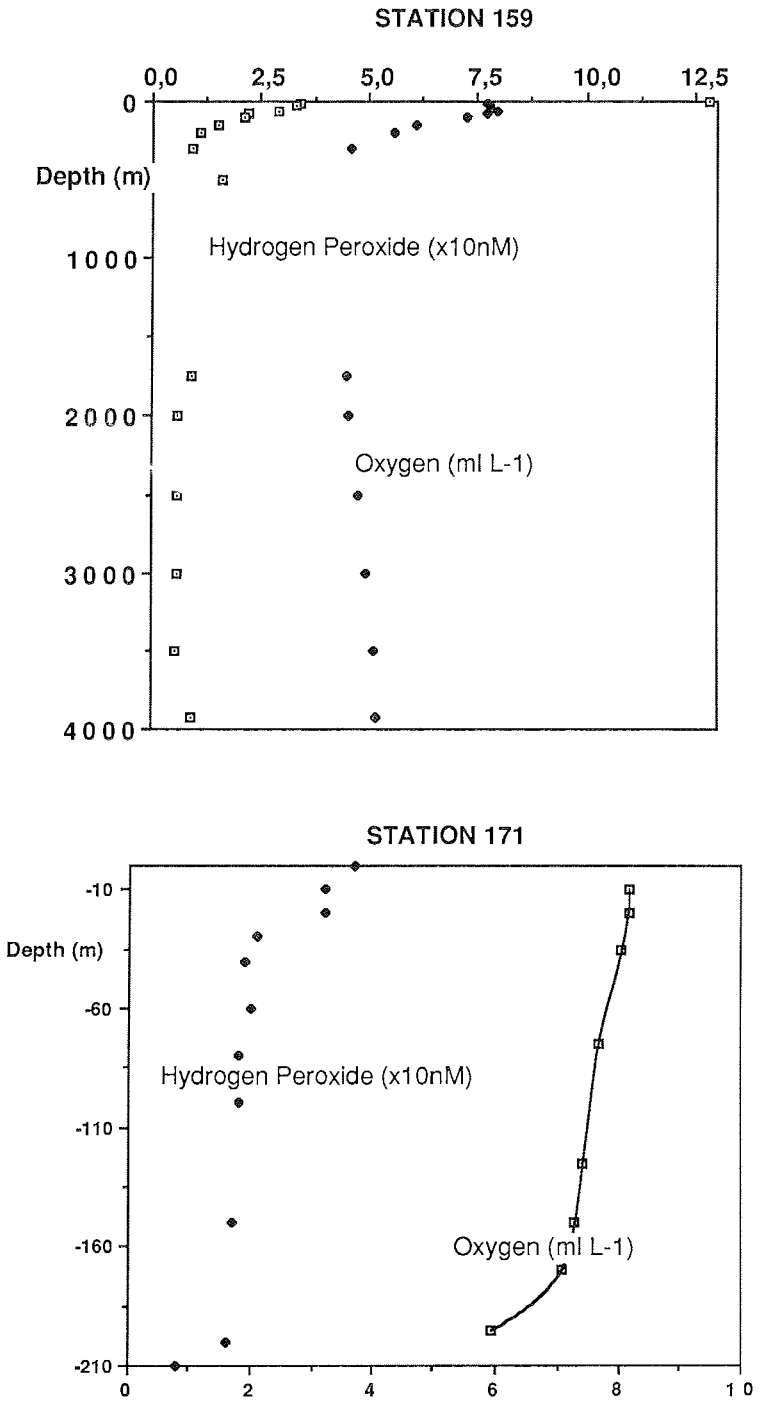

Figure 19:

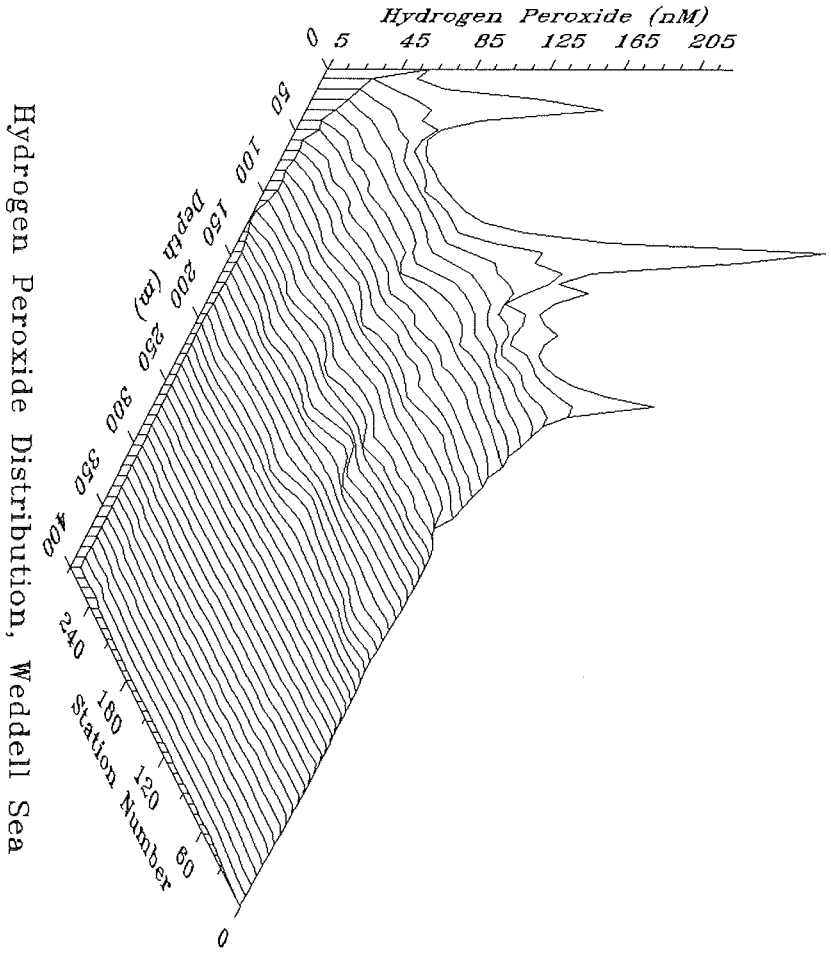
Hydrogen Peroxide Distribution, Weddell Sea
Hydrogen Peroxide (nM)
0 5 45 85 125 165 205
Depth (m)
50 100 150 200 250 300 350 400
Station Number
0 60 120 180 240

4.1.4 Trace Metals - Iron and Manganese Effects on Phytoplankton Growth

H.J.W. de Baar, A.G.J. Buma, G.Jacques, R.F. Nolting, P. J.Treguer

Objectives

In the past decade reliable data have become available on the oceanic distributions of many trace elements. Very low concentrations in the nanomolar to picomolar range have been reported, requiring ultraclean methodology throughout for their determinations. Among these trace elements quite a few (Ba, Cd, Cu, Ni, Zn, the Rare Earths, Al sometimes, etc.) were shown to exhibit vertical and interoceanic distributions very similar to those of the macronutrients, i.e. Nitrate, Phosphate, Silicate (and Alkalinity). Presumably these elements are intimately involved in the major biological cycles within the oceans. However the overall data set for metals in the oceans is still quite limited. Thus far there exists no reliable data set of transition element concentrations in Antarctic waters.

The anomalously high nutrient levels in the surface waters of the Southern Ocean accompanied by rather modest standing stocks of plankton biomass (Siegfried et al., 1985) contrasts with the much more efficient utilization of nutrients in temperate oceanic surface waters (where as a result very low nutrient levels are found). This is often referred to as the Antarctic paradox (Treguer & Jaques, 1986). The older and more recent literature contains several suggestions about limitation of the Antarctic marine system by nano-nutrients, notably Mn and Fe, as well as Co, Zn or vitamin B-12 (also containing Co). Fe is an important component in many algal metabolic pathways. Chlorophyll synthesis is dependent on Fe nutrition and iron-starved algae exhibit deviations in pigment composition. Given aforementioned metal-nutrient relations elsewhere one may also speculate about high levels of, say, Cu or Cd to be found in Antarctic surface waters, possibly leading to inhibition rather than stimulation of plankton growth.

While our EPOS trace metal project was still in the planning stages attention was drawn to two recent studies with potential relevance for the Southern Ocean. Two independent research teams reported simultaneous experiments (August 1987, RV WACOMA) in the Subarctic Pacific Ocean (Ocean Station Papa, 50°N, 145°W), an area also characterized by unusually high nutrient levels in the surface waters. Enhanced phytoplankton growth upon addition of nanoMolar levels of Fe was found in both studies, while the controls exhibited no or very little growth. A truly bio-limiting role for Fe in those regions was suggested, while it was speculated that Southern Ocean short supply in production may also be limited by Fe. Lacking any reliable data on Antarctic waters, there has been ample room for creative speculation. Obviously a study of the distribution and fate of trace metals in Antarctic waters is not only of great interest in itself for marine chemistry, but would also provide the necessary constraints for evaluating some of the above hypotheses regarding the role of metals in the pelagic ecosystem of the Southern Ocean.

Work at Sea

During EPOS Leg 2 we had the opportunity to work on both the distributions of transition metals in the waters as well as the possible role of Fe and Mn (Cu, Zn) as regulators of plankton growth. Throughout the project, clean methods and rigorously pre-cleaned materials (Teflon PTFE, FEP, Polyethylene, Polycarbonate) were applied. Ultraclean sampling operations depended on 12 to 17 modified Teflon-coated GOFLO (General Oceanics) samplers mounted on our specially built Teflon-coated CTD/Rosette frame, used for the first time during the EPOS campaign. Upon recovery, the samplers were taken off the Rosette, mounted on the outside of our Class-100 clean air container (extensively refitted for EPOS Leg 2), and connected to the inside through Teflon FEP tubing with Teflon PTFE stopcocks. For culture studies the water was directly led into the 20 ltr. Polycarbonate vessels. For assessment of vertical profiles in the water column the GOFLO samplers were pressurized (about 1 atm filtered N2 gas) in order to pass the seawater through 0.4 micron precleaned, preweighed Nuclepore filters mounted in all-Teflon PTFE filter holders. The filters were kept for later analyses, the water samples were acidified to pH 2 and stored.

For our study of trace metal abundances we also collected clean surface water samples and samples of ice, snow and ice algae by utilizing the rubber zodiac boat, weather permitting. Altogether, we collected some 400 samples, focussing mostly on the 49 W transect (Tab. 4). Some 50 samples (2 or 5 ltr each) were taken for determinations of Rare Earth Elements by Schijf and De Baar at the NWO Laboratory for Isotope Geology, Amsterdam. Another set of samples (100 ml each) was collected for Van der Weijden (Utrecht), who will assess his expectation of Fluorine anomalies in seawater resulting from uptake by Krill. Most samples were, however, collected for determination of trace metals by GFAAS in our shore laboratory. Of these samples, the majority were already processed on board ship, utilizing two different lines of extraction. All sample processing was done inside laminary flow benches inside the clean air container. Some 200 samples of seawater, snow, etc. were purified and 100-fold preconcentrated with a solvent extraction method (APDC/Freon, APDC/MIBK) for future analyses of Cu, Cd, Ni, Zn, Fe. Some 100 samples were preconcentrated and purified (separation of sea salt) with chromatography (Chelex-100) for future analyses of Mn, Fe, Cu, Cd, Ni, Zn. For several stations, duplicate samples were extracted with the two different techniques, with the hope of obtaining a consistent, hence reliable data set. Upon final analyses of seawater extracts and particles (filters) in the shore laboratory the final interpretation will rely on variables measured by others during EPOS Leg 2, notably for hydrography, dissolved oxygen, nutrients and chlorophyll a.

The practical arrangements for this study were planned and executed in conjunction with the parallel Al enrichment project reported elsewhere. Experimental design was modified after Coale & Bruland (pers. comm.). In our refrigerated container the sealed culture vessels were subjected to appr. 100 $\mu E\ m^{-2}\ s^{-1}$ light intensity in a light/dark cycle (16/8 hours), saturation light level for local plankton communities as assessed independently during EPOS Leg 2. Our light benches with motor-driven slowly revolving culture vessels functioned most satisfactorily. For manipulation and subsampling

(every 24 hours) the vessels were brought into the clean air container. Subsamples were taken for shipboard determinations of Nitrate, Phosphate, Ammonium, Silicate and chlorophyll a, the latter by acetone extraction (Exps. II to V) and initially by in vivo fluorescence (Exp. I). In the final experiment, uptake rate studies were executed for ^{14}C incorporation (total and proteins only), ^{3}H-Thymidine incorporation and $^{32}Si/^{32}P$ incorporation. The flow cytometry group kindly offered to run determinations also done on shipboard but the ensuing data awaits final processing ashore by the instrument manufacturer. Samples for microscopic assessment of species and their abundance, trace metal levels, Particulate Organic Carbon (POC) and pigment composition were taken and processed for future determinations in the shore laboratory.

Tab. 4. Inventory of collected and filtered seawater samples, some of them already processed aboard as indicated by crosses. At a given sampling depth, in fact, several samples were collected, ranging from 2-4 and volumes from 0.25 to 5 ltr, most of them stored away for future analyses and also as back-up in case the shipboard extractions became contaminated.

Station	Depth Interval with No of Depths	Processed Aboard	APDC/MIBK	Chelex
147	10-1000	12	-	x
151	0-1500	13	x	x
153	10-1500	12	x	x
154	0	1	x	-
156	0-2200	25	x	x
157	0-3900	25	x	x
158	0-300	13	x	x
159	0-3900	34	x	x
169	0-450	12	x	-
171	10-230	9	x	-
172	0	1	x	-
174	0-300	13	x	-
175	0	1	x	-
176	0	1	x	-
177	0	1	x	-
182	0	1	x	-
183	0	1	x	-
186	10-300	13	x	-
189	0	1	x	-
192	0	1	x	-
193	0	1	x	-

Preliminary results

Five experimental series (I-V), comprising 2 to 7 cultures simultaneously, were run over time periods from 8 to 15 days (Tab. 5). The seawater represented the Scotia Sea with very low (III) and elevated (bloom, V) biomass, the North flank of the Weddell-Scotia Confluence (I), bloom conditions at its Southern flank (II) as well as Weddell Sea Water proper under more than 90 % ice cover (IV). Different plankton communities were encountered, dominated by the diatom *Corethron criophilum* and nanoflagellates (mainly Cryptomonads) in Exp. I; nanoflagellates (mainly Cryptomonads) in Exp. II; the diatoms *Corethron criophilum*, *Chaetoceros dichaeta* and *Chaetoceros neglectus* (III & V), and *Corethron criophilum* (IV). Preliminary shipboard microscopic inspection during the course of the

experiments revealed slight changes in relative species composition, but definitely no complete take-over by a single species and generally excellent physiological condition, the latter also monitored by the ratio Chlorophyll/Phaeophytin (mostly higher than 10, never below 2). In total 8 cultures ran with Fe additions, 4 with Fe+EDTA, 4 with Mn additions, next to 8 untreated controls and 2 EDTA controls (Tab.6).

In all cases both the enriched and control cultures show an immediate increase in biomass (Chl a) and decrease of nutrients, suggesting normal growth and little or no traumatic effects due to initial handling (Fig. 20-22). In the second experiment the metal additions were done only at t=2 days, at which point in time the reproducibility (Chl a = 3.9± 0.2 ; NO_3 = 22.3 ± 0.2; PO_4 = 1.45 ± 0.02) between 8 cultures underlines the overall reliability of our methods. During an initial period, lasting from about 3 to 5 days, no significant responses to the metal enrichment were observed in any of the five experimental series. Small grazers were and remained quite abundant throughout the experiments, levels of ammonia remained fairly constant around their starting values (the latter ranging from 0.1 to 0.5 µM) in most experiments. Only in the third experiment ammonia gradually decreased from 0.47 to 0.08 µM, presumably due to phytoplankton uptake. Apparently, the absence of larger grazers such as copepods or *Euphausia superba* (Krill) as well as the saturating light level lead to enhanced biomass accumulation in enriched and control cultures alike. The duration of this initial non-responsive period appears to relate to the initial (t=0) biomass (Chl a) of the culture.

Only after 3-5 days of consistent growth the enriched cultures begin to outgrow the controls. At that point in time the levels of biomass and nutrients in the cultures had developed near the highest and lowest levels respectively found in the ambient surface waters. During EPOS Leg 2 the highest Chl a values encountered were about 4.5 $\mu g.l^{-1}$, consistent with earlier reported ranges (Sullivan et al. 1988). Spring or summer values for Nitrate and Phosphate rarely drop below 20 and 1.5 µM respectively, only about 25 % below the winter values of 25-30 µM and 2 µM respectively. Silicate levels (not shown) in the Weddell Sea and Scotia Sea rarely drop more than 25 % below their respective winter values of about 80 and 25 µM.

In all cases where just Fe was added we subsequently observed enhanced growth and rapid utilization of available nutrients. Curiously enough the level of added Fe (1 nM or 10 nM) does not appear to make much difference, in contrast with one of the North Pacific studies (Martin and Fitzwater 1988). In experiment II the metals were added only at t=2 days, for Fe at 1 nM and at 10 nM, as well as at 1 nM (t=2) with daily extra 1 nM additions up to 6 nM at t=8 (Fig.20). For all three cases similar growth enhancement was observed. Most experiments (I, II, V) were run until nutrient exhaustion of the metal enriched vessels was reached, at which time the biomass (Chl a) was 1.5 to 2.1 times that in the controls. In general NO_3 was the first nutrient to be completely (I, II) or largely (III, IV) depleted. In the Scotia Sea with lower initial Silicate levels, the latter was exhausted first for the Fe = 10 nM culture in the final bloom experiment (V, not shown). Experiments III and IV also showed very distinct Fe stimulation but had to be aborted somewhat prematurely for logistical reasons (Fig.21,22).

In two series (IV and V) we also added a prepared stock of Fe with EDTA, and a separate EDTA control. These Fe+EDTA enriched and EDTA control cultures did by and large exhibit the same trends as for the Fe enriched and untreated control cultures respectively. In the first 4 days (Fig. 22) all developed very similarly, at t=6 the Fe+EDTA picks up at enhanced rate, yet eventually both Fe enriched and both control cultures end up at same levels, notwithstanding the EDTA. At t=6 the EDTA might have made the Fe more readily available. Detoxification of possibly high levels (in analogy with high ambient nutrients) of adversely acting metals like Cd or Cu would have been an alternative mechanism but is not supported by the identical development of untreated and EDTA controls, as also found in experiment V (not shown).

Manganese was added in experiment II (at t=2 days) to a level of 10 nM, as well as to 1 nM with daily additions of 1 nM up to 6 nM in total at the end (Fig.21). Latter culture showed distinctly more biomass than the control. Curiously enough the higher addition of 10 nM showed very little effect. Removal of Mn, for example by slow oxidation or wall adsorption, might negate any possible effect in the 10 nM culture, whereas the daily addition of fresh Mn in the other would sustain enhanced growth. Future analyses of Mn levels in stored samples may provide the answer here. Another run with a 10 nM addition (Fig. 22) shows little effect, only at the end of the run we see enhanced biomass but curiously enough slightly less nutrient uptake. In the final study (V, not shown) a 1nM addition eventually led to a 15% enhancement of biomass and similar decrease of nutrients. In summary we found a distinct effect for Mn in only one out of five experiments, the other four only exhibiting modest trends as also reported for one Mn experiment in the North Pacific (Coale and Bruland, pers. comm.).

For a range of plankton communities encountered in waters of the Weddell Sea, the Scotia Sea and the Confluence we have always found Fe to stimulate biomass accumulation. When extrapolating these observations to the in situ ecosystem it appears conceivable that Fe would stimulate phytoplankton growth and utilization of macronutrients in Scotia-Weddell Sea waters, without however acting as the single limiting factor. It is interesting to note that the added Fe only shows an effect once the cultures have reached levels of Chl a and nutrients comparable to the maximum and minimum levels observed respectively in the real field situation during EPOS Leg 2. This may suggest that there is adequate Fe in Antarctic waters to support modest growth and biomass, but not enough for optimum utilization of macronutrient resources. Here we observe that the ice zone blooms are associated with less saline meltwater, meltwater which may also carry an elevated trace metal signal from dust input. Future analyses of the surface water and ice/snow samples collected with the zodiac may provide an answer. At low ambient nitrate levels (say 20 µM) Antarctic algae may have more difficulty metabolizing nitrate effectively, and there the extra Fe boost in our cultures would make the difference.

Assuming steady state, the surface waters appear to either recycle their Fe resources quite efficiently, or there is an adequate supply from external sources. In this respect the EPOS Leg 2 study site, downwind and downstream from relatively nearby land-masses (S-America, Antarctic Peninsula) may receive adequate inputs from both aeolian and continental shelf sources. In this respect the more remote Indian and Pacific sections of

the Southern Ocean might be a more likely candidate for testing the hypothesis of singular Fe limitation, without ignoring the importance of our Weddell-Scotia Sea study area for the overall Southern Ocean. On the other hand one cannot avoid observing the many "dirty" icebergs which slowly melt while drifting away from the Antarctic continent. They are literally carrying along dirt, weathered material rich in Al and Fe of which at least a portion would dissolve and become available for plant uptake. These icebergs exist all around the Antarctic continent and might well contribute to the Fe budget of the Southern Ocean (Martin & Fitzwater, 1988).

Table 5: Shipboard data of five cultures series.

EXPERIMENT	I	II	III	IV	V
EPOS Station	145	158	159	169	182
Latitude °S	58	59	57	62	57
Longitude °W	49	49	49	47	49
Day	27	8	12	17	27
Month (1988)	11	12	12	12	12
Ice cover	-	-	-	over90%	-
Sampling depth (meter)	35	20	50	40	40
Number of Cultures	4	7	2	6	7
Begin Values (t=0):					
Temperature °C	-0.6	-1.3	0.08	-1.77	1.62
Chlorophyll a ($\mu g\ l^{-1}$)	1.65	2.24	0.15	0.83	0.89
Nitrate (μM)	27.9	26.0	29.8	28.1	27.9
Phosphate (μM)	1.87	1.55	1.81	1.89	1.74
End values:					
Time (days)	10	8	12	9	8
Temperature °C	3.5	3.5	3.5	3.5	3.5
Chl a ($\mu g\ l^{-1}$) for Fe=10 nM	18.8	10.6	10.6	12.0	13.9
Nitrate (μM)	N.D.	N.D.	7.2	15.8	4.5
Phosphate (μM)	0.14	-	0.3	0.73	0.1
Chl a ($\mu g\ l^{-1}$) for Control	13.0	6.0	5.1	7.6	10.6
Nitrate (μM)	2,9	5.7	16.4	18.5	7.3
Phosphate (μM)	0.25	-	0.79	0.91	0.18
Depletion of:	NO_3	NO_3	NO_3	NO_3	Si

Table 6: Number of untreated controls and nominal concentrations (nanoMolar) of trace metals and EDTA in the culture solutions. Metal additions usually at t=0, except for Exp. II at t=2 and for an addition of Fe + EDTA at t=4 in Exp. V.

EXPERIMENT	I	II	III	IV	V
Controls	two	two	two	two	two
Fe (nM)	10	1 at t=2	-	-	-
	10	10 at t=2	10	10	10
		1 at t=2, with daily 1 nM addition until 6 at t=8			
Fe + EDTA	-	-	-	10+15	10+30at t=0
					10+30at t=4
Fe + EDTA + Mn					1+30+1
EDTA (nM) Control				15	30
Mn (nM)	-	1 at t=2, with daily 1 nM until 1			
				6 at t=8	-
	-				
Mn	10	-	10		

We conclude that Fe is not the single limiting factor for the biota in the Scotia-Weddell Sea, an important sector of the Southern Ocean. On the other hand Fe might conceivably stimulate phytoplankton accumulation, effectively acting as one of several growth-limiting factors.

Literature Cited

Martin, J. H., & Fitzwater, S. E., 1988. Iron deficiency limits phytoplankton growth in the northeast Pacific subarctic. Nature, 331: 341-343

Siegfried, W. R., Condy, P. R. & Laws, R. M., 1985. Antarctic Nutrients Cycles and Food Webs. Springer-Verlag, Heidelberg.

Sullivan, C. W., McClain, C. R., Comiso, J. C. & Smith, W. O., 1988. J. geophys. Res., 93 (C 10) 12,487 - 12,498.

Treguer, P. & Jacques, G., 1986. L´Ocean Antarctique. La Recherche, 178: 746-755

Fig. 20 Experiment II. Concentrations of chlorophyll a (μg l^{-1}), dissolved nitrate (μM) and phosphate (μM) versus time (days) .

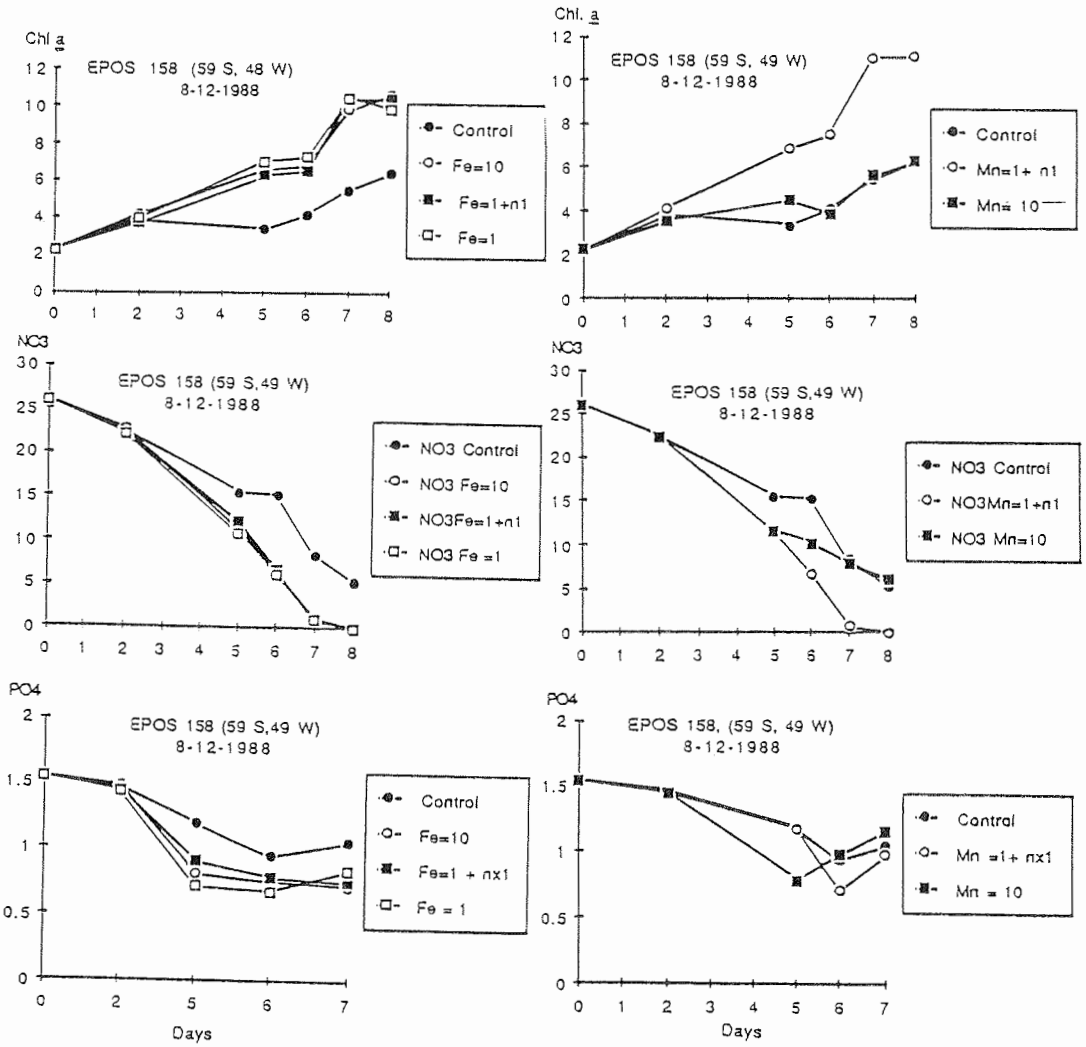

Fig. 21 Experiment III. Concentrations of chlorophyll a ($\mu g\ l^{-1}$), dissolved nitrate (μM) and phosphate (μM) versus time (days) .

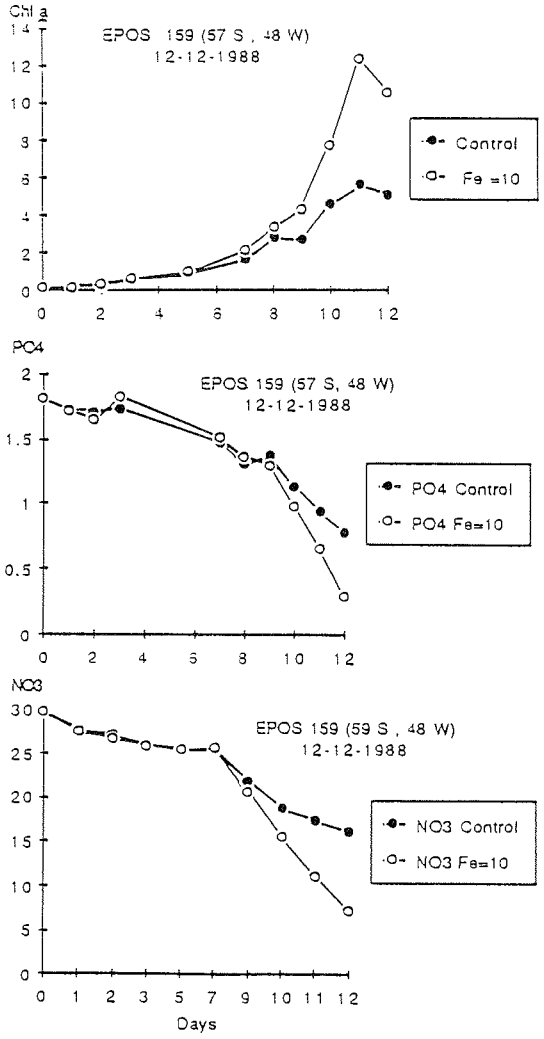

Fig. 22 Experiment IV. Concentrations of chlorophyll a (μg l^{-1}), dissolved nitrate (μM) and phosphate (μM) versus time (days) .

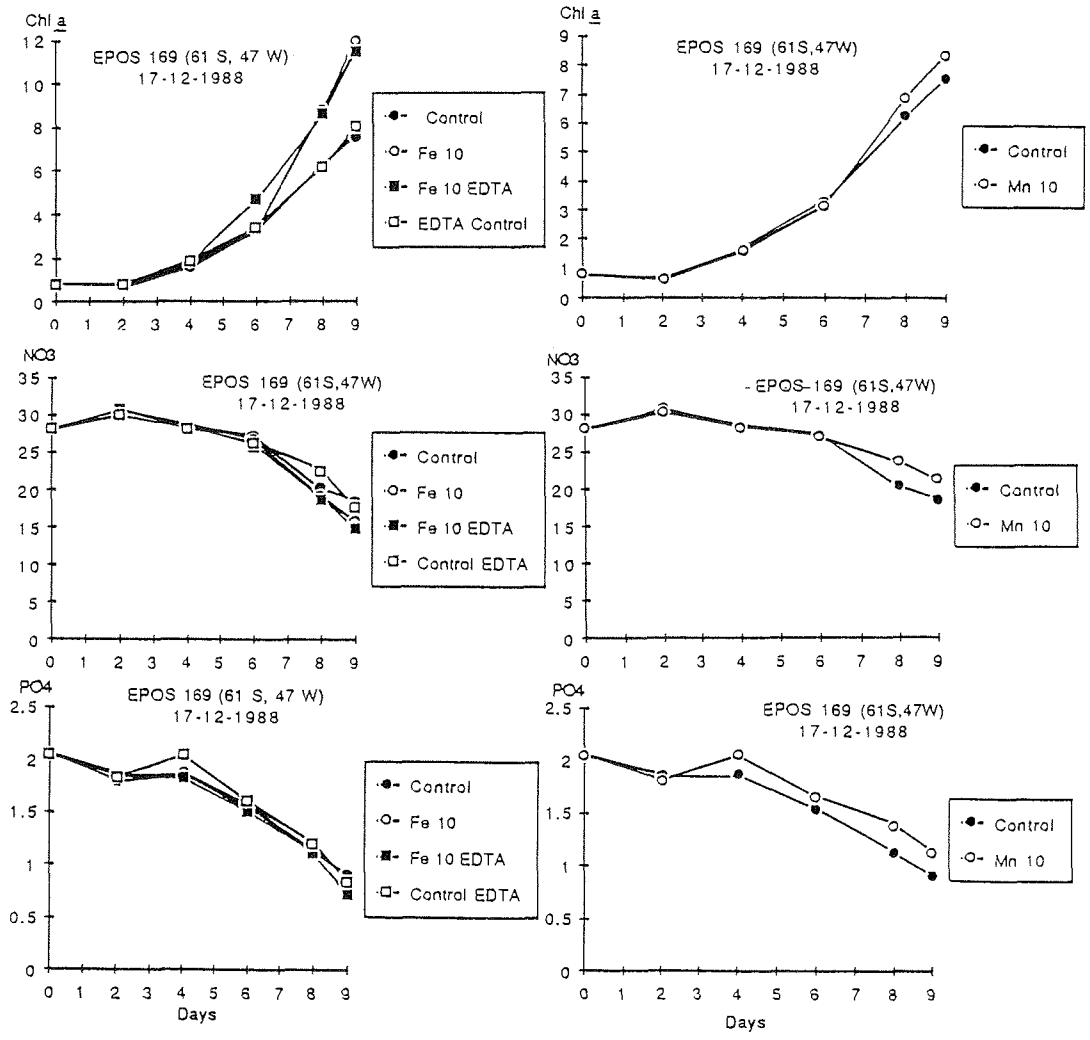

4.1.5 Barium Biogeochemistry

J. van Bennekom, F. Dehairs, L. Goeyens, M. Pamatmat, P. Treguer

Objectives

This discussion is intended to highlight the usefulness of barium as a tracer of both biological and hydrological processes. It is based on the knowledge we gathered from the Atlantic Ocean (GEOSECS campaigns) and the Southern Ocean (INDIGO 3 campaign; Indian sector of the Southern Ocean; January - February 1987).

Data for the Atlantic Ocean indicate the occurrence of a positive relationship between primary production and particulate barium in surface water. The biological control upon the barium cycle resides in the production of suspended microcrystalline (av. diam. 1 µm) barite ($BaSO_4$). This production of barite can occur intracellularly, in active plankton, and/or in microenvironments such as aggregates of biogenic detritus.

INDIGO 3 results showed that in the euphotic layer, occasional extreme particulate Ba concentrations (>1500 pM, as compared to <250 pM on average) coincided with "high" Chl a (between 1.0 and 1.2 µg/l, relative to values < 0.4 µg/l) and "low" nitrate (between 20 and 24 µM relative to concentrations between 24 and 27 µM) concentrations. At first sight this suggests active production of barite by the phytoplankton. However, the fact that particulate Ba in the euphotic layer generally correlates positively with remineralization rates, indicates that heterotrophic processes as well could control barite production in surface water.

We will be able to document both these processes of active and passive barite production in more detail from the EPOS Leg 2 data set, since the upper 100 m of the water column along the studied transects cover a wide range of Chl a concentrations (0.1 - 3 µg/l) and show local high values for ammonia (up to 3 µM; § 4.1.6) coinciding with higher bacterioplankton production (up to 0.16 µg C/l/h; § 4.2.11).

In order to check if faeces and plankton aggregates are indeed sites of barite production, fecal pellets, as collected with the Fransz net (samples provided by Fransz), and with the 30 l Niskins (samples provided by H. Gonzalez) were prepared for SEM-EMP investigation. Some sediment trap samples are also intended for total Ba analysis in order to estimate the fluxes. Furthermore, Riebesell prepared sets of decaying ice algae aggregates, which were sampled every 3 or 4 days and prepared for SEM-EMP analysis; the idea being to check a possible relationship between appearance of barite and aging of the aggregates.

Although the biologically produced barite dissolves in undersaturated seawater, dissolution is slow, which makes the barite microcrystals behave conservatively, at least relative to organic carbon. As a result, suspended barite concentrations reflect and integrate former biological activities. We documented this for the Southern Ocean during the INDIGO 3 cruise. For the region south of the Polar Front, barite content was observed to peak in the

oxygen minimum and to correlate positively with AOU in the oxygen minimum. This feature is unique for the area south of the Polar Front. There is evidence for it to be the result of
(1) advection of deep water (the NADW component) with low oxygen to the south, followed by upwelling in the Divergence area and spread out of this water to the N and NE in a shallower, sub-euphotic depth range (100 to 500 m), and
(2) consumption of this advected oxygen, due to heterotrophic activity on settling organic detritus which creates the oxygen minimum and results in the release of barite microcrystals.

The picture for the production and release of barite to the water column we hope to construct from the available data is as follows: organic matter produced in the euphotic layer provides either the crystallization site for barite or is the carrier of barite to deeper layers. Heterotrophic degradation of these organic microenvironments consumes oxygen and sets free the internal individual barite crystals. Within a limited time lapse, these crystals tend to accumulate in a fixed ratio to oxygen consumption. This picture probably applies for the World Ocean, but the coincidence of barite and oxygen minimum is typical for the Southern Ocean, due to a combination of characteristic hydrological conditions and of biological effects.

The sharply defined and relatively shallow oxygen minima (between 500 and 100 m), observed during INDIGO 3, are absent in the Scotia Sea, the Confluence and Weddell Gyre area. We expect, however, to find the subsurface barite maximum which is an ubiquitous phenomenon. Within this barite maximum layer the relationship between AOU and barium content, observed during INDIGO 3, should also hold. The expected decrease of oxygen and increase of barium in the Ba maximum layer might be detected going from the 49° to the 47° W meridian and probably also going south to north along each meridian, which means downstream of the general water flow in the area. It could be, however, that distances considered are too small to see any significant changes and also that due to the observed north/south exchange of water across the Confluence, the picture is obscured.

This biologically mediated production of barite and its subsequent dissolution in the water column controls the distribution of dissolved barium. Dissolved Ba concentrations should follow those of silicate rather closely, especially the concentration decrease in the lower part of the water column due to the influence of newly formed bottom water. We also infer this from our earlier observations indicating dissolved Ba to be a very sensitive tracer of bottom water formation along the shelf and slope in the Amery Basin area (Indian Ocean sector).

Based on the large spatial and temporal variability of Chl a and primary production we expect some variability of dissolved Ba due to translocations into the particulate phase as well.

Work at Sea

Total suspended matter (TSM)

The sampling of suspended matter for Ba and other parameters reflecting biomass (POC, PN, Si, Ca) was conducted with high resolution in the first 100 m of the water column and was frequently coupled with $^{15}NH_4$ incubation experiments for assessing organic matter remineralization rates.

TSM was sampled using 30 l-Niskin bottles mounted on the 6 mm diameter hydrowire. The seawater was filtered under pressure of filtered air, using on-line filter holders fitted directly to the bottom lids of the Niskins, to avoid loss of large particles by sedimentation. Four to eight litres were filtered on Whatman GF/F (d. 47 mm) for POC and PON determination; 6 to 24 l were filtered over Millipore membranes (HAWP; 0.45 µm pore size; Ø 47 mm) for ICP determination of Ba, Ca, Sr, Al, Si.

At meso-stations, 10 depths were sampled between surface and 500 or 1000 m (26 stations between 57° S and 62° S, along 49° and the 47° W). At time-stations, sampling was done over the whole water column (30 depths). During these stations we also filtered 500 to 1000 ml seawater through Nuclepore membranes (0.4 µm pore size; Ø 25 mm) for SEM-EMP investigation of barite association with other biogenic phases. Filters for ICP and SEM analyses were rinsed with 25 ml of deionized water for sea salt removal and dried at 50 °C. Filters for POC and PON were kept deep-frozen.

Dissolved barium

For dissolved barium 50 ml unfiltered seawater were taken, acidified to pH 1 and kept at room temperature. We sampled at the same depths as for the nutrients, including silica (from the CTD- rosette). This was done during the meso- and the time-stations. For the surface water, rosette sampling occurred with a 10 m resolution.

Preliminary results

No direct measurements of dissolved and particulate barium were done on board. Determinations will be performed in the home-based laboratory, using Inductively Coupled Plasma Optical Emission Spectroscopy (ICP-OES). For suspended matter Ca, Sr, Al, Si and POC, PN will be determined as well.

4.1.6 Distribution of Nutrients in Surface, Subsurface and Deep Layers

J. van Bennekom, M. Estrada, L. Goeyens, B. Magas, A Masson, J. Morvan, P. Tréguer, A. Svansson, C. Veth

Objectives

Due to intense upwelling of Warm Deep Water, the Weddell Gyre is among the nutrient-richest areas of the World Ocean. Huge fluxes of nutrients reaching the surface layer support the regional biological activity (Jacques and Tréguer, 1986). The macronutrients are generally considered as non-limiting factors for phytoplankton growth in Antarctic areas (although significant depletion has been reported during summer in the Atlantic sector of the Southern Ocean, and especially in the ice platelet layer under sea ice during early spring).

During EPOS Leg 2, our objective was to examine the distributions of the nutrients in five main subsystems in the Southern Ocean which are located on both sides of the Weddell Scotia Confluence (WSC): the typical ocean well mixed system of the Scotia Sea, the frontal area of the WSC, the marginal ice zone system, the under ice water layer and finally the deep water layers

.

Work at Sea

The distribution of nutrients (ammonium, nitrate + nitrite, phosphate and silicate) were studied along two sections (49°W and 47°W), going from 57°S to 62°S. We focussed on the 49°W section where two complementary transects were performed (26-29 November) and (27-30 December), completed by a so-called "Marginal Ice Zone" transect, south of 59°S (20-22 December). Surface surveys were also carried out south of and through the frontal zone. In this report we use the first transect down to 49°W (Fig. 23,24,25 and 26) as a reference situation.

It must be noted, however, that the whole water column was moving eastwards (Circumpolar Current and Weddell Gyre), and that some of the latitudinal variations observed might also result from modifications in the water mass properties due to this advection.

On 5 deep-water stations, 2 in the Powell Basin, 2 in the Scotia Sea and 1 on the saddle at 49°W, the entire water column was sampled down to 5 m from the sediment. Nutrients, dissolved Aluminium, dissolved Barium were determined at all deep stations; in the Powell Basin potential ETS activity was also measured

Preliminary Results

The Winter Water in the Weddell Sea

The characteristics of the Under Ice Water Layer (UIWL) may be taken as representative of those of Winter Water (34.35 PSU, -1.83°C), since biological activity and physical processes have not affected its initial

composition (southern part of the transect). From data of both transects and analyses of samples pumped from directly under the ice, the UIWL composition was near 31 μM $N\text{-}NO_3$ (Fig. 23), 2.1 μM $P\text{-}PO_4$ (Fig. 24) and 80 mM $Si\text{-}Si(OH)_4$ (Fig. 25); ammonium concentrations, lower than 0.3 μM $N\text{-}NH_4$, indicate a moderate biological activity beneath an ice coverage of 0.8 to 1. During the first transect (26-29.11.88) down 49°S this quite homogeneous water mass spreads northwards until only 61°S, its characteristics being modified northwards by phytoplankton uptake favoured during the ice melting (see below).

The Frontal Zone

During the first 49° W transect, a strong gradient of silicate (30 - 55 μM, Fig. 25), located near 57°45′ S, was present over about 30 miles, related to the WSC. Unlike silicate, nitrate (27 - 29 μM, Fig. 23) and phosphate (1.8 - 1.9 μM, Fig. 24) did not exhibit large variations in this area. Within the WSC area, during the first transect (26-29.11.88), distributions of all nutrients as well as those of temperature and salinity, show vertical homogeneity until 60 - 80 m.

Numerous authors have documented that the presence of the frontal area of the WSC becomes less evident eastward; in fact, the surface latitudinal gradients of both physical and chemical properties measured during our 47°W transect (not represented herein) exhibit some dilution. Nevertheless, a silicate gradient was still present: an enhancement of about 20 μM Si being observed within a distance of about 100 miles.

At the southern flank of the Confluence, the presence of a reduced nutrient area associated with a phytoplankton bloom patch, extending over 60 miles (Fig. 23, 24 and 25) was one of the main features we met during EPOS Leg 2. It may be characteristic either of a frontal zone, the phytoplankton growth and related consumption in nutrients being favoured in more stable waters at the southern flank, as compared to the more turbulent waters north of the front, or by the seasonal retreat of the MIZ which releases low salinity water and hence a stabilized shallow mixed layer, see Sullivan et al. (1988). It must be noticed that during winter the whole frontal area is covered by ice. At the beginning of EPOS Leg 2 the limit of the ice was located about 100 km south of the frontal zone. Such a distance corresponds to one or two weeks of ice retreat, which is also the time needed for a phytoplankton bloom. This leads to some confusion in determining which phenomenon (frontal stabilization or ice retreating) is predominant. As the presence of this large impoverished nutrient patch was encountered at the same position during our 3 transects along 49°W, the first hypothesis (frontal stabilization) received some support. Nevertheless, we suggest that both mechanisms might act together as they help in creating accumulation of biomass and more stable conditions at the southern border of the Confluence. Such an ecological situation will follow the same pattern as long as quiet weather remains established over the Weddell basin.

Two points must be highlighted as far as the southern flank of the WSC is concerned. First, although the impoverishment of nutrients was clearly evidenced by our data, it must be noted that both phytoplankton biomass (maximum less than 4 μg chlorophyll a/l) and consumption of nutrients

(nutrient concentrations are still over 19 µM for nitrate, 0.99 µM for phosphate and 35 - 38 µM for silicate) are moderate. This might be explained by biological limitation (grazing) and/or micronutrient limitation (§ 4.1.4). Secondly, a spectacular ammonium maximum seems to be "hanging" (Fig. 26) southwards at the base of the reduced nutrient layer; it turns out that the heterotrophic activity (Krill, bacteria, see § 4.3.3, 4.2.10 and 4.2.11) is very intense in this layer: the biological origin of ammonium is undoubted.

The Well-Mixed Surface Waters of the Scotia Sea

Although only a few stations were located within this area, the nutrient distributions encountered during EPOS Leg 2 show a very typical summer situation characterized by a surface well-mixed layer separated from the Winter Water by a well-defined pycnocline (below 60 m). This surface layer was dramatically reduced in silicate (concentrations lower than 30 µM Si during late November, decreasing by about 10 µM in the beginning of January, the corresponding concentrations of nitrate and phosphate were 25-20 µM N and 1.8-1.2 µM P). We focus on the difference in Si/N ratios for the Weddell Sea and Scotia Sea: respectively about 2.5 and 0.5. The silicate concentrations are lower in the Scotia Sea and it turns out that Si does appear as a limiting factor for diatom growth during EPOS Leg 2 (see next chapter)

The Marginal Ice Zone

As the ice is retreating southward, a moderate consumption of nutrients follows the exposure of the surface layer to increased light: in the neighbourhood of the northern limit of the ice (i.e. about 60°30´S), during the MIZ transect (20-22.12.88, not represented herein), the consumption of nitrate (taking WW as reference) reached 4 µM; it was 0.2 µM P for phosphate and 8 µM-Si for silicate. This nutrient impoverishment is associated with an increase in phytoplankton biomass (chlorophyll a rose to 1.8 µg/l).

Deep layers

The low temperatures and the low concentrations of silicic acid in the Powell Basin clearly indicated the influence of Western Weddell Sea Bottom Water in the lowermost 400 m of the water column. Both the temperature and the silicic acid concentration were lower than reported before. The intermediate maximum at about 1750 m depth due to dissolution of biogenic silica was much less pronounced than found during the AJAX expedition in February 1985. This could indicate a seasonal development of this maximum.

The Powell Basin is of special interest because the bottom water contains newly formed Weddell Sea Bottom Water, as can be seen from the decrease in silicic acid (Fig. 27) and the low temperatures below 2500 m depth. This water mass in turn is a major component of Antarctic Bottom Water, the influence of which can be felt in all oceans. At this station also, samples for determination of biogenic and mineral silica were taken, while ETS activity was measured in deep and bottom waters.

The silicic acid concentration was slightly but significantly lower than reported before, while phosphate was identical. ETS activity was detectable at all depths measured; it increased in bottom waters. This tallies with recent observations on the dissolved oxygen distribution in the Weddell Sea.

Aluminium concentrations

The concentration of dissolved Aluminium, determined on board with fluorimetry of the lumogallion complex, was low compared to that in other oceans. The lowest concentrations were found in open ocean surface waters (about 1.5 nM). Contamination of surface waters by the ship was of course clearly noticeable and rubberboat sampling was essential. Between the ice sometimes higher concentrations were found, which can be explained by the high amount of dissolved Al found in snow on ice floes. An intermediate maximum of about 2.5 nM in dissolved Al was encountered at 1000 m depth in the Scotia Sea, while the bottom water had up to 3 nM.

The Circulation of Nitrogenous Compounds Through the Ecosystem

One of the major interests of EPOS Leg 2 was centered on the transition of the ecological situation we encountered, as we went from a first period still dominated by new production to a second one, where regenerated production seemed to predominate. Examining the distribution of nitrogenous compounds may help to support this general conclusion of the cruise.

1. According to previous results, we must focus again on the fact that the whole studied area was characterized by high nitrate concentrations: in late November the concentrations ranged between 27 and 32 µM in surface waters. Only slight variations occurred during December and even in the somewhat reduced nitrate patch south of the WSC, the nitrate concentration remained higher than 19 µM. This confirms that $N\text{-}NO_3$ can certainly not be a limiting factor for phytoplankton growth in the Antarctic region.

2. The presence of high ammonium concentrations in this ecosystem: although this has been previously documented (e.g. Tréguer et al. have measured concentrations reaching 1.3 µM-N in the Scotia Sea during fall 1987, in areas dominated by nanoflagellates), the level we measured during EPOS Leg 2 was exceptionally high (reaching 3 µM-N). This is in agreement with general observations about the dominance of heterotrophic activity during the cruise.

3. A general scheme about the functioning of the Weddell-Scotia Sea ecosystem related to nitrogen circulation based on EPOS Leg 1 and Leg 2.

3.1 During winter, the biomass of phytoplankton in open water of the circumpolar ring is low, unlike that of ice algae located in the infiltration layer (between snow and ice). These algae might preferably use nitrate (and the other nutrients) provided by the sea water. The populations of both systems are mainly diatoms. As shown by previous "Polarstern" cruises, some depletion of nitrate may occur in certain conditions below the young transparent ice (but in a very shallow layer, i.e. less than 1 m depth).

Nevertheless, considering the EPOS Leg 1 and Leg 2 data it seems that the concentrations of nitrate in the WW are only slightly affected.

3.2 In early spring the melting of the ice and the retreating ice edge introduce epontic diatoms in the water column. This results in chlorophyll a concentrations up to 0.4 µg /l. Phytoplankton blooms (chlorophyll a can reach about 10 µg/l) grow in the stabilized, less saline surface layer. These blooms are located either at about 100 km north of the MIZ (according to the theory of the retreating ice edge, Smith and Nelson, 1985; Sullivan et al., 1988), and/or at the southern boundary of the frontal WSC (where primary production as high as 1 gC m^{-2} d^{-1} was measured, during EPOS Leg 1). This results in a significant reduction of nitrate, but a complete depletion seems exceptional.

Table 7: Ammonium Content in the 0-300 m Layer at the 49°W Sections

Subsystem concentration	Latitude (°S)	Date	NH_4^+ mmol N m^{-2}
North WSC	57	11.26.88	50.2
		27.12.88	46.6
South WSC	59	28.11.88	77.8
		20.12.88	188.3
		28.12.88	128.2
ice-edge/MIZ	61	29.11.88	27.7
		22.12.88	20.0
		01.01.89	27.8c

3.3 Consequently an extensive grazing activity (especially of the Krill) occurs in the different subsystems, the phytoplankton biomass is reduced to low levels, and the pressure on nitrate is dramatically reduced: within a month the "nitrate hole" located at the southern border of the WSC does not exhibit any important variation. This means the nitrogen demand is either oriented towards other nitrogen sources, and/or the nitrate losses are almost balanced by the gains of diffusion and advection. The increased heterotrophic activity results in a spectacular increase in ammonium in the whole water column. This ammonium and very likely other nitrogenous metabolites unfortunately not measured during EPOS Leg 2 might support the growth of nano-phytoplankton species (Tab. 7). During such a period, in the "impoverished patch" hanging on the southern flank of the WSC, the ammonium content decreases by 1/3. The reason why the diatoms are not able to grow in a medium so rich in nitrate (and other macronutrients) remains presently unclear.

An extensive study of the nitrogen cycle, especially during spring and summer is therefore suggested for the next Cruises.

Literature Cited

Jacques G. and Tréguer P., 1986. Les écosystemes pélagiques marins III, L'océan Austral, Masson Pub., 250 pp.

Smith W. O. and Nelson D. M. (1985). Phytoplankton bloom produced by a receding ice edge in the Ross Sea: spatial coherence with the density field. Science 227, 136 - 166.

Sullivan, C.W., G.R. McClain, J.C. Comiso, W.O. Smith, 1988, J. Geophys. Res. 93, C 10, 12487 - 12498.

Figure 23: EPOS Leg 2 - 49°W Section (26-29 Nov. 1988)
Nitrate and Nitrite in µM-N

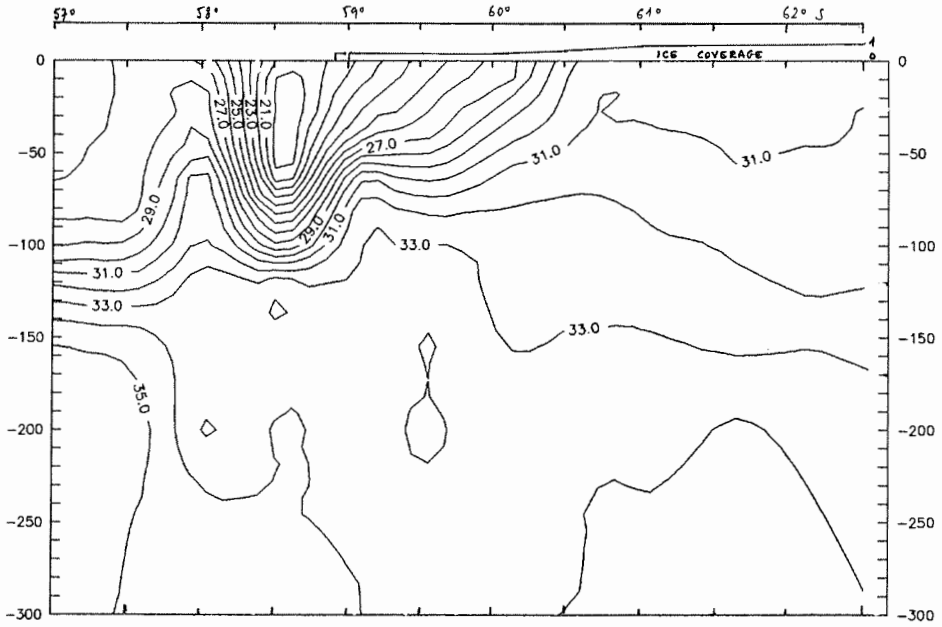

Figure 24: EPOS Leg 2 - 49°W Section (26-29 Nov. 1988)
Phosphate in µM-P

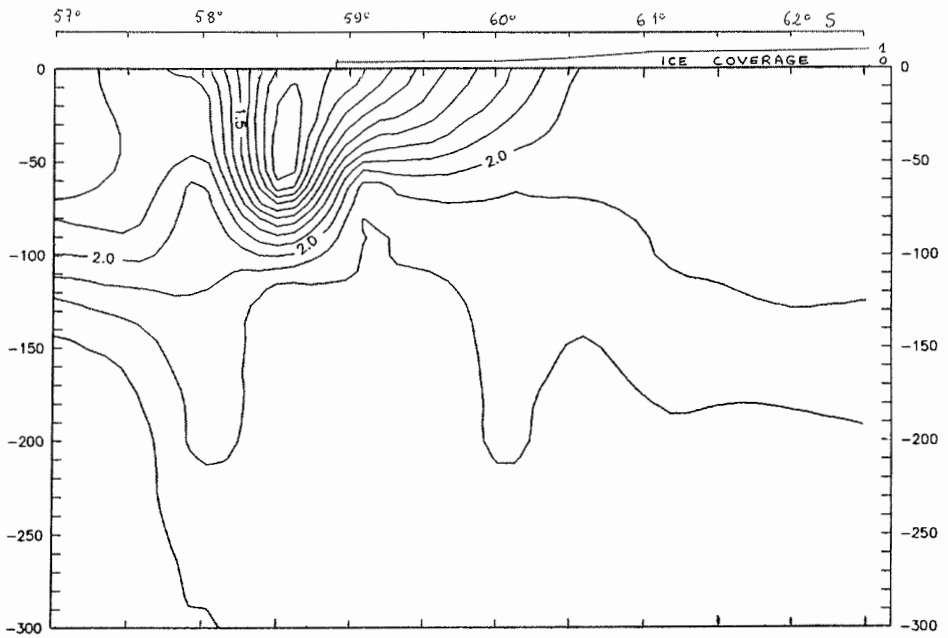

Figure 25: EPOS Leg 2 - 49°W Section (26-29 Nov. 1988)
Silicate in µM-Si

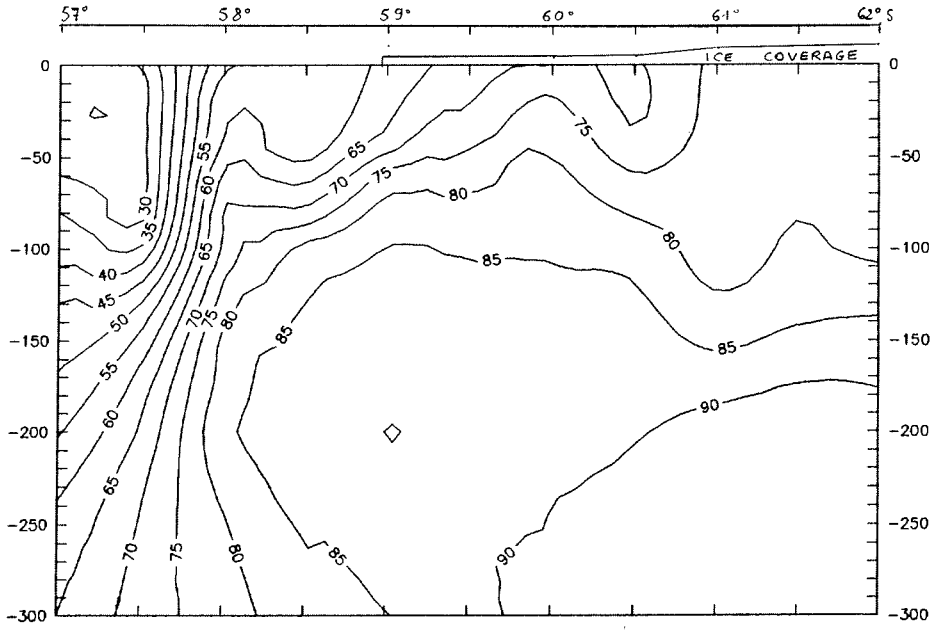

Figure 26: EPOS Leg 2 - 49°W Section (26-29 Nov. 1988)
Ammonium in µM-N

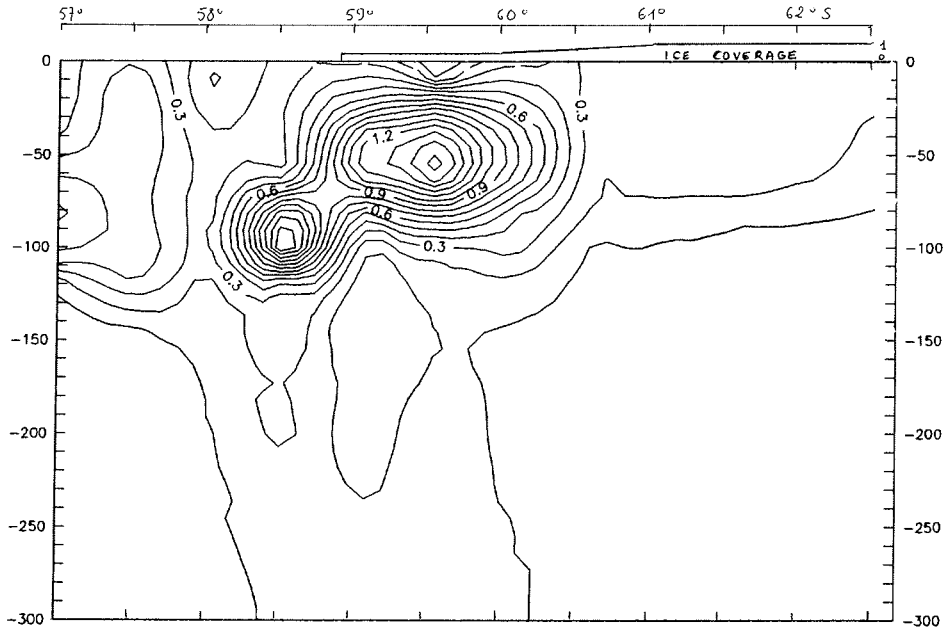

Figure 27: Vertical Profiles of NO3 and H_4SiO_4 in the deep water (mmol m^{-3})

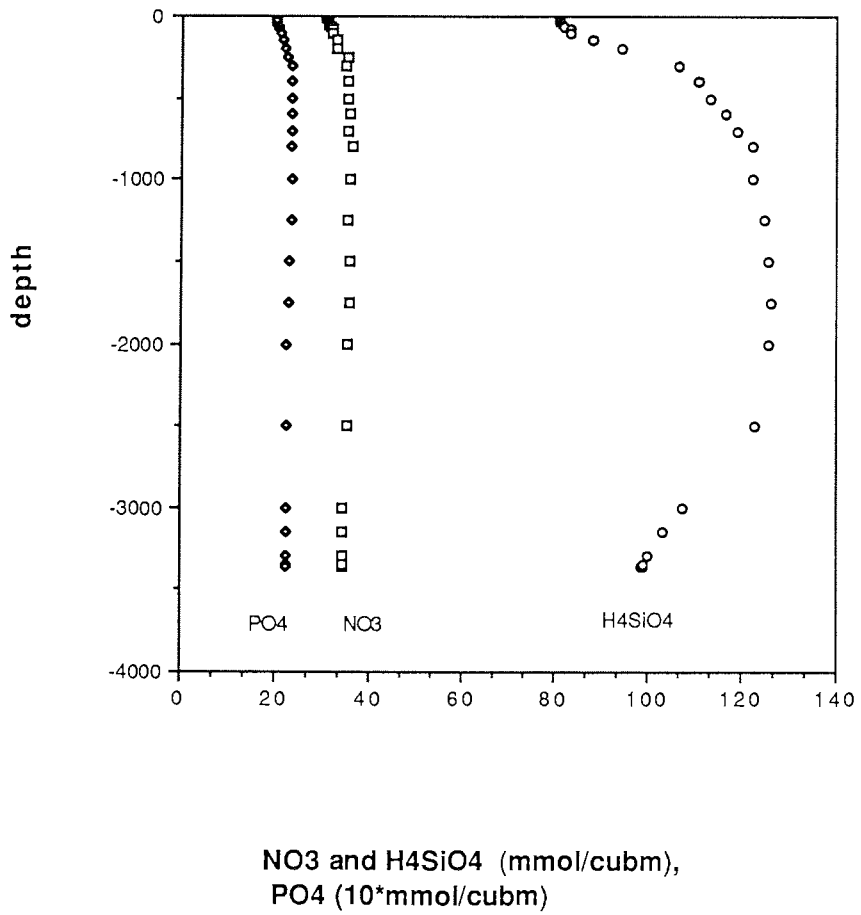

4.1.7 Uptake and Regeneration of Nitrogen, Silica and Phosphorous

J. van Bennekom, A. Buma, L. Goeyens, L. Lindner, J. Morvan, R. Nolting, M. Panouse, F. Sörensson, P. Treguer

Objectives

1. Nitrogen

The total amount of inorganic nitrogen present in the Southern Ocean is generally higher than even the winter values in temperate waters, and is not depleted during the summers. The form in which it is present may, however, play a role in determining the growth rates. Reduced nitrogen nutrients, such as ammonium or urea are less energy-demanding to utilize. If the productivity - as has been suggested - is controlled by light limitation, this can be an important factor.

The distinction between new and regenerated production can be made by applying the nitrogen uptake models of Dugdale and Goering (1967) and Eppley and Peterson (1979), which are based on the assumption that reduced nitrogen is formed within the euphotic zone, while nitrate is supplied through transport from deeper layers. Since both the ammonium levels in deeper waters and also nitrification rates in the euphotic zone are very low, this seems to be a valid model for the open Southern Ocean. This can then be used as a method to estimate the amount of the primary production that can be exported from the euphotic zone without affecting the steady-state biomass.

The purpose of the nitrogen studies during EPOS Leg 2 was to study the changes in nutrient utilization in transects across the Confluence and the edge of the melting pack ice, to see whether there was a shift in relative use of regenerated nutrients (ammonium and urea) compared to nitrate, and also to study the coupling of this to the regeneration of ammonium. The regeneration of ammonium was also used as a measure of heterotrophic activity, especially in conjunction with the barium studies. The dependency on nitrate could be supposed to increase in stations with a high biomass and production, while high production rates at the same time as high heterotrophic activity (maintaining the standing stock at low levels) would mean a rapid turnover of ammonium. There is not always a balance between the uptake and regeneration of ammonium, as is shown by the repeated findings of high ammonium levels in subsurface waters (50-100 m) of the Confluence area. In most marine (supposedly nitrogen-limited) euphotic plankton communities, the ammonium concentration is kept at a few tenths of a micromole per liter or lower.

2. Silica uptake using a stable isotope ^{30}Si

Although a major part of the silicon cycle is controlled by processes occurring in the Southern Ocean, measurements of the production and dissolution of biogenic silica by diatoms in this area are scarce (e.g. Nelson and Gordon, 1982; Nelson and Smith, 1986). These data have been determined by experiments with enriched stable isotopes (^{29}Si or ^{30}Si), the

change in the isotopic composition of suspended matter collected by filtration measured afterwards by mass spectrometry (see Nelson and Gordon, 1982 for details about the technique used). Within a bloom patch associated with the seasonal retreat of the MIZ in the Ross Sea, Si-uptake ranged between 7 to 93 μmol m^{-2} d^{-1}, unlike the situation described during summer in the Pacific sector where lower Si-uptake was measured (0.9 to 6.8 μmol m^{-2} d^{-1}).

3. Silica and phosphorous uptake using the radio-nuclide ^{32}Si

This technique was employed here for the first time in marine research. A few weeks before the start of EPOS Leg 2 it turned out that L. Lindner could make available a small stock of ^{32}Si and was able to take part in the cruise.

^{32}Si is a weak beta-emitter (E(max) = 0.2 MeV) with an as yet much disputed half-life (140 ± 30 years). It is the parent of ^{32}P, itself a strong beta-emitter (E(max) = 1.7 MeV, $t_{1/2}$ = 14.2 days). In secular equilibrium, the parent and daughter activities are equal to each other. Because of its strong beta emissions, ^{32}P can be readily radio-assayed (50% efficiency) in aqueous solutions by means of its Cerenkov radiation, thus without the use of scintillator cocktails. The Cerenkov spectrum of ^{32}P is by chance very similar to that of an unquenched liquid scintillation spectrum of ^{3}H. The beta emissions of ^{32}Si itself are too weak to generate Cerenkov radiation. In practice during EPOS Leg 2 , all ^{32}Si samples were measured in aqueous media by Cerenkov counting of daughter ^{32}P, whereas deduction of the equilibrium value of ^{32}Si at infinity was achieved by analysis of the activity vs time plot.

Initial readings of ^{32}P, usually in disequilibrium in the various types of samples measured, yielded valuable information regarding ^{32}P-phosphate in the systems under investigation. It should be noted that nascent ^{32}P from radioactive decay of ^{32}Si in aqueous silicate solutions, ends up as ^{32}P-phosphate as was shown recently by research conducted in NIKHEF - Amsterdam.

Apart from its elegance and high efficiency, an important additional consideration for using the technique of Cerenkov counting has been the possibility of re-using aqueous waste solutions from ^{32}Si-uptake experiments.

4. Silica dissolution

The dissolution rate of biogenic silica plays a key role in the silica paradox of the Southern Ocean. Two different factors counteract each other: the dissolution rate decreases with temperature, but increases when the content of Al is low. Using the cultures from various uptake experiments, dissolution rates were followed subsequently in subsamples with and without added Al.

Work at sea

1. Nitrogen

Uptake rates were studied by incubation experiments with additions of ^{15}N-labelled nutrients, ammonium, nitrate and urea (Rönner et al., 1983). The regeneration rates were determined with ^{15}N-isotope dilution techniques (Goeyens et al., 1987; Selmer and Sörensson, 1986). The ^{15}N content of the samples will be analyzed by emission spectrometry on return to the labs in Göteborg and Brussels, and no results on uptake or regeneration can therefore be presented here.

To elucidate whether the uptake systems are saturated at the ambient nutrient levels, the uptake rates at a series of concentrations have been performed for both ammonium and urea. The effect of high concentrations of ammonium on the uptake of nitrate have also been studied. In some experiments, the difference between uptake and incorporation of nitrogen into cellular components has been investigated by studying the uptake of nutrients into both whole particulate material and into proteins.

The nitrogen studies were centered on the euphotic zone, except for some of the regeneration experiments, carried out on water from greater depths. For some of these, nitrification rates and changes in oxygen concentration were also determined, the latter in cooperation with M. Pamatmat. Production of ammonium during the mineralization process was also monitored in bacterioplankton cultures set up by Kuparinen and Björnsen.

2. Si-uptake Using Stable Isotope Method

During EPOS Leg 2 , 69 samples (fifteen stations, Tab. 8) enriched with ^{30}Si were incubated on deck (simulated in-situ device: flasks wrapped with neutral screens, natural light, temperature fixed by running seawater). They will be analyzed in the course of 1989 by P. Treguer and B. Queguiner (LCEM, IEM, Brest) at Corvallis, in cooperation with D. Nelson (CO, OSV, USA).

Table 8: Si, P and C Uptakes: Stations

Station No.	Date	Location		Level (% incident light)
156	04.12.88	61°S	49°W	100/10/1
157	07.12.88	58°57S	48°W	100/50/25/10/3/1/0.1
158	09.12.88	59°24S	48°43W	100/25/10/3/1/0.1
159	12.12.88	56°59S	48°23W	100/25/10/3/1/0.1
169	17.12.88	61°31S	46°52W	100/25/10/3/1/0.1
172	20.12.88	59°00S	48°59W	100/25/10/3/1/0.1
173	20.12.88	59°29S	49°W	100
174	21.12.88	60°S	49°W	100/25/10/3/1/0.1
175	21.12.88	60°30S	49°W	100
176	22.12.88	61°S	49°W	100/25/10/3/1/0.1
177	22.12.88	81°30S	49°W	100
178	23.12.88	61°30S	49°W	100/25/10/3/1/0.1
188	29.12.88	59°S	49°W	100/25/10/3/1/0.1
205	03.01.89	57°15S	48°10W	100/25/10/3/1/0.1
207	04.01.89	57°26S	48°35W	100 (kinetics of uptake

3. Silica uptake using the radio-nuclide ^{32} Si.

Different types of experiments were carried out with ^{32}Si on board "Polarstern". The first one mentioned - uptake - constitutes the main effort; the other ones should be viewed as demonstration projects.

i) ^{32}Si-silicate uptake from ocean waters by diatoms (and silico-flagellates)

ii) Labelling of diatoms with ^{32}Si in light specific activity by growing cultures in the waste-water of the uptake studies

iii) A time study of the influence of iron, as a trace metal, on the uptake of silicate by phytoplankton.

iv) Feeding of Krill with cultures from ii) subsequently following the uptake and excretion of ^{32}Si, and its distribution in Krill tissue.

In parallel with the stable isotope incubations, the ^{32}Si and ^{14}C uptake were measured at sixteen stations. Since ^{32}Si ($t_{1/2}$= 140±30y) decays by β^- emission (0.2 Mev) to ^{32}P, itself a β^- emitter, phosphate uptake could also be traced. Concentrations of silicate and phosphate in samples to be incubated were measured directly. Filtrations (of 1 l on 0.4 µm Nuclepore membranes) for later determination of biogenic silica and particulate phosphorus were also carried out. Si uptake was also measured using a diatom culture under different environmental conditions (exp. VI, see de Baar et al.). A kinetics experiment was carried out at Sta. 202 in parallel with N and C uptake measurements

4. Dissolution of Biogenic Silica.

At 16 stations, samples were incubated with stable isotopes to study dissolution of biogenic silica following uptake. ^{32}Si was incorporated into biogenic silica of a growing diatom culture. After filtration, careful washing and resuspension in sea water, there was an increase in radioactivity in solution.

Preliminary Results

1. Nitrogen

As mentioned above, the samples will be analysed in the home lab and hence no results can be presented here.

2. and 3. Silica and Phosphorous uptake rates

The present data indicate fluxes ranging between 3 and 14 µmol-Si m^{-2} d^{-1}, i.e. moderate Si uptake as compared with previous results for the Antarctic spring (see above). This is consistent with the general idea that during EPOS Leg 2 the phytoplankton activity was not dominated by diatoms. In the various stations, C uptake ranged from 24 - 106 µmol m^{-2} d^{-1} and P uptake from 0.14 - 0.84 µmol m^{-2} d^{-1}.

4. Silica dissolution rates

The role of Al was investigated in natural as well as in cultured diatoms. The conclusions of previous work carried out in the Southern Ocean that the Al/Si ratios in the water column are very low was confirmed. To test the hypothesis that these low ratios cause a high dissolution rate of biogenic silica, net samples were taken in areas with abundant diatoms. At 3 stations (marginal ice zone; Scotia Sea and Signy shelf) water from the surface mixed layer was incubated under clean conditions (see chapter by Buma et al.), untreated and with addition of 100 nM of Al.

In all cases diatoms grew well after a lag time of about 5 days. After 12 to 14 days one of the nutrient elements was nearly totally depleted; Si for the Scotia Sea culture and N for the others. This tallies with the nutrient ratios in the different water masses; the Si/N ratio being much higher in the Weddell Sea water than in the Scotia Sea water north of the Confluence.

In order to increase the harvest of biogenic silica grown in waters with different Al/Si ratios, deep-sea water was added until 30-50 mg SiO_2 was produced. In the course of the experiment, the phytoplankton community changed in composition: especially small *Chaetoceros* species grew to higher abundance, but there was no significant difference between the culture with Al and the control.

Dissolved Al steadily decreased in the cultures with added Al. As far as preliminary conclusions could be drawn on board, culturing of Antarctic diatoms with enhanced Al seems possible; the influence on the dissolution rate and solubility of the biogenic silica will be studied on shore.

Literature Cited

Dugdale, R.C., Goering, J.J., 1967. Uptake of new and regenerated forms of nitrogen in primary productivity. Limn. Oceanogr. 12:196-206.

Eppley, R.W., Peterson, B.J., 1979. Particulate organic matter flux and planktonic new production in the deep ocean. Nature 282:677-680.

Goeyens, L., de Vries, R.T.P., Bakker, J.F., Helder, W., 1987. An experiment on the relative importance of denitrification, nitrate reduction and ammonification in coastal marine sediment. Netherlands J. Sea Res. 21:171-175.

Nelson D.M. and Gordon L.I., 1982. Production and pelagic dissolution of biogenic silica in the Southern Ocean. Geochim. Cosmochim. Acta 46: 491-501

Nelson D.M. and Smith W.O., 1986. Phytoplankton bloom dynamics of the western Ross Sea ice-edge. II. Mesoscale cycling of nitrogen and silicon. Deep-Sea Res. 33: 1389-1412

Rönner, U., Sörensson, F., Holm-Hansen, O., 1983. Nitrogen assimilation by phytoplankton in the Scotia Sea. Polar Biology 2:137-147.

Selmer, J.-S., Sörensson, F., 1986. New procedure for extraction of ammonium from natural waters for ^{15}N isotopic ration determinations. Appl. Environm. Microbiol. 52:577-579

4.2 PHYTOPLANKTON, PROTOZOOPLANKTON AND BACTERIOPLANKTON

4.2.1 Phytoplankton Biomass Distribution

G. Jacques, M. Panouse

Objectives

The interaction between water column chemistry and biology as influenced by physical factors such as mixed layer depth and sea ice was studied in some of the major sub-systems of the Antarctic Ocean: the open water of the Scotia Sea, the frontal zone of the Weddell-Scotia Confluence, the marginal ice zone and, partly, the pack-ice.

Recent reviews of the Antarctic aquatic ecosystems (Fogg, 1977; El-Sayed, 1984; Jacques and Tréguer, 1986; Priddle *et al.*, 1986; Tréguer and Jacques, 1986) clearly state that primary production in the Antarctic is low. Against this background, mean biomass of the area studied has to be considered as high. This is not really surprising, as the idea of great richness of the Antarctic Ocean, accepted in the seventies, rests first on the observation of blooms in the areas frequently visited by ships supplying the Antarctic bases, such as the Drake Passage, the approaches to the Antarctic Peninsula, the coastal regions, and the ice-edge. At the beginning of the austral summer, the usual season of these missions, these areas are often the site of noteworthy blooms, either in ice (epontic algae) or in open water.

Work at Sea

About 1200 measurements of chlorophylls *a*, *b*, *c* and their corresponding pheophytins were carried out during EPOS Leg 2:

- 450 as routine measurements at each station.
- 400 devoted to the sized fraction study.
- 280 at the request of other scientists (mainly for the trace metals enrichment experiments).
- 40 for methodological comparisons.

The measurements were carried out according to the following procedure:

- filtration of 300 ml on Whatman GF/F® membrane filter (47 mm).
- manual destruction of the filter with a glass rod.
- extraction at 5°C in 90% acetone with a duration of at least 2 hours.
- centrifugation for 7 min at 5°C and 200 rpm.
- measurement of the extract on an Aminco-Bowman® spectrofluorometer, following Neveux and Panouse (1987) at six sets of wavelengths: 432-667 nm, 412-669 nm, 430-718 nm, 437-655,5 nm, 463-652 nm, 451.5-633 nm.
- calibration by comparison with a pigment standard embedded in metacrylate.

During the cruise, some methodological tests were conducted. We must emphasize that, most of the time, a dominance of nano- and pico-plankton was observed; this has a bearing on interpretation of the preliminary results:

1) In most cases, the GF/C filters, used during EPOS Leg 1, yielded higher chlorophyll values than the GF/F filters, used routinely during EPOS Leg 2, with values 5% higher on average. We tentatively ascribe this difference to the more difficult extraction of pigments from GF/F filters where the very small cells are sequestered in the deeper structure of the filter.

2) In all cases, the 0.2 µm polycarbonate Nuclepore® filters yielded much higher values than the above mentioned fibreglass filters: as an example, +15% compared to GF/F. With regard to efficiency, this therefore is the filter of choice. Unfortunately, its high price and slow filtration rate are two obstacles.

3) Various tests were carried out in order to compare the two extraction methods used on board. The manual extraction method as applied to the routine samples was compared with the grinding technique (Derenbach 1969) utilized by the AWI research group. The latter technique has the advantage of allowing an immediate measurement and moreover, it has a better performance. For the kind of plankton encountered during EPOS Leg 2, the latter extraction method leads to final values which, on average, are 15 % higher.

4) Various comparisons were also conducted between two methods for fluorescence measurements: the above mentioned spectrofluorometric technique versus the fluorometric technique using a Turner Design® model 10, calibrated with the spectrophotometric method. For chlorophyll values in the higher range (> 3 mg m^{-3}), the latter method provides results which are 20 to 30% higher. Further comparative tests will be executed in the laboratory in order to investigate the reason for this divergence.

Spatial distribution along the first Transect

Fig. 28 reveals the following patterns:

- Low values in the Scotia Sea (< 0.3 mg m^{-3}). The major part of this biomass (30 -70%) was due to large diatoms (§ 4.2.2).
- Low values at the ice-edge and into the pack (<0.6 mg m^{-3}) ·
- A large bloom area with values reaching 4.5 mg m^{-3} in between; the bloom was spread over an area more than 50 miles wide, and comprised mainly large phytoplankters. At Sta. 146 and 147, in the heart of this bloom, more than 80% of the biomass was contributed by cells greater than 10 µm.

We can not determine yet whether this large diatom bloom was linked to the meandering Confluence or to a marginal ice zone effect. Numerous papers have shown that blooms are generally observed on shallow mixed layers formed by addition of melt water from the retreating ice-edge. The variability of the vertical profiles in the northern border of the Confluence area (Sta. 159 in the Scotia Sea), due to physical factors in a frontal zone, contrast with the clear surface maximum, found in the open Weddell Sea (Stat 158).

Evolution with Time

The short-term variations observed during time stations will not be dealt with here. The interpretation of the long term evolution needs a knowledge of the main features of this kind of variation. For example, in the northern part of the Weddell-Scotia frontal zone, we can observe evident short term variations in the physical structure, and hence in the profiles of biological parameters. In contrast, in the open ocean waters of the Weddell Sea, chlorophyll profiles generally show little change (Fig. 29).

Scotia Sea
Each short time investigation in the Scotia Sea confirmed the dominance of diatoms and showed a regular increase of the mean biomass: 0.8 mg Chl a m^{-3} at the beginning of the third transect and 1.0 to 1.5 just in the beginning of January. At this time, most of the diatoms were not healthy; is it an indication for a next shift of the community towards a more heterotrophic system such as in the Weddell Sea?

Weddell Sea
The association between a high level of biomass and large diatoms was no longer recorded later during the cruise. Very probably, this kind of community expands at the beginning of the spring, and these blooms are the starting point of the flux of organic matter and silica towards the deep waters and the sediment. The time station 157 (Fig. 31), where, in a few hours, most of the plankton biomass was grazed by the Krill, strikingly shows the evolution of the system at the time of change from spring to summer.

The Krill clearly appears as the key component of the ecosystem in the western Weddell Sea and its surroundings. The trophic web seems to topple from the classical cycle based principally on new production with a large fraction of the organic matter produced by large diatoms (exported into the deep water through their rapid sinking or by the way of faeces) towards the microbial loop which is a weak exporter of organic matter. Some vertical profiles of chlorophyll clearly underline that evolution (Fig. 30). By the way, during the second transect, the maxima of biomass (between 0.8 and 1.1 mgChl a m^{-3}) decreased and were, at a more than 90% level, due to particles smaller than 10 µm. We observed (Fig. 28) the southward shift of the rich chlorophyll area; this observation may reinforce the hypothesis of a MIZ effect.

Marginal Ice Zone (MIZ)

An optimistic view would be to consider that the melting of the pack-ice is accompanied by a bloom over the 20 million km^2 that it sweeps across. The observations done during the EPOS Leg 2 point to a more realistic point of view: the diatom bloom seems to be limited to the period when the ice breaks up at the beginning of spring. After that, the receding ice-edge is clearly a chlorophyll-poor area. The supply of algae from the pack-ice, which some time after melting can represent a significant part of the biomass (El-Sayed and Taguchi, 1981; Smith and Nelson, 1985), does not raise the Chl a concentrations in the water column towards an high level.

Recent studies show that the "macro" pathway is preponderant whenever the total primary production is high (blooms), and the "micro" pathway is preponderant in situations where plankton is scarce. But continuous surface monitoring operations have shown that the Antarctic Ocean does not violate the rule, which is becoming more and more evident, of high variability of structures in space and time. Also, as Platt and Harrison (1985) predicted, we should expect that each province of the Southern Ocean can occupy, at a given time, in a given place, at a given depth, any position at all in the range extending from extreme oligotrophy to eutrophy. This view is much more realistic than one which definitively classifies a given oceanic region as either eutrophic or oligotrophic.

Literature Cited

Derenbach, J. 1969. Zur Homogenisation des Phytoplanktons für die Chlorophyllbestimmung. Kieler Meeresforsch. 25: 166-171.

El-Sayed S. Z., 1984. Productivity of the Antarctic waters - A reappraisal. *In* Marine Phytoplankton and Productivity. Edited by O. Holm-Hansen, L. Bolis, R. Gilles, Springer-Verlag, Berlin, 19-34.

El-Sayed, S. Z., Taguchi, S., 1981. Primary production and standing crop of phytoplankton along the ice-edge in the Weddell Sea. *Deep-Sea Res.*, 28: 1017-1032.

Fogg G.E., 1977. Aquatic primary production in the Antarctic. *Philosophical Trans. R. Soc. Lond.*, B, 279: 27-38.

Jacques, G., Treguer, P., 1986. L' Océan Antarctique. *In* Ecosystèmes Pélagiques Marins. Edited by G. Jacques and P. Tréguer, Masson, Coll. Ecologie 19, 101-162.

Neveux, J., Panouse, M., 1987. Spectrofluorometric determination of chlorophylls and pheophytins. *Arch. fur Hydrobiol.*, 109: 567-581.

Platt, T., Harrison, W. G., 1985. Biogenic fluxes of carbon and oxygen in the ocean. *Nature*, 318: 55-58.

Priddle, J.,Hawes, I., Ellis-Evans, J.C., 1986. Antarctic aquatic ecosystems as habitats for phytoplankton. *Biol. Rev* ., 61: 199-238.

Smith, W. O., Nelson, D.M., 1985. Phytoplankton bloom produced by a receding ice edge in the Ross Sea: spatial coherence with the density field. *Science*, 227: 163-166.

Treguer, P., Jacques, G., 1986. L'océan Antarctique. *La Recherche*, 178: 746-755.

Fig. 28 - Chl a distribution from 57°S to 62°S
- during the first 49°W transect (26 to 30.11.88, a)
- during the third 49°W transect (27 to 31.12.88, b)

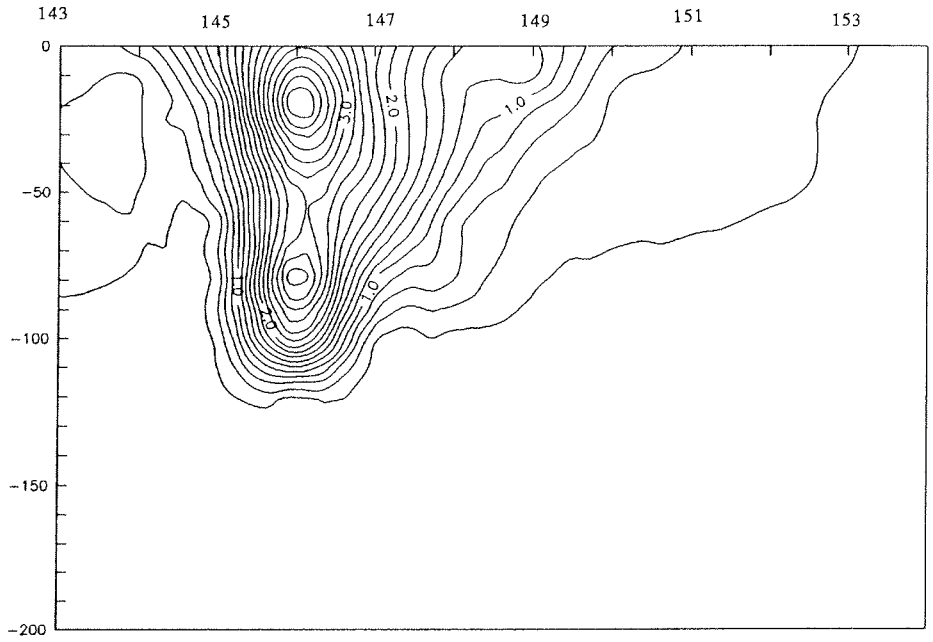

CHLOROPHYLL A SECTION FROM STATION 143 TO 154

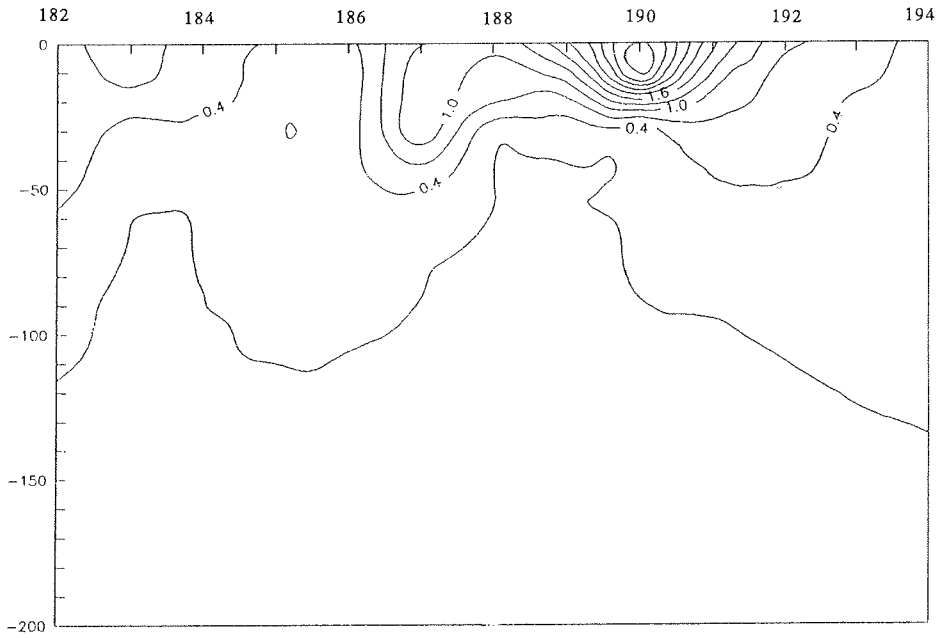

CHLOROPHYLL A SECTION FROM STATION 182 TO 194

Fig. 29 - Comparative short-term variations of the vertical distribution of Chl a (mg m^{-3}) observed during two time stations.

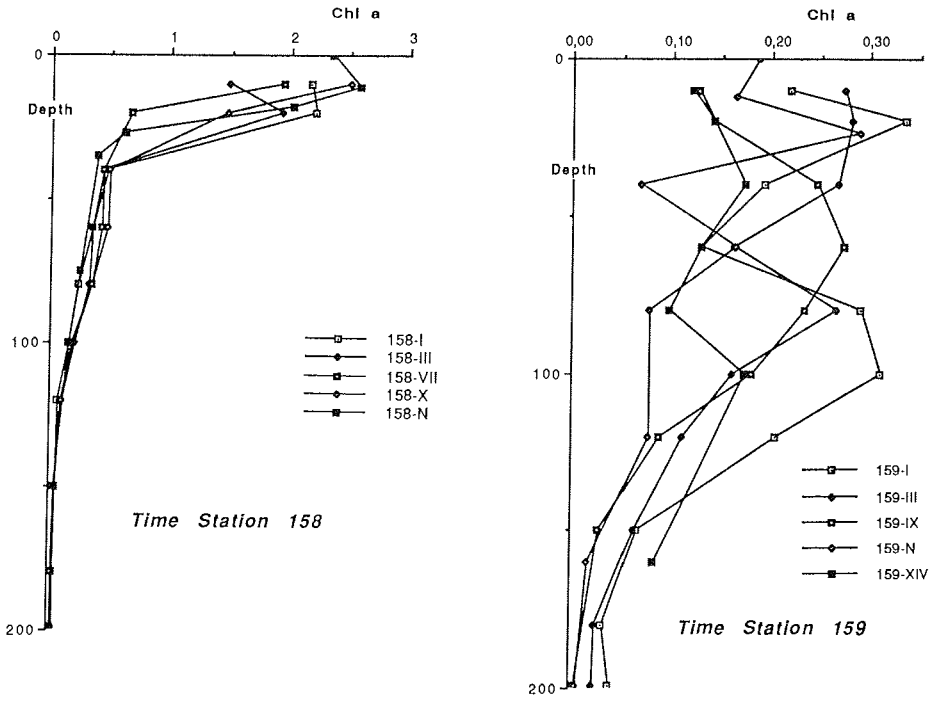

Fig. 31 - Three-dimensional evolution of a diatom bloom at the time station 157 in the Weddell Sea.In a few hours, a Krill swarm, located in the subsurface layer, grazed down the diatom bloom

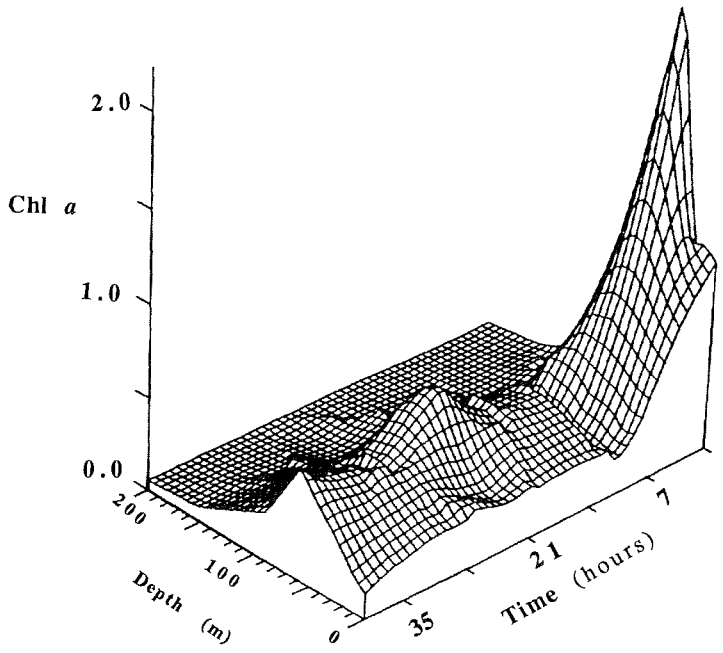

Fig. 30 - Caricatured features of the Chl a (mg m^{-3}) distribution at the Sta.146: 27-11-88) and at the beginning of the summer (Sta. 190: 29-12-88) in the open Weddell Sea.
If the maximal amounts of Chl a can be compared, the integrated value 0 - 100 m completely differs: 203 mg Chl a m^{-2} at station 146 but only 74 mg Chl a m^{-2} at station 190. In the same area (59°S - 60°S), the food web shifted from a diatom bloom within the whole euphotic layer towards a flagellate-dominated system in which heterotrophs were important.

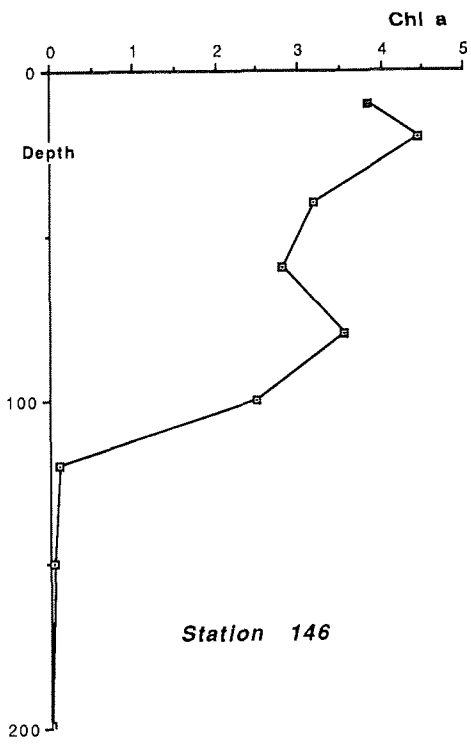

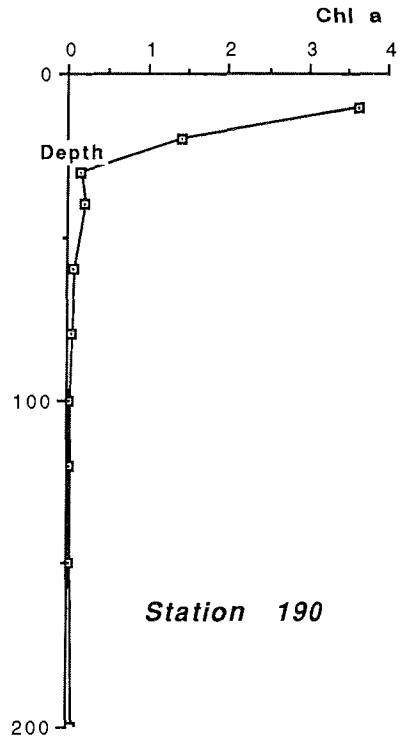

4.2.2 Phytoplankton - Size Fractionation

M. Eckernkemper, G. Jacques, M. Panouse,

Objectives

As in other areas, both types of pelagic system (those based on new and regenerated production) have been encountered in the Antarctic Ocean. Some data suggest that they succeed each other rapidly, being controlled by the depletion of nitrate in the mixed layer. Directly, this pelagic succession emphasizes the problem of the real abundance of the nano- and pico-phytoplankton and of its relationship with the ciliates, that is to say the significance and the pathway of the so-called "microbial loop". Effectively, starting with the paper of Bröckel (1981), the question of the relative importance of the smallest forms within the pelagic Antarctic ecosystem has been hardly discussed; recent papers bring increased recognition of the regeneration community as an important pathway also in Antarctic waters. Hewes *et al.*, (1985) assert, as Brandini and Kutner (1987), that a large percentage (>50%) of total chlorophyll found in waters surrounding Antarctica is contained in the pico- and nano-plankton size fractions (<20µm). Does this information require that we revise the classical concept of the Antarctic diatom-Krill food chain to one which incorporates the feeding by Krill on many large-volume particles (protozoans as well as diatoms) with protozoans acting as a link which couples pico- and nano-plankton production to higher trophic levels? A recent review (Weber and El-Sayed, 1985) confirms that large particles would be retained with maximum efficiency by Krill and that for particles < 6 µm, retention drops off rapidly.

Work at Sea

We chose to study the smallest phytoplankters by three convergent ways:

- The pigment composition of different size fractions, filtering replicates on different Nuclepore® membrane filters of 10 µm, 3µm and 1 µm pore-size compared with the classical glass-fiber Whatman® GF/F used routinely during the cruise. Due to the regular dominance of smallest forms, filtration on 0.2 µm Nuclepore filter was added beginning with station 156.

- P/I curves of size-fractionated phytoplankton communities. For this purpose, according to the technique described by Sheldon and Rassoulzadegan (1987), three fractions were separated through gentle filtration of natural samples on Nuclepore® membrane filters:< 10 µm, < 3 µm and < 1 µm. From these fractions, subsamples were taken for PI curves by means of ^{14}C uptake experiments (and also, for Chl a measurements). Fifty µCi of $NaH^{14}CO_3$ were added to each 25 ml subsample. The incubation was run for 3 hours in an artificial light incubator, at 7 levels of irradiance, ranging from 0.2 to 750 µE m^{-2} s^{-1}. The temperature was kept as close as possible (within 1.2 °C) to the *in situ* temperature by means of a cooling unit. After filtration through Whatman® GF/F, the filters were counted in a Beckman® LS 1800 scintillation counter.

- Flow cytometry has been quite recently applied to the study of marine organisms (Yentsch *et al.*, 1983). The apparatus used (ACR 1000 ODAM®), equipped with a high-pressure mercury lamp, provides, for each particle passing through the light beam, two physical parameters (the mean diameter and the surface properties) and two autofluorescences from photosynthetic pigments (the chlorophyll a red fluorescence and the phycoerythrin orange fluorescence). These pigments are specific to Cyanobacteria (Marchant *et al.*, 1987) and Cryptophyceans occurring in the Antarctic waters. This complete set of analyses was carried out at each station starting from the second north-south transect, both on natural sea-water and on a concentrated centrifugate.

Preliminary Results

Size-Class Distribution during the N-S Transects

The stations situated in the Scotia Sea are characterized by low biomasses, which are mainly (for 30 to 70%) due to diatoms with sizes greater than 10 µm.The only exception was found at the beginning of the third transect with biomasses reaching 0.8 mg Chl a m^{-3}. Each passage through such a purely oceanic area confirmed this typical feature.

But the most interesting fact concerns the productive area south of the Weddell-Scotia Confluence, some 80 nautical miles away from the pack-ice. During the first transect, the bloom (between 1 and more than 4 mg Chl a m^{-3}) was spread over a vast area more than 50 miles wide, and it was mainly due to large phytoplankters (Fig. 32 and 33). At Sta. 146 and 147, right in the heart of this bloom, more than 80% of the biomass was provided by cells greater than 10 µm.

In the whole area between this rich core and the pack, and particularly near the ice-edge, the picture is reversed, with a very low biomass and a dominance of nano- and pico-plankton: between 30 and 50% of this biomass lies in the range of 3 to 10 µm. This confirms the recorded predominance of Cryptophyceans along with small diatoms, the lack of Chl b excluding the Chlorophyceans; one must keep in mind that *Nitzschia nana*, *Chaetoceros neglectus* and *C. tortissimum* smaller than 10 µm are often the dominant species of the Antarctic marine ecosystem (Hewes *et al.*, 1985; Brandini and Kutner, 1987).

If large diatoms represent the bulk of the biomass in the Scotia Sea (Sts 143 and 160), the chlorophyll-rich area of the Weddell Sea develops from a microplankton-rich bloom (first section) to a nanoplanktonic dominated community (second section) in the whole area south of Confluence.

Evolution of the Ecosystem

The association between a high level of biomass and large diatoms was no longer recorded later during the cruise. Very probably, this kind of community expands at the beginning of the spring, and these blooms are the starting point of the flux of organic matter and silica towards the deep waters and the sediment.

The time station 157, where, in a few hours, most of the planktonic biomass seems to have been grazed by the Krill, shows the evolution of the system at the time of change from spring to summer (Tab. 9).

Tab. 9: Changes in Chl content and size fractionation of the phytoplankton, 10 hours apart, at 10 m depth at Station 157

	Chl a amount	% Chl a > 10µm
Cast 157-I	2.4 mg m^{-3}	70%
Cast 157-N	0.5 mg m^{-3}	30%

The Krill clearly appears as the key component of the ecosystem in the Weddell Sea and its surroundings. The trophic web seems to topple from the classical cycle based principally on new production with a large fraction of the organic matter produced by large diatoms (exported to deep water through rapid sinking or by the way of fecal pellets), towards the microbial loop which is a weak exporter of organic matter. By the way, during the second transect, the maxima of biomass (between 0.8 and 1.1 mg Chl a m^{-3}) drop down and are, at a more than 90% level, due to particles smaller than 10 µm in size.

Production of the Different Size Classes

The data have been only partly processed, and the following results are subject to further developments. For example, the determination by visual means of I_k, considered as an index of the photo-adaptation, only can lead to strongly erroneous results. Therefore, we will await more data processing before proceeding in the analysis of the part played by size fractions in the overall primary production of the phytoplankton.

A quick look at the results obtained so far shows that the amounts of biomass encountered in the original samples cover a wide range, between 2.6 mg Chl a m^{-3} (Station 158) and 0.2 mg Chl a m^{-3} (Station 186). Meanwhile the biomasses recorded in the three fractions (F 10 = < 10 µm; F 3 = < 3 µm; F 1 = < 1µm) also vary largely, with an average decreasing from 0.73 (F 10) to 0.16 mg Chl a m^{-3} (F 1), while, inversely, the relative variation coefficient increases steadily from F10 (105%) to F1 (210%). The use of the ratio of biomasses in the fractions F3 and F10, as an index of the relative abundance of large phytoplankton cells in the original samples, enables us to cross-sort the stations in 4 major categories (Tab. 10).

Tab. 10 - Stations sorted according to both biomass and cell size

HS = High biomass, Small cells, HL = High biomass, Large cells
LS = Low biomass, Small cells, LL = Low biomass, Large cells

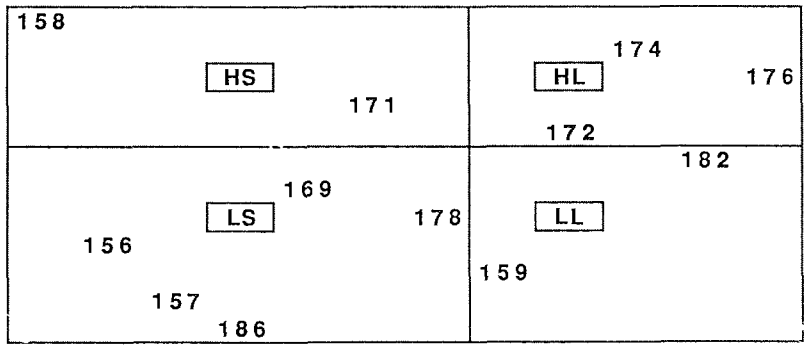

Applying the same kind of analysis to the carbon uptake rates in the PI curves, we can observe also a rather wide dispersion in the maximum values recorded, between 0.08 (Sta.172, fraction F1) and 1.52 mg C m^{-3} h^{-1} (Sta. 152, F3). However, if the increase between the mean maximum value of uptake in the F1 fraction and that one in the F10 fraction is 90%, it corresponds to an increase of about 356% in the related values of biomass; this seems to indicate a far better efficiency of the small phytoplankton cells compared to the large ones. This is confronted by the fact that if, instead of the uptake rate values, the efficiency ratio P/B is taken into account, then the increase between fractions F10 and F1 will be in the order of 800%.

Talking about PI curves, it is of interest to have a look at their shape; here are presented two sets of curves coming from stations chosen from opposite categories (fig. 34 and 35): 174 (HL) and 186 (LS). In sta.174, with high levels of biomass, either total or fractional, the F10 curve differs strongly from the others, with a maximum far higher and a marked decrease due to strong photo-inhibition; besides, F3 and F1 curves are quite similar, even if the biomasses are different by a factor of 6, and show low maxima with late inhibition. This could mean that, among the small phytoplankton cells, the fraction between 1 and 3 µm does not improve the overall efficiency much. On the other hand, considering the PI curves from Sta.186 (drawn at the same scale), where the total biomass is far lower while the F1 and F10 biomasses differ by a factor of 10, the F10 curve is only slightly above the F1 curve. Moreover, despite a ratio of 7 between the F3 and F1 biomasses, the curves are confounded, reinforcing the impression drawn from the observation of the previous set of curves. The best efficiency of the smallest

cells do not support the idea expressed by Gieskes and Elbrächter (1986), that part of the chlorophyll-containing particles are free-floating chloroplasts.

Conclusion

Kosaki *et al.* (1985), said that while the pico plankton fraction (whether this is defined as <3 µm or < 1µm), which predominates in tropical waters, is negligible in the Antarctic, the nano plankton (3 to 20 µm) constitute as much as 55% of the chlorophyll biomass. This is not the case in the area studied during EPOS Leg 2 where the smaller fraction predominates. During the last days of November, some diatom blooms, probably prevailing just earlier, were still present in the Weddell Sea. At Sta. 146 to 150 and just on arrival at the time station 157, at least 75% of the phytoplanktonic biomass was due to diatoms larger than 10 µm. After that time, south of the Weddell-Scotia Confluence, the mean biomass of the size fraction > 10 µm was always < 20%, very often even < 10% of the total biomass.

The combined practice of differential filtration (a technique still open to question), flow cytometry, and PI curves on small fractions gives a coherent picture of the ecosystem. At least two interesting questions remain to be solved. The first one is the reason why the food web suddenly shifts from the classical pathway towards a microbial loop with a high proportion of regenerated production. The second one is to find out if a constant and widespread Krill grazing pressure can be strong enough to prevent any diatom bloom.

Note:

- The clear photo-inhibition of the large-cell fraction at Sta. 174
- The best efficiency of the smallest cells at Sta. 186 where the absolute production of the < 10 µm and < 1 µm fractions are relatively similar while their biomasses differ by a factor 10

Literature Cited

Brandini, F. P., Kutner, M. B. B., 1987. Phytoplankton and nutrient distributions off the northern South Shetland Islands (summer 1984 BIOMASS-SIBEX). *La Mer*, 25: 93-103.

Bröckel, K. von, 1981. The importance of nanoplankton within the pelagic Antarctic ecosystem. *Kiel. Meeres.*, 5: 61-67.

Gieskes, W. W. C., Elbrächter, M., 1986. Abundance of nanoplankton-size chlorophyll-containing particles caused by diatom disruption in surface waters of the Southern Ocean (Antarctic Peninsula): *Neth. J. Sea Res.*, 20: 291-303.

Hewes, C. D., Holm-Hansen, O, Sakshaug, E., 1985. Alternate carbon pathways at lower trophic levels in the Antarctic food web. *In* W. R. Siegfried, P. R. Condy and R. M. Laws (eds) Antarctic nutrient cycles and food web. Springer Verlag, Berlin, Heidelberg, 277-283.

Kosaki, S., Takahashi, M., Yamagushi, Y., Aruga, Y., 1985. Size characteristics of chlorophyll particles in the Southern Ocean. *Trans. Tokyo Univ. Fish.*, 6: 85-97.

Marchant, H. J., Davidson, A. T., Wright, S. W., 1987. The distribution and abundance of chroococcoid cyanobacteria in the Southern Ocean. *Proc. NIPR Symp. Polar Biol.*, 1: 1-9.

Sheldon, R. W., Rassoulzadegan, F., 1987. A method for measuring plankton production by particle counting. *Mar. Microbial. Food Webs*, 2: 29-44.

Weber, L. H., El-Sayed, S. Z., 1985. Spatial variability of phytoplankton and the distribution and abundance of Krill in the Indian sector of the Southern Ocean. *In* W. R. Siegfried, P. R. Condy and R. M. Laws (ed.) Antarctic nutrient cycles and food web. Springer Verlag, Berlin, Heidelberg, 284-293.

Yentsch, C. M., Horan, P. K., Muirhead, K., Dortch, Q., Haugen, E. M., Legendre, L., Murphy, L. S., Perry, M. J., Phinney, D., Pomponi, D., Spinrad, R. W., Wood, A. M., Yentsch, C. S., Zahurenec, B. J., 1983. Flow cytometry and sorting: a powerful technique with potential applications in aquatic sciences. *Limnol. Oceanogr.*, 28: 1275-1280.

Figure 32 - Relative importance of sized fractions at the first transect .

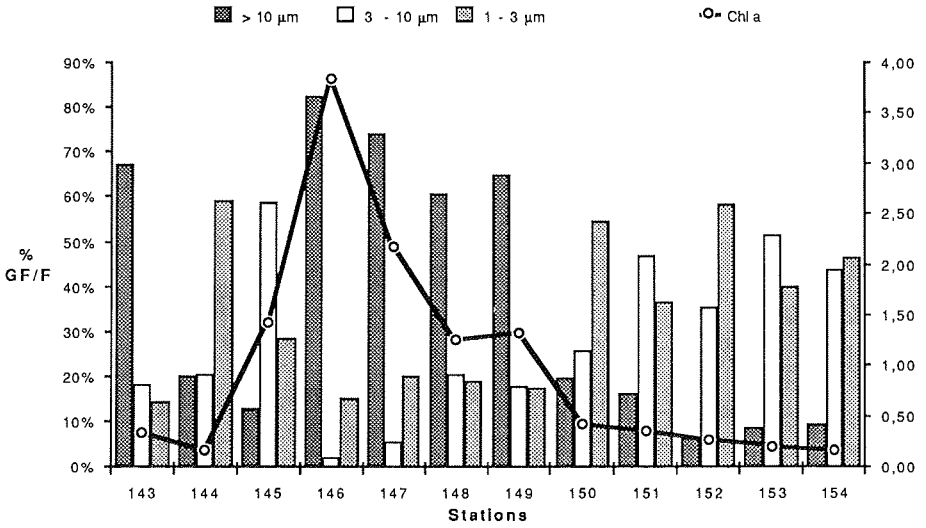

Figure 33 - Relative importance of sized fractions at the second transect .

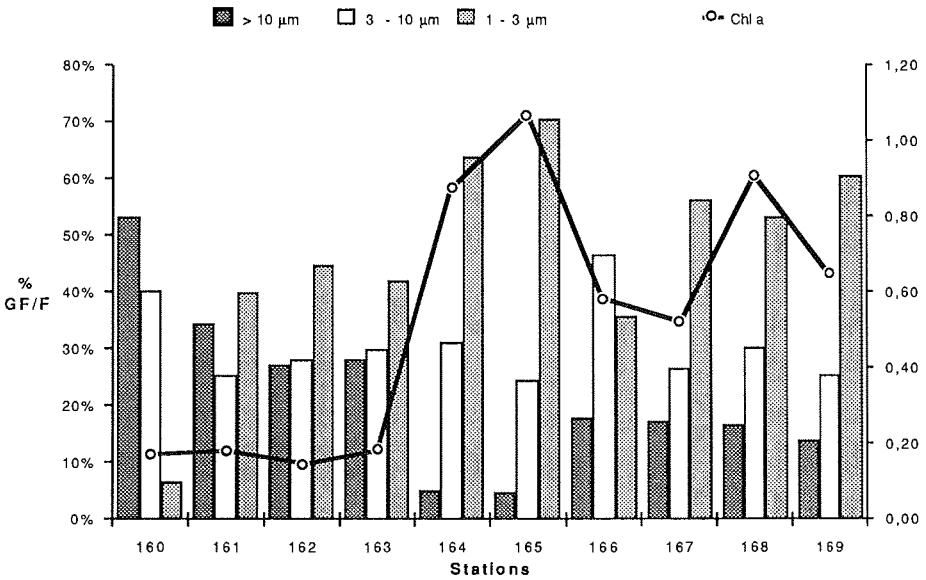

Figure 34: PI curves of three size fractions from station 174, with high biomass and large cells

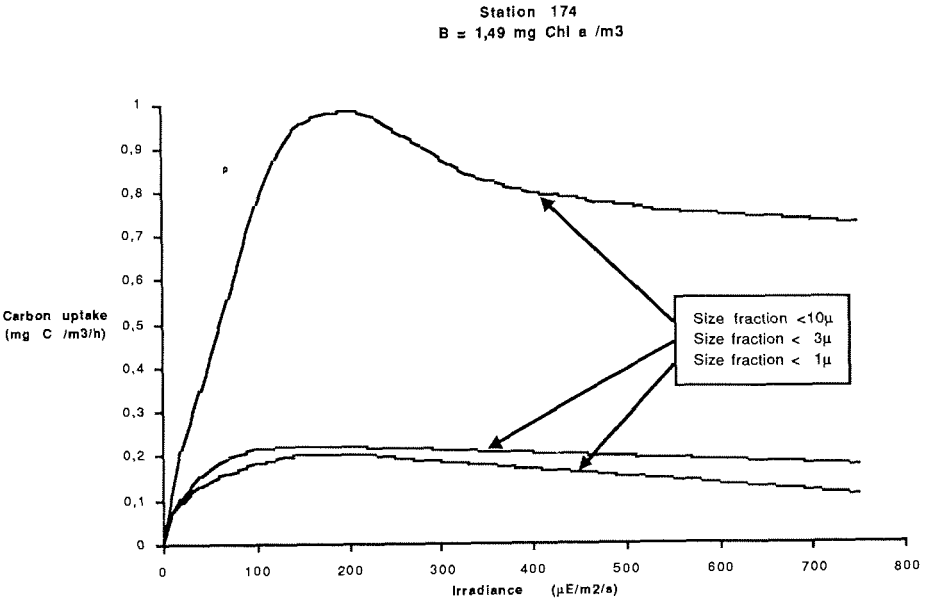

Figure 35: PI curves of three size fractions from station 186 with low biomass and small cells

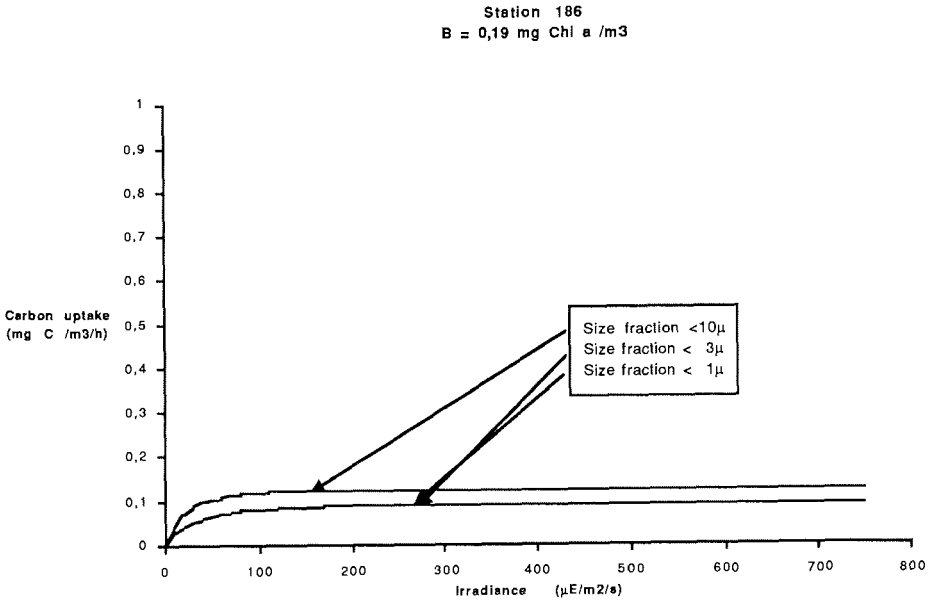

4.2.3 Phytoplankton Pigment Measurements by HPLC

A. Buma, J. Larsen

Objectives.

We studied spatial distribution of phytoplankton populations by means of pigment fingerprints, as measured by HPLC (High Performance Liquid Chromatography).

Pigment fingerprints can give an adequate indication of the algal classes present in phytoplankton populations. For instance Chl b is typical for green algae; peridinin is, with a few exceptions (see below) the main carotenoid in photosynthetic dinoflagellates. The carotenoids, alloxanthin and zeaxanthin, are markers for Cryptophyceae and Cyanobacteria, respectively. Whereas microscopy of water and net samples gives a rapid first order picture of the general composition of the phytoplankton crop, HPLC analyses can be quantitatively more reliable, particularly for smaller forms such as Cyanobacteria that are difficult to distinguish by eye. Thus, microscopical analyses of samples from the cruise (see elsewhere in this report), indicate that alloxanthin, Chl b, peridinin, and also several fucoxanthins are major components of the pigment composition, along with Chl a. We will pay special attention to the fucoxanthins, i.e. the "real" fucoxanthin and two fucoxanthin derivatives: butanoyloxyfucoxanthin and 19´ hexanyloxy-fucoxanthin that can provide interesting information..

Fucoxanthin is the main light harvesting carotenoid in diatoms and therefore a common pigment in Antarctic waters, whereas all three fucoxanthins can be found in prymnesiophytes, such as *Phaeocystis pouchetii,* a common algae in the Antarctic. Culture experiments on an Antarctic isolate of *P. pouchetii* have shown that especially the derivatives are present in high amounts as compared to the real fucoxanthin, which is only present in trace amounts. Occurrence of the latter depends on stage in the life cycle and physiological condition (nutritional status). *P. pouchetii* strains, isolated from the North Sea also contain these fuco derivatives, but only as minor components. Here fucoxanthin is the major light-harvesting carotenoid. A comparative study on different strains of *P. pouchetii* (North Sea and Antarctic strains) has revealed significant differences in pigmentation especially of the fucoxanthins, when cultured under the same environmental conditions (T,S,I and chemical composition of the medium).

The taxonomy of *Phaeocystis* at the species level is still not entirely clear. More cultures of *Phaeocystis* will be established from samples collected on the cruise. These cultures (together with those already established) will be investigated ultrastructurally and for pigment composition, attempting to unravel the taxonomic problems. Also more information on the life cycle of *Phaeocystis* may result from these studies.

It is still a matter of discussion as to which extent pigment fingerprints can be used for reliable quantitative estimates of algal class biomass. Although all diatoms show a clear uniformity in the pigment composition in the qualitative sense, relative amounts of pigments (versus Chl a) can vary considerably between species. For instance, ice algae are believed to contain relatively

high amounts of Chl c, due to chromatic adaptation. However, pelagic diatoms of the genus *Chaetoceros*, isolated from the Scotia Sea, also contain high amounts of Chl c. As mentioned above, peridinin is a common light harvesting carotenoid in dinoflagellates, but some representatives of this group contain 19´hexanoyloxyfucoxanthin instead of peridinin, supposedly due to prymnesiophyte endosymbionts.

Whether this is the case in Antarctic waters is still unclear, but future experiments will probably clarify this point. When interpreting pigment data, also the effect of environmental conditions has to be considered. Whereas Antarctic diatoms so far investigated hardly change their pigment ratios with changing environmental conditions (spectral changes, nutritional changes), the pigment composition of the prymnesiophyte, *Phaeocystis pouchetii,* shifts considerably depending on life cycle stages and physiological condition. This variability in the pigment composition could partly be the reason for the ecological success of this organism.

HPLC analyses also provide information on recent grazing and physiological state of the community (senescence), from phaeophorbide and phaeophytin, (chlorophyll breakdown products) respectively. These measurements will be done routinely on the water samples taken during EPOS Leg 2. Samples have also been taken for pigment analysis of Krill gut material. Spatial distribution patterns of pigments will be related to other biological data as well as to hydrographical parameters.

Work at Sea

Some 80 samples for pigment analysis were taken: 36 from sub-surface depths, several ice samples and 9 profiles (4 depths: 80, 40, 20, 10 m). On all stations also, samples were fixed for miscroscopic counts at home. The fixative used (a mixture of lugol, glutaraldehyde and ethanol) is considered to be a good fixative for diatoms and flagellates as well, but for nanoplankton composition of the samples better techniques are available.

10 - 30 L of seawater were filtered through 47 mm GFF glass-fiber filter in dark pressure containers, with slight overpressure (less than 0.2 bar), and stored at - 27°C immediately after filtration. At home, filters will be homogenized in a homogenizator (with glasspearls), in methanol buffer, just prior to injection in the HPLC system.

Separation of pigments will be done on a reversed phase gradient elution system (linear gradient from 100 % A to 100 % B in 20 min. where A= methanol in phosphate buffer (70/30), and B= Methanol & Ethylacetate (80/20)). Detection of pigments: Absorbancy at 436 nm (total pigments) and at 658 nm (breakdown products). Integration of peak areas by a recording integrator.

4.2.4 Phytoplankton: Photosynthesis, Growth and Respiration

C.Lancelot, S.Mathot

Objectives

The proverbial richness of the Antarctic Ocean originates from the observation of tremendous biomasses of Krill, whales, seals and birds. This richness seems paradoxical since primary production and phytoplankton biomasses as low as in oligotrophic oceanic regions were generally reported in the Southern Ocean in spite of high macronutrient levels. It therefore seems difficult to explain how biomass of higher trophic levels can be sustained by this low oceanic primary production.

Indeed, algal blooms have occasionally been found within the marginal ice zone (El Sayed, 1971, Smith & Nelson, 1986) and in sea ice microhabitats (Whitaker, 1977, Garrison et al. 1986, McGrath-Grossi et al. 1987). The enhanced vertical stability of the surface layer resulting from the physical properties of both these particular phytoplankton habitats provides a stable environment with light levels favourable for phytoplankton growth.

Contribution of ice edge phytoplankton to overall primary production could be very important as the marginal ice zone covers a wide area. It is, however, difficult to evaluate because the rate of ice retreat is closely linked to meteorological conditions. Also, the contribution of sea-ice algal production is an important question that cannot be presently answered because both the physical and chemical properties of the ice habitat and the physiology of ice algal communities are still not well known. This is partly because of a lack of consistency both in collection methods and process measurements. Nevertheless, sea ice provides unique physical and chemical conditions to which physiological processes of associated biota have adapted. The success of some microalgae in colonizing and growing in sea ice would reflect, therefore, partly metabolic adaptations to this particular environment.

Because of the large variety of phytoplankton habitats in Antarctica (ice, melting ice, oceanic water), accurate estimates of overall primary production should only be provided by means of predictive mathematical models which would take into account *the physiology of phytoplankton and its interaction with the habitat as well as the species dominance of the community.* Such a model was successfully developed for the study of phytoplankton growth in Prydz Bay waters during later summer 1987 (Lancelot et al. 1988). Its general applicability to the Antarctic ecosystem was to be established during the summer EPOS Leg 2 cruise where the physiological characteristics of algal communities from different habitats were to be determined. Particular attention was paid to phytoplankton from the Confluence and marginal ice zone areas. Physiological properties of sea ice communities were also studied and their role as an inoculum to the water column following ice melting was addressed.

Work at Sea

Sampling strategy: Physiological experiments were conducted during various periods of the vegetation period on the different phytoplankton communities that characterize the Southern ecosystem presently studied: The Scotia Sea, the Confluence area, the marginal ice zone (Weddell Sea), the sea-ice environment.

Sampling depths were determined according to the vertical structure of the water column provided by the CTD profile (see § 4.1.1) and the depth of the euphotic layer estimated from colour index measurements (see § 4.1.2). Sea-ice communities from surface water surrounding and from the infiltration layer of ice floes were collected by rubber-boat. Sea-ice communities from interior layers within annual sea ice were sampled by cores taken in the middle of the ice floes. Light measurements indicated that these last communities would receive about 15% of incident available light. Sea-ice communities collected were gently melted in GF/C filtered seawater in order to avoid osmotic shock. Melting was conducted in darkness.

Physiological experiments

*Concept:*Phytoplankton activities -photosynthesis, growth, respiration- are determined by means of a mathematical model based on elementary cellular biochemistry. This model assumes that synthesis of functional cellular constituents (F, composed of 80% of proteins) constitutes the best index of cellular growth. The structure of the model is illustrated by Fig.36. Three pools of cellular constituents are to be considered on the basis of their biological function: the functional and structural macromolecules (F), the reserve products (R, composed of lipids and polysaccharides), and the small metabolites (S, precursors of macromolecule synthesis). Mathematical equations that describe the metabolic processes of their synthesis and catabolism, symbols and units of parameters and variables involved in the equations are reported in Lancelot et al. (1988).

Experiment: Experimental determination of the parameters characterizing the equations of the model was carried out based on two kinds of experiments combining radio-tracer technology and classical biochemical procedures.

(i) the experimental determination of photosynthetic parameters involving short-term ^{14}C incubation - Steemann-Nielsen standard method - performed at different light intensities (1-900 $\mu E\ m^{-2}\ s^{-1}$). Photosynthetic parameters Kmax, a, ß are then statistically estimated by means of the Platt et al (1980) equation.

(ii) The experimental determination of growth parameters will be performed by mathematical adjustment based on data relative to long-term (24 hours) kinetics of ^{14}C assimilation into 4 pools of cellular constituents easily separable by simple biochemical procedures: lipids, small metabolites, polysaccharides and proteins. Experimental determination of the energetic requirements for cellular maintenance was carried out on some occasions with parallel 24 hours kinetics experiments in which specific growth inhibitors were added two hours before the dark period. Cellular

maintenance should be indeed very essential for both pelagic and ice algae since they are confined to long dark period during the winter season. ^{14}C incubations were performed in a thermostatic incubator illuminated by halogen lamps. The light-dark period was adjusted to the natural photoperiod and the light intensity to light saturation value i.e. 120 $\mu E\ m^{-2}\ s^{-1}$.

Calculations: Daily integrated values of photosynthesis and growth will be provided by integration of the equations describing the model on the variations of light both in the water column and during the photoperiod. Available incident light intensity PAR was effectively continuously recorded by means of a cosine Li-Cor light sensor (Data recorded on floppy disks).

Preliminary Results

Only photosynthetic parameters are presently available. The time-consuming biochemical determinations will be performed later in the laboratory.

Tab. 11 gathers extreme values of photosynthetic parameters as graphically calculated for the different algal communities studied. These are obtained from the analysis of 50 photosynthesis-light experiments conducted during the cruise. The most relevant data are illustrated by Fig. 37 to 41. Precise values of photosynthetic parameters will be computed later by statistical fitting of experimental data, using the Platt et al. (1980) equation. It is important to note that no significant time and space variations in photosynthetic parameters were to be found within each specific area sampled, at least during the summer period considered. This can be explained by the lack of important change in species dominance.

Assimilation numbers, Kmax, are remarkably similar for different areas sampled, the sea-ice communities excepted, where a wide range of values were calculated (Tab. 11). Kmax values relative to pelagic communities are of the same order of magnitude as those generally reported for temperate waters, indicating that the Antarctic algae are well adapted to the low temperatures prevailing in this ecosystem. Assimilation numbers of ice communities on the other hand have to be examined carefully as a function of species composition and their location within the ice floes. Communities from infiltration layers are composed exclusively of ice algae that can grow very rapidly and efficiently in spring when the snow load depresses the floe into the sea. In agreement with this is the increase of the calculated assimilation numbers from 0,35 to 3,8 for ice algae sampled from the beginning up to the end of December (Tab. 11). In contrast, communities of the interior layer contain both ice algae and frozen-in phytoplankton, such as centric diatoms. The latter community is photosynthetically inactive, being in a resting stage, with to many dead cells and empty frustules. Assimilation numbers as commonly expressed per chlorophyll a unit are therefore very low (Tab. 11) since inactive cells do still contain chlorophyll a. Assimilation numbers characteristic of the ice algae will therefore be recalculated on the basis of chlorophyll content of those algae only. This latter will be estimated at home from microscopical analysis of Lugol samples, combining the enumeration of the sea ice algae and the measurement of their respective biovolumes.

Photosynthetic adaptation of phytoplankton to their light regime is currently expressed by the value of the light saturation parameter I_k and the occurrence of photo-inhibition at high light intensities. Photo-inhibition was never observed regardless of the origin of the algal community (see Fig.37 to 41). This suggests that Antarctic algae are well adapted to the high light levels they encounter during the spring-summer period as illustrated by Fig.42. which shows one example of daily photosynthetically active radiation. Higher values of I_k observed for Scotia Sea phytoplankton could be explained by the dominance of diatoms in the community as compared with the Confluence and marginal areas where nanoplankton forms like cryptomonads were always dominant.

More interesting is the rapid adaptative capability of sea ice communities to the light regime they encounter. This is clearly illustrated by comparison of Fig.41a,b,c,d that show data on photosynthesis-light relationship respectively established for ice communities sampled in the interior (Fig. 41a) and infiltration (Fig. 41b) layers of an ice floe, together with that from planktonic algae from the surface water layer between floes (Fig. 41c), and from the adjacent mixed layer (Fig. 41d). Examination of these figures clearly indicates that ice algae of the interior layer, receiving about 15% of the incident light, are typically shade-adapted. I_k values range between 15 and 50 $\mu E\ m^{-2}\ s^{-1}$ in agreement with previous studies in Mc Murdo Sound (see Horner, 1985).
On the contrary, ice algae from the surface and infiltration layer, fully exposed to light are typically sun-adapted, I_k values ranging between 100 and 167 $\mu E\ m^{-2}\ s^{-1}$.
In agreement with this are the very similar values of the photosynthetic parameters of the adjacent planktonic community which is liberated from the ice during the melting process.

Conclusion

Preliminary results on photosynthesis reveal that Antarctic phytoplankton seems to be well adapted to the different temperature and light regimes encountered, either in the water column or in the ice. Values of photosynthetic parameters will, however, be accurately recalculated following computer treatment and phytoplankton species analysis. Daily integrated primary production values would then indicate the importance of phytoplankton activity in the Scotia-Weddell Sea area investigated during the vegetative period.

Literature Cited

El-Sayed, S.Z. (1971). Observations of phytoplankton bloom in the Weddell Sea. Antarct. Res. Ser. 17: 301-312

Garrison, D.L.; Sullivan, C.W. & Ackley, S.F. (1986). Sea Ice microbial communities in Antarctica. Bioscience 36(4): 243-249

Lancelot, C. et al. (1988). Ecophysiology of Phyto- and Bacterioplankton Growth in the Prydz Bay Area During the Austral Summer 1987. I. Modelling phytoplankton growth.J. Proceedings of the Belgian National Colloquium on Antarctic Research Brussels, October 20, 1987, 115-132

Mc.Grath Grossi, S.; Kottmeier, S.T.; Moe, R.L.; Taylor, G.T. & Sullivan, C.W. (1987). Sea ice microbial communities. VI. Growth and primary production in bottom ice under graded snow cover. Mar. Ecol. Progr. Ser. 35: 153-164

Platt, T.; Galleyas, C.C.; Harrison, W.G. (1980). Photoinhibition of photosynthesis in natural assemblages of marine phytoplankton. J. Mar. Res. 38(4): 687-701

Smith, W.O.Jr. & Nelson, D.M. (1986). Importance of ice edge phytoplankton production in the Southern Ocean. Bioscience 4: 251-257

Whitaker, T.M. (1977). Sea ice habitats of Signy Island (South Orkneys) and their primary productivity. In: Adaptations within Antarctic ecosystems. Llano G.A. (ed.) Gilf. Publ. Houston Texas, 75-83

Figure 36: Diagrammatic representation of phytoplankton cellular constituents and metabolic activities

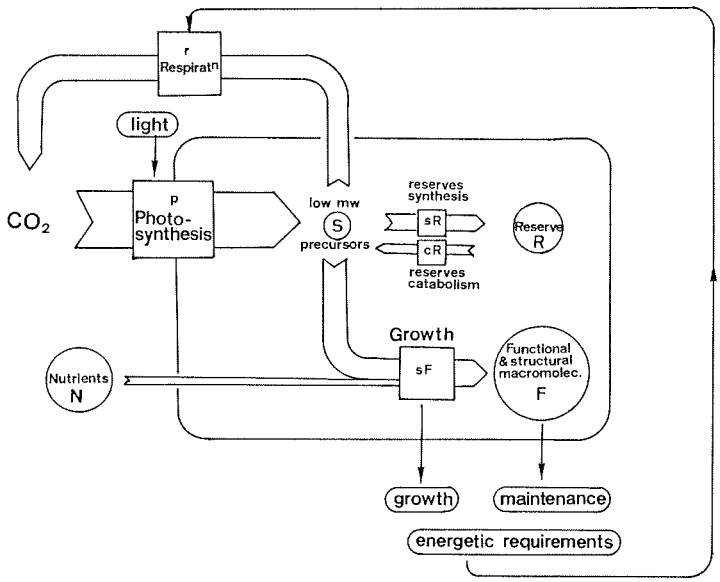

Figure 42: Example of the daily photosynthetical active radiation on December 23rd 1988

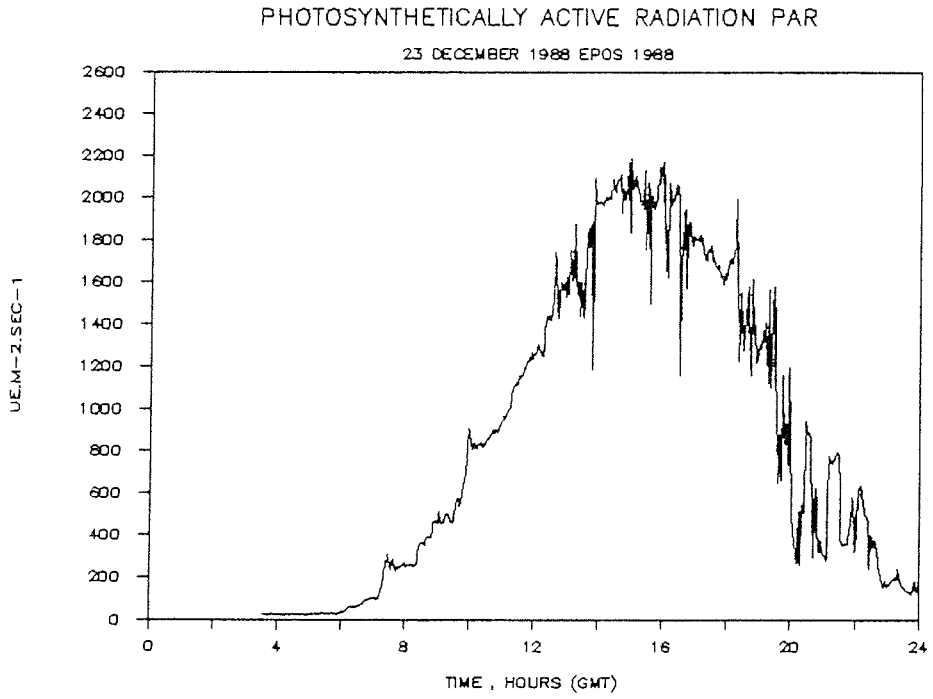

Figures 37 - 40: Phytosynthesis-light experiments on samples from various stations

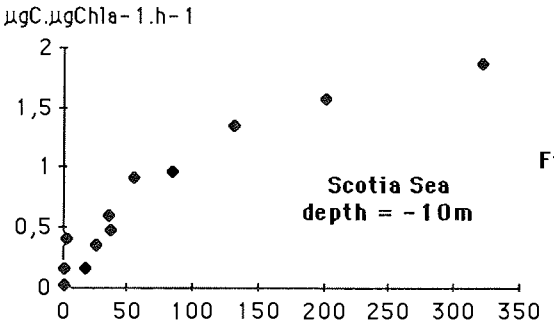

Fig.37

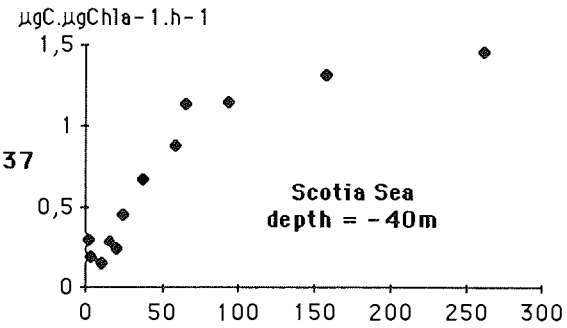

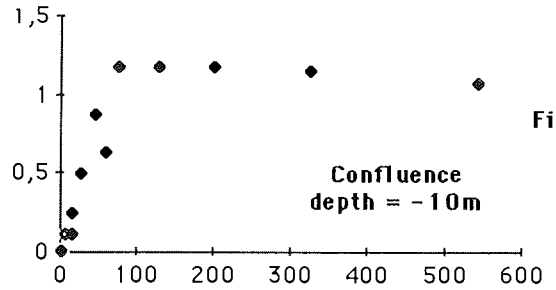

Fig.38

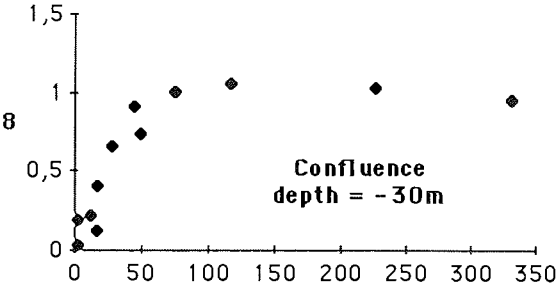

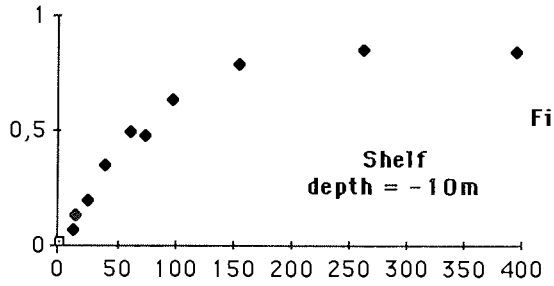

Fig.39

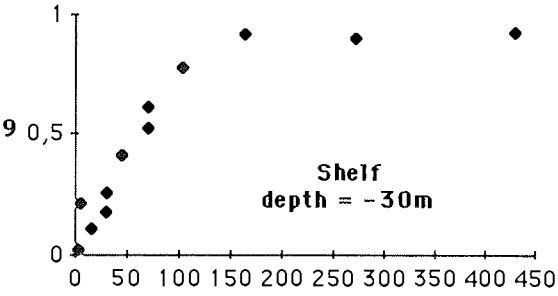

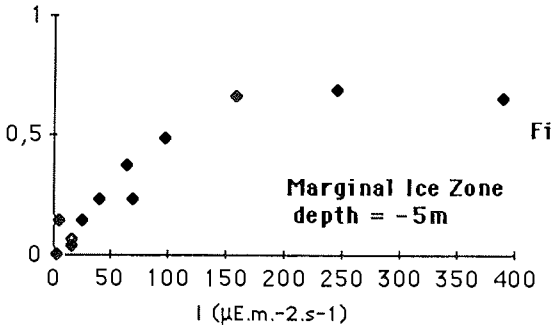

Fig.40

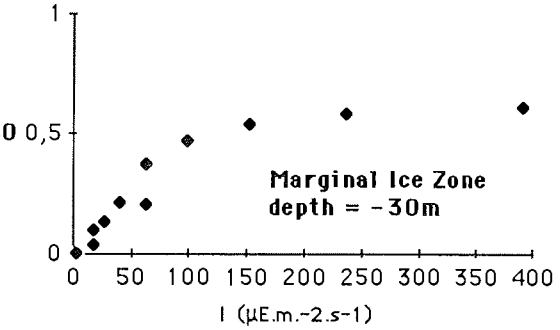

Figures 41 a-d: Photosynthesis-light experiments on samples from various stations

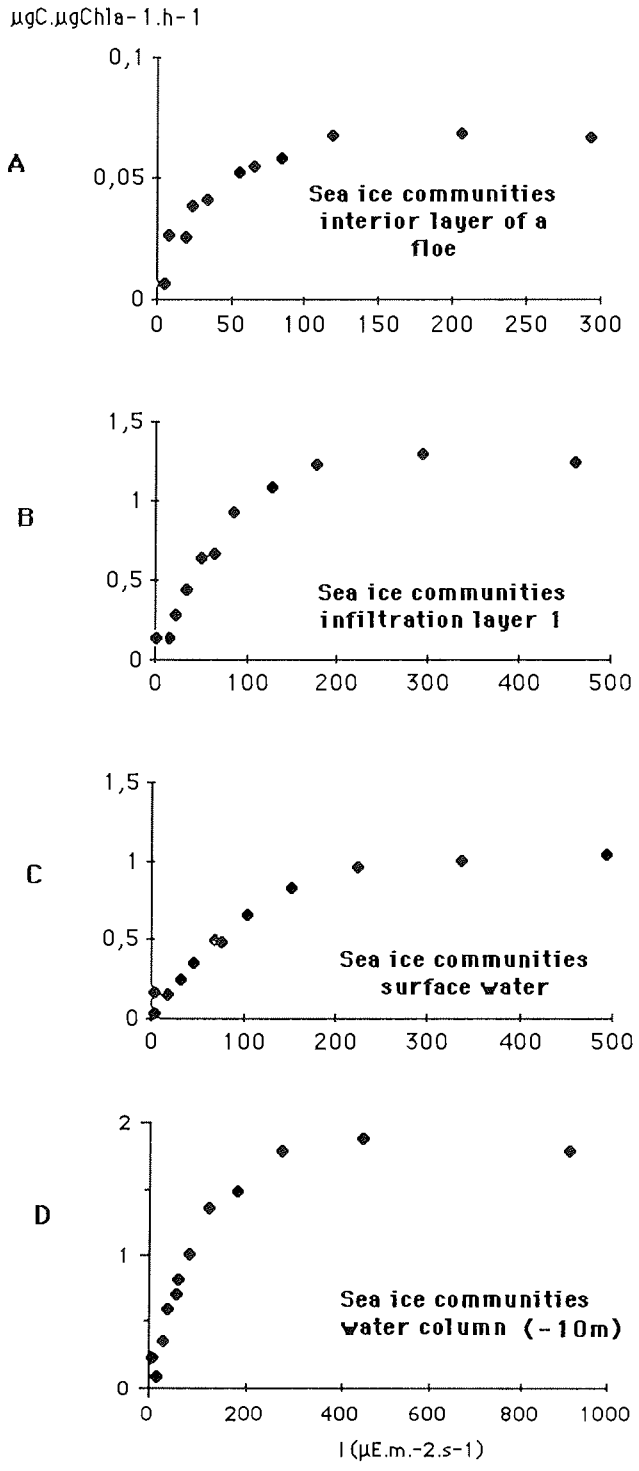

Table 11: Photosynthetic Parameters

BIOTOPE		PHYTOPLANKTON DOMINANT SPECIES	K MAX (1) ($\mu gC\ \mu gChla^{-1}\ h^{-1}$)	ALPHA (1)/(2)	I K (2) ($\mu E\ m^{-2}\ s^{-1}$)	TEMPERATURE (°C)
Scotia Sea		Common diatom species: Chaetoceros, Thalassiosira, Rhizosolenia, Corethron, Dactyliosolen, Coscinodiscus...	1,1-2	0,01-0,02	105-150	+1,3- +1,8
Confluence area		Diatoms dominating with high species diversity	0,7-2	0,01-0,02	72-124	0
Marginal zone		Nanoplankton dominated system main species: Cryptomonads	0,7-2	0,01-0,03	65-100	-1,0- -1,5
Shelf		?	0,8-0,9	0,01	80-95	-1,1
Sea Ice communities:						
Infiltration layer	04/12	Typical ice flora: Pennate diatoms (many species of Nitzschia, Amphiprora),Phaeocystis, many flagellates	0,35	0,0035	99	
	16/12		0,99-0,84	0,006-0,008	104-167	
	31/12		1,3-3,8	0,02-0,04	90-100	
Interior layer	3/12	Combination of typical ice algae and frozen in Centric diatoms	0,1-0,3	0,005-0,007	15- 50	
Surface water	23/12		1,04	0,01	118	
Water column			1,87/1,63/1,56	0,02	104/95/75	-1,2- -1,4

4.2.5 Phytoplankton Metabolic Activity Studied by Tracer Technology

C. Lancelot, L. Lindner, S. Mathot, F. Sorenssen, P. Tréguer

Objective

Accurate determination of net primary production, i.e. the food available for higher trophic levels, is essential for the study of marine ecosystems. Net primary production can be expressed in terms of biomass or cell increase. Knowledge of both is important for estimating activity of heterotrophic organisms. Presently no simple method satisfies this demand and the ^{14}C method as currently used by phytoplanktologists measures something between gross and net primary production, depending on the physiological state of the algae and the incubation times used. Different alternatives to the ^{14}C method were therefore recently proposed, as for example, nutrient uptake measurements by means of natural isotopes such as ^{15}N and ^{32}Si. These, unfortunately, describe only one particular process without taking into account the global growth metabolism of phytoplankton. As a tentative alternative for better understanding phytoplankton metabolism, we had the opportunity to conduct, in parallel, incubations employing different radiotracers on the same natural phytoplankton community. Comparison of these data should provide new information on factors controlling cell division and biomass production.

Work at Sea

A diatom-dominated phytoplankton community was sampled before sunrise in the Scotia Sea. The station was located at 57°29′S 48°32′W and sampling depth was 10 m. Kinetics of 24-hour-tracer incubations were run in parallel from sunrise to sunrise under semi in-situ simulated conditions. The incubator was located in the middle of the helicopter deck. Temperature was kept constant with running seawater. A difference of 1°C was observed between deck and in situ temperature.

The following radioactive and natural isotopes were used:

^{14}C-bicarbonate was used for estimating photosynthesis, growth and respiration (see § 4.2.4)

$^{15}N\ NO_3^-$ and $^{15}N\ NH_4^+$ were used for the study of nitrogen metabolism i.e., its uptake and its assimilation into proteins. (see § 4.1.7)

Natural and radioactive silicate were used for the study of silicate metabolism (see § 4.1.7)

At different times during the photo- and dark period subsamples were simultaneously taken and filtered for specific isotope incorporation measurements. These will be performed at home by each experimentalist.

4.2.6 Phytoplankton - Inorganic Carbon Uptake and Respiratory ETS Activity.

M. Estrada

Objectives

The existence of diel rhythms in the photosynthetic activity of phytoplankton in temperate and tropical waters has been demonstrated in numerous studies (see, for example, Doty and Oguri, 1957; Sournia, 1974; Harding et al. 1981). In general, the rates of photosynthesis, both under conditions of light saturation and of light limitation, show maxima and minima in the light and dark periods, respectively. Doty (1959) suggested that the cycle amplitude was inversely correlated with the latitude of the sampling locality. Later, Lorenzen (1963) proposed that the variable of interest was not the latitude but the relative duration of day and night. Given that Antarctic phytoplankton is exposed to an illumination regime with extreme seasonal variations, it is interesting to know if its response is similar to that of phytoplankton from other regions. Recently, Rivkin and Putt (1987) have shown that the time of maximum photosynthetic capacity in the phytoplankton of McMurdo, Antarctica, shifted from mid-day, at the beginning of September, to mid-night, at the end of October. The consideration of these variations in photosynthetic capacity lead to estimates of primary production up to 4 times higher than those based only on mid-day incubations.
The consumption of oxygen in the sea is due mainly to the respiratory activity of plankton. The determination of respiration rates provides valuable information on the energetic metabolism of aquatic ecosystems and may give insight into oceanic phenomena such as the calculation of the ages and circulation patterns of deep water masses (Packard, 1979). However, respiration rates are often low, especially in cold waters, and difficult to measure directly. An alternative indirect method (Packard, 1971) is the determination of the activity of the enzymes of the respiratory electron transport system (ETS). Several studies (Kenner and Ahmed, 1975; Packard and Williams, 1981) have shown that the ETS and the oxygen consumption rates are well correlated, although the actual ratios may vary in different environments.

According to some authors (Fogg, 1977), the adjustments between the rates of photosynthesis, respiration and photorespiration in algae from cold environments are different from those in algae from temperate waters. Harrison (1986), in a study of microplankton of the Canadian Arctic, found fluxes of oxygen of the same order of magnitude as those recorded in coastal zones of temperate areas, but significantly higher than the limited data available from Antarctic waters (Williams, 1984).

The aim of this research project was to obtain information on the diel patterns of photosynthetic capacity in the phytoplankton of the EPOS area, and to ascertain if the findings of Rivkin and Putt could be generalized to other Antarctic regions. With the ETS measurements information on potential respiratory rates of Antarctic microplanktonic communities was obtained which enables verification of any peculiarities in the relationships between ETS and other physiological parameters.

Work at Sea

Phytoplankton samples were collected at the time stations from 10 m (Sta.156) or from 10 m and a subsurface depth (in the others), at 4-6 hour intervals during a period of 24 hours. The water was introduced in transparent 125 ml Pyrex bottles and 10 μCi of ^{14}C-bicarbonate were added to each bottle. From each depth, bottles were incubated in duplicate during 2-3 hours under 6 different values of photosynthetically active radiation. One dark bottle from each depth was also included in the incubation. By means of a thermostatic system, the temperature was kept at -1.7° C at Sta.156 to 158 and at 2° C at Sta.169. A description of the incubator used can be found in Tilzer et al. (1986). Parallel samples were taken for fluorimetric pigment analysis and for phytoplankton counts.

Clearly, the proposed method has several weak points. The characteristics of the water mass and the phytoplankton community at a given point may vary much with time, introducing other factors of variability in the photosynthetic rates and the assimilation numbers. This happened during some of the stations.

The ETS determinations were carried out according to a modification of Kenner and Ahmed (1975) of the tetrazolium reduction technique proposed by Packard (1971). At each mesostation, seawater samples of 4-10 l from six depths (generally between 0 and 150 m) were filtered through 47 mm Whatman GF/F filters and stored in liquid nitrogen. Some deep water and melted brown ice samples were also processed. For the analysis, the filters were ground with 3-6 ml of a phosphate buffer in a teflon-glass tissue grinder. The assay was carried out adding 0.5^{-1} ml of the crude homogenate to a reaction mixture containing 1 ml of a tetrazolium solution and 3 ml of a phosphate buffer containing NADH and NADPH. Two kinds of blanks were also run. The reaction was stopped with 1 ml of a mixture of formalin and phosphoric acid. The quenched reaction mixture was centrifuged (30 m at 3600 rpm) and the absorbencies of the supernatant at 750 and 490 nm were recorded. The incubation temperature was generally 0°C (25°C for the samples from 1000 m or below). On several occasions, the temperature dependence of ETS activity was checked assaying aliquots of the same homogenate at different temperatures. The results may be converted to in situ temperatures using the equation: $E \times (1/T1-1/T2)/R$
ETS (in situ temp) = ETS (incub. temp) x e, where T1 and T2 are the incubation and in situ temperatures in degrees Kelvin; E is close to 15000 Kcal/mole and R = 1.98 Kcal $Mole^{-1}$ degree.

Preliminary Results

At Sta.158, the samples taken at mid-night showed light-saturated assimilation numbers (mg C/mg chlorophyll a/hour) which were significantly higher than those of the other samples. This observation, which would agree with the suggestions of Rivkin and Putt (1987) is difficult to explain on the basis of the chlorophyll variability alone, but a definite conclusion cannot be reached until the composition of the community is examined. No significant variations in the light-saturated assimilation numbers were apparent in the

other stations. Given the limited set of data available, it is not possible to make any generalizations.

The following comments on ETS measurements are based on the data of the first transect (mesostations 143-154), referred to a temperature of 0° C. The main feature of the distribution of ETS activity in the first transect was the presence of a maximum between Sta.145 and 147, coinciding with the peak of phytoplankton biomass in the Confluence area (Fig. 43). The integrated ETS activity between 0 and 100 m ranged from 22.8 mg O_2 h^{-1} m^{-2} in Sta.154, to 100.5 mg O_2 h^{-1} m^{-2} in Sta.147. The bloom stations showed the lowest ETS /chlorophyll ratios (Fig. 44), indicating the relatively higher importance of the autotrophic component of the microplankton community.
Only a few ETS determinations were carried out for the time stations. However, it is interesting to note that the 10 and 40 m samples of Sta.157 (cast 9) showed a strikingly high ETS/chlorophyll ratio (Fig. 44). This observation suggests a high degree of heterotrophy and agrees with changes in dissolved oxygen in incubated samples (see § 4.1.3).
Some experiments to compare oxygen consumption and ETS activity were attempted, but not enough data were obtained to allow any solid conclusion.

Literature Cited

Doty, M.S. (1959). Phytoplankton photosynthetic periodicity as a function of latitude. J. of the Marine Biological Association of India 1(1): 60-68
Doty, M.S. & Oguri, M. (1957). Evidence for a photosynthetic daily periodicity. Limnol. Oceanogr. 2: 37-40.
Fogg, G.E.(1977). Aquatic primary production in the Antarctic. Phil. Trans. R. Soc. London (B) Biol. Sci., 279: 27-38.
Harding, L.W., Meeson, B.W., Prezelin, B.B. & Sweeney, B.M. (1981). Diel periodicity of photosynthesis in marine phytoplankton. Mar. Biol., 61: 95-105.
Harrison, W.G. (1986). Respiration and its size-dependence in microplankton populations from surface waters of the Canadian Arctic. Pol. Biol. 6: 145-152
Kenner, R.A. & Ahmed, S.L. (1975). Measurement of electron transport activities in marine phytoplankton. Mar. Biol., 33: 119-128.
Lorenzen, C.G. (1963). Diurnal variation in photosynthetic activity of natural phytoplankton populations. Limnol. Oceanogr. 8: 56-62.
Packard, T.T. (1971). The measurement of electron transport activity in marine phytoplankton. J. Mar. Res., 29: 235-244.
Packard, T.T. (1979)Respiration and respiratory electron transport activity in plankton from the Northwest African upwelling area. J. Mar. Res., 37: 711-742.
Packard, T.T. & Williams, P.J.leB. (1981). Rates of respiratory oxygen consumption and electron transport in surface seawater from the northwest Atlantic. Oceanologica Acta, 4: 351-358.
Rivkin, R.B. & Putt, M. (1987). Diel periodicity of photosynthesis in polar phytoplankton: Influence on primary production. Science, 238: 1285-1288.
Sournia, A. (1974). Circadian periodicities in natural populations of marine phytoplankton. Adv. Mar. Biol. 12: 325-389.

Tilzer, M.M.; Elbrächter, M.; Gieskes, W.W. & Beese, B. (1986). Light-temperature interactions in the control of photosynthesis in Antarctic phytoplankton. Polar Biol., 5: 105-111.

Williams, P.J.leB. (1984).A review of measurements of respiration rates. In: Heterotrophic activity in the sea, IV, 15. (J. E. Hobbie and P. J. leB. Williams, eds). Plenum Press, New York: 357-390.

Fig. 43: Distribution of ETS activity (measured at 0°C) along the first transect of EPOS Leg 2

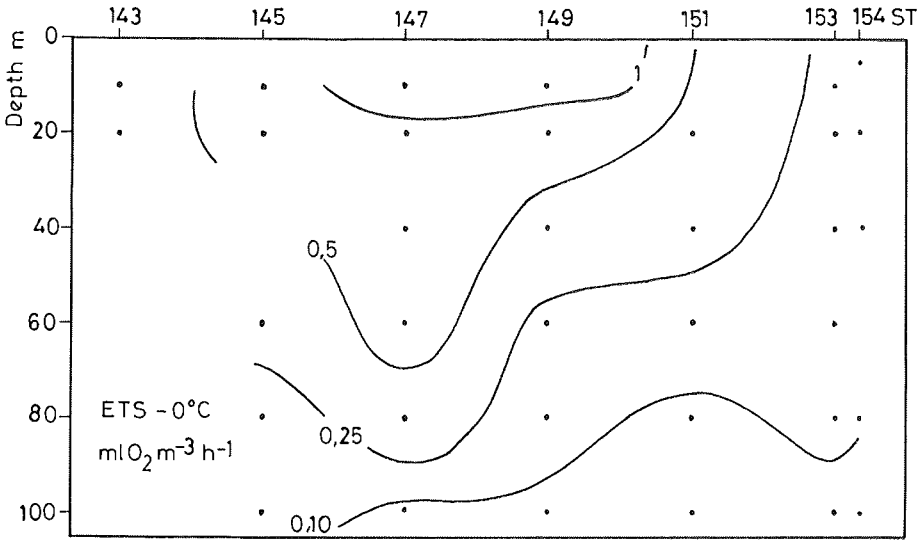

Fig. 44: Relationship between ETS activity (measured at 0°C) and chlorophyll concentration for the samples of the first transect of EPOS Leg 2

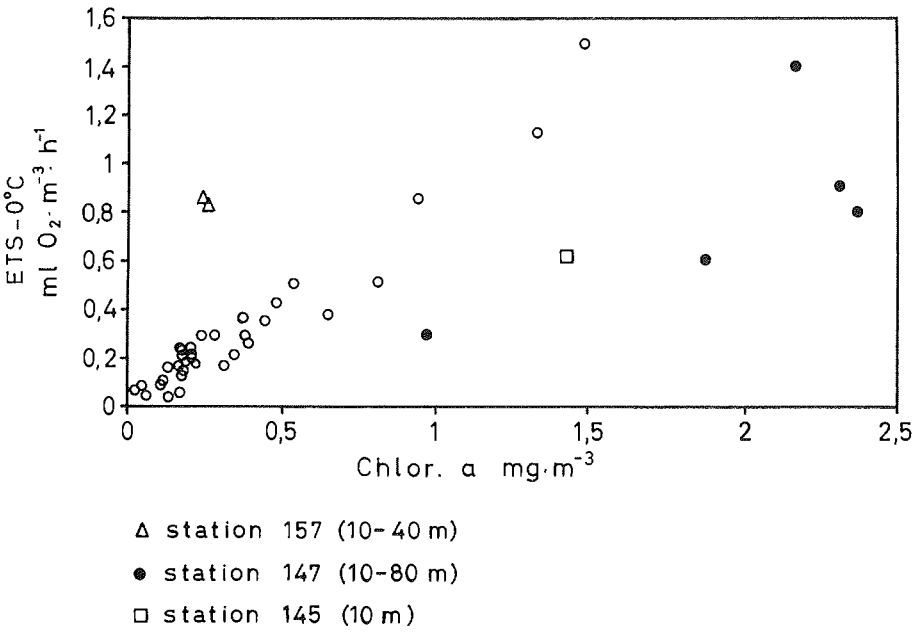

4.2.7 Ecological Aspects of Aggregates

M. Pamatmat, U. Riebesell, S. Schiel, I. Schloss,

Fragile aggregated particles, or 'marine snow', are a common feature of the pelagic ecosystem. These aggregates, ranging in size from a few hundred micrometres to several centimetres in diameter, are very diverse in structure and composition. They often include both organic and inorganic components. The processes leading to the formation of aggregates are still poorly understood.

The study of marine aggregates is of considerable value to several oceanographic disciplines. The aggregation of microscopic particles to macroscopic conglomerations leads to an alteration of particle sinking rate which can result in a substantial increase of vertical flux. Chemical conditions within aggregates can differ significantly from the surrounding water, resulting in chemical heterogeneity and small-scale patchiness in the pelagic system. The aggregation of small particles to larger ones can also be of importance to the pelagic food web.

Conventional oceanographic sampling methods (such as nets or water bottles) have failed to collect the fragile aggregates without disrupting them. In this study, we used an experimental apparatus (roller table, see later for details) which has been shown to reform disrupted aggregates and maintain them in the laboratory (Shanks and Edmondson, in press). Consequently, aggregated material obtained by this method can be interpreted as marine snow which was present in the water column before sampling. Applying this method to melted brown-ice will create new aggregates which have not necessarily existed in the ice. Therefore, aggregates produced under these conditions will be interpreted as aggregates that potentially would have been formed during and after ice-melting.

Objectives

Different experiments were conducted with lab-synthesized aggregates to address the following questions:
1) Rate of aggregate formation.
2) Species composition of the aggregate components in comparison to the composition of the suspended material.
3) Sinking rates of aggregated versus non-aggregated phytoplankton.
4) Oxygen production and consumption of intact and disrupted aggregates.
5) Dependency of the extent of aggregation and aggregate size on the amount of suspended phytoplankton biomass.
6) Effects of nutrient concentrations on aggregation-disaggregation processes.
7) Bacterial colonization on aggregates kept under light and dark conditions.
8) Grazing on aggregates by Krill and copepods.
9) Barium precipitation in aggregates.

Work at Sea

Field observations

During the N-S transects from the ice edge into the pack-ice, fields of 'brown-ice' were frequently encountered. Patches of brown-ice were hundreds of meters and up to several kilometers in dimension. The greenish-brown color was the result of concentrated algal biomass enclosed in the ice. Such concentration of biomass was often found in the form of well-defined horizontal layers in the ice or in the underlayer of ice floes. The algal material producing the brown ice consisted of a distinct algal community, dominated by pennate diatoms. The good condition of the algae and their concentrated occurrence in distinct layers in the ice suggests that they were growing in and on the ice rather than being frozen in during the ice formation in such high concentrations.

During rubberboat excursions in brown-ice fields, aggregates ranging from a few millimeters to 2 or 3 centimeters in size were observed. Aggregates were found lying on top of water-covered extensions at the edges of ice floes, floating within brash ice fields, and in open waters adjacent to the melting ice. Aggregation of material was also observed inside the ice. Brownish spots in the millimeter to centimeter size range were enclosed in the ice and in some cases were seen to horizontally spread to larger patches, similar in appearance to bacterial cultures on agar plates.

The microscopic examination of free and ice-enclosed aggregates revealed a predominantly algal composition. In all samples, pennate diatoms were the most abundant organisms, in many cases contributing more than 90% of the biomass. Species of the genus *Nitzschia* (e.g. *N. closterium, N. cylindrus, N. curta, N. kerguelensis*) were always abundant. Other genera (in order of abundance) included *Amphiprora, Phaeocystis, Tropidoneis, Rhizosolenia, Corethron* and many forms of autotrophic and heterotrophic dinoflagellates, some of which were identified as close relatives of benthic flagellates (J. Larsen, pers. comm.). The heterotrophic community included ciliates and nauplii of different zooplankters.

Sampling and incubations

During the time stations, water samples from different depths in the euphotic zone were collected in Niskin bottles, while surface water was sampled with a bucket. Sea ice-related samples of high phytoplankton biomass were collected in the form of 1) brown-water from the infiltration layer (the thin layer of high algal biomass in ice floes lying between the solid ice and the overlying snow cover), 2) brown-ice from the edges of ice floes, from ice cores, and from brash ice fields floating at the water surface. In order to avoid a decrease in salinity, melting of the brown-ice was conducted in large volumes of GF/C-filtered sea water. Both the water samples and the melted brown-ice were immediately placed into cylindrical 10-litre tanks made of clear plexiglass which were rotated on a roller table at a temperature of 0°C. The light regime was kept constant with a L/D cycle of 16/8 hours and a light intensity of 60 $\mu E\ m^{-2}s^{-1}$.

Experimental work

1) Rate of aggregate formation:
Immediately after the tanks were filled, photographs were taken of the enclosed water samples in short intervals while they rotated on the roller table. The photographs will be enlarged and analyzed to obtain a two-dimensional size frequency distribution of the aggregates forming inside the tanks as a function of time.

2) Species composition:
Subsamples of aggregated and suspended material were taken from the rotating cylinders at different times. The material was fixed with formalin for later analysis of the phytoplankton species composition.

3) Sinking rate measurements:
Aggregates having a wide range of size and age were removed from the roller table cultures and, after a rough determination of their volume, were placed into the upper portion of a 110 cm-long water column. The speed of sinking was determined at 5 cm intervals. The sinking rate for individual aggregates was calculated only for those that showed constant sinking speed over several intervals. The sinking rate of the non-aggregated phytoplankton was determined using a homogenous sample method called SETCOL (Bienfang, 1981). Aggregate-free water samples were taken from the same roller table cultures from which the aggregates were collected and used to fill settling tubes (length: 50 cm, volume: 1150 ml). Subsamples were taken to determine the initial concentration of phytoplankton biomass. After a settling period of 4 hours, the top 100 ml was sampled by carefully siphoning the water from the top of the column. After discarding the central portion of the column (950 ml), the bottom 100 ml was also collected. Sinking rates were calculated according to the equations outlined by Bienfang (1981).

4) Oxygen production and consumption:
Lab-produced aggregates were placed into 20 ml glass vials filled with GF/F-filtered sea water and incubated for 16 hours at a temperature of 0°C and a light intensity of 95 $\mu E\ m^{-2}s^{-1}$. In half of the incubation vials, aggregates were destroyed by small glass beads in the vials. Oxygen concentration was measured with a Radiometer oxygen electrode. Oxygen production was calculated from the change in concentration between initial and final sampling. The chlorophyll a concentration of the incubated sample was determined, and the rate of oxygen production expressed per unit of chlorophyll a (i.e. ml $O_2\ h^{-1}\ \mu g\ Chl\ a^{-1}$). Equivalent incubations were carried out in the dark to determine oxygen consumption per unit of aggregated chlorophyll a.

5) Concentration-size relationship:
Brown-water samples were diluted with GF/C-filtered seawater to final concentrations of 50%, 20%, and 10% of the initial pure water sample. The diluted cultures were then rotated on the roller table and photographs were taken for later analysis. The size-frequency distribution of aggregates as a function of phytoplankton concentration will be established from this data.

6) Effect of nutrient concentration:
Nutrient concentrations (NO_3, PO_4, SiO_4) were closely monitored in some of the rotating cultures. Formation and break-up of aggregates in the cultures were noted and related to the prevailing nutrient conditions.

7) Bacterial colonization:
Subsamples of aggregated and non-aggregated material were regularly taken from rotating cultures kept in the light and in the dark. The samples were preserved with neutral formalin for later analysis of bacterial abundance.

For points 8) and 9), please refer to *3.2.29 Grazing Rates* and *3.2.10 Barium Biogeochemistry in the Southern Ocean* in this volume.

Preliminary Results

In brown-ice fields and next to brown-ice patches we frequently observed algal aggregates floating in the water and lying on or sticking to the ice. The algal composition in these aggregates (90% pennate diatoms) was identical to that of the brown-ice. Similarly, aggregates artificially produced in the lab from melted brown-ice samples displayed the same algal composition as those aggregates collected *in situ.* As a result of our observations, we hypothesize that when their substrate (the ice) is melting away pennate diatoms create their own substrate by sticking to each other and thereby forming compact aggregates. As we observed *in situ,* these aggregates are then released into the open water or adhere to the ice.

The rate of aggregate formation in samples rotating on the roller table was significantly different for the various kinds of samples tested. In brown-water samples collected from the infiltration layer, most of the algal biomass was still in suspension after 48 hours of rotation and the maximum size of aggregates was well below 1 mm. On the other hand, in brown-ice samples from different sources, aggregate formation was observed after less than 15 minutes and a substantial amount of biomass was concentrated in aggregates as large as 10-12 mm in their longest dimension after only 90 minutes (Fig. 45 a, b).

Sporadic microscopic examination of both aggregated and non-aggregated material revealed some differences in the species composition. In cultures with high abundances of *Nitzschia cylindrus*, for example, a higher proportion of cells of this species tended to remain in the non-aggregated rather than in the aggregated state. However, a detailed microscopic analysis of the collected material is required before more quantitative relationships can be established.

Sinking rates of individual aggregates ranging in size from 1 to 325 mm^3 varied between 95 and 690 m d^{-1}. Although in general larger aggregates tended to sink faster, the relationship between aggregate volume and sinking rate seems to be non-linear (Fig. 46). Despite a high degree of scatter a correlation coefficient of $r=0.87$ can be achieved when a logarithmic regression is applied to the data. The logarithmic relationship between aggregate volume and sinking rate suggests that for this type of aggregate, sinking rate does not increase in proportion to an increase in

aggregate size. However, if aggregate size is plotted in a two-dimensional (i.e. surface area) rather than in the three-dimensional form (i.e. volume) versus sinking rate, a linear relationship is found (r=0.86). This suggests that the sinking rate is a direct function of aggregate surface area rather than of volume.

Sinking rates of the non-aggregated phytoplankton were more than two orders of magnitude lower than those of the aggregated material. Rates estimated with the SETCOL-method varied between 0.25 and 0.38 m d^{-1}, sinking rates normally measured for natural phytoplankton.

During sinking rate measurements in the 1 m water column we frequently observed that small portions of material were torn off the settling aggregates, possibly due to friction along the edges of the aggregates. This observation could suggest that despite their high sinking rates, aggregates might not reach the sediments of the Weddell Sea (water depth: 4000 meter) but might disaggregate on their way to the bottom.

Oxygen production measurements of aggregated and non-aggregated phytoplankton indicated that under equivalent light conditions phytoplankton aggregates produce significantly less oxygen per unit of chlorophyll a than non-aggregated phytoplankton. In two sets of experiments oxygen production was measured as 1.09 (±0.28) and 3.16 (±1.87) ml O_2 h^{-1} mg Chl a^{-1}, and 2.40 (±0.11) and 3.37 (±0.45) ml O_2 h^{-1} mg Chl a^{-1} for aggregated and non-aggregated phytoplankton, respectively. Similarly, oxygen consumption of non-aggregated phytoplankton was also higher than of the same material in the aggregated form (aggregated : 0.161 ±0.002 ml O_2 h^{-1} mg Chl a^{-1}; non-aggregated: 0.245 ± 0.037 ml O_2 h^{-1} mg Chl a^{-1}). At least two factors could be responsible for lower values of oxygen production of aggregated phytoplankton: a) reduction of light availability due to shading in aggregates; b) reduced rate of replenishment of nutrients (including CO_2) due to decrease of turbulent diffusion in aggregates, i.e. for cells in aggregates molecular diffusion is the sole source of nutrient supply. In the same way, lower values of oxygen consumption of aggregated phytoplankton in the dark could be caused by low oxygen availability due to a reduction of turbulent diffusion in aggregates. Considering the oxygen production/consumption rates as an indication for phytoplankton activity one might say that due to physical constraints, aggregated phytoplankton on the whole is less active than the same phytoplankton in a non-aggregated state. However, within an individual aggregate one might expect a strong gradient of activity from the outer surface to the center.

An effect of nutrient concentration on aggregation was observed in material collected in the Weddell-Scotia Confluence. In the rotating cultures, large aggregates dominated by the genera *Rhizosolenia, Chaetoceros, Phaeocystis*, and a colonial form of *Thalassiosira*, formed within the first 12 hours of incubation. Immediate break-up of these aggregates repeatedly coincided with the depletion of nitrate in the culture medium. Replenishment of the depleted nutrients in all cases resulted in reaggregation.

No obvious relationship could be found between the concentration of biomass and the size of aggregates formed in the rotating cultures. While in

some cases aggregates of comparable size formed in both the pure and the diluted cultures, in other cases dilution retarded aggregate formation.

Literature Cited

Bienfang, P.K. (1981). SETCOL - a technologically simple and reliable method for measuring phytoplankton sinking rates. Can. J. Fish. Aqua. Sci. 38: 1289-1294.

Shanks, L.A. and Edmondson, E.W. (1989). Laboratory-made artificial marine snow: a biological model of the real thing. Mar. Biol. 101: 463-470

Figure 45: Aggregate formation of melted brown-ice (collected at Sta.180) while rotating on a roller table; A. after 15 minutes of rotation; B. after 90 minutes of rotation.

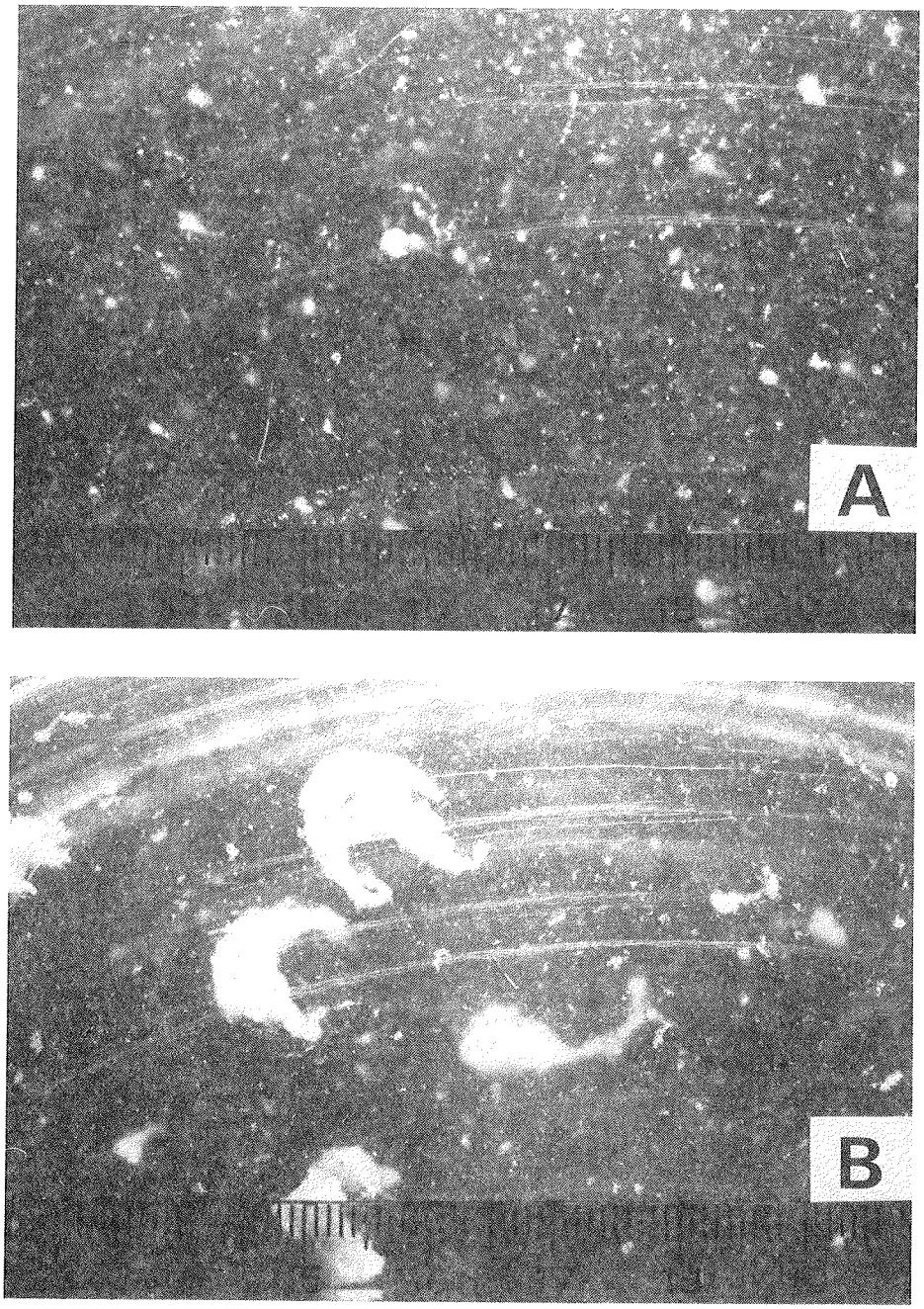

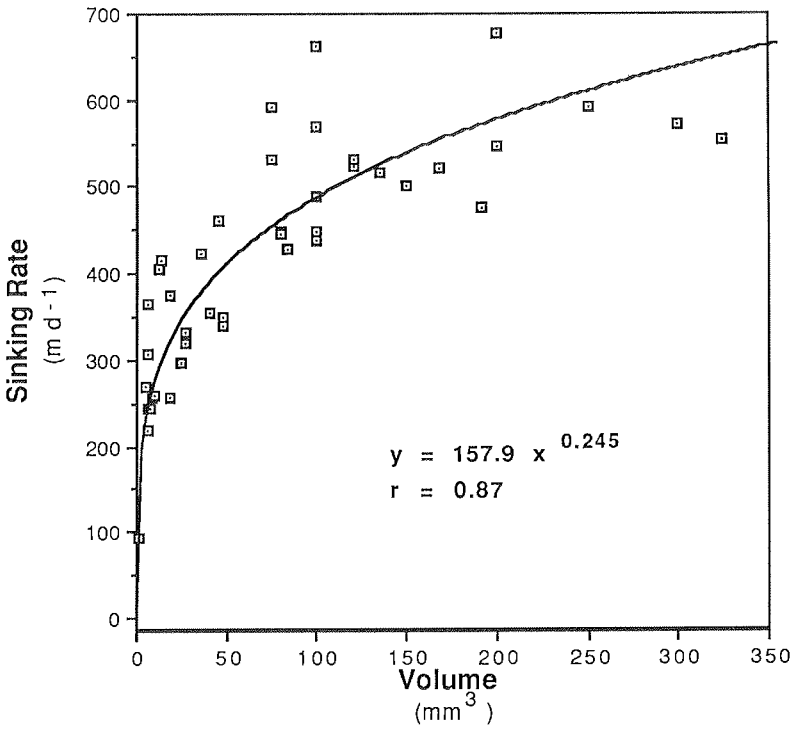

Fig. 46 Sinking rate (m d^{-1}) versus volume (mm^3) of lab-made aggregates from brown-ice collected at Sta. 180.

4.2.8 Particulate and Dissolved Organic Carbon

G. Cadée

Objectives

The total amount of organic carbon in the water column represents important background information for assessment of biological activity and distribution of biomass. Organic carbon is present in both particulate (POC) and dissolved (DOC) states, and whereas the former can be determined with some degree of accuracy, measurement of the dissolved pool is much more difficult. Nevertheless, the use of a standardized method provides data of use for regional and seasonal comparisons. The objectives of this study were to assess the standing stocks of POC and DOC in relation to the physico-chemical environment, biological activity and vertical flux.

Work at Sea

Samples for POC and DOC were taken from mesostations and standard depths. Particles were collected on pre-combusted glass-fibre filters and frozen for later assessment. DOC samples were acidified, bubbled with N_2 gas and sealed in glass ampoules. POC and DOC will be measured by a wet oxidation method using potassium persulphate. Analysis will be conducted at NIOZ, Texel with an Oceanography International TOC apparatus equipped with an infrared analyzer.

4.2.9 Unicellular Organisms Studied Alive Using Photographic and Video Techniques.

A. Buma, M. Estrada, J. Larsen, U. Riebesell, I. Schloss, H.A. Thomsen

Water samples and net plankton samples preserved with different kinds of fixatives form the basis of many post-EPOS research activities related to the unicellular plankton organisms. Diatoms and also the thecate dinoflagellates preserve well, even though the beauty of the living cell is lost forever. Identification of many smaller, "naked" flagellates is difficult or even impossible after fixation. In some cases, a characteristic pattern of movement is crucial for the identification, and in other cases delicate morphological characteristics have to be noted. Flash-photography, which we have used extensively to record in particular the "naked" dinoflagellate diversity of the area, is one means to overcome some of the problems caused by the necessity of having to preserve samples. Another possibility to store information on living material is to use modern video-technology.

Work at Sea

The study of flagellates has been based on examination of qualitative net samples (organisms generally larger than 20 µm) as well as quantitative water samples. Various observation techniques and treatments have to be applied to identify flagellates of particular interest to this study.
All samples have been inspected routinely by the light microscope for a general assessment of the composition of the phytoplankton. Several plankton organisms typical for the Antarctic region have been recorded on video tape. Light microscopy (LM) in combination with flash microphotography has been used for a more detailed study of the so-called unarmoured dinoflagellates. About 300 video recordings (140 min.) of Antarctic microplankton organisms have been made during EPOS leg 2. An edited tape, showing characteristic Antarctic phyto-and protozooplankton organisms, will be prepared and made available (at cost price) to anyone interested. A list of all video recordings is deposited at the AWI.
A number of flagellates can only be identified after electron microscopical (EM) examination, including scale bearing flagellates (*Prymnesiophyceae* and *Prasinophyceae*) and choanoflagellates in which the taxonomy is based on the structure of the lorica. For EM water samples were concentrated by centrifuging (2000 rpm) for 7 min with a cooling centrifuge and droplets of the concentrated sample with living organisms were placed on coated grids with a micropipette (whole mount technique). Fixation by osmium vapour for about 30 sec followed by drying and rinsing in distilled water. For ultra struc-tural examination, fixation by glutaraldehyde in cacodylate buffer followed by osmication, dehydration in alcohol, and embedding in Spurrs resin.
A number of crude cultures has been established during the cruise which were taken home to establish unialgal cultures. Cultures of*Cryptomonas* sp., *Phaeocystis pouchetii*, *Pyramimonas* spp, and possibly some autotrophic dinoflagellates, may form the basis for studies of ultra structure, pigment composition, autecology etc.
Water samples from three transects have been preserved in lugol and/or glutaraldehyde. With the species composition known from LM of live

samples and/or EM of whole mounts, it might be possible to identify at the least some flagellates to species in the preserved water samples. If so, the most abundant flagellates or groups of flagellates will be counted using an inverted microscope in order to give an estimate of their biomass.

Preliminary Results

A detailed quantitative description of the phytoplankton communities and taxonomic investigations must await elaborate studies. The general trends in species composition observed during the cruise will be of relevance for the interpretation of other data, and for the formulation of hypotheses concerning the development in time and space of the Antarctic ecosystem studied. Live samples of net-plankton from the surface layer and concentrated water samples from 10+20 metres depths form the basis of the following general account of the phytoplankton communities.

1st transect, 26-30 Nov 1988; Sta.143-153.

Net-plankton organisms were abundant in the Scotia Sea and in the Confluence area (Sta.143-149). Diatom species *Chaetoceros*, *Corethron*, *Coscinodiscus, Dactyliosolen, Rhizosolenia, Thalassiosira* were dominating and typical for the region. The species diversity varied considerably along the transect being high at Sta.143,147 and 149, while at Sta.145 a single species, *Corethron criophilum*, was dominant. A species of *Thalassiosira* forming huge colonies was abundant in the southernmost Confluence area (Sta.149). Thecate dinoflagellates were abundant in the Scotia Sea only. Colonies of the prymnesiophyte *Phaeocystis pouchetii* occurred in net samples from most stations. The Weddell Sea net-plankton was poor and only *Corethron criophilum* was observed regularly.
The autotrophic nanoplankton in the central Scotia Sea was dominated by the prymnesiophytes, *Emiliana huxleyi* and *Phaeocystis pouchetii* (the flagellate stage), while in the southernmost part towards the Confluence (Sta.145), a reddish-brown cryptomonad (8-12x3-5 µm) was totally dominating (Fig. 47[C]). At all following Sta.(147-153), the autotrophic nanoplankton community comprised the same complex of species: the cryptomonad, diatoms (mostly small *Nitzschia* spp), unarmoured dinoflagellates, *Phaeocystis pouchetii* (the flagellate stage), and *Pyramimonas* spp *(Prasinophyceae)* (Fig. 47). The characteristic pyramid-shaped, green flagellates of the genus *Pyramimonas* (Fig. 47[D]) became more abundant as we approached the ice edge.
Heterotrophic nanoflagellates were abundant at several stations (Fig. 47). In all samples several taxa of non-photosynthetic, naked dinoflagellates occurred. Bacteria grazers, such as the choanoflagellates, with their highly characteristic "houses" of silicified rods, were particularly abundant in the Confluence area (Sta.147,149), and here often formed large spherical colonies. A "droplet"-shaped heterotrophic flagellate with two slightly unequal posterior flagella was common at Sta.153.

2nd transect, 13-16 Dec 1988; Sta.160-169.

The contribution of the net-plankton to the biomass along this transect was only evident at the northernmost Scotia Sea stations (diatoms dominating / high species diversity). The autotrophic nanoplankton in the Scotia Sea was

dominated by *Emiliana huxleyi*. In the Confluence area and in the Weddell Sea (from Sta.164 and further south), the autotrophic nanoplankton community was similar to what was found in these areas during the first transect.In the heterotrophic nanoplankton, a "comma"-shaped amoeba (Fig. 47) was particularly abundant along this transect.

Marginal Ice Zone Transect, 20-24 Dec 1988; Sta.172-179.

The marginal ice zone transect corresponds to the southernmost part of the first transect along 49°W. The most characteristic changes observed were the impoverished net-plankton found at all stations, and the ubiquitous development of a highly uniform autotrophic nanoplankton community similar to that found in the Weddell Sea area during the two earlier transects (Fig. 47). In the heterotrophic nanoplankton, the "droplet"-shaped flagellate observed during the first transect and the "comma"-shaped amoeba during the second transect were both abundant. The flagellate appears to be a voracious grazer. Almost all cells observed contain a large food-vacuole. The chloroplasts of the prey (often *Phaeocystis* cells or diatoms) may give the impression that this is in fact a photosynthetic flagellate. The occurrence of such food vacuoles may have implications for the distinction between auto- and heterotrophic organisms using epifluorescence microscopy only.

3rd transect, 27-31 Dec 1988; Sta.182-194.

This transect along 49°W showed net-plankton dominance at the Scotia Sea station only (Sta.182); diatoms (several species), thecate dinoflagellates and the silicoflagellate *Distephanus speculum* were dominating. The coccolithophorid *Emiliana huxleyi* was still abundant in the Scotia Sea area and the diatom *Dactyliosolen tenuijunctus*. The autotrophic nanoplankton communities in the Confluence and Weddell Sea areas were similar to those encountered during the marginal ice zone transect. Sta. 190 was remarkable in being (almost) an unialgal soup of the reddish-brown cryptomonad.

The ice biota

Diatoms are by far the most important group of organisms in the ice biota. The flagellate ice community is usually dominated by *Phaeocystis pouchetii*. Ice samples have been studied on four occasions and each time the same community was encountered. Several choanoflagellates were recorded. The dominant form was in all cases a morphological variant of *Diaphanoeca multiannulata* (Fig. 48[B]) with smaller loricas than found in typical *D. multiannulata* from open water localities. Other species associated with ice are *Acanthoecopsis unguiculata* aff., *Bicosta antennigera, Saepicula leadbeateri*, and three undescribed species (Fig. 48), one of them identical to sp.nov. 24 in Takahashi (1981; ice samples from Lützow-Holm Bay, Antarctica). Another species is similar to *Parvicorbicula quadricostata* although there are differences in size and in morphological details of the lorica. It is interesting that all new forms possess elaborate posterior stalks. This might be an adaptation to the interstitial life in ice. Other flagellates usually found in interstital habitats were seen in the ice, including the dinoflagellates *Amphidinium pellucidum* and *A. semilunatum*, the euglenid *Anisonema* cfr. *acinus*, *Protaspis* spp and *Phyllomonas simplex* (in.sed.).

Observations on Selected Groups

The species composition of the planktonic choanoflagellate (*Choanoflagellida, Acanthoecidae*) fauna appears to be similar throughout the Antarctic waters (e.g. Takahashi, 1981; Buck & Garrison, 1988; Thomsen et al., 1989). The most important individual species were *Bicosta spinifera*, *Crinolina aperta*, *Diaphanoeca pedicellata* and above all *Parvicorbicula socialis*. All species observed in the plankton have been recorded previously from Antarctic waters. Very little is known about distribution and abundance of choanoflagellate species. Buck & Garrison (1988) and Thomsen et al. (1989) suggest a dramatic change in species composition moving from the ice edge towards the open sea.

During the 1st transect (Fig. 49), Choanoflagellates were abundant in the southern part of the Confluence area (Sta.147,149). Weddell Sea stations and the Confluence station dominated by the *Corethron criophilum* and the cryptomonad were almost without choanoflagellates. The most common choanoflagellate species along this transect were *Crinolina aperta*, *Diaphanoeca pedicellata* and *Parvicorbicula socialis*.
At the 2nd transect (Fig. 50) along the 47th meridian differences between the stations were less pronounced. However, also on this transect there is a gradual decrease in abundance towards the southernmost stations. The general species composition is markedly different from that observed on the first transect. The dominant species were *Bicosta spinifera, Calliacantha natans* and *Parvicorbicula socialis.*

Choanoflagellates are believed to multiply by mitotic division of the protoplast. In most species, the cell produces the number of costal strips needed to form the new "house" of a daughter cell prior to division. Following division of the protoplast, one daughter cell remains in the old "house", whereas the other daughter cell is liberated from this together with a "complete construction kit" for a new lorica, which is assembled in a few minutes. A number of choanoflagellates (e.g. *Bicosta spinifera, Calliacantha natans, Calliacantha simplex, Cosmoeca ventricosa)* occur in small and large varieties, which differ only in the size of the lorica. Costal strips from the large specimens of *Bicosta spinifera* are considerably longer than the protoplast. It has remained an enigma how the cell manages to produce these strips intracellularly.
The present observations indicate, however, that the cell is temporarily prolonged at the posterior end (Fig. 51[A]) in order to produce such long costal strips. To our surprise we observed that also the small cells of *Bicosta spinifera* frequently had a posterior prolongation similar in size to that of the large forms (Fig. 51[D]). This indicates that such small cells would, after the next cell division, 'jump' in size and belong in the population of large cells. The nanoplankton samples from sta.159 contained approximately 20.000 cells/litre of *Bicosta spinifera*, of these 60% were large forms and 40% were small forms. The size distribution within 324 specimens is given in Fig. 52. *Bicosta spinifera* from the stations along the second transect were analyzed with respect to lorica size (Fig. 53a,b). Scotia Sea samples (Sta.160-163) contained almost exclusively large forms, whereas samples from the Confluence area and the Weddell Sea showed a predominance of small forms. Sta.159 (Fig. 52) appears to be unique in having almost equally sized

populations of small and large cells. Cells of all sizes preparing for division by producing large costal strips were recorded from Sta.159 (Fig. 52; division events). Abrupt changes in size occur in other groups of unicellular organisms (e.g. the diatoms) and are here related to sexual reproduction. It is tempting to envisage that the 2-peaked size distribution observed in *Bicosta spinifera* is also related to sexual reproduction. If so, the large specimens may represent the diploid generation, whereas the smaller cells are haploid and may function as gametes. The small cells forming long costal strips, and thus likely to 'jump' to be included in the large size group after division, may be interpreted as planozygotes. Observations of *Bicosta spinifera* populations on the second transect suggest that populations of large or small cells only may persist, indicating that both types of populations are capable of mitotic divisions (Fig. 51[A, B]).
To investigate whether different ploidy levels exist in *Bicosta spinifera,* the DNA-contents of proflavine stained specimens will be examined. Finally, it should be mentioned that also *Calliacantha natans* occurred in two size variants along the second transect, showing a distribution pattern similar to that of *Bicosta spinifera.* Large specimens dominated in the Scotia Sea area, while the vast majority of cells in the Confluence area were small. Are the unimodal, size distributional patterns observed in the Confluence area the result of selective grazing?

The dinoflagellates (*Dinophyceae, Gymnodiniales*), colloquially known as the naked or unarmoured dinoflagellates, are one of the most poorly known groups in the phytoplankton, mainly because they do not preserve well. Live cells from net and water samples were studied in detail by light microscopy using flash microphotography for documentation. Almost 40 different species were observed and about 30 of these are likely to be undescribed taxa. Naked dinoflagellates are rarely dominating but appear to be almost ubiquitously present in marine waters. At least half of the species observed here are heterotrophic and may be an important component of the microbial food web. A series of samples were preserved with the intention of counting and estimating the biomass of the naked dinoflagellates in the investigated area. With the species composition known from the examination of the live samples, it might be possible to recognize at least some species in the preserved samples and enable us to carry out cell countings.

Prymnesiophyceae (Coccolithophorids) were present in almost all water samples examined. In the Scotia Sea area, the dominant organism in the nanoplanktonic fraction (organisms < 20 µm) was the coccolithophorid *Emiliana huxleyi.* It was also present, though more scattered, in the Confluence area, whereas it appeared to be absent in the Weddell Sea area. In the ultraplanktonic fraction (organisms < 5 µm), a coccolithophorid community was found to be a characteristic component of the plankton in most areas including the Scotia Sea, the Confluence, and the Weddell Sea. A detailed description of this community is only possible after electron microscopical examination of the whole mounts prepared. It is, however, evident from light microscopical examination of dried preparations, that the dominant species are *Trigonaspis melvillea* and *Wigwamma antarctica* (both described from the Weddell Sea). Counting of the Lugol-fixed samples from this cruise may give, for the first time, an indication of the ecological importance (density and biomass) of these flagellates in Antarctic waters. An ultraplanktonic community of coccolithophorids is well-known from the

arctic/subarctic region, and also recently described from the Antarctic (Thomsen et al., 1988). A comparison between the communities of the two polar regions shows considerable differences at the species level. At the generic level, it has so far been possible to accommodate Antarctic species within the established arctic/subarctic genera.

Conclusions

The most important general trend observed during the cruise is the transition from a mixed net-plankton/nanoplankton community towards a highly uniform nanoplankton dominated system especially in the Weddell Sea area. On the first transect only the southernmost Weddell Sea stations were dominated by nanoplanktonic species, whereas at the end of the cruise period, only samples from the Scotia Sea contained significant amounts of larger phytoplankton organisms. Hydrographical, physical and chemical conditions can apparently not explain the changes from net/nanoplankton dominated communities to those dominated entirely by nanoplankton. Mesocosm grazing experiments with Krill, *Euphausia superba*, (see § 4.2.12) have shown such changes to occur as a result of grazing. After having grazed down the diatoms, the Krill was removed from the culture tanks and a nanoplankton community, similar to that found in the Weddell Sea and in the Confluence Area during the latter part of the cruise, developed. The plankton of the Weddell Sea and the Confluence Area were dominated by flagellates rather than diatoms. The reddish-brown cryptomonad is probably the most abundant individual species. To our knowledge this is the first time an Antarctic ecosystem is found to be dominated by a cryptomonad species throughout a vast geographical area, therefore estimation of its biomass is particularly important. This will be one of our main goals in the period following this cruise.

Literature Cited

Buck, K.R. & Garrison, D.L. 1988. Distribution and abundance of choanoflagellates (Acanthoecidae) across the ice-edge zone in the Weddell Sea, Antarctica. Mar. Biol. 98: 263-269.

Takahashi, E. 1981. Loricate and scale-bearing protists from Lützow-Holm Bay, Antarctica. I. Species of the *Acanthoecidae* and the *Centrohelida* found at a site selected on the fast ice. Ant. Rec. 73: 1-22.

Thomsen, H.A., Buck, K.R., Coale, S.L., Garrison, D.L., Gowing, M.M. 1988. Nanoplanktonic coccolithophorids (Prymnesiophyceae, Haptophyceae) from the Weddell Sea, Antarctica, Nord. J. Bot. 8: 419-436.

Thomsen, H.A., Buck, K.R., Coale, S.S., Gowing, M.M. & Garrison, D.L. 1989. Nanoplankton from the Weddell Sea, Antarctica, with particular emphasis on the choanoflagellates (Acanthoecidae, Choanoflagellida). (in prep)

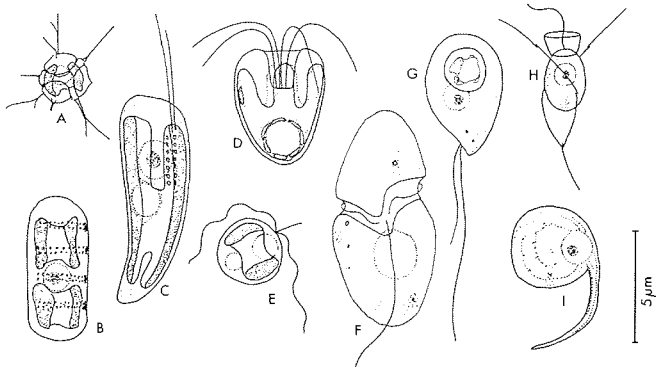

Fig. 47.
The typical nanoplankton community from the Weddell Sea:
A. *Triparma* sp.,
B. *Nitzschia* sp.,
C. *Cryptomonad*,
D. *Pyramimonas* sp.,
E. *Phaeocystis Pouchetii*,
F. *Cyrodinium* sp.,
G. The "Droplet",
H. *Bicosta spinifera*,
I. The Amoeba

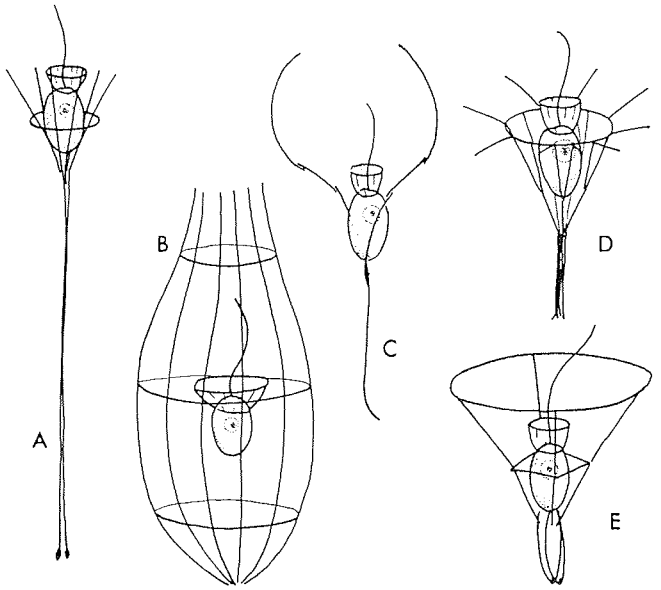

Fig. 48.
Choanoflagellates from the ice community (A,B,C: undescribed species; D: *Diaphanoeca multiannulata* aff.; E: *Bicosta antennigera).*

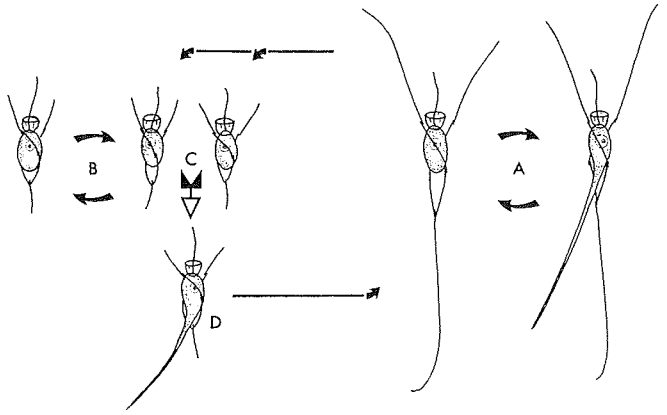

Fig. 51.
A hypothetical choanoflagellate life cycle (*Bicosta spinifera*).
A: vegetative division of diploid specimens;
B: vegetative division of haploid specimens;
C: fusion of gametes;
D: Planozygote in preparation for lorica enlargement.

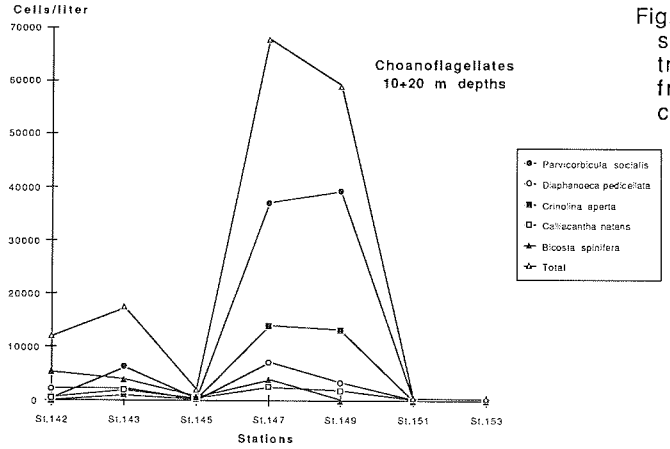

Fig. 49. The abundance in surface water samples (1st transect) of the most frequently observed choano-flagellate species.

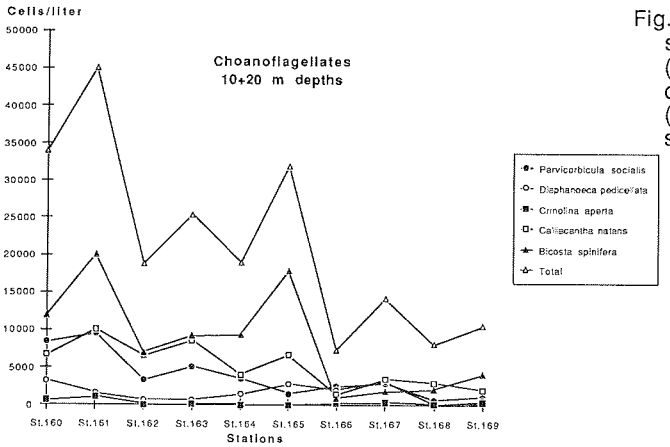

Fig. 50. The abundance in surface water samples (2nd transect) of five choanoflagellate species (same sequence of species as in Fig.49).

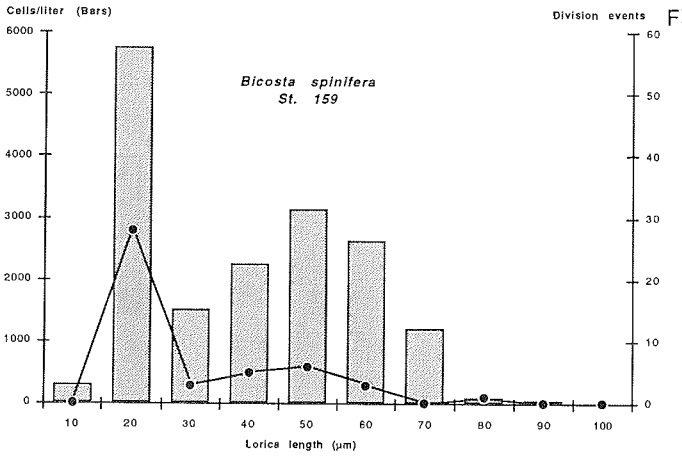

Fig. 52. The variation in *Bicosta spinifera* lorica length (µm) encountered in surface water samples from Sta. 159. Notice the bimodal distribution. The line graph shows division events (i.e. cells with posterior cell prolongations) observed while examining a single droplet of dried cells.

Fig. 53 a,b. The variation in lorica length of surface water *Bicosta spinifera* populations along the 2nd transect. Small cells predominate at Sta.164 and at St. 165 .

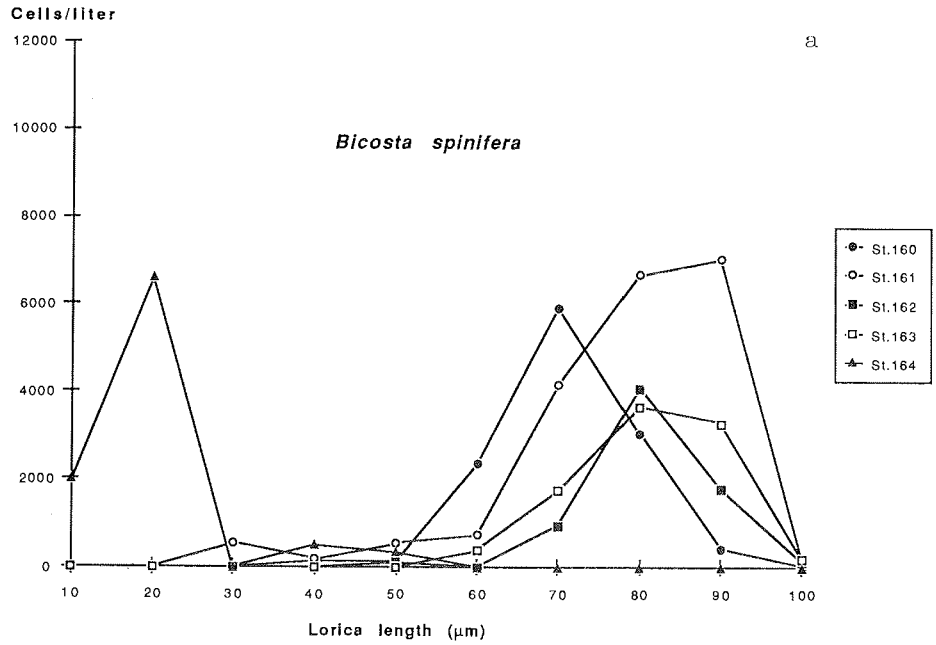

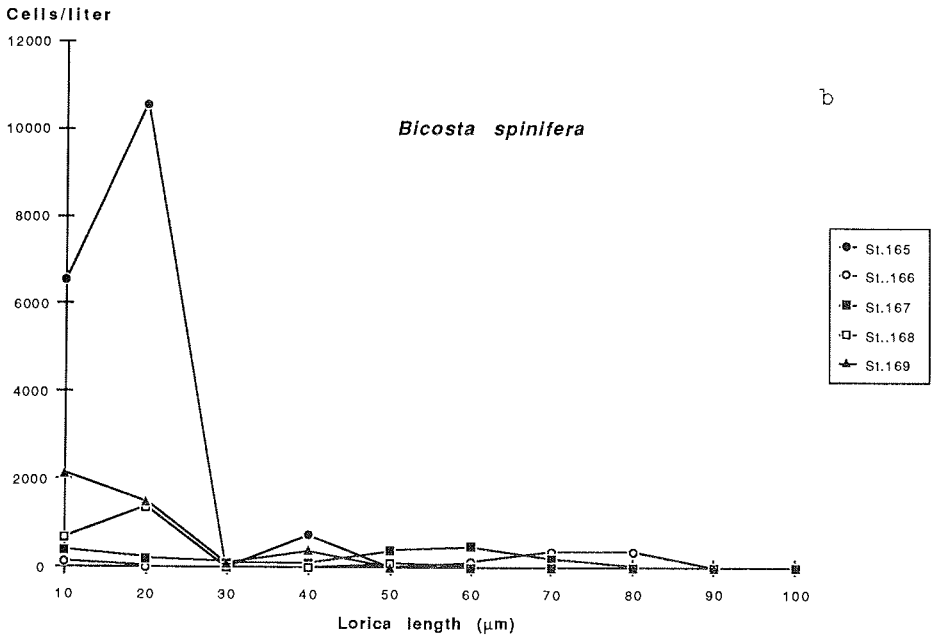

4.2.10 The microbial loop

S. Becquevort

Objectives

The importance of the microbial food web in most marine ecosystems is now generally recognized. A significant fraction of primary production is channelled via dissolved organic matter and utilized by planktonic bacteria. Grazing by phagotrophic nanoprotozoa is the major process of bacterial biomass control, allowing the transfer of bacterial production to the higher levels of the food web.

Very little is known about the Southern Ocean microbial loop, and its role in the overall functioning of the ecosystem is still a matter of controversy. Although, several authors (Hodson et al., 1981, Hanson et al., 1983) reported measurements of microbial activities of the same order of magnitude as those observed in temperate areas, others (Sorokin, 1971; Pomeroy & Deibel, 1986) claimed that a dramatic decrease of bacterial activity occurs at temperatures below 2°C which leaves a larger part of primary production for remineralization by grazers or results in accumulation of dissolved organic matter.

We developed a general methodology for measuring and understanding the role of the microbial loop in aquatic environments. Our approach is based on the direct measurement of some basic processes involved in microbial loop dynamics, together with the characterization of chemical and biological compartments concerned, i.e. the dissolved organic carbon, the bacterial biomass, the density of phagotrophic nanoprotozoa, and the growth and mortality rates of bacteria. Our purpose is to check the applicability of this approach to Antarctic waters and to provide new information to the controversy on the role of the microbial loop in that ecosystem (see also § 4.2.11).

Previous measurements carried out in the Prydz Bay during late summer 1987 (Billen et al. 1988) indicate that the overall importance of the microbial loop does not differ much in this area compared to temperate marine systems. However, a much larger delay was observed in the response of bacteria to phytoplankton development. The existence of such a delay would explain the low bacterial activities measured by several authors at the early stage of the vegetation season. During the EPOS cruise, we had the opportunity to test this assumption in the Scotia-Weddell Sea area during the vegetative season and to enlarge our knowledge of the importance of the microbial loop in the Antarctic ecosystem.

Work at sea

Routine measurements

Samples were collected in the surface mixed layer at each micro- and mesostation along different transects, 49°W, 47°W and marginal ice zone.
Bacterial production was measured by ^{3}H-thymidine incorporation in bacterial DNA. Samples were collected for bacterial biomass determination

and phagotrophic nanoprotozoa enumeration. These measurements will be performed at home by epifluorescence microscopy.

Extra measurements
Additional measurements were performed at different times during the cruise in the different areas characteristic of the Antarctic ecosystem studied: Scotia Sea, Confluence area, Marginal ice zone, Ice communities

They include:
(i) The study of the vertical distribution of bacterial production and the determination of bacterial biomasses and phagotrophic nanoprotozoa densities in the upper 150 meters of the water column.

(ii) The study of the diel cycle of bacterial production as measured during the time stations.

(iii) The measurement of bacterial mortality. This refers to the loss of functional and morphological integrity of bacteria, including lysis and destruction of genetic material. The method used consists in following the disappearance of radioactive tracer from the DNA of ^{3}H-thymidine-labeled bacteria. Selective filtration and use of eukaryotic metabolic inhibitors allow distinguishing between grazing by heterotrophs and bacterial mortality due to the other causes.

In addition, control by temperature of these mortality rates and bacterial production has been occasionally measured.

Preliminary Results

Some first results on bacterial production and bacterial mortality rates are reported here. An average bacterial biovolume of 0,05μm^3 was used to convert bacterial cell production into bacterial carbon production. Accurate biovolumes will be calculated at home for each sample. Bacterial production rates will be, therefore, reevaluated later. Data reported here have to be considered as trends and not as exact values.

Table 12: Geographical and time variations of bacterial production ($\mu g\ C\ l^{-1}\ h^{-1}$) in the upper mixed layer along transects 49°W

Transect 49°W

AREA	PERIOD 26 - 30 Nov. 88	PERIOD 10 - 23 Dec. 88	PERIOD 27 - 31 Dec. 88
Scotia Sea	0.0108	0.0522	0.0534
Confluence	0.117-0.387	0.0344-0.041	0.1772
Marginal Zone	0.0032-0.0219	0.0288-0.0744	0.0313-0.0894

Table 12 (cont'd.): Geographical and time variations of bacterial production ($\mu g\ C\ l^{-1}\ h^{-1}$) in the upper mixed layer along transects 47°W

Transect 47°W

AREA	PERIOD 13 - 16 Dec. 88
Scotia Sea	0.0289-0.0335
Confluence	0.0379-0.0580
Marginal Zone	0.0123-0.0390

Table 13: Bacterial mortality

AREA	BACTERIAL MORTALITY grazing h^{-1}	non/grazing h^{-1}
Scotia Sea	0.002	0.0016
Confluence	0.0039	0.0019
Marginal Zone	0.0031	0.0018

Tabs. 12 present data relative to geographical and time variations of bacterial production in the upper mixed layer along transects 49°W and 47°W. Examination of this table indicates that the lowest bacterial production rates are to be found in the marginal ice zone whereas the highest ones are located in the Weddell-Scotia Confluence, specially after the "pillage" of diatoms by Krill. In this case, the delay in the response of bacteria to phytoplankton is particularly short (Fig.54). At a higher time scale, we had observed an increase of bacterial production on repeating the 49°W transect (Tab. 12), the Weddell-Scotia Sea Confluence area excepted. However, subsurface measurements must be carefully interpreted with regard to the vertical profiles. Fig.55.a,b,c illustrate the vertical distribution of the bacterial production for three characteristic stations of the studied area of the Antarctic ecosystem. Examination of these figures indicates higher bacterial production rates in the mixed layer with maxima occurring between 20 and 40 meters. Below this depth, bacterial production decreases down to very low values. In the Confluence area however, a second peak was observed at 80 meters. This has to be correlated to the very complex physics of this area, which indicates warmer water mass at this depth (see § 4.1.1). As a general rule, vertical profiles of bacterial production rate will be carefully examined according to the physics of the water column and the availability of dissolved organic matter. Integrated values of bacterial production will be calculated later on the basis of the knowledge of the mixed-layer depth. These values will be compared to phytoplankton availability and activity.

Preliminary results on sea ice communities indicate very high uptake rates of ^{3}H-thymidine, i.e. about one order of magnitude greater than in the adjacent water column. Their importance compared to planktonic bacterial uptake will be deduced only after measurement of bacterial biomass which will lead to an accurate estimate of absolute rates of bacterial growth.

Tab. 13 reports data of bacterial mortality. These are significantly lower than those measured in temperate marine systems. This apparently contrasts with data of direct microscopical observations indicating high numbers of bacteriovores. However, ingestion rates can vary greatly depending on protozoan cell size, total bacterial abundance and temperature. Results of Tab. 14 will be, therefore, reexamined carefully when data relative to the measurements mentioned above will be available.

References.

Billen, G., C. Lancelot & S. Mathot, 1988. Ecophysiology of phyto- and bacterioplankton growth in the Prydz Bay area during the austral summer, 1987. II. Bacterioplankton activity. In: Proceedings of the Belgian National Colloquium on Antarctic Research. Brussels, Oktober 20, 1987. Prime Ministers Services

Hanson, R.B., H.K. Lowery, D. Shafer, R. Sorocco & D.H. Popoe, 1983. Microbes in Antarctic waters of the Drake Passage: vertical patterns of substrate uptake, productivity and biomass in January 1980. Polar Biol.2: 179-188

Hodson, R.E., F. Azam, A.F. Carluci, J.A. Fuhrman, D.M. Karl & O. Holm-Hansen, 1981. Microbial uptake of dissolved organic matter in McMurdo Sound, Antarctica. Mar.Biol.61: 89-94

Pomeroy, L.R. & D. Deibel, 1986. Temperature regulation of bacterial activity during the spring bloom in Newfoundland coastal waters. Science 233: 359-361

Sorokin, Y.I., 1971. On the role of bacteria in the productivity of tropical ocean waters. Int.Rev.Ges.Hydrobiol.56: 1-48

Figure 54: Time variations of chlorophyll a (data of G. Jacques) and bacterial production in the upper layer. Time station 14/157

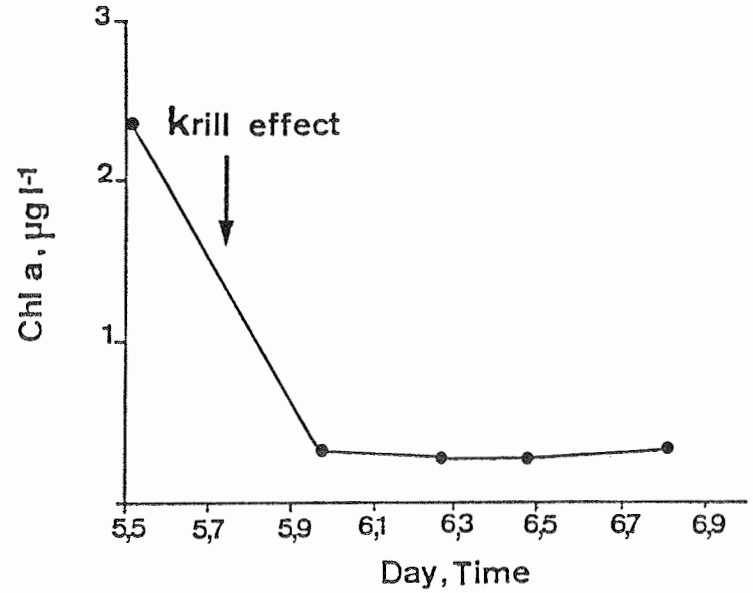

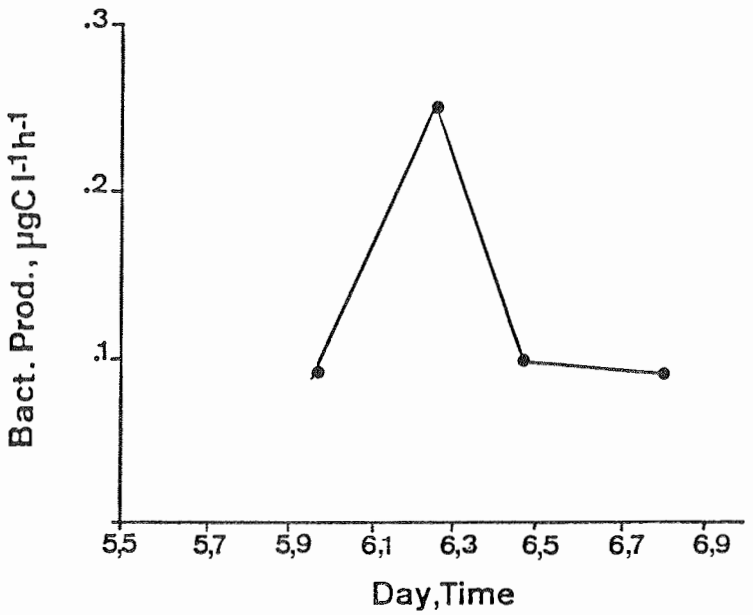

Figure 55: Vertical profiles of bacterial production in different characteristic areas: a- Scotia Sea, b- Confluence, c- Marginal zone

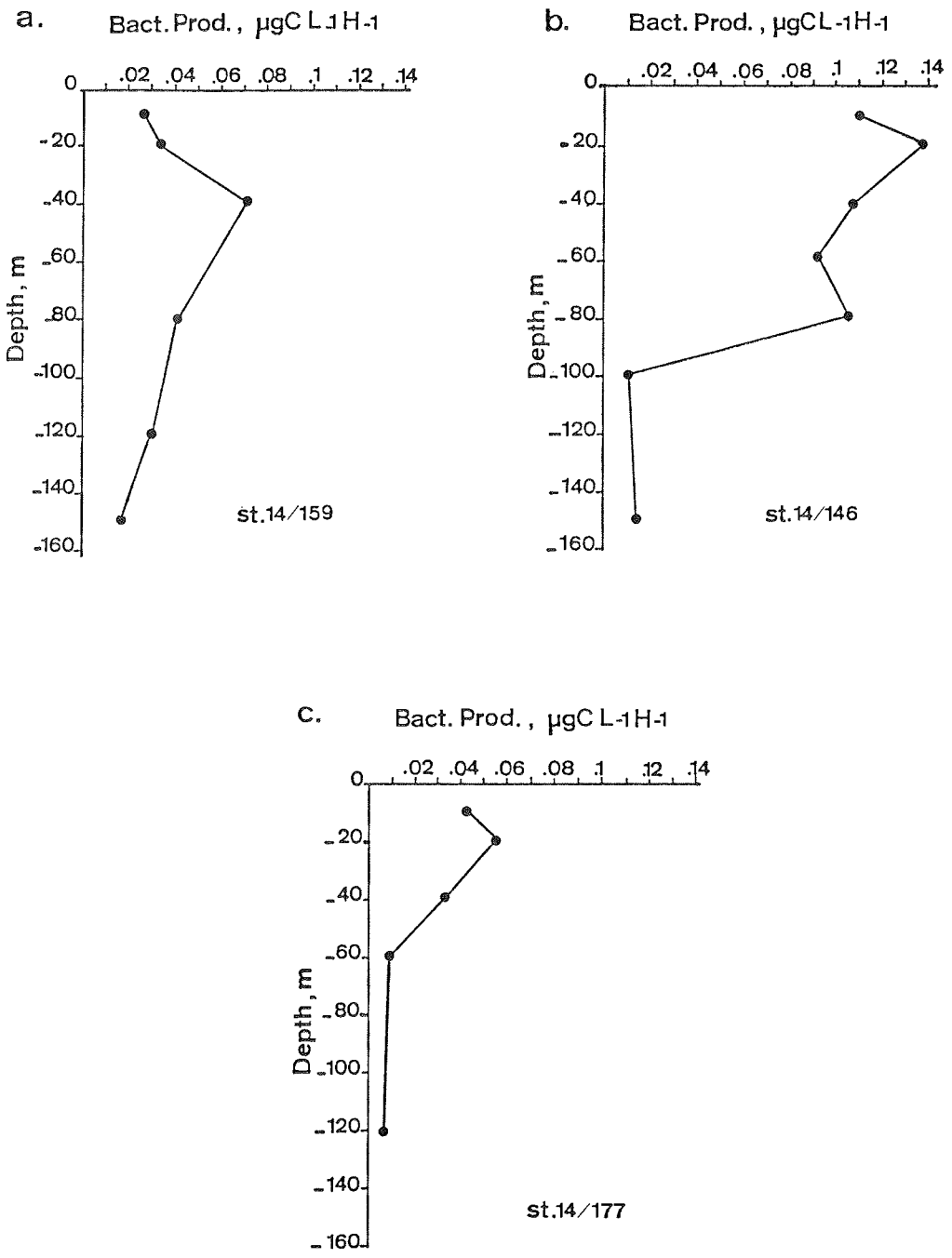

4.2.11 Experiments with the Microbial Food Web

P. Bjornsen, J. Kuparinen

Work at Sea

Bacterioplankton carbon net production was estimated from incorporation of tritiated thymidine (5 nM) during 1 hour incubations. Samples were filtered onto 0.2 µm cellulose acetate filters and extracted 10 times with cold trichloroacetic acid. Incorporation rates were converted into net carbon production by multiplication with 1,100 cells per femtomol thymidine, 0.045 μm^3 per cell and 2.7 pgC per μm^3.

Incorporation of tritiated leucine (10 nM) was measured analogously to thymidine incorporation and expressed arbitrarily as nmol per litre and hour.

Bacterioplankton biomass will be estimated from counts of acridine orange stained cells in epifluorescence microscope combined with cell volume measurements by image analysis or by calibrated ocular grid.

Primary productivity in the microcosm experiments was measured from 4 hour incubation of 8 ml samples with 4 µCi of $NaH^{14}CO_3$. Incubations were stopped by adding 200 µl of 1-N HCl. Four ml aliquots were allowed to stay in the fumehood for at least 24 hour to release unassimilated inorganic ^{14}C-carbonate, before addition of 7 ml of PCS scintillation cocktail. Parallel dark incubations were subtracted as blanks. Dissolved inorganic carbon was measured by infrared gas analysis.

Chlorophyll a was measured fluorometrically from triplicate samples filtered on GF/F filter and extracted in ethanol (94%) for 24 hours. Calibration was done by spectrophotometry according to Lorenzen (1967) using chl. extracts from a flagellate dominated community.

Samples for POC measurements were filtered onto precombusted GF/F filters for infrared gas analysis at home.

Conversion Factor Experiments

The uptake of tritiated thymidine incorporation (TTI) into bacterial macromolecules as estimators of bacterial production relies on conversion factors from the measured thymidine incorporation to cell production, and further to produced biovolume and carbon net and gross production. These conversion factors can be obtained theoretically or empirically, by comparing different growth estimators in controlled systems. Only a limited number of such experiments have been carried out in open ocean systems, particularly in Antarctic waters. While tritiated thymidine is supposed to be incorporated exclusively into bacterial DNA, and thus to be an estimator of bacterial cell production, tritiated leucine is presumably incorporated mainly into bacterial protein, and may thus serve as a direct estimator of bacterial biomass production. The ratio of leucine to thymidine incorporation would then indicate the mean size of the produced bacteria.

We evaluated the thymidine and leucine incorporation methods in a number of batch experiments, where sterile-filtered ambient sea water was inoculated with a natural assemblage of bacterioplankton obtained as a one micron filtrate. The growth of bacteria was followed during 12 days by daily samplings for measuring incorporation of thymidine and leucine, for counting and sizing of bacterial cells by epifluorescence microscopy, and for determination of POC. In some batches, the medium content of dissolved inorganic carbon (DIC) had been reduced to <50 µM by acidification, bubbling and reneutralization to pH 8. These batches further allowed us to assess the bacterial respiration by measuring the increase of DIC by infrared gas analysis. Comparison of produced DIC with produced POC will reveal bacterioplankton growth efficiency, and thereby contribute to the discussion whether the microbial loop acts as a link or a sink in the pelagic carbon metabolism. In two experiments nitrate uptake and remineralization was followed by LG using ^{15}N.

Determinations of POC and cell numbers and volumes will be done at our home laboratories before the set of conversion factors can be estimated. From the measurements done on board it was apparent, that the filtered sea water supported a growth of bacteria far above in situ rates. Increases in DIC indicated substrate consumptions during 6 days of 100 - 500 µg C per litre. A tentative relationship between leucine incorporation and DIC production was established, which if extrapolated to in situ measurements of leucine incorporation suggests bacterial respiration to amount to about 100 mgC per m^2 and day as an order of magnitude.

Microcosm Experiments

Two microcosm experiments of 12 days' duration were carried out in 100 litre aquaria on board. The aims of these experiments were primarily to study trophic interactions and control mechanisms within the microbial food web, by comparing development patterns of differently manipulated microcosms, and secondly to establish carbon balances for each microcosm in order to quantitatively assess the transfer of matter through the microbial loop.

Six perspex aquaria of 100 litre were filled at Sta.149 (Weddell Sea) and 173 (Southern Confluence). We warmly acknowledge the assistance of several volunteers, who increased their gorilla index[1] whilst helping us.

The aquaria were manipulated in a factorial pattern with respect to light intensity (approximately 90 vs. 5 µE/m^2sec), concentration of inorganic nutrients (ambient vs. double concentration of nitrate and phosphate) and size fractionation (<200 µm vs <20 µm or <5 µm). Some of the small fractions were incubated in 2 litre polycarbonate bottles.

The microcosms were sampled every second day for measurements of Chlorophyll a, POC, flow cytometry (during exp. 2), primary production, bacterioplankton production, bacterial biomass and biomass of auto- and

[1] The gorilla index is defined as the relative arm length divided by the slope of the forehead

heterotrophic nano- and microplankton. Inorganic nutrients were measured at start and end of the experiments.

Chlorophyll a values for selected microcosms are showed in Fig. 56 and 57. The phytoplankton was dominated by nanoflagellates, and in the second experiment almost exclusively by cryptomonads. During the first experiment, chlorophyll a increased exponentially in all microcosms with no apparent lag phase. Nutrient and light manipulations significantly affected the rate of increase. Fractionation at 20 µm and 3 µm reduced the increase rate, indicating that grazers smaller than 200 µm were not a controlling factor for the build up of phytoplankton biomass. In the second experiment, however, micrograzers (20-200 µm) had a significant impact on the development of chlorophyll a. In the low light microcosms, these organisms (dominated by dinoflagellates and the so-called "droplet amoeba", (see § 4.2.12) were capable of keeping the cryptomonads in check, while the parallel 20 µm screened microcosm showed steadily increasing chlorophyll concentration. In the high light microcosms, chlorophyll increased until nitrate depletion at day 8-10. For the unenriched microcosms, nitrate depletion occurred at 12-14 µg Chlorophyll a per litre, several fold less than expected from conventional conversion factors. Part of the "missing" nitrogen may have been immobilized in heterotrophic biomass and in dead organic material. While ignoring the grazers larger than 200 µm, our experiments clearly demonstrated the controlling potential of micrograzers at a late stage of a bloom scenario, in relation to the more traditionally considered "bottom-up" control by nutrient and light availability.

The heterotrophic response to the manipulations and the induced change in phytoplankton cannot be fully evaluated before the biomasses have been estimated from microscopy. Only bacterioplankton production was measured on board. In the first experiment, bacterial production seemed to parallel the development of chlorophyll in the different microcosms, apparently with a response time of few days. During the second experiment, the low light microcosms showed increased bacterial production, in spite of the slower development of phytoplankton in these microcosms. Whether this difference is caused by grazing control or by higher substrate availability must await a thorough evaluation of all microbial pools.

The measured bacterioplankton production rates will be compared to actually observed changes in bacterioplankton biomass to reveal bacterioplankton mortality rates, and these estimates will further be related to biomass and development of heterotrophic nanoflagellates to elucidate functional and numerical responses of these bacteriovores and their carbon conversion efficiency. Finally the information obtained from the enclosure experiments will be applied to the collected field data on bacterial production and biomasses of bacteria and nanoflagellates.

Spatial Distribution of Bacterioplankton Production Across the Confluence

The horizontal and vertical variation of bacterioplankton production rates along transects 2 and 3 (47°W and 49°W) are shown as isopleths in Fig. 58 and 59. Bacterioplankton production seemed to be restricted to the upper 100 meters of the water column with highest values close to the surface. Along the transects, highest bacterial production rates were found in the

Confluence area. The spatial distribution of bacterial production showed striking covariance with chlorophyll a (r=0.68, n=66) and with ammonia.

At each station, leucine incorporation was proportional to thymidine incorporation (r=0.911, n=66) along the vertical profile, suggesting constant size of the active bacteria, although epifluorescence microscopy of the total bacterial assemblage (comprising active as well as inactive cells) indicated that the mean bacterial cell size decreased with depth. Counts of bacteria cells at station 143 showed a vertical distribution similar to thymidine uptake, with cell numbers ranging from 3.8 10^5/ml at the surface to 1.5 10^5/ml at 200 m.

Figure 56 : Chlorophyll a, Microcosms Experiment 1

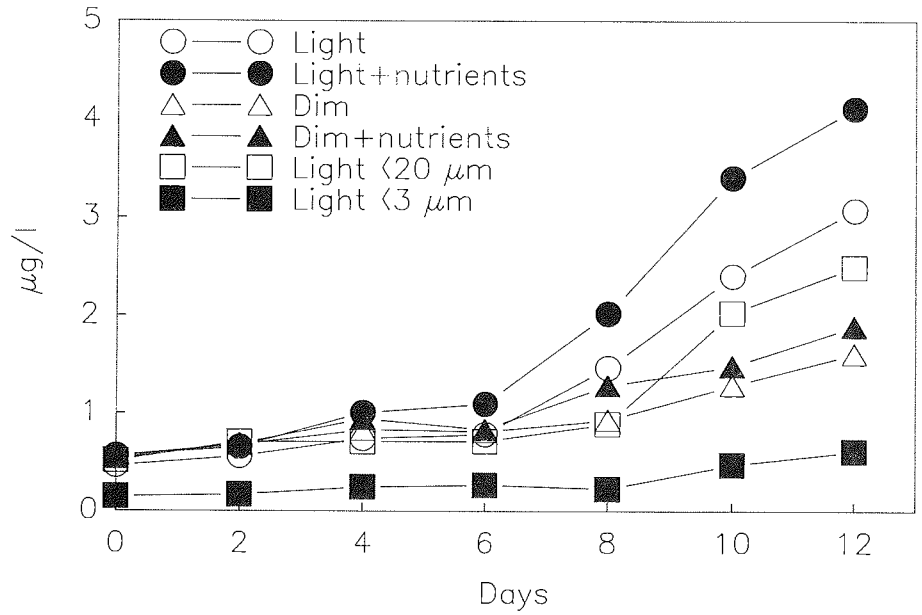

Figure 57: Chlorophyll a, Microcosms Experiment 2

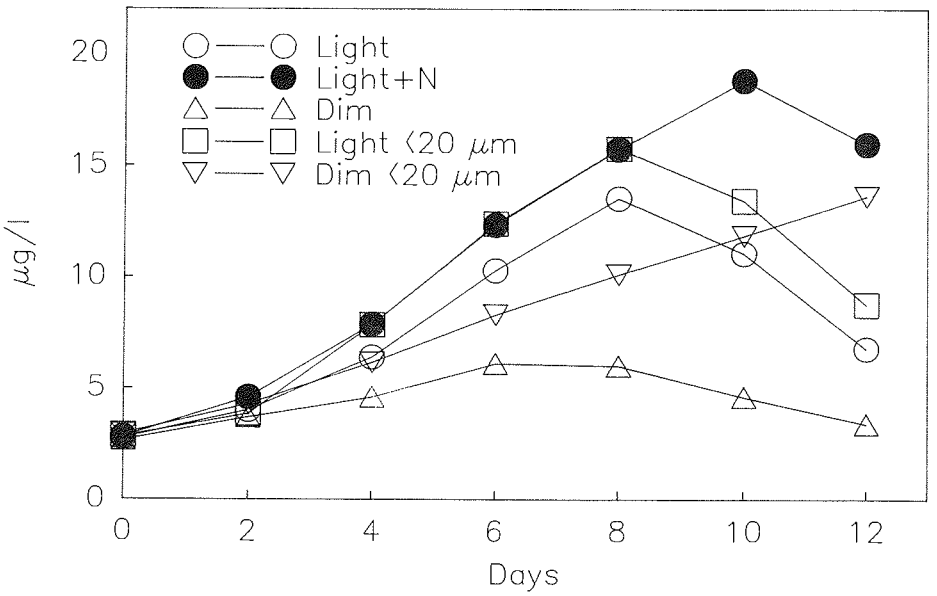

Figure 58: Profile of Bacterioplankton Production in Transect 2

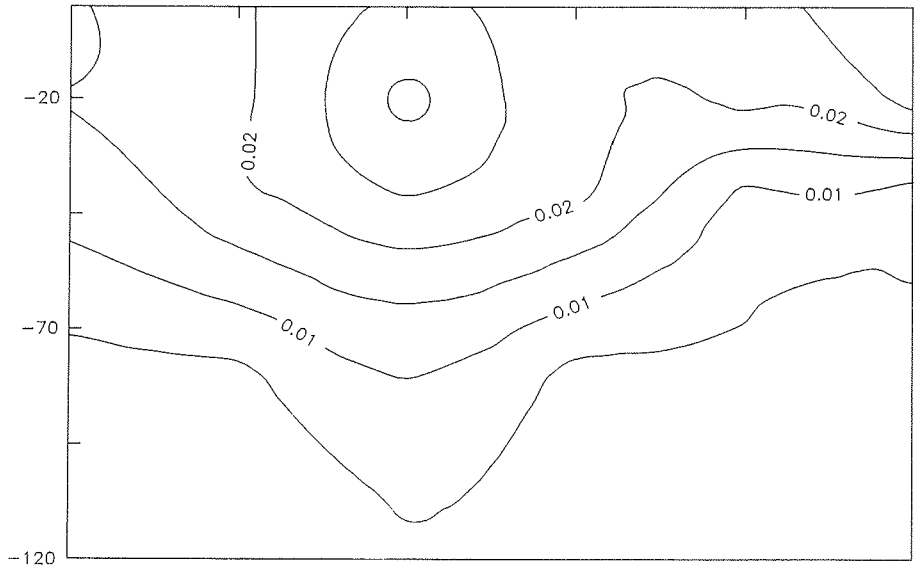

Figure 59: Profile of Bacterioplankton Production in Transect 3

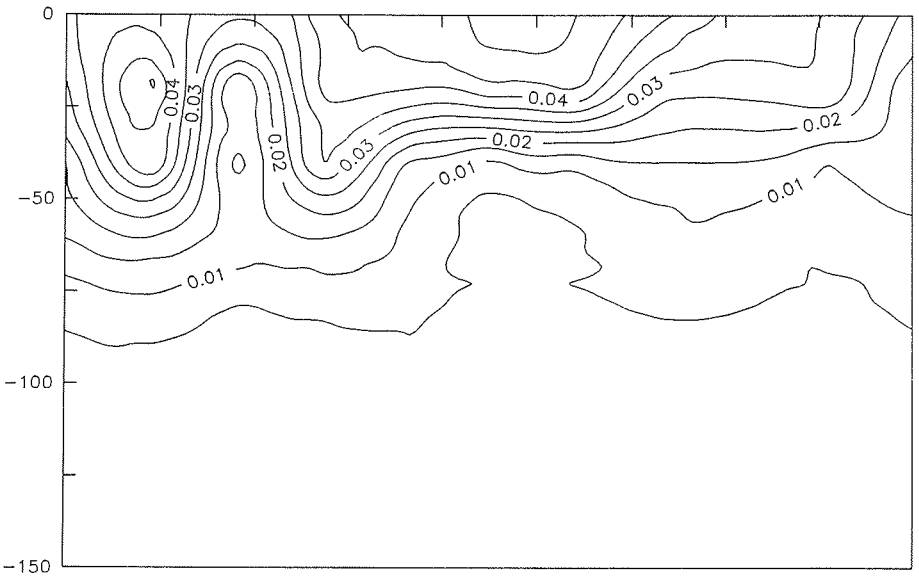

4.2.12 Macro- and Micrograzing Effects on Phytoplankton Communities

V. Alder, J. Cuzin-Roudy, G. Fransz, E. Granéli, J. Larsen, M Rabbani, H. Thomsen.

Objectives

Many theories have been put forward in order to explain algal blooms in general or the growth and accumulation of specific groups or species. Such theories do not always treat the ultimate "forcing function" or do not explain the mechanisms involved. In general, theories formulated in connection with specific blooms tend to be either monocausal theories or explanations encompassing a broad suite of factors. Among the first category can be mentioned effects on algae by specific chemicals, e.g. trace metals (Ingle and Martin, 1971). In the second category are explanations like eutrophication or long-term climatic changes. Biotic factors in the population dynamics of phytoplankton, e.g. resource competition (Sommer and Kilham, 1985; Kilham and Hecky, 1988) and selective grazing by zooplankton have been much neglected.

Grazers have two general effects on phytoplankton: they ingest them, thereby causing mortality, but they also excrete nutrients, thereby enhancing growth. The net effect on phytoplankton can be both positive and negative, depending on the rate of grazing (Carpenter et al., 1985). Grazing on phytoplankton as an important species-specific loss factor has been getting increasing attention during the last decade as it has become evident that abiotic factors alone cannot explain the biomass and species composition of phytoplankton assemblages (e.g. Vanni 1987, Granéli et al., in press).

In Antarctic waters, however, phytoplankton biomass is low in spite of high levels of inorganic nutrients. Thus, phytoplankton does not utilize these nutrients fully. The reasons may be that the phytoplankton in Antarctic waters is limited by trace metals, as suggested by Martin and Fitzwater (1988) and/or that Krill (Euphausia superba) is a very efficient herbivore maintaining phytoplankton biomass at low levels.

Work at Sea

Experiments on light and nutrient (bottom up) versus grazer (top down) control of phytoplankton species composition, size spectrum and biomass were performed by us during Leg II of EPOS. See Tab. 14 for number, type of experiments stations and depths from where natural phytoplankton assemblages were sampled.

Experimental Design

All experiments, except for those using Krill, were performed in glass flasks exposed to cool white fluorescent tubes, ca 0°C, 18:6 light-dark cycle. The size of the flasks varied from 2 to 10 litres volume. The Krill experiments differed by the use of 25 litre polythene jerry cans filled with 18 litres water + inoculum of phytoplankton concentrated in a 20 µm nylon net. Every 2 or 3 days, subsamples were taken and the phytoplankton was fractionated to

less than 20 µm (filtering the water through nylon net) and to less than 3 µm after filtering through a 3 µm Nucleopore filter. The Total, < 20 µm and < 3 µm fractions were then measured as in vivo chlorophyll in a Turner fluorometer model 112. The results presented here will deal mostly with the effect on the total phytoplankton community, the other fractions will be discussed latter on. During the course of the experiments, extra samples were taken for extraction of chlorophyll a with acetone to provide a means of transforming the in vivo chlorophyll to extracted chlorophyll a values.

Table: 14

EXPERIMENT	LIGHT INTENSITY µE m^{-2} s^{-1}	STATION	DEPTH (M)
LIGHT	70 and 11	143	30
	70 and 11	148	30
	100 and 11	167	20
NUTRIENTS + VITAMINS + Fe+EDTA.	70 and 11	143	30
	70 and 11	148	30
ZOOPLANKTON IMPACT ON PHYTOPLANKTON	70 and 11	143	30
	70 and 11	148	30
	100 and 11	167	20
KRILL IMPACT ON PHYTOPLANKTON AND ZOOPLANKTON	100	158	20
	100	167	20

Light Experiments

Of all 3 experiments, Sta. 143 produced the lowest biomass (Fig. 60 a-e). The reason may be that just after the start, the temperature in the cool container rose to 8°C during the second day due to a technical defect in the container. However, the pattern was the same as for Sta. 148: growing at 70 µE m^{-2} s^{-1}, the chlorophyll concentrations attained 4 times higher values than when growing at 11 µE m^{-2} s^{-1}. For Sta. 167, however, the chlorophyll produced in the bottles exposed to 100 and 11 µE m^{-2} s^{-1} were almost the same (Fig. 60e).

Effects of Nutrients

For Sta. 143, nutrient additions had no greater stimulatory effect over phytoplankton biomass production when growing at 11 µE m^{-2} s^{-1} while Sta. 148 showed a very positive effect. At 70 µE m^{-2} s^{-1}, however, the biomass produced was 2 times higher for Sta. 143 and 3 times for Sta. 148 (Fig. 60 a-d). For the light and nutrient additions experiments we have the phytoplankton species composition and biomass only for Sta.148, as it was difficult to sediment the samples for counting on board. At this station *Chaetoceros neglectum* dominated at the beginning and end of the experiment.

Zooplankton Impact on Phytoplankton

These experiments were performed by adding different concentrations of zooplankton after collection with a Nansen net, mesh size 200 µm (Sta. 143 and 148) and with Fransz net, mesh size 50 µm for Sta. 167.

For Stas. 143 and 148 no clear effect of grazing by the mesozooplankton was found (Fig. 61). This is explained by the fact that the zooplankton was probably injured during sampling, as very few copepods and nauplii were found at the end of the experiment. For Sta. 167 additions of 5 X and 10 X zooplankton lowered the biomass in comparison with the control (where no extra zooplankton was added). For all experiments *Oithona similis* and copepod nauplii dominated the mesozooplankton community (Fig. 61)

Krill Impact on Phyto- and Zooplankton

Four jerry cans were used for the Krill experiments: Control (no additions of zooplankton or Krill), Zooplankton (ca. 10 X the natural zooplankton concentrations), Krill (Exp. Sta. 158= 6 juvenile + 2 adult Krill; Exp. Sta. 167= 6 juveniles + 2 adults, and then 4 more adults after 4 days), Krill + zooplankton (additions were a combination of the zooplankton + Krill jerry cans). In all jerry cans, phytoplankton collected with a 20 µm nylon net was added to start with a high phytoplankton level (ca. 5 µg chlorophyll *a* l^{-1}).

In both experiments with Krill, the algal biomass decreased to less than 1 µg chlorophyll *a* l^{-1} during the first 3 days. The experiment with water from Sta. 158, the Krill and Krill + zooplankton showed the same trend, and the same happened for the control and zooplankton jerry can. The explanation is the same as above: the Nansen net killed the zooplankton. For the second experiment (Sta. 167) zooplankton addition had a positive effect on the total phytoplankton community, with values above the control. During the first days of the experiments the Krill + zooplankton had a positive effect on the phytoplankton with chlorophyll values above the control. The possible explanation is that the Krill grazed first on the zooplankton; after 7 days they started to graze on the phytoplankton. For the experiment with water from Sta.158, the large diatoms such as *Corethron criophilum* and *Chaetoceros neglectum* dominated the control and zooplankton jerry cans at the beginning and end of the experiments. In Krill and Krill + zooplankton jerry cans following the removal of the Krill, the plankton community was at the end of the experiment dominated by autotrophic nanoflagellates (*Pyramimonas* sp ., *Cryptomonas* sp .) and a "droplet"-shaped heterotrophic flagellate dominated completely at the end of the experiment. The same situation was found in control, zooplankton and Krill + zooplankton jerry cans from Sta. 168, except that throughout the experiment the dominating diatom was a large *Thalassiosira* sp. Small flagellates similarly dominated at the end of the experiment. The nanoplankton community that developed in the course of the experiments was basically identical to that observed in Weddell Sea samples from the latter part of the cruise period (see § 4.2.9).

Micrograzing

To check the micrograzing effect on the phytoplankton, at the beginning of the experiments with light and/or nutrient, water was filtered through a 20 µm nylon net and with a Nuclepore 3 µm filter, and poured in pyrex bottles (2 litres). For all stations the less than 20 and less than 3 µm fractions isolated initially, increased to several fold higher biomass than the same fractions incubated in 10 litre bottles containing all the plankton; this suggests that micrograzing is a very efficient in keeping the small algae at low levels (see e.g. Fig. 63.)

Acknowledgement

We wish to thank Sigrid Schiel for the use of the Nansen net, Guy Jacques and Ulf Riebesell for some of the chlorophyll extractions, Johan van Bennekom, Leo Goeyens, Annick Masson and Fred Sörensson for the nutrient analyses, the crew for helping us to take all the 100 litres of water we needed for the experiments and finally to the chief scientist of EPOS Leg 2, Prof. Victor Smetacek for solving the technical (and other) problems in his very relaxed way.

Literature cited

Carpenter, S. R., J. F. Kitchell and J. R. Hodgson, 1985. Cascading trophic interactions and lake productivity. BioScience, 35:634-639.

Granéli, E., P. Carlsson, P. Olsson, B. Sundström, W. Granéli and O. Lindahl (In press). From anoxia to fish poisoning: The last ten years of phytoplankton blooms in Swedish marine waters. In: E. Cosper et al. (Ed.). Novel phytoplankton blooms: causes and impacts of recurrent brown tides and other unusual blooms. Springer Verlag.

Ingle, R. M. and D.F. Martin, 1971. Prediction of the Florida red tide by means of the iron index. Environ. Lett. 1: 69-74.

Kilham, P. and R. E. Heckey, 1988. Comparative ecology of marine and freshwater phytoplankton. Limnol. Oceanogr. 33: 776-795.

Martin J. H. and S. E. F. Fitzwater 1988. Iron deficiency limits phytoplankton growth in the north-east Pacific Subarctic. Nature, 331: 341-343.

Sommer, U. and S. S. Kilham, 1985. Phytoplankton natural community competition experiments: a reinterpretation. Limnol. Oceanogr. 30: 436-440.

Vanni, M. J. 1987. Effects of nutrients and zooplankton size on the structure of a phytoplankton community. Ecology 68: 624-635.

Fig. 60: Biomass (measured as chlorophyll a) produced by the phytoplankton in the bottles exposed to high (70 and 100 µE m^{-2} s^{-1}) and low (11 µE m^{-2} s^{-1}) light, and between the bottles with and without nutrient additions. (A and B = parallel bottles)

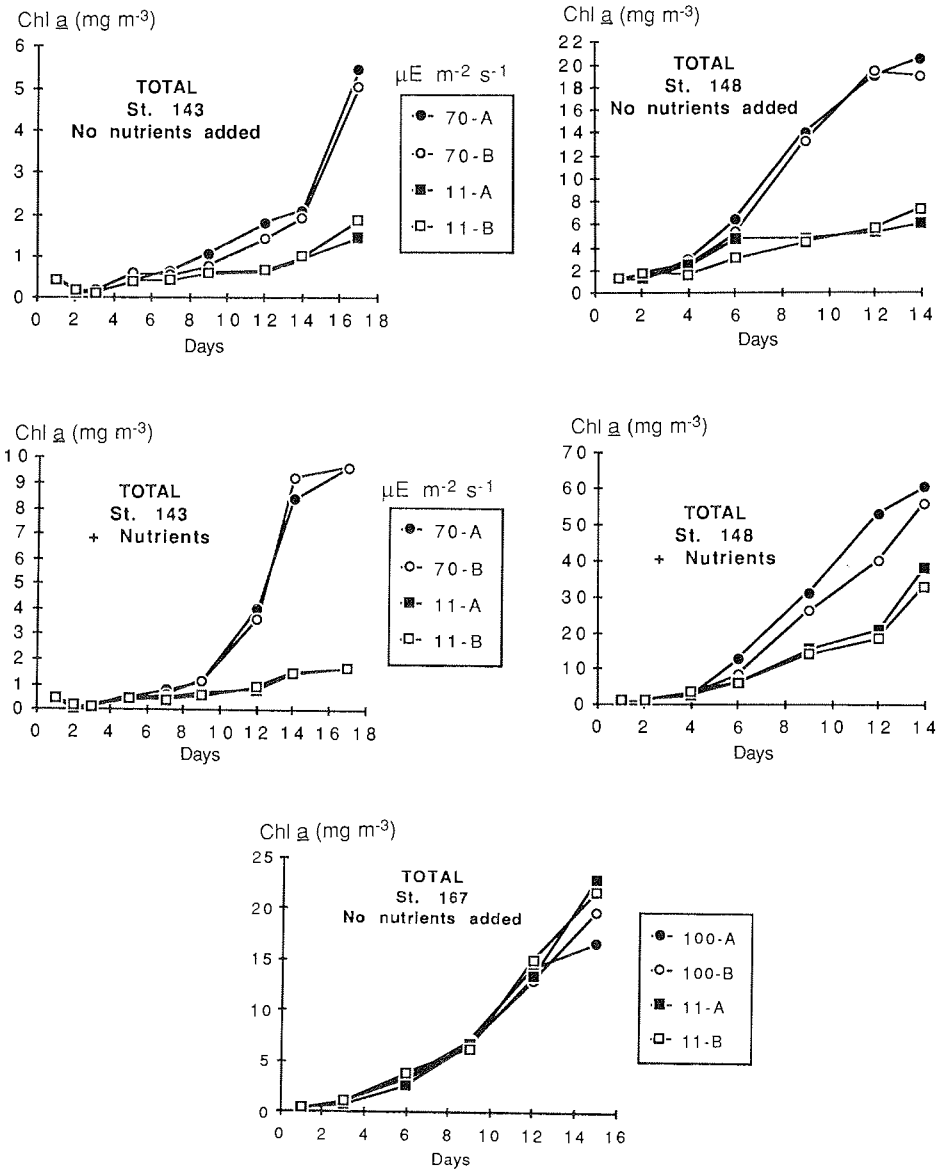

Fig. 61: Biomass (measured as chlorophyll a) produced by the phytoplankton in the bottles with and without different concentrations of mesozooplankton.

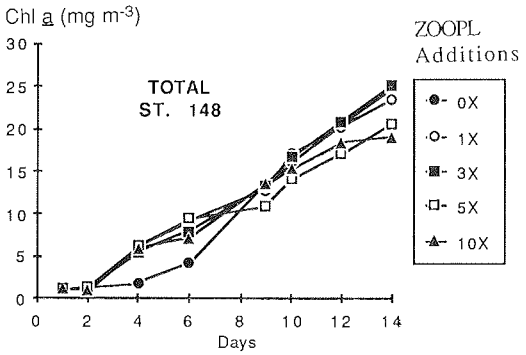

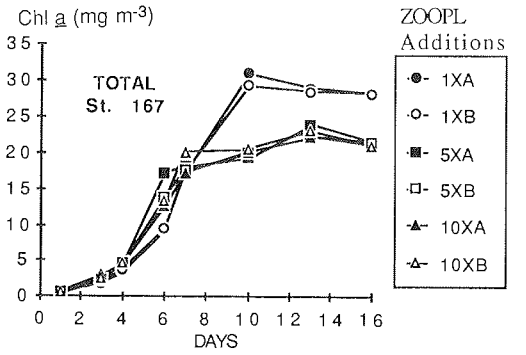

Fig. 62: Effects of Krill, mesozooplankton, and Krill+mesozooplankton on phytoplankton biomass formation. C= control, Z=10 X the natural mesozooplankton concentration, K= Krill addition (see experiment design), KZ= Krill+mesozooplankton.

Chart1

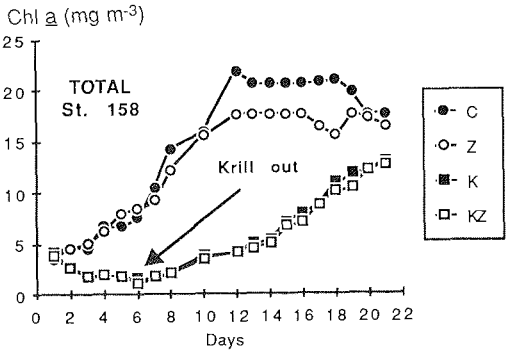

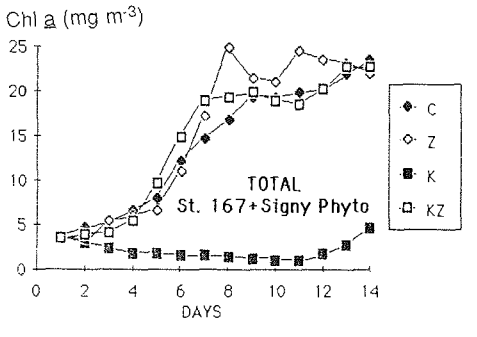

Fig. 63: Effects of micrograzers on the nano- and picoplankton biomass formation. D= Nano- and picoplankton, daily fractionated from bottles containing the whole plankton community being subject to heavier grazing than in I: where they were isolated at the beginning of the experiment and let grown alone.

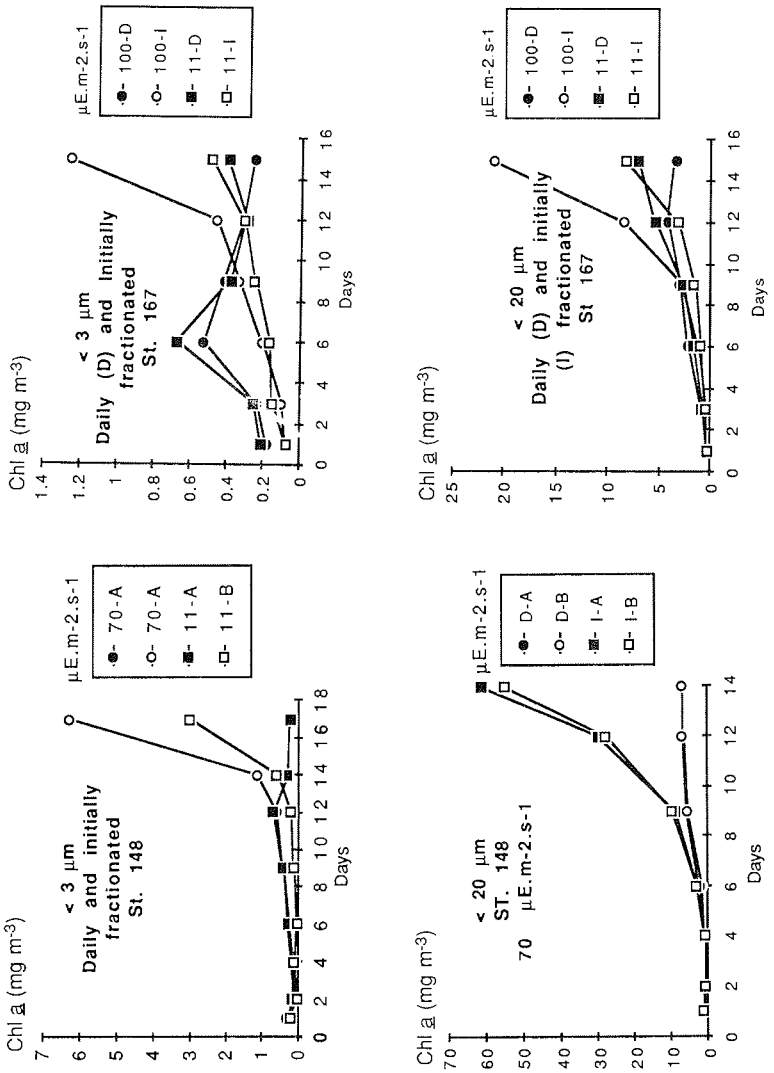

4.3 ZOOPLANKTON/MICRONEKTON DISTRIBUTION, COMMUNITY STRUCTURE AND ACTIVITY

Introduction

The zooplankton group united different expertise, interest and application of gear in such a way that the study of zooplankton distribution, development and its activity broadly covered all relevant size classes and species. The species group studied range from microplankton protozoans (Alder), herbivorous and omnivorous metazoans in the size range of 10 to 10,000 µm (Fransz, Gonzalez, Mizdalski, Schiel) to the macroplanktonic and micronektonic organisms (Cuzin-Roudy, Schalk).

Sampling counting and experiments were conducted to clarify the main aspects of species abundance, biomass and diversity, population dynamics, spatial distribution, food uptake, growth and reproductive biology.

The following chapters highlight the approach and preliminary results of the various subgroups. However, the main results will be revealed after time-consuming quantitative analysis of the samples, which could be carried out only partially on board. After completion these results will lead to a fruitful synthesis of the zooplankton work in all its aspects, and will hopefully contribute to an explanation of the planktonic processes observed.

4.3.1 Protozooplankton - Tintinnid Distribution

V. A. Alder

Objectives

The protozooplankton of the Southern Ocean, such as ciliates (oligotrichs and tintinnids), radiolarians, phaeodarians, foraminiferans and large heterotrophic dinoflagellates, have received up to now less attention from Antarctic plankton researchers than the primary producers and the larger zooplankton. Although this group is not dominant in the zooplankton biomass, their role in the marine food web is important, since they have very high reproduction and metabolic rates and, as has been recently published, they can put a considerable grazing pressure on the lower levels of the food web (Heinbokel & Beers, 1979, Heinbokel & Coats, 1986, Verity, 1985). Ciliates feed on smaller particles - nanoplankton, flagellates, and bacteria - which are normally not utilized directly by mesozooplanktonic consumers. So they form an intermediate step between the two basic trophic levels. Therefore, a more detailed analysis of the protozooplankton community is required.

The objectives of the research during the EPOS Leg 2 cruise were:

1. To investigate horizontal, but in particular vertical distribution of the protozooplankton in relation to variability in environmental parameters:

a) Physical factors, such as hydrography and ice coverage, will be taken into account to determine whether species are useful as biological indicators of water masses.

b) Biological factors, especially relationships between different trophic levels to find out about the structure and flows in the food web.

2. To conduct a detailed taxonomic, biogeographic study on tintinnids of the Antarctic waters.

Work at Sea

Protozooplankton was sampled with three different methods:

1. Niskin bottles and rosette casts for collecting samples from various depths (10, 20, 40, 60, 80, 100, 120, 150, 180, 200, 300 m) at the micro and time stations (Sta. 144 to 193). In total, 120 litres of water were filtered from each station (about 10 litre/sample/depth). The protozooplankton was concentrated by using a 15 µm sieve. A volume of approx. 3000 litres of water was filtered by this method to obtain 300 samples.

2. Vertical hauls from 100-0, 200-0, and 300-0 m were made with a 50 µm mesh plankton net. At 12 stations, 36 samples were collected in this way.

3. During the hydrographical grid from 1 to 3 January, surface water samples were collected continuously (at the stations and in between) from

the sea water tap system of the ship, using 10, 15, and 50 µm mesh filters. In total 60 samples were collected.

All samples were preserved in an acid Lugol's solution.

Preliminary Results.

Due to the protozooplankton biomass in the area it was not possible to do on board a detailed counting of a representative number of samples with the inverted microscope because of the risk of loosing part of the sample. Thus the water samples from the Niskin bottles and rosette were preserved for qualitative and quantitative analysis in the laboratory. However, material from net catches and sediment traps offered an opportunity to get a general impression about the species composition in the area.

Table 15: Some of the most abundant tintinnid taxa in the Weddell and Scotia Sea water masses. Abundant (+++), frequent (++), rare (+), absent (-).

Taxa	Region	
	Weddell Sea	Scotia Sea
Laackmanniella naviculaefera	+++	++
Codonellopsis gaussi	+++	+++
Codonellopsis glacialis, fa typica	+++	+
Cymatocylis drygalskii, fa typica	+++	-
Cymatocylis drygalskii, fa ovata	+++	-
Codonellopsis glacialis, fa conica	++	-
Laackmanniella prolongata	++	+
Coxliella	+	?
Salpingella sp.	-	-
Cymatocylis vanhoeffeni	++	++
Cymatocylis flava	++	++
Cymatocylis affinis/convallaria (smooth horn)	++	+++
Cymatocylis affinis/convallaria (striate horn)	++	+++
Cymatocylis antarctica	-	++
Amphorellopsis sp.	-	++
Codonellopsis pusilla	-	+

Differences in species composition of tintinnids between the Weddell and Scotia Sea watermasses (Tab.15) were expected as they have been found during earlier work in the Weddell Sea (Boltovskoy et al., 1989). *Cymatocylis affinis/convallaria* (smooth and striate forms) and *Codonellopsis gaussi* were very abundant in the northern part of the transect, the Scotia Sea - Polar Front, but they were also observed in the Weddell Sea. *Amphorellopsis* sp. is typical for the Scotia Sea water mass and was only found at the northern stations. *Cymatocylis drygalskii fa typica* and *fa ovata* were very abundant in the Weddell Sea and are considered to be typical for Antarctic waters. The genera *Coxliella* and *Laackmanniella* are supposed to occur only in the Weddell Sea; however, present findings show that the latter may not be that characteristic as it was also found in the northern part of the transect in large numbers.

In general, the size of most of the tintinnid species increases from north to south, which was confirmed by material from the currently studied transect. Previous to this cruise, no data on vertical size distribution were available. The present samples show also an increase of size with depth. Is there a

relation between water temperature or density and size in this group of ciliates?

In the sediment trap samples from the southern part of the transect the large species *Cymatolocylus flava* and *C. vanhoeffeni*, which were found in the deeper water layers (>100 m), were more abundant than the smaller surface species. This may point to differences in sedimentation rates of, or grazing pressures, on the different size classes. This species has also been described as being typical for Antarctic waters, but appeared also to be present in the Polar Front - Confluence Waters at the "Scotia Sea" stations.

As a preliminary conclusion, it may be suggested that the difference between Weddell Sea and Scotia Sea water was not as distinctly present in the Tintinnid population as could be expected, and that in general a "Weddell Sea Community" was found practically along the whole section studied. This Weddell Sea Community showed similarities to the tintinnid assemblage of the retreating pack ice (Boltovskoy et al., 1989). Only very few "typical" Scotia Sea species were found at the most northern stations. Furthermore, *Codonellopsis balechii*, which occurs in high abundances at the northern part of the Antarctic Peninsula, was expected to be found in the northern part of the transect, transported eastwards by the Circumpolar Current. But this species was not found either. Did the transect really enter Scotia Sea waters or only a boundary zone? The hydrographical profiles show that at the most northern stations, only in the deeper layers (>200 m) real Scotia Sea water was present and that in the surface layer only mixed Scotia Sea / Weddell Sea water was encountered .

Further studies on species composition and morphological variation from the discrete depth layers sampled in combination with physical, chemical and biological data will reveal in greater detail distribution patterns and the value of the various species as watermass indicators.

Refrences

Boltovskoy, D, V.A. Alder and F. Spinelli, 1989 (subm.). Summer Weddel Sea microplankton: assemblage structure, distribution and abundance, with special emphasis on the tintinnina

Heinbokel, J.F. and J.R. Beers, 1979. Study on the functional of tintinnids in the Southern California Bight. III. Grazing impact on natural assemblages. Mar.Biol.52: 23-32

Heinbokel J.F. and D.W. Coats, 1986. Patterns of tintinnid abundance and reproduction near the edge of seasonal pack-ice in the Weddel Sea, November 1983. Mar.Ecol.Progr.Ser.33: 71-80

Verity, P.G., 1985. Grazing, respiration, excretion and growth rates of tintinnids. Limnol.Oceanogr.30: 1268-1282

4.3.2 Mesozooplankton - Distribution and development of Copepods

H.G. Fransz, S.R. Gonzalez, E. Mizdalski, S. Schiel

Objectives

Herbivorous zooplankton reflects in its abundance and growth rate the plankton productivity and the grazing pressure exerted on the algae. For the comparison of the productivity of water masses and the study of plankton succession in the upper 300 m, samples were collected to estimate the biomass, species and stage composition and rates of development and egg production of the zooplankton group in the size class of 50 to 10,000 µm. In this size class the different developmental stages of copepod species dominate the biomass to such an extent that this contribution is basically a copepod study.To find some answers to the intriguing question of how pelagic copepod populations can maintain themselves at the extremely low Antarctic water temperature and the short food season, the life and reproduction cycles of dominant species will be followed during the spring/summer period covered by the 3 EPOS legs. The concurrent hibernation of adult and subadult copepodids, in combination with early prebloom spawning, (Fransz, 1988) suggest that most species have either a 2-year life cycle, or a 1-year cycle with 2 subpopulations with separated spawning periods in spring and summer. Hence this contribution refers to copepod population biology as well as systems ecology.

Work at Sea

Samples were taken at two transects: along 49°W and along 47°W, both running from open water into the pack-ice. Sampling along the 47°W transect was already conducted during EPOS Leg 1 and will be repeated during EPOS Leg 3, so that a continuous series from November 1988 untill February 1989 will be available for the study of both spatial and temporal patterns in the copepod population.
During EPOS Leg 2 three different nets were deployed for sampling mesozooplankton: the 50µm Fransznet, the 200 µm Multinet (for discrete depthsampling) and the 300µm Bongonets (as a reference between the three EPOS cruises)

Fransz net.
Depth integrated samples were collected with a 50 µm vertical Fransz net hauled from 100, 200 or 300 m at 1 m/s. The volume filtered was measured with a flow meter and approached 4.2, 8.3 and 12.5 m^3 respectively. The stations sampled are arranged according to transect in Tab. 16.

At all mesostations and shelf Sta.171, one haul was made from 300 m for counting. At all other stations 3 hauls were made from different depths, at the time Sta.at noon and midnight. In addition, at all stations samples were collected from 300 to 0 m for fecal pellets (Gonzalez) and micro-zooplankton (Alder) analysis, or samples were shared for this purpose.
Except at the shelf station and the diatom patch stations near the Confluence (207 to 209), at all stations additional samples were collected to enclose copepod stages in glass ampoules for carbon determination

according to the method of wet oxidation (see § 4.2.8), and for incubation experiments to measure rates of development and egg production.

Of a total of 93 samples collected for quantitative analysis, 62 were counted on board. For counting, the samples were fractionated with a 1 mm screen to separate the larger organisms, which were identified and counted. Subsamples of 1 ml out of 50 to 500 (depending on the amount of algae in the samples) from the suspended fine fraction were pipetted into a micro-cuvette and counted at a magnification of 25x to 50x until 100 to 200 organisms were identified. Copepods were identified to species and developmental stage and counted in length classes. As far as time permitted the counts were entered into a HP85 computer to derive densities and dry weight estimates according to dry weight - length relationships (Fransz, 1988).

Live material was incubated in 5 l polyethylene buckets (Fransz, 1988), kept at 0°C for 72 h. Size fractions of 100 to 200 µm and 200 to 500 µm were incubated in 50 µm filtered sea water to study growth from shifts in mean stage. The 21x4=84 size fractions fixed before and after incubation will be analysed later. Of different dominant species 1 to 20 females were incubated in 5 l 50 µm filtered sea water. Females and eggs laid were counted after 72 h.

Table 16 : stations sampled at the two transects

STATIONS									
LEG 1; 19/10 - 12/11	84	87	89	92	96	109	117	132	135
1. Mesostations transect 49°W 26/11 - 30/11	143	145	147	149	151	153			
1. Time stations transect 49°W 03/12 - 11/12	156	157	158	159					
2. Mesostations transect 47°W 13/12 - 16/12	160	162	164	166	169				
Time station 47°W 16/12 - 17/12	169								
Shelf station 19/12	171								
Ice survey transect 49°W 20/12 - 24/12	172	173	174	175	176	177	178	179	
3. Mesostations transect 49°W	27/12 - 31/12			182	186	188	190	192	194
Selective sampling near Confluence 03/01 - 04/01	207	208	209						

Multinet and Bongonet.
The Multinet was equipped with five nets (each 200 µm). Discrete depth hauls were made with 5 standard depth ranges from 1000 m to the surface. Samples were taken at the six mesostations along the 49° and 47°W

transects. During the grid survey (st. 207, 208, 209) Multinet hauls were made down to 300 m and the depth ranges sampled were defined according to the vertical temperature profile.
The Bongo net was employed vertically down to 300 m at the six mesostations along the 47° transect.

Copepods of the families Calanidae *(Calanoides acutus, Calanus propinquus, C. simillimus),* Eucalanidae *(Rhincalanus gigas)* and Metridae *(Metridia gerlachei, M. curticauda, M. lucens, Pleuromamma* sp.) from the Multinet samples of the two 49° transects were identified, sorted and counted on board .
The calanoid copepods in the Multi net samples and the total zooplankton in the Bongo net samples from the 47° transect were as far as possible identified, sorted and counted.

All samples were preserved in 4 % formaldehyd - seawater solution.

Preliminary Results

The following preliminary results illustrate some levels and trends. To stress the main difference in water-masses the stations were divided over the Scotia and Weddell Sea, with the Confluence zone in between (the 2 middle stations of the transects). The following results present means of these areas.

1. Biomass and density distribution

Tab.17 presents for small (<1 mm) and large (>1 mm) copepods the dry weight and number per m^3 for some of the transects distributed over time. It seems that dry weight was almost evenly distributed over large and small copepods, but the small ones (small species and small stages of large species) were very dominant in number. Activities such as production, feeding, respiration and excretion will also have been considerably higher in the small size fraction.

Total copepod dry weight ranged from about 20 mg m^{-3} in the Scotia Sea to about 1 to 3 mg m^{-3} in the Weddell Sea. The distribution pattern of total copepod dry weight per m^3 in the upper 300 m during the first mesostation transect is given in Tab.18. There was no evident progression in time. Nor was there any consistent depth distribution pattern or diurnal change in distribution in the upper 300 m.

Table 17: Biomass and density of copepods.

COPEPOD BIOMASS

mg ADW m^{-3} (small / large)

	Scotia Sea	Confluence	Weddell Sea
EPOS Leg 1 (19/10 - 12/11)	--	7.4 / 5.5	0.5 / 0.3
Mesostations 49°W 26/11 - 30/11)	2.0 / 3.0	3.8 / 6.1	1.0 / 2.4
Time stations 49°W (03/12 - 11/12)			
Day: upper 100 m	10.2 / 5.1	6.9 / 4.3	0.3 / 1.1
upper 200 m	12.6 / 1.5	7.1 / 4.7	0.2 / 0.3
upper 300 m	15.9 / 6.6	4.7 / 2.0	2.8 / 3.2
Night: upper 100 m	13.9 / 2.3	5.1 / 5.3	0.3 / 0.2
upper 200 m	13.2 / 24.8	5.0 / 3.1	0.5 / 1.5
upper 300 m	5.4 / 5.6	4.3 / 2.3	0.7 / 2.8
Mesostations 49°W (27/12 - 31/12)	5.0 / 4.5	1.1 / 1.1	0.8 / 2.5

COPEPOD DENSITY

number per m^{-3} (small / large)

	Scotia Sea	Confluence	Weddell Sea
EPOS Leg 1 (19/10 - 12/11)	--	3656 / 37	767 / 0.4
Mesostations 49°W (26/11 - 30/11)	3155 / 23	2290 / 31	641 / 3
Time stations 49°W (03/12 - 11/12)			
Day: upper 100 m	3786 / 53	4088 / 5	95 / 1
upper 200 m	5783 / 5	4095 / 6	154 / 0.5
upper 300 m	7560 / 13	2587 / 4	5060 / 3.5
Night: upper 100 m	5442 / 6.2	1942 / 9	179 / 1
upper 200 m	6506 /192	3715 / 13	753 / 2
upper 300 m	2880 / 52	1789 / 9	676 / 7
Mesostations 49°W (27/12 - 31/12)	2620 / 48	588 / 3.3	662 / 2.7

Tab.18: Distribution of copepod dry weight at the first mesostation transect.

Station:	143	145	147	149	151	153
mg ADW m^{-3}:	7.5	2.4	4.0	15.7	5.1	1.6

2. Species composition

The distribution of dominant species is given in the Tab.19.

Table 19: Dominant copepod species in the upper 300m.

	DOMINANT SPECIES		
	Scotia Sea	Confluence	Weddell Sea
LEG 1	---	*Oithona similis* *Calanoides acutus* *Calanus propinquus* *Metridia gerlachei*	*Oithona similis*
1. Meso transect 49°W			
	Oithona similis	*Oithona similis* *Calanus propinquus*	*Oithona similis* *Metridia gerlachei*
	Calanoides acutus	*Rhincalanus gigas*	*Calanoides acutus*
Time transect			
	Oithona similis	*Oithona similis* *Metridia gerlachei*	*Oithona similis* *Calanoides acutus*
	Calanoides acutus	*Calanoides acutus* *Rhincalanus gigas* *Euchirella sp.* *Calanus similimus*	*Metridia gerlachei*
2. Meso transect 49°W			
		Oithona similis	*Oithona similis*
	Oithona similis	*Metridia gerlachei*	*Calanoides acutus*
	Calanoides acutus	*Calanoides acutus* *Rhincalanus gigas* *Euchirella sp.* *Calanus similimus*	

This indicates that the highest species diversity was in the Confluence Zone. *Oithona similis* is a dominant small species, the others are large species.

Species and stage composition may be used to identify the origin of plankton patches as observed during the first transects and the selective sampling near the Confluence. This has not been worked out yet.

3. Fecundity

Daily egg production per incubated female is indicated in the next Tab.20.

Table 20: Daily fecundity in Scotia Sea / Confluence / Weddell Sea

	Oithona	*Calanoides*	*Metridia*	*Calanus*
1. Meso stations transect 49°W	0/0/0	12.1/16/0.02	2.5/0.3/-	-/-/0
1. Time stations transect 49°W	0/0.2/0	-/14.4/0	0/0.6/-	-/-/-
2. Meso stations transect 47°W	0/0/0	4.3/0/-	-/-/-	-/-/0
Ice survey transect 49°W	-/-/0	-/-/0	-/-/-	-/-/6.1
3. Meso stations transect 49°W	0/0.04/0	-/0/0	-/0/0	-/29.8/2.4

If no females were found in the samples this is indicated by a hyphen (-). *Rhincalanus gigas* produced eggs only in one of 7 experiments (22 per female per day at Sta. 182). *Oithona similis* showed a very low production rate. But because it lays eggs in batches (egg sacs) in contrast to the others, it may spawn less frequently and require longer incubation times at prevalent food densities. Most productive were *Calanoides acutus* in the early Scotia and Confluence blooms at 49°W, and remarkably *Calanus propinquus* in the Weddell Sea and Confluence at the end of December. Fig.64 displays the regions of highest egg production of the different species.

4. Population development

To give an example, the stage distribution of the most abundant species, Oithona similis, is given in Tab.21 in course of time for the different areas.

In the Weddell Sea a shift was observed from C4 to C6 (adult), and from N2/N3 to at most N5/N6, in about one month. In the Scotia Sea and Confluence zone this development apparently started earlier in season, probably due to the early diatom blooms. The egg/female ratio seemed to decline. The distribution in the "Confluence Zone", which was initially intermediate between the Scotia and the Weddell Sea, became identical to the Weddell Sea distribution at the end of December, which indicates a shift in water mass from south to north.

The slow growth of about 2 to 3 stages per month and the declining egg production point to a 2-year life cycle rather than to a 1-year cycle with divided subpopulations. Estimates of growth rate may later add more information about population development.

Table 21: Mean Abundance (number/m^3) of the different stages of *Oithona* (in brackets number of samples

	STAGE												
	1 egg	2 n1	3 n2	4 n3	5 n4	6 n5	7 n6	8 C1	9 C2	10 C3	11 C4	12 C5	13 C6
EPOS Leg 1 (29/10 - 12/11)													
Confluence (2)													
	953	2	65	47	21	21	41	0	31	100	124	234	274
Weddell Sea (7)													
	41	57	91	119	21	9	4	7	9	20	72	54	21
1. Mesostation transect 49°W (26/11 - 30/11)													
Scotia Sea (6)													
	755	75	280	215	220	00	15	50	50	80	130	110	90
Confluence (2)													
	626	63	217	185	109	84	7	0	0	28	23	38	24
Weddell Sea (2)													
	130	17	32	21	16	4	0	0	16	22	52	39	1
Time stations 49°W (3/12 - 11/12)													
Scotia Sea (6)													
	653	142	208	202	140	94	148	73	64	80	85	188	349
Confluence (15)													
	681	62	153	185	100	76	97	13	34	58	43	29	123
Weddell Sea (6)													
	215	25	118	143	69	22	27	23	33	25	20	20	23
2. Mesostation transect 49°W (27/12 - 31/12)													
Scotia Sea (2)													
	900	64	150	120	112	154	110	2	10	38	56	102	238
Confluence (2)													
	170	40	26	20	8	36	12	0	0	4	4	12	52
Weddell Sea (2)													
	200	20	38	28	18	16	14	0	0	16	8	8	54

Fig.64: Diagram showing the regions of highest egg production of the various species.

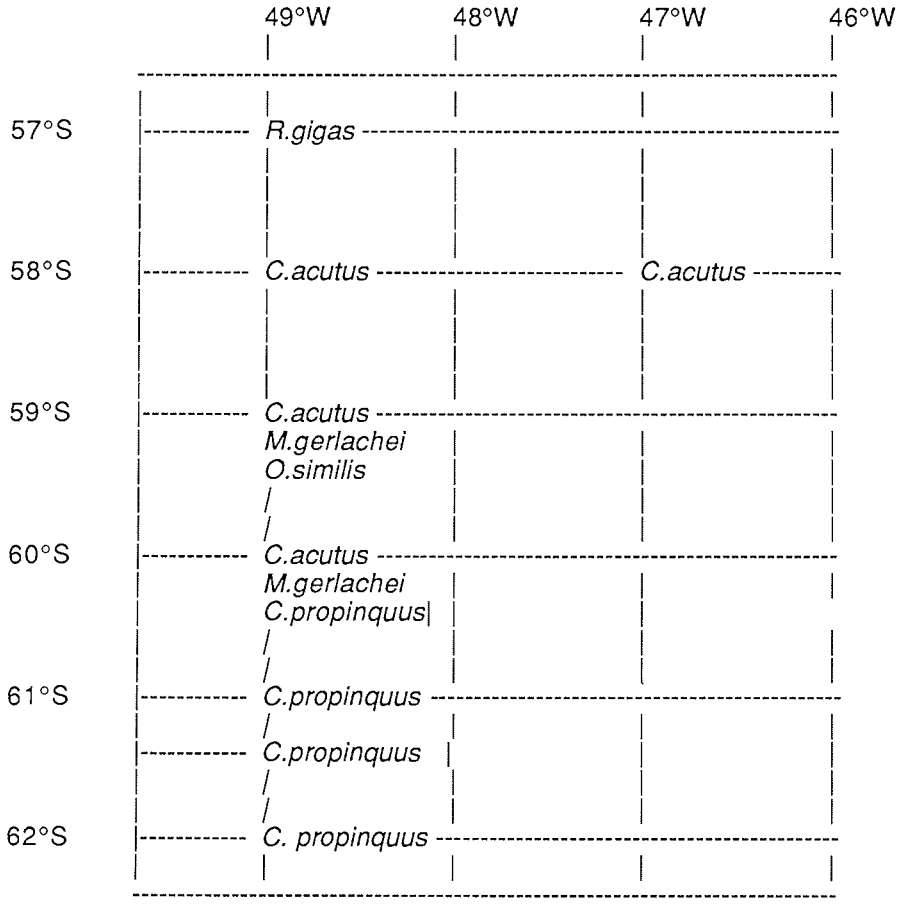

5. Vertical distribution

The 49° transect. A very low abundance of all species was found at Station 145 which is located just south of the front. The subantarctic species *C. simillimus, M. lucens, Pleuromamma* sp. only occurred at the stations in Scotia Sea water (no. 143) and in the Confluence zone (no. 145, 147) with main abundance at Station 143. The most abundant species, *Calanoides acutus* and *Metridia gerlachei* occurred in greater numbers in the upper water layers (300 - 0 m) at the stations in the Scotia Sea, whereas the bulk is found in the deeper water depths in the Weddell Sea (Fig. 65 and 66). The composition of the developmental stages changed also from north to south, with younger stages in the north to older ones in the south. *Calanus propinquus* does not show great differences between the stations with highest numbers always in the upper 150 m meters. *Rhincalanus gigas* had its main distribution at the station located in Scotia Sea water (Fig. 65 and 66).

The 47° transect. A very low abundance of copepods at the station close to the front could not be detected at this transect. Lowest total numbers combined with the lowest numbers of copepod species were found at the most northern station, highest abundance of copepods at Station 162 in the upper 50 m. Like the transect at 49° the largest stock of copepods is in the upper water layers in the Scotia Sea and in the deeper layers in the Weddell Sea.

The small calanoid copepod species *Microcalanus pygmaeus* made up the highest fraction at most stations. *Metridia gerlachei* as well as *Rhincalanus gigas* occurred in high numbers in some water layers at the most northern station, whereas *Ctenocalanus* sp. in the upper 150 m at the two stations close to the front.

Literature Cited

Fransz, H.G. (1988). Vernal abundance, structure and development of epipelagic copepod populations in the eastern Weddell Sea. Polar. Biol. 9: 107-114

Figure 65: Vertical distribution of C. acutus, C. propinquus (all stages combined) along the 49° transect (26.11. - 30.11.88).

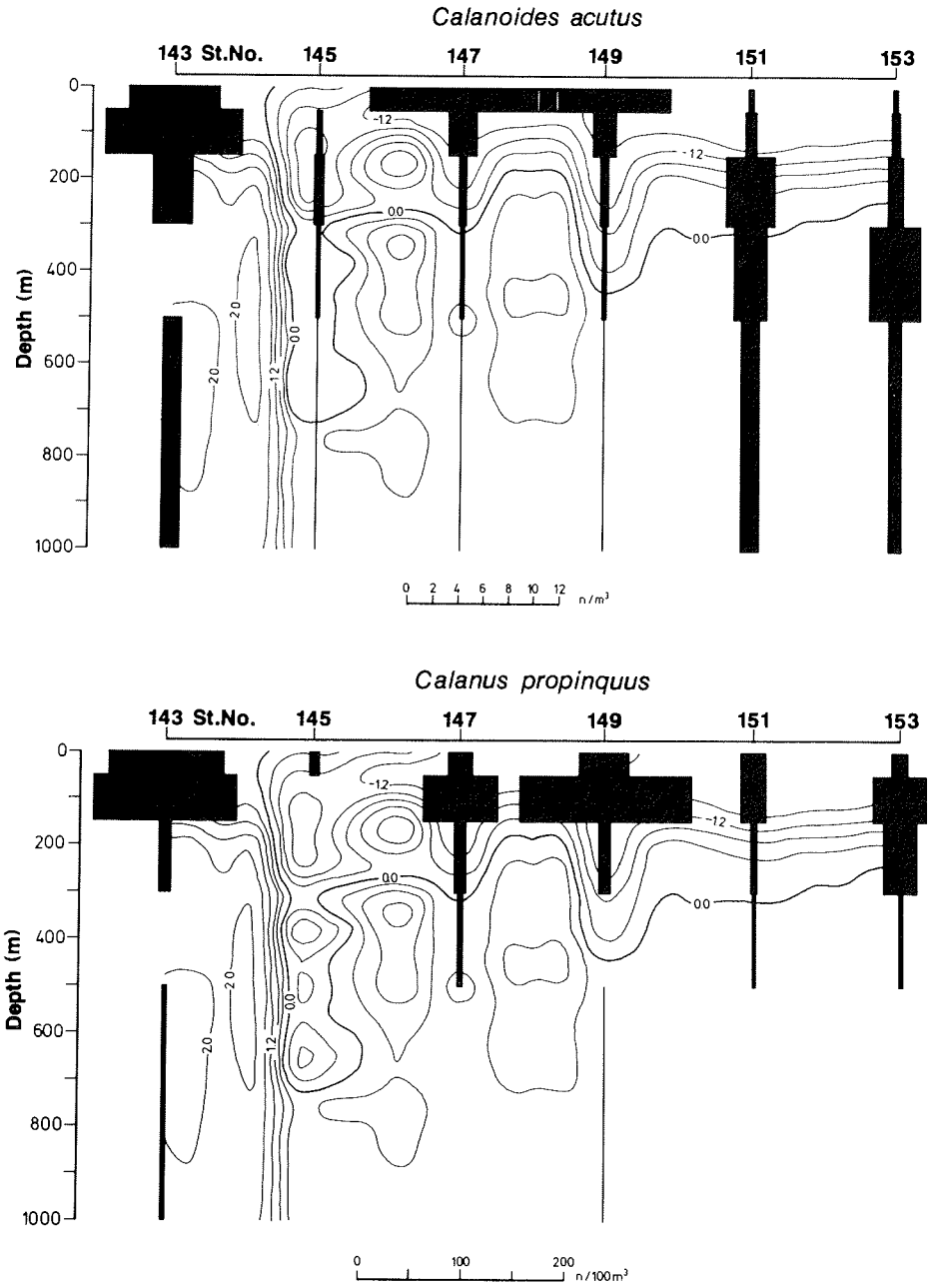

Figure 66: Vertical distribution of R. gigas and M. gerlachei (all stages combined) along the 49° transect (26.11. - 30.11.88).

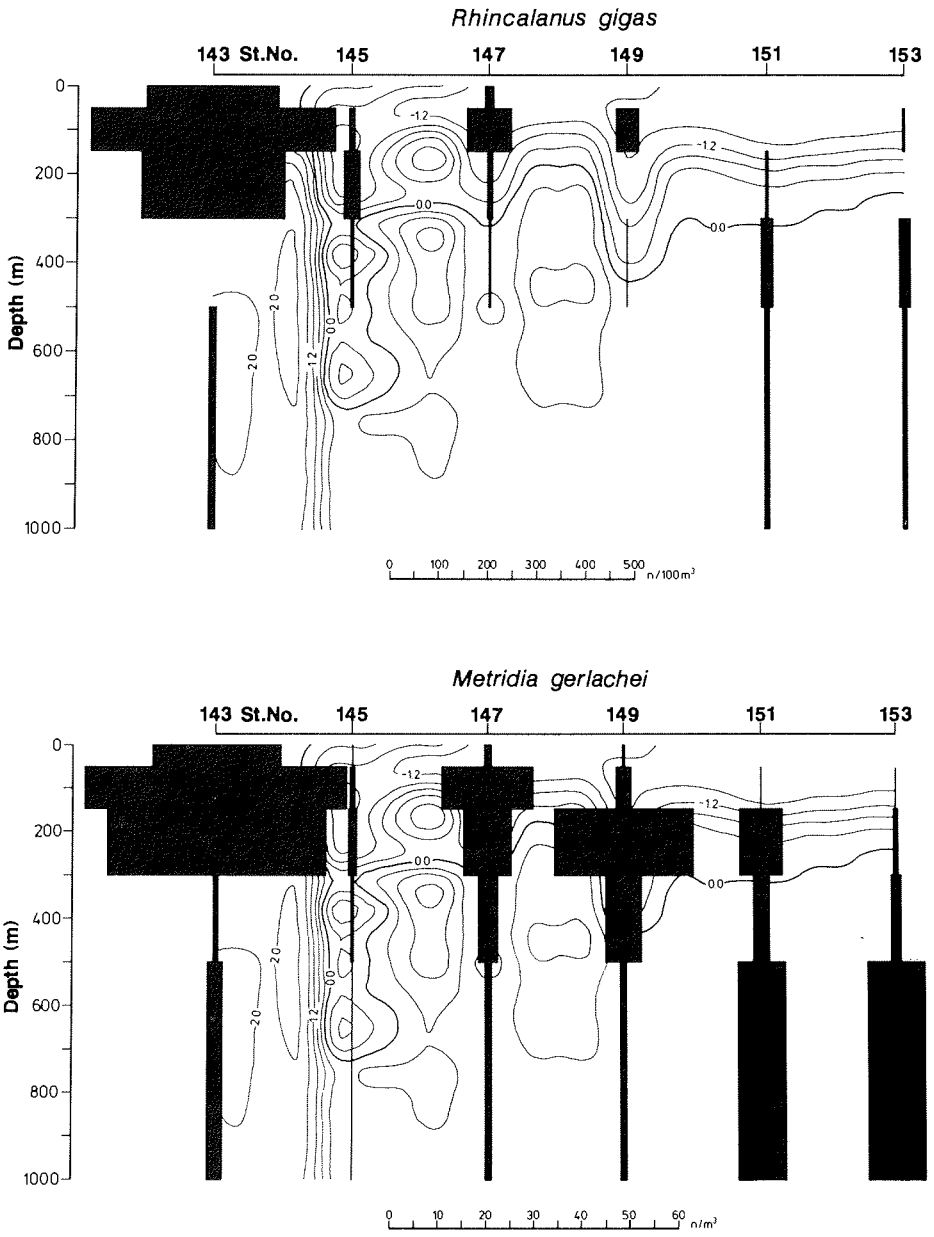

4.3.3 Macrozooplankton - Biomass, Development and Activity

J. Cuzin-Roudy, P.H. Schalk

Objectives

The Antarctic pelagic ecosystem is one of the most intriguing systems, with its extreme conditions and large seasonal fluctuations.For only a short period of the year, in the Austral summer, phytoplankton blooms produce food for the secondary producers; during the long period of winter the water is virtually devoid of food. The zooplankton and micronekton stock of these waters must have developed special life strategies to cope with the poor winter conditions and profit from the bloom the next summer; for example life cycles geared to the seasonal changes, or special adaptations in the metabolic system. As the ice edge may play an important role in generating the summer development of the pelagic ecosystem (i.e. Fryxell and Kendrick, 1988; Daly and Macaulay, 1988), the research programme was carried out at two north-south running transects at 49 and 47° W running from the open Scotia Sea (57°S), through the Confluence Zone, into the ice covered area of the Weddell Sea (62°S) from 22th November 1988 till 6th January 1989.

The objectives of the mesozooplankton and micronekton research during the EPOS leg 2 cruise were to study:

1. spatial and temporal variation in the community structure, biomass and respiratory activity, and

2. in a number of selected species, the developmental stages, morphologic and cytologic differences and N14/N15 ratio.

As Krill forms a major component of the macroplankton in these waters and is of great importance to the lower trophic levels of the ecosystem (grazing), much of the attention was focussed on this species.
It is now well admitted that Krill populations are able to maintain survival in winter under the ice by feeding on ice-algae. But winter condition for Krill means biological activities reduced to a minimum, with moulting, but eventually regressive growth, and no reproduction. Moreover, at the end of the summer, after the reproductive season, adult Krill undergo a sexual regression which attains a degree never described in other crustaceans: secondary sexual characters disappear completely through successive moults and the gonads regress to a juvenile structure. In consequence, when the next reproductive season starts, large adults of several years old have to go through the same steps of sexual differentiation as the young sub-adults which will reproduce for the first time. This life-cycle pattern implies a special adaptative strategy for Krill concerning the hormonal balance (ecdysteroids and eyestalk neurohormones, which is known to control moulting and reproduction in other crustaceans) and metabolic activity, but has never been investigated in pelagic shrimp-like crustaceans.
Food is believed to be the limiting factor for active growth through moulting, sexual development and egg production in Krill. A generally well accepted hypothesis is that ice-algae are sufficient for sustaining the fundamental

metabolic needs in winter, but that spring phytoplankton blooms are necessary for the physiological shift leading to Krill production in summer. By relating the steps of the changing physiology of Krill during the period of investigation along the N-S transect to the physical, chemical and biological structure of the studied zone, we expect to establish a general pattern for the onset of seasonal sexual maturity in Krill populations during the transitional period of spring. We expect also to gather arguments to support the hypothesis that the qualitative and quantitative value of the food available to Krill from spring production in this particular hydrological structure is responsible for the shift from a winter to a summer adaptative strategy in Antarctic Krill.

Work at Sea

The mesozooplankton was sampled with an Omori trawl net (mouth area 2 m^2, mesh size 500 µm), which was converted to be used as a vertical net by adding a cod-end line and connecting a 35 kg weight to the collector. This (only) Omori net was lost on 21-12 at Sta.174 and was replaced by a Bongo net with the same mesh size and a total mouth area of 1.5 m^2 (two nets). Hauls were made in duplicate from 400m depth to the surface as a standard, with a lowering speed of 0.5 m/s and a hauling speed of 1.0 m/s.

Displacement volumes were measured on the fresh catch and a 2 ml subsample was taken of the "plankton community", as sampled by the net, for determining respiratory (ETS) activity.

In open water, free of pack-ice or ice floes, an open RMT 1+8 (Baker et al., 1973) was used for sampling mesozooplankton and micronekton in the upper 100, 300 and 400m of the water column, with a towing speed of approximately 2.6 knots. The wet weights of the total RMT 8 catches were measured. Respiratory (ETS) activity of various organisms from these catches were determined.

Net samples were taken along 49°W between 57° and 62°S and along 47°W between 57° and 61°30'S. The three nets deployed also provided organisms for use in various experiments on board by other scientists (grazing, fecal pellet production, uptake measurements).

Records of acoustic backscattering were obtained continuously during the cruise with one ELAC echo-sounder operating at 30 and another at 150 kc. The depth range of the 30 kc sounder was set either to 0-200 or to 0-500m, depending whether backscattering in the deeper water layers was present. The 150 kc sounder was kept constantly at the 0-200m range. Gain setting, noise suppression, chart speed etc. were set at optimal range on the echogram at the beginning of the cruise and kept at that setting to obtain comparable records. Although no echo-integrator was used the records present a rough picture of the relative amount of backscattering and vertical distribution and diel migration.

Krill from the different samples were observed alive for simultaneous scoring of i) body length, ii) moult stage and iii) external sexual maturity. In order to assess more precisely the gonadal structure, a "squash" technique was devised for the instantaneous scoring of the sexual maturity stage (SMS) on

freshly caught Krill. This new scoring system is based on a former histological description of the structure of the juvenile, sub-adult and adult gonads during the reproductive season (Cuzin-Roudy, 1987).
The most lively Krill from the net catches were kept on board in sea water tanks (50 l, renewed every 2 days), maintained in a cold container (0°C). They were fed with phytoplankton collected at the corresponding stations or with "brown ice" from the ice stations. The daily observation of the live animals kept on board allowed us to follow the succession of ovarian transformations during early spring development and then during egg-maturation (with two phases of yolk accumulation). The period preceding and following spawning in females was also observed in isolated individual Krill in an attempt to estimate the time for ovarian regression and reactivation after a spawning event. Observations were also made about moulting, mating and feeding behaviour, for juvenile, sub-adult and adult Krill of both sexes.

The "squash" technique devised for live Krill was also adapted for scoring formalin-fixed samples. The relative proportions of the different SMS will be estimated for the different samples, and a sexual maturity index (SMI) will be established for the different Krill populations sampled in the different water masses along the EPOS Leg 2 transects.
Krill representative of the different sexual maturity stages were also preserved for the histological study of the developing ovary and of the main endocrine centers controlling growth, moulting and reproduction.
Haemolymph samples were also collected for qualitative and quantitative studies of the ecdysteroid balance ("moulting hormone"), using HPLC resolution and radio-immunoassay (RIA).

Preliminary Results.

The observations made along the beginning of EPOS Leg 2 confirmed our former results concerning the structure of the inactive ovary in winter conditions. Krill found in ice-covered areas were at a juvenile stage or at the very beginning of development of the gonad (SMS: 0 to 3, gametogenesis phase). Krill caught during the first transect of EPOS Leg 2 were either immature or poorly advanced in sexual maturity and never approaching egg-maturation (Tab. 22, see also EPOS Leg 1 report). Then, the different steps of female sexual maturity, between resting ovaries and egg-production, were encountered, starting from the winter condition found in ice to breeding Krill in the region of the Confluence. Spawning was first observed in this area which appeared as the most suitable for Krill reproduction. Small and large adults (of different age classes) were undergoing simultaneous gonadal development.

The changes along the scale of progressive gonadal development for the Krill kept on board paralleled the one observed in samples taken at the same positions at repetitive times. For example, females from Sta.148, maintained on board, were laying eggs when spawning females were found at the same location (Sta.158) eleven days later.

A preliminary general distribution of Krill sexual maturity stages in the geographic area studied is given in Fig. 67. The first females ready for spawning were found at Sta. 158 (59°S, 49°W), in December. At later

passages though this area (Sta.173, 188), the population contained mostly females recovering from the first egg-laying. As no females ready for spawning were seen during EPOS Leg 1, these observations indicate that the second phase of yolk accumulation (SMS 5 to 8) is rapid in rich spring conditions, and also confirms that female Krill spawn repetitively during their reproductive season. Mature males were found from Sta. 157, but females were never observed mated before their second phase of egg-maturation. Breeding females lose the thelycum content when moulting, but were observed mated in our tanks as early as postmoult stage B.

Tab. 22: Sexual maturity of Antarctic Krill *Euphausia superba* Dana along EPOS Leg 2 transects, ad.: adults, with developed secondary sexual characters (thelycum or petasma); sub-ad.: sub-adults developing secondary sexual characters; juv.: juveniles, no secondary sexual characters; Imm.: males with differentiated but not functional testis; Met.: males producing spermatophores. The sexual maturity stages for females are scored on an 8 steps scale, from 0: ovary reduced to the germinal zones - juvenile or adult winter condition; 8: mature eggs in ovary - spawning condition (Cuzin-Roudy, Ross and Quetin, in preparation).

Station	Position	Krill catches	Sexual maturity stages	
			males	females
First transect: 49°W				
145	57°S	ad., sub-ad., juv.	Met.	0 to 4
146	58°S	juv.	Imm.	0
148	69°S	ad., juv.	Imm.	0
150	60°S	juv., sub-ad.	Imm.	0 to 3
153	61°S	sub-ad.	Imm.	0 to 3
156	60°S	juv.	Imm.	0
157	58°S	ad., sub-ad.	Met.	5 to 6
158	59°S	ad., juv.	Met.	6 to 7
159	57°S	juv., ad.	Met.	5
Second transect: 47°W				
162	58°S	ad., sub-ad., juv.	Met.	5 to 6
164	59°S	ad., sub-ad., juv.	Met.	5 to 6
166	60°S	ad., sub-ad., juv.	Met.	5 to 6
169	61°S	juv.	Imm.	0
Third transect: 49°W				
172	59°S	ad.	Met.	5 to 6
173	59°S	ad., juv.	Met.	5
174	60°S	ad.	Met.	4 to 5
178	61°S	juv.	Imm.	0
179	62°S	juv.	Imm.	0
182	67°S	ad. (1 male)	Met.	----
186	58°S	ad. (2males)	Met.	----
188	59°S	ad.	Met.	4 to 5
190	60°S	ad.	Met.	1 to 5
192	61°S	juv.	Imm.	0
194	62°S	juv.	Imm.	----
207	57°S	ad. (1 male)	Met.	----
208	57°34´S	ad.	Met.	7

These observations will have to be confirmed and quantified by the scoring of sexual maturity states (along with body size and moult stage) in samples and sub-samples fixed in formalin. The new scoring system for fixed samples leading to the estimation of a SMS can also be applied to preserved sample from other cruises. It will therefore be useful for comparisons between samples from different areas of the Antarctic ocean and from various years or times of the year.

ETS Measurements.

The respiratory activity of various zooplankton and micronekton species as well as the activity of the zooplankton community in general was determined by ETS measurements. ETS stands for Electron Transport System and the activity of this enzyme system is a relative measure of the actual in situ respiration of the organism (Schalk, 1988). One of the major objects of this study was Krill, *Euphausia superba*. The development from juvenile to sexual maturity until spawning was followed during the time of the cruise and the ETS activities of the various stages were measured. In the beginning of the cruise (second half of November) at the first section at 49°W, mostly juvenile and immature adult Krill were found. The juveniles, as expected, showed high activities, probably related to growth. All sub-adult stages had comparably low activities (Tab.23). When the same section was sampled for the second time in the end of December and beginning of January, fully mature Krill was found which showed increased respiratory activities. During the 7 weeks of sampling, the respiratory activity of the maturing Krill went up by about a factor four (from ±20 to ±80 µgat O/gr hr). Apart from this, the respiratory enzyme activity is strongly related to temperature (Fig.68). The Krill migrating from their winter habitat, the ice edge, to open waters (Daly and Macaulay, 1988) matures and experiences a temperature rise of about 2°C, corresponding with an increase in ETS activity of about a factor of 1.5 (Fig.68). The combination of these two factors increases the respiratory activity by a factor of 6 and the swarms must have a large impact on the phytoplankton stock.
Comparison with respiratory activities of other organisms (Tab.24) indicated that *Thysanoessa macrura* and *Euphausia superba* had highest respiratory activities, of which the latter showed by far the highest biomasses throughout the cruise. Next to Krill, salps were most abundant in the net catches, but although they also can occur in vast numbers, their activity is much lower, an indication that their role in the ecosystem is less important. All the investigated taxa had, despite the low water temperatures, relatively high respiratory activities compared to taxa from temperate and warmer waters.

Tab. 23: The increase in ETS activities with the sexual maturity stages according to Makarov & Denys(1982).

station	date	sex.mat.stage	n	ETS activity
145	27-11	male III B	10	29.7
148	28-11	juveniles	7	36.7
153	30-11	juveniles	2	36.6
		male II B/D	2	17.8
		fem. II B/A-C	2	18.1
		fem. II B/D	5	17.6
		fem. III A/A-C	5	13.2
		fem. III A/D	2	18.4
157	6-12	juveniles	5	28.8
158	9-12	male full.mat.	4	61.4
175	21-12	fem. III B	2	47.4
		male III B	2	46.7
188	29-12	male full.mat.	1	56.3
		fem. III C	1	51.6
208	4-1	male full.mat.	1	80.1
		fem. full.mat.	1	68.4

Measurements of the ETS activities of the plankton community as sampled by the nets revealed distinct spatial differences. As an example, the figures of the last 49°W section are given (Fig.69). Biomass figures obtained from both the vertical nets and the RMT 8 displayed highest values in the Scotia Sea waters, then a sharp dip crossing the Confluence zone and an increase towards the ice edge. The ETS activities per gram "zooplankton" (from the vertical nets) showed a similar trend as the biomass: higher activities in the north and near the ice edge, with a low in between. Finally, expressed as activity per m^2 sea surface, the graph demonstrates clearly that close to the ice edge the respiration is relatively high. A similar, but somewhat shifted, trend was found at the 47°W section. Fryxell and Kendrick (1988) found higher abundances of algal cells close to the ice-edge and suggested that the ice has a generating effect upon phytoplankton blooms. The increased biomass and ETS activities in zooplankton indicate that near the ice-edge also enhanced activity at higher levels of the ecosystem occur.

Tab. 24: Range in ETS activities of the various taxa investigated.

Taxum	min. ETS	max. ETS
Thysanoessa macrura	32.0	71.6
Euphausia superba	12.8	80.1
Mysidae	21.2	30.8
Clio pyramidata	25.0	25.6
Limacina antarctica	19.5	19.5
Gymnosomata	12.1	18.0
Chaetognatha	4.0	10.5
Salpida	0.8	4.8
Siphonophora	1.6	6.0
Tomopteris spec	28.0	28.0
Copepoda	9.0	10.4
"zooplankton"	7.5	22.0

Acoustic Observations.

In addition to the net catches the acoustic backscattering in the water column was continuously monitored with a 30 and a 150 kc echosounder. Only the general trend along the 49°W section can be sketched here as most of the echograms have not been processed yet and only a quick survey of the data has been carried out.

As a measure of biomass, the schools present on the echograms were counted and their depth, vertical and horizontal extension measured (Everson, 1983). In some cases, verification of the organisms responsible for the observed backscattering was attempted by making RMT 1+8 hauls through the depth layers where echo traces were observed. These catches yielded, as most abundant organisms, invariably Krill when dense schools were observed, and salps and siphonophores when faint curtain like structures were present. The overall tendency was that more backscattering was measured during the second visit (end of December) to the 49°W section as compared to the first (end of November), and that the vertical extent of backscattering increased from 200 to 400 m depth respectively. This gives the impression that the amount of biomass of micronekton in the water increased during this period. Treguer (4.1.6) found in the same period an evident increase of ammonium in the upper 100 m of the water column, which supports the suggested biomass increase. The observed schools showed a distinct diel vertical migration (Fig.70) and dispersed in the "night" between 2200 and 0200 hours local time. The depth of occurrence decreased nearer to the ice edge. In the ice, hardly any schools were observed, although there was in general a high abundance of Krill as could be deduced from the large numbers washed onto the ice in the ships wake, and large numbers of observed penguins and seals in this area (Van Franeker, 4.4). This agrees with the observations that Krill stays directly under the ice floes to graze on the ice algae (Daly and Macaulay, 1988; Marshall, 1988), invisible to the echo-sounders (Everson and Murphy, 1987). Possibly, the gradual blocking of light in the water column by the increasing numbers of ice floes triggers upward migration and subsequent dispersal of the Krill under the floes (Fig.71).

In general, the amount of backscattering on the echograms from the ice edge into open water seems to be in agreement with the numbers of birds observed (Van Franeker, 4.4), however, a detailed further study of this material has still to be done. A comparison between ammonia profiles (see § 4.1.6) and depth distribution of schools might provide interesting results, as well as a correlation between chlorophyll a distribution and numbers of Krill schools observed to test wether the grazing hypothesis (disappearance of a phytoplankton bloom within hours supposedly due to grazing of Krill swarms) may hold.

To conclude, although much work remains to be done (sorting, identifying, morphometric measurements, hystology, cytology, N14/N15 ratio), work that can only be carried out in the various home laboratories, the results of this cruise promise to be a success. A multitude of net samples was gathered and will offer good material for a detailed description of the developments in the larger plankters in both the spatial and time scales.

Some of the measurements on board (ETS, sexual maturity of Krill, grazing experiments, acoustic measurements) revealed new insights and new lines to follow in future research. The zooplankton community showed elevated biomasses and respiratory activities near the ice-edge. This supports the theory that the ice-edge acts as a frontal zone with enhanced productivity and stocks at all consumer levels (Fraser and Ainley, 1986; Ross and Quetin, 1986; Garrison et al., 1986; Fryxell and Kendrick, 1988).

The metabolic activity of Krill was documented during the cruise period of two months and showed an increase both with sexual development and with the temperature gradient encountered when migrating from ice covered to open waters. This increase of metabolic activity amounted to a factor of 6 and indicates a growing grazing pressure during the summer development of the pelagic ecosystem. Moreover, also schooling behaviour seemed to be enhanced during the two months of observation, which must result in increasingly high stresses on the primary producers of the system during the summer development. The sudden and substantial decreases overnight in some observed chlorophyll maxima patches (4.2.1) may be related to these dense and highly active mature Krill schools and seem to point to an active search for food by these schools, as suggested by Hamner et al. (1983).

The importance of knowledge about patchiness in both the spatial and temporal scale, and about relations between patches of producers and consumers was once again made clear during this cruise. This is a subject that obviously needs more attention in future, as it makes the interpretation and correlation of studies on the various ecological compartments difficult.

Literature Cited

Cuzin-Roudy, J. 1987. Gonad history of the Antarctic Krill *Euphausia superba* DANA during its breeding season. Polar Biol.7(4):237-244

Daly, K.L. and M.C. Macaulay, 1988. Abundance and the distribution of Krill in the ice-edge zone of the Weddell Sea, austral spring 1983. Deep Sea Res.35(1):21-41

Everson, I, 1983. Variations in vertical distribution and density of Krill swarms in the vicinity of South Georgia. Mem.Nat.Inst.Polar Res.Spec.Iss.27:84-92

Everson, I. and E. Murphy, 1987. Mesoscale variability in the distribution of Krill, *Euphausia superba.*

Fraser, W.R. and D.G. Ainley, 1986. Ice edges and sea-bird occurrence in Antarctica. BioScience 36:258-263

Fryxell, G.A. and G.A. Kendrick, 1988. Austral spring microalgae across the Weddell Sea ice-edge: spatial relationships found along a northward transect during AMERIEZ 83. Deep Sea Res.35(1):1-20

Garrison, D.L., C.W. Sullivan and S.F. Ackley, 1986. Sea ice microbial activities in Antarctica. BioScience 36:243-250

Hamner, W.M., P.P. Hamner, S.W. Strand, and R.W. Gilmer, 1983. Behaviour of Antarctic Krill, *Euphausia superba*: chemoreception, feeding, schooling and moulting. Science 220:433-435

Marshall, P., 1988. The overwintering strategies of Krill under the pack ice of the Weddell Sea. Polar Biol.9: 129-135

Ross, R.M. and L.B. Quetin, 1986. How productive are Antarctic Krill? BioScience 36:264-269

Schalk, P.H., 1988. Respiratory electron transport system (ETS) activities in zooplankton and micronekton of the Indo-Pacific region. Mar.Ecol.Progr.Ser.44:25-35

Figure 67: Preliminary spatial distribution of sexual maturity of Krill *Euphausia superba*, in December, along EPOS Leg 2 transects. C: Confluence; F: frontal zone of the Confluence; I E: ice-edge

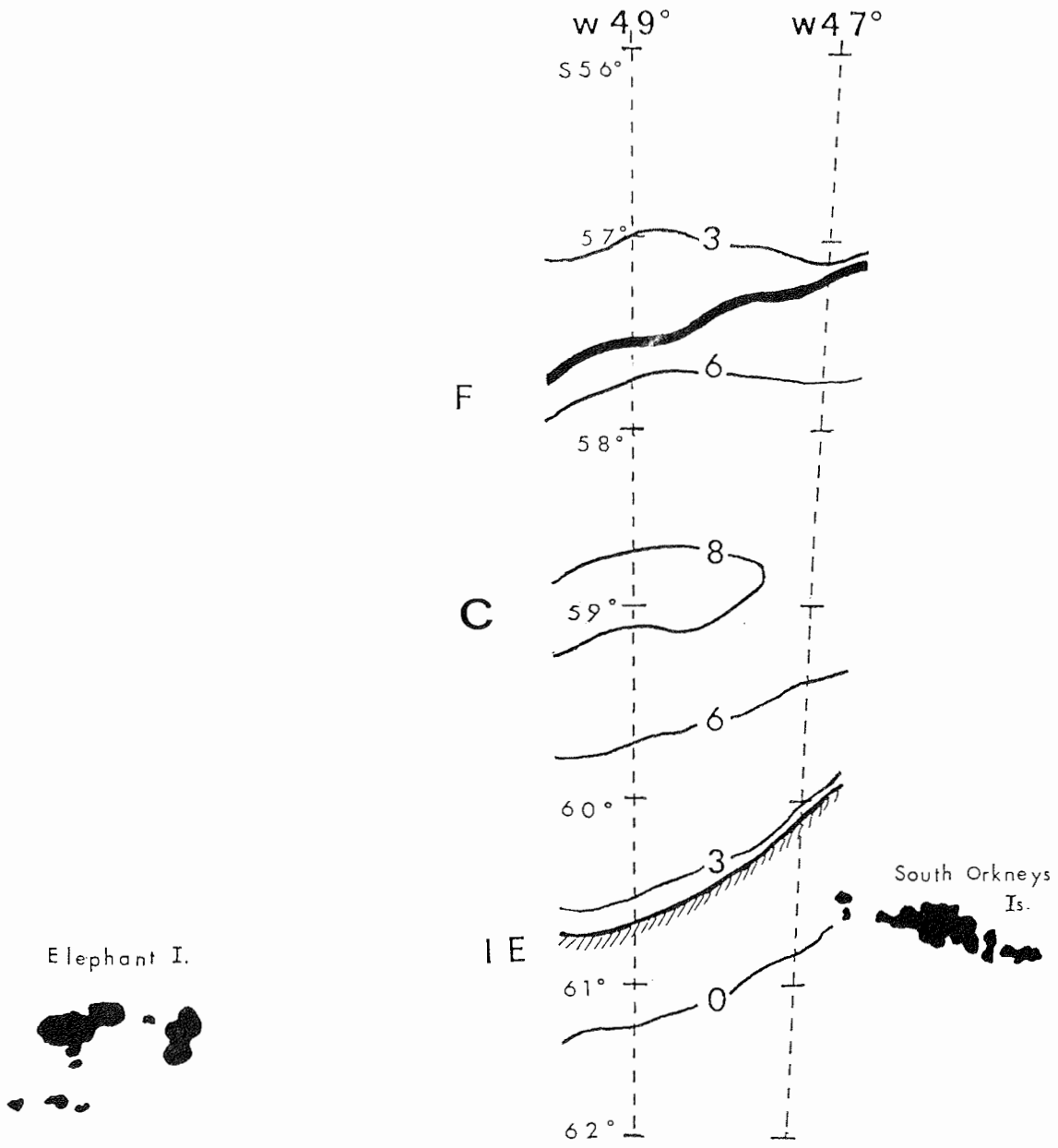

Figure 68. The temperature dependence of the specific ETS activities of some of the organisms investigated. Different symbols for a species represent measurements at two or more stations; the darkened area indicates the total range in ETS activity.

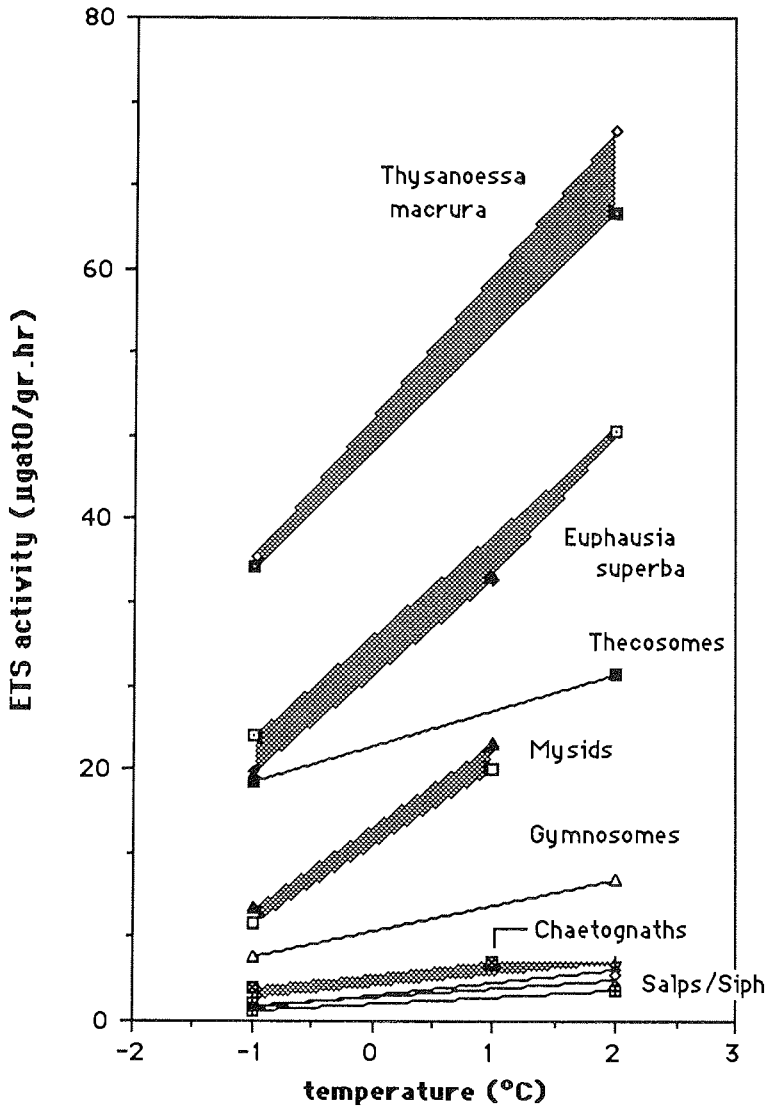

Figure 69. Upper graph: the biomasses of zooplankton from Omori net catches (in ml displacement volume) and of micronekton from RMT8 catches (in kg wet weight) per standard haul along the 49°W section. Lower graph: ETS activities of the zooplankton expressed as specific activity per gram zooplankton and as total activity per m^2 sea-surface. The rectangles in the upper right corner of both graphs indicate the northward extent of the icefield in the sections.

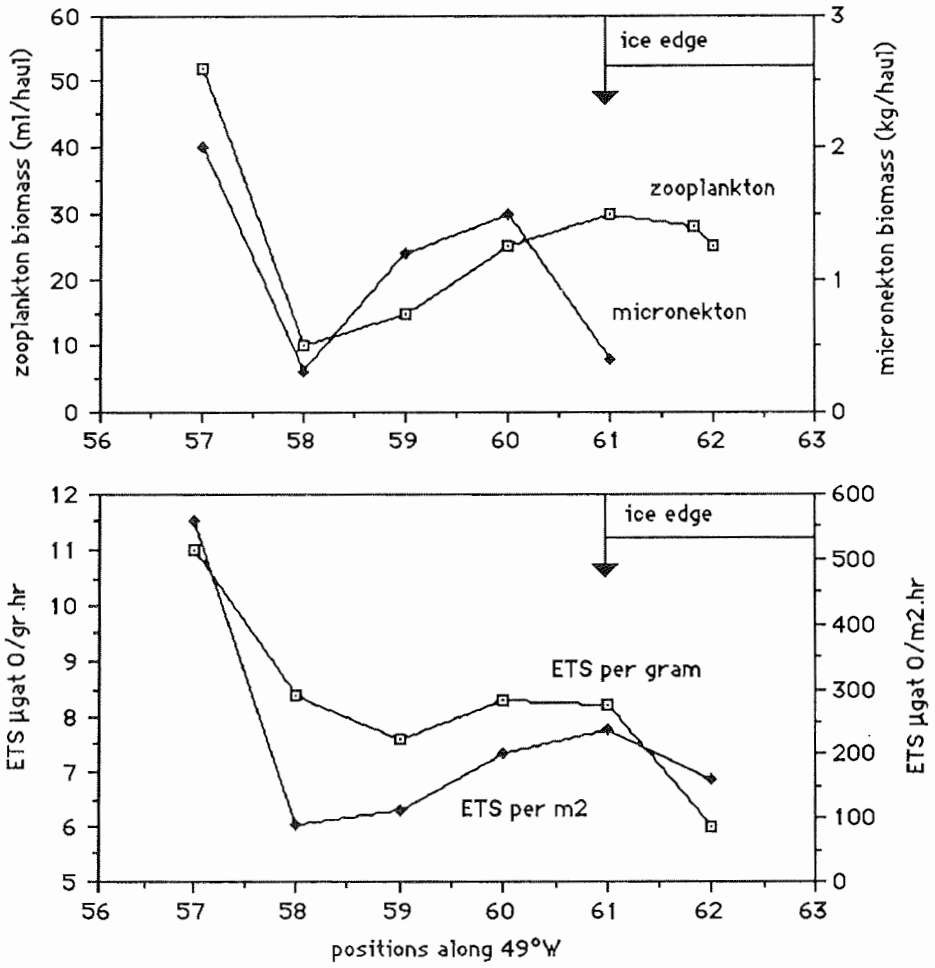

Figure 70. The frequency distribution of schools observed on the records of the 150 kc echosounder (upper graph). Schools mainly occurred during hours of daylight and showed a peak in abundance around midday. The schools were found deeper during day-time, with a maximum depth of 90m, than during twilight hours and exhibited diel migration. Thickness of the bars indicate the numbers of schools observed in the various depth layers. These observations concern in total 189 schools seen during the first visit to the 49°W transect from 28 November till 4 December 1988.

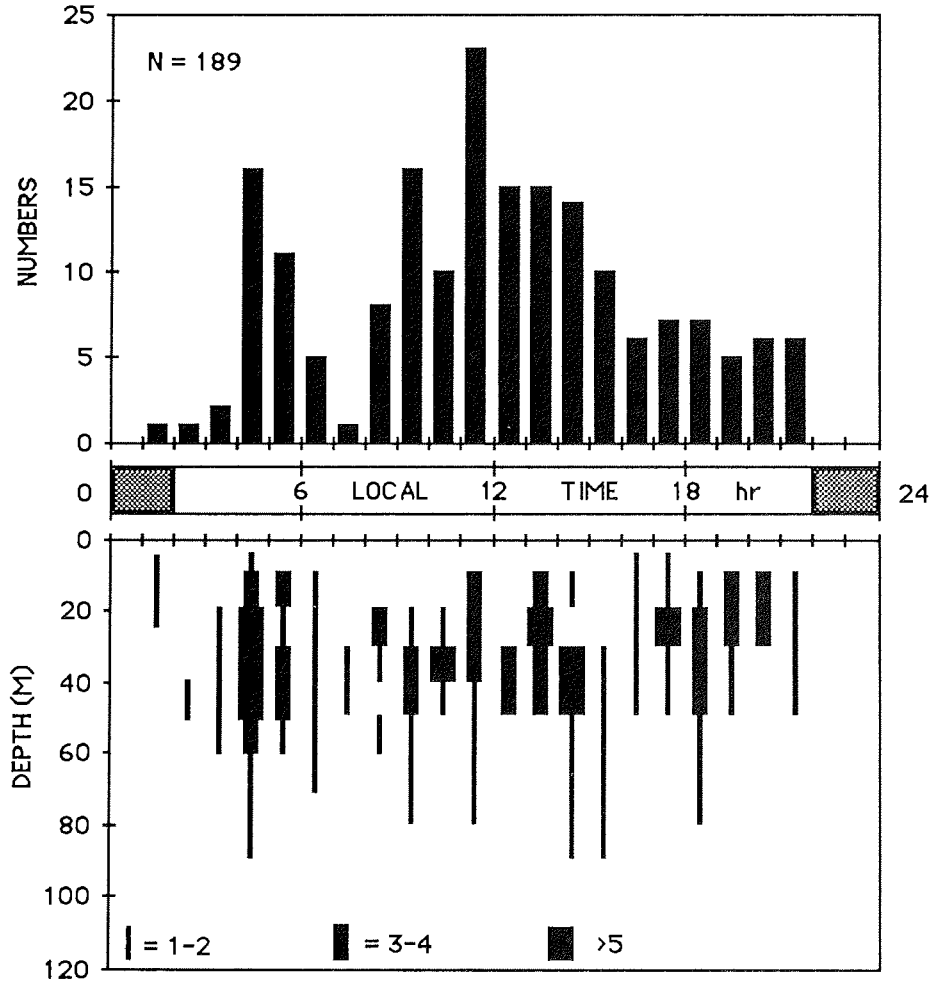

Figure 71. Diagram showing a rough schematic representation of the numbers and depth distribution of the schools detected with the 30kc echosounder along the 49°W section. In the ice, hardly any schools were detected; along the ice-edge with icefloes and open leads, some shallow small schools occurred, while in open water towards the north increasing numbers of large schools were observed at greater depths. It is suggested that the gradual blocking of daylight by the ice triggers an upward migration and subsequent dispersal of the schools.

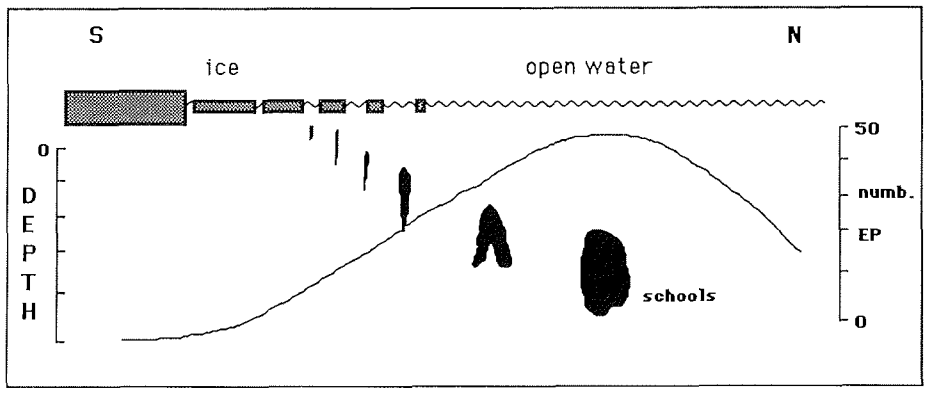

4.3.4 Grazing Rates in Relation to Food Supply

U. Riebesell, S. Schiel, I. Schloss

Zooplankton is exposed to a great variety of food organisms and concentrations. Both the abundance and size of food particles influence feeding rates. Preferential grazing on certain size classes of phytoplankton can lead to an alteration of the phytoplankton species composition. Euphausiids and many copepods, for example, feed most efficiently on larger particles, thereby changing both the cell size spectrum and, consequently, the phytoplankton species composition in the direction of smaller species. With decreasing food abundance, however, selective feeding becomes less important.

The general scope of this study is to gain a deeper understanding of the feeding behaviour of the Krill *Euphausia superba* and the dominant copepod species in Antarctic waters. Specific objectives were to determine, for different species of copepods and different size classes of *Euphausia superba.,* the following:
1) the relationship between particle size and feeding rates, and
2) the effect of decreasing concentrations of various sizes of food particles on feeding rates

Work at Sea

The experiments were conducted in 5-liter glass beakers at a temperature of 0°C and light intensities between 0.5 and 1 $\mu E\ m^{-2}\ s^{-1}$. In the beakers, a flow-through system, driven by a peristaltic pump ensured that the particulate material was kept in suspension. Known numbers of copepodite stages and adult females of the species *Calanus propinquus, Calanoides acutus, Rhincalanus gigas* and *Metridia gerlachei* as well as of different size classes of Krill were placed in the beakers. In several sets of experiments, feeding rates of these zooplankters were estimated for a variety of food particles of different sizes and concentrations:

1) natural plankton assemblages collected with Niskin bottles at 20 m water depth at Sta.156, 157, 158 and 159

2) as under 1), here the particulate material was artificially concentrated

3) culture of *cryptomonads* (initial chl a conc. : 13 $\mu g\ l^{-1}$)

4) brown ice which was collected at Stat 180, 195 and melted in GF/F-filtered seawater (initial chl a conc. : 36 and 14.5 $\mu g\ l^{-1}$, respectively)

5) culture of *Phaeocystis* (initial chl a conc. : 3 and 6.5 $\mu g\ l^{-1}$)

6) culture of *cryptomonads* + a mixture of diatoms (initial chl a conc. : 6 and 13 $\mu g\ l^{-1}$)

Both the brown ice samples and the *Phaeocystis* culture consisted of aggregated material which was pretreated by rotating the samples on a

roller table for about 24 hours (for details please refer to § 4.2.7). Two sets of feeding experiments were conducted with the assemblage outlined under 6): a. with equal amounts of Crytomonads and diatoms , and b. with a higher concentration of diatoms (biomass estimates on the basis of chlorophyll a). Particle sizes in the different experiments ranged from <10 µm to >1-2 mm.

For each set of experiments, at least one beaker without zooplankton was monitored as a control. The feeding experiments lasted between 42 and 72 hours. Chlorophyll a concentrations were measured every 6 to 8 hours in each of the beakers. Subsamples for cell counts and POC were taken at the beginning and end of the experiments; however, during the cryptomonad / diatom-experiments subsamples for cell counts were taken at all sampling times.

Upon termination of the experiments the animals were picked out and deep frozen for later determination of their carbon content. The faecal material which had accumulated in the beakers over the course of the experiment was collected and washed in filtered sea water. A portion of the faecal material was deep frozen for determination of the assimilation rates, while the remainder was used for the measurement of chlorophyll a content .

Preliminary Results

As a first evaluation of the feeding activities of the different grazers, the change of phytoplankton biomass over time was examined. Based on these data and other variables still to be measured (e.g. POC content of grazers and faecal pellets, phytoplankton cell counts) weight-specific feeding rates and assimilation efficiencies as well as the impact of selective feeding will be addressed. Results from 4 of the 6 types of feeding experiments are presented below.

Effect of food particle size:

The different phytoplankton groups used as food organisms covered a size range between <10 µm (pure culture of Cryptomonads) and >1-2 mm (aggregated diatoms from brown ice samples and aggregated colonies of *Phaeocystis*). In our experiment, particles over the entire size range were efficiently grazed by *Euphausia superba*. The three size classes of Krill (small, medium, large) fed equally well on all food particles tested except the Cryptomonads (8-10 µm). In the cryptomonad culture, the biomass decreased continuously only in the beakers containing small and medium-sized Krill (Fig.72). Large Krill, however, was not able to efficiently graze on such small particles. This is indicated by the slow decrease in cryptomonad biomass during the first 30 hours and the stagnation in biomass thereafter. On the other hand, extremely large food particles (brown ice and *Phaeocystis* aggregates) could be accommodated equally well by all three size classes (Fig. 73 and 74). In fact, individual Krill were observed to capture large aggregates in their feeding baskets. Krill feeding on such concentrated food packages produced extremely long faeces (up to 20 cm), which often remained attached to the animals. In a mixture of small cryptomonads and large diatoms, the phytoplankton biomass was diminished just as fast as in beakers with only one size of food particles

(Fig. 75). Phytoplankton cell counts for each sample interval will show whether the different-sized particles are grazed upon preferentially.
In contrast to Krill, the three species of copepods used in our experiments did not seem to feed efficiently on any of the food organisms. In most cases, the change in phytoplankton biomass in beakers with copepods was very similar to the change in the control beakers (Fig. 72, 74, and 75). In the experiment where brown ice aggregates were used as food particles, the phytoplankton biomass in the copepod beakers even seemed to increase when compared to the control (Fig. 73).

Effect of food concentration

The initial food concentrations in the different experiments ranged between 6 and 41 µg chl a l^{-1}. In the case of high initial concentration, the phytoplankton biomass decreased almost linearly over a period of 72 hours (Fig. 72) to values smaller than 3 µg chl a l^{-1} (small Krill). However, once a certain lower limit of food concentration was reached, the decrease in biomass slowly levelled off (Fig. 74 and 75). This lower limit was largely independent of both the size of the food particles and the size class of the Krill, although a slighty higher threshold limit of larger Krill seems to be indicated in Fig. 75a. In all except this case, final concentrations were well below 1 µg chl a l^{-1}. Such levels were commonly encountered *in situ* over most of the area studied during this cruise.

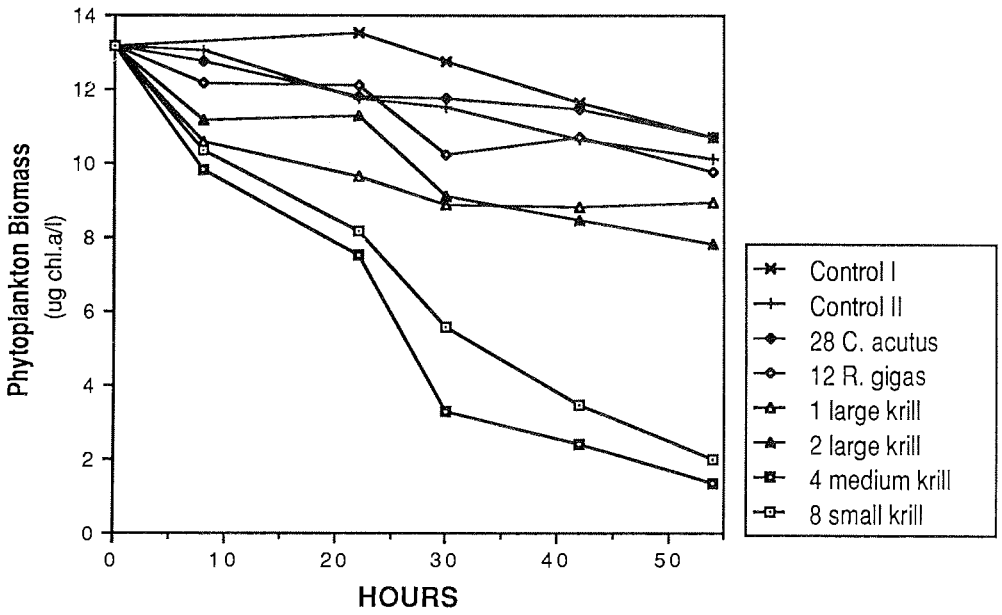

Fig. 72: Effect of different grazers on a culture of Cryptomonads (particle size 8-10 µm).

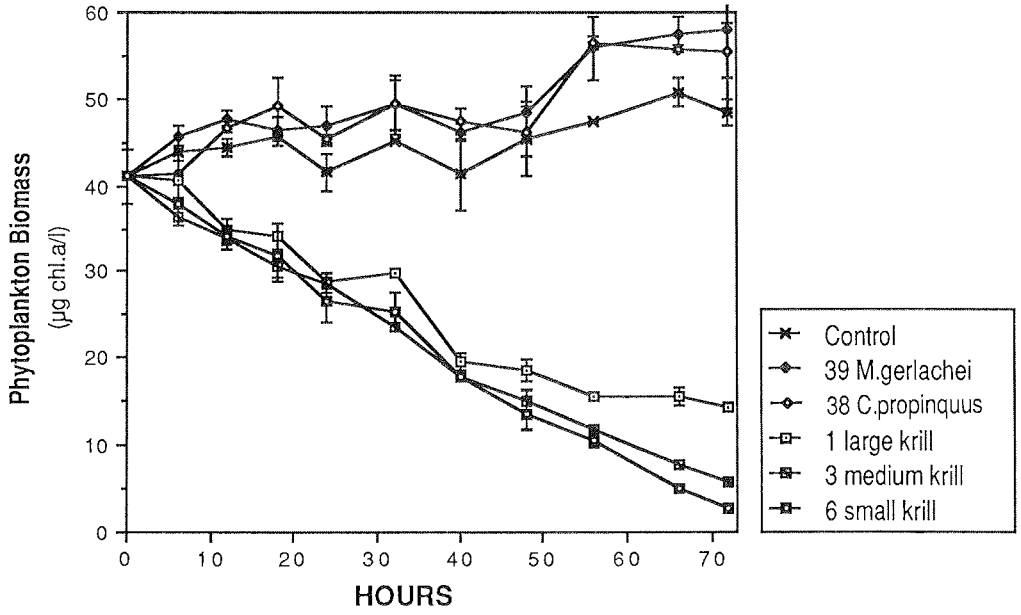

Fig. 73: Effect of different grazers on aggregated brown ice (Sta. 180) phytoplankton (particle size 0.5-4 mm).

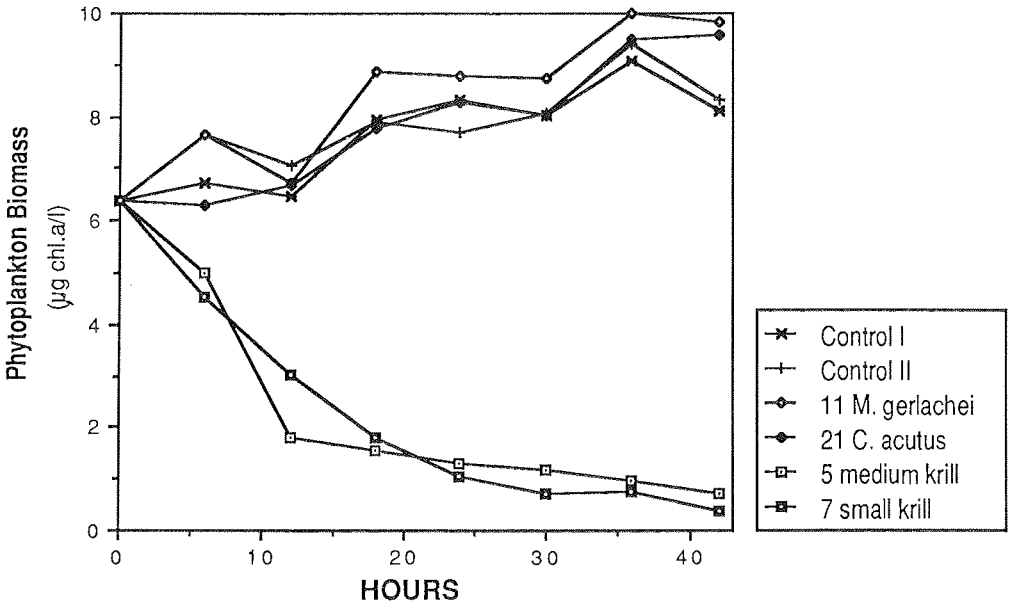

Fig. 74: Effect of different grazers on aggregated *Phaeocystis* colonies (particle size 0.2-2 mm)

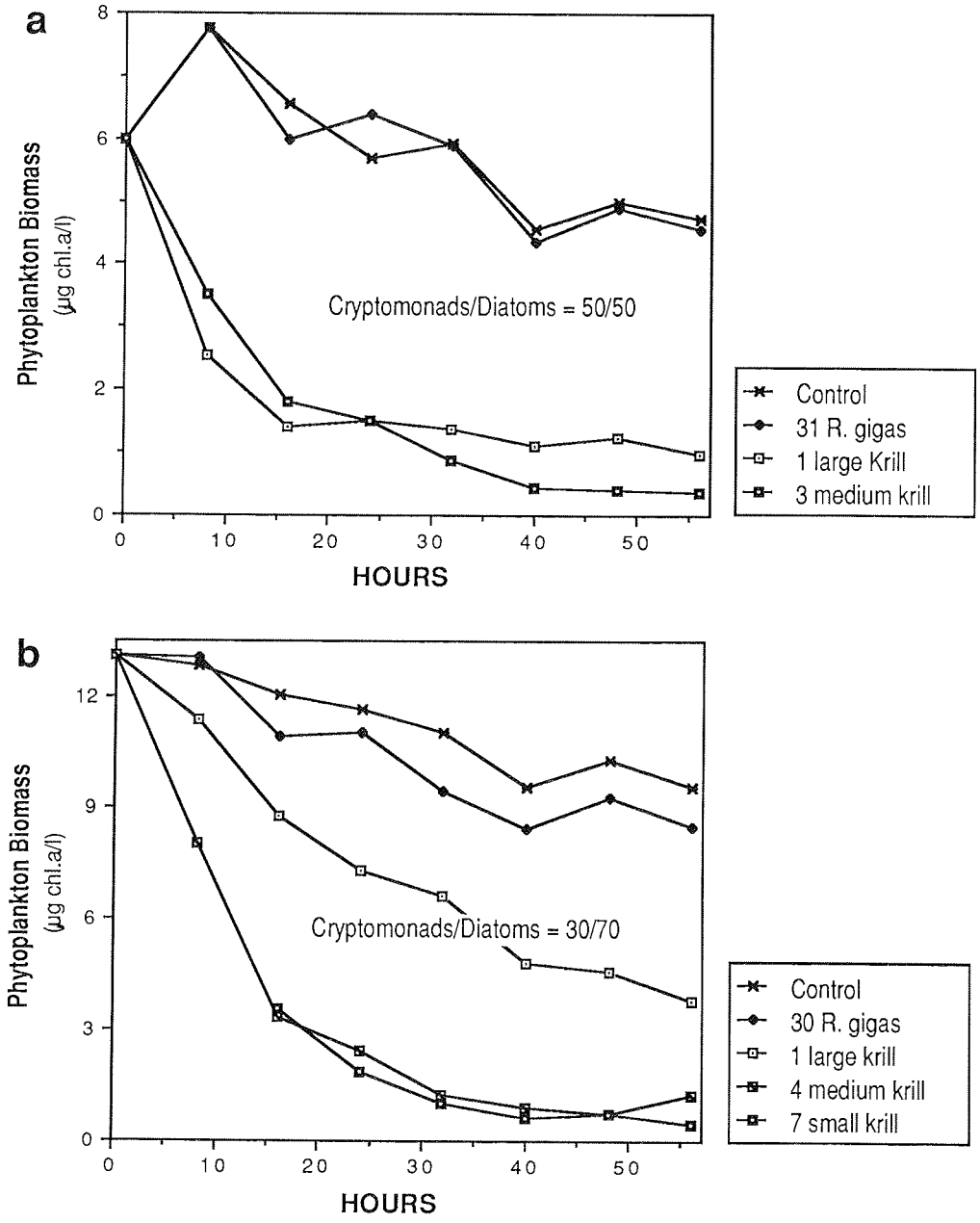

Fig. 75: Effect of different grazers on a mixture of Cryptomonads and large diatoms; a. Cryptomonad biomass / diatom biomass = 50 / 50; b. Cryptomonad biomass / diatom biomass = 30 / 70

4.3.5 Faeces Sedimentation

G.Cadee, H. Gonzalez

Objectives

Vertical flux of particulate material is an important process diverting organic substance from the surface to deeper layers. The composition of sinking particles can further provide information on processes occurring in surface layers. We measured vertical particle flux using free-floating sediment traps deployed at selected time stations.

Work at Sea

Funnel-shaped (Kiel-Type) sediment traps were used for 10 to 24 hours at time stations, usually at 2 depths (75 and 150 m). Before homogenizing and subsampling for POC, PON, Chlorophyll, Biogenic Si, Faecal pellets and Ba, a small aliquot of the samples was inspected microscopically. Chlorophyll and pheopigment were measured by Jaques. The chloroform used in the traps as a poison changes part of the chlorophyll into pheopigment; accordingly, chlorophyll and pheopigment are combined as "chlorophyll equivalents". Faecal pellet size was measured; other data will follow later. An ingenious method of anchoring traps to an icefloe was invented by the ships crew.

Samples for faecal pellets were collected in the upper 300 m: ca. 30 Niskin bottle samples (30 l each) were filtered for pellets, and samples were taken with nets (mess size 50 µm) hauled vertically. These samples will be analysed in Bremerhaven by Gonzalez for pellet types and pellet composition in order to assess food consumed and possible selective feeding by herbivores. In addition, ca. 400 water samples of 0.2 l each were collected to study phytoplankton abundance and composition (= food available for the herbivores).

Preliminary Results

Time Stations

Sediment traps deployed at Sta. 159 (Scotia Sea, 150 m only) indicated sedimentation of mainly faecal material, probably salp faeces. The daily flux of chlorophyll + pheopigment amounted to only 0.1% of the standing stock above the trap, indicating efficient recycling in the upper layer.

Sediment traps deployed at 75 and 150 m at Sta. 157 (Krill station) indicated sedimentation of appreciable amounts of faecal strings of Krill. In the 150 m trap, moreover, oval pellets occurred in larger amounts than in the 75 m trap, pointing to a higher production of these pellets below 75 m. The average width of Krill faeces in the 150 m trap was larger than in the 75 m trap (400 and 300 µm, respectively), they also showed a higher state of degradation in the deeper trap. Krill faecal strings contained many diatom fragments. The daily flux of chlorophyll *a* + pheopigment was largest at this station, amounting to ca 3.5% of the standing stock above the trap of 75 m and 2.5% for the 150 m trap.

Sediment traps at ice-stations (156, 169 and 178) gave comparable results: euphausiid ("Krill") faecal strings, although less abundant than at the Krill station, dominated, indicating the presence of euphausiids under the ice. Particularly at Sta.156 a marked difference was found in width of Krill faecal strings at the two depths: at 50 m the average width was 150 µm, at 150 m 250 µm, faecal strings of less than 100 µm width abounded in the 50 m trap, but were absent at 150 m. This suggests that the smaller faecal strings have a low settling velocity and could be degraded before reaching greater depths. Experiments were therefore started measuring settling velocities of Krill faeces (see section Experiments). As observed at the Krill station, oval pellets were more abundant in the deeper traps. The daily flux of chlorophyll a + pheopigment varied from 0.1 to 0.7% of the standing stock, indicating efficient recycling in the upper layer.

Experiments: Faeces

A number of zooplankton organisms were kept alive in order to study the type of faecal pellets they produce. This enabled us to get information on pellet types of some euphausiids, salps, amphipods, mysids and Tomopteris. The oval pellets observed in sediment trap and net samples appear not to be produced by these organisms. Chaetognaths and / or ctenophores could be the producers of these mysterious oval pellets, but such predators proved to be difficult to keep alive and feeding.

A good relation was found between age (length) of Krill and width of faecal strings produced, although size range is large: juvenile Krill (22 mm length) produced strings of 48 - 144 µm (mode 96 µm), adult Krill (45 - 50 µm length) strings of 120 - 335 µm (mode 240 µm).

Potential settling velocities of Krill faecal strings and oval faecal pellets were measured in settling tubes at ca 0°C and 34 ‰ S in order to explain differences observed in material settling in sediment traps used at different depths. Oval pellets were obtained from vertical nets, Krill faecal strings were obtained by RMT and Bongo nets.
Oval pellets showed sinking rates from 100 to 300 m/day, with a steep increase with size. Small Krill faecal strings of the same volume as the largest oval pellets had sinking rates of ca. 100 m/day; also for Krill faecal strings sinking rate increased with size (volume), but this increase was less steep than in oval pellets (related to the difference in form and compaction). Food appeared to be a dominant factor in sinking rate: faecal strings from Krill fed on *Phaeocystis* or Cryptomonas showed a lower sinking rate than those from Krill fed on ice-algae. Faecal strings of Krill in nature had settling velocities in between.

Highest sinking rates measured were ca. 500 m/day for a "natural" faecal string of 10.5 mm long and 0.24 mm wide. However, in the deeper sediment traps broader faecal strings were collected, these could not be collected later for our settling experiments, but extrapolating from our experiments, they must have sinking rates of up to 1000 m/day.

4.3.6 A Multiparameter Approach to Krill Ecology: An attempt to summarize.

G.C. Cadee, J. Cuzin-Roudy, H. Gonzalez, E. Graneli, L. Lindner, U. Riebesell, P. Schalk, S. Schiel, I. Schloss.

Introduction

Many references can be found on the study of Krill and research on this dominating species of the Antarctic waters has been conducted from a multitude of scientific angles. However when one wants to compose a complete picture of the life history and ecological significance of Krill the pieces of the puzzle have to be derived from data of different areas and different seasons and years. During the EPOS leg 2 cruise, research was conducted along a transect from the Weddell Sea pack ice well into the open Weddell-Scotia Sea Confluence waters during a period of 7 weeks, which permitted us to follow the summer development of the Antarctic pelagic ecosystem. Investigations were conducted on hydrography, chemistry and all levels of the food web, offering an ideal opportunity to sketch a complete Krill picture from one continuous data set. In this paper we sumarize EPOS data on growth, sexual development, respiratory activity, grazing, silica uptake, migratory behaviour and schooling and match this with the background of the vast amount of literature available.

Development and sexual maturity

The area investigated by leg 2 is known to be one of the main spawning sites of Krill, *Euphausia superba*, during the Antarctic summer. The period covered by our cruise corresponded to a phase of transition in Krill physiology, between a winter adaptation to the ice biota and a summer pelagic life. Food requirements for Krill change as they develop from the juvenile to the adult stage, but also when they move from the sexually inactive phase in winter to the summer phase of brood maturation. Ice-edge phytoplankton blooms are believed to provide the source of food which is necessary for the fulfillment of the enlarged energy requirements for gametogenesis and yolk accumulation in eggs. Then the grazing pressure exerted on ice-edge phytoplanktonic production by maturing Krill is likely to be the determinant biological factor for the changes in the structure of the pelagic communities.

Respiratory activity.

The respiratory activity of different developmental stages of Krill has been measured by determining the activity of the Electron Transport System (ETS), which gives a relative measure for the respiration rate of the organism (Schalk, 1988). Distinct differences in respiratory activity were found for the various developmental stages of Krill. Juveniles showed relatively high activities (± 30 µg-at O/g h), probably related to enhanced growth rates. The sexually inactive adults captured in November showed rather low activities (± 20 µg-at O/g h), increasing gradually with the further development of sexual maturity to a four times higher activity in fully mature specimens (± 80 µg-at O/g h) captured in the beginning of January. The temperature dependence of the respiratory enzymes showed a large

increase of a factor two from 0°C at the ice edge to 2°C in the open water. These two factors together, maturing and the increasing water temperatures encountered during the summer migration to open waters, increase respiratory activity by a factor six, which considerably enhances the grazing pressure on the Antarctic pelagic ecosystem.

Effects of Krill grazing on phytoplankton communities

Experiments were performed in 25-litre jerry cans exposed to 16:8 light dark cycle and ca 0°C. The cans were filled with 18 litres of unfiltered seawater containing the indigenous plankton communities + an "extra" inoculum of phytoplankton collected on a 20µm mesh size nylon net to start with a high phytoplankton level (ca. 5 µg chlorophyll a l^{-1}). Four jerry cans were used for the Krill experiments: Control (no additions of zooplankton or Krill), Zooplankton (ca 10 x the natural zooplankton concentrations), Krill (Exp. Sta. 158= 6 juvenile + 2 adult Krill; Exp. Sta. 167= 6 juvenile + 2 adults, and then 4 more adults after 4 days), Krill + zooplankton (additions were a combination of the "zooplankton" and "Krill" jerry cans). The results show that Krill is a very efficient grazer, decreasing chlorophyll a values to nearly zero within 3 days. Afterwards the Krill were removed from the jerry cans, the phytoplankton community that developed in the cans was basically identical to that observed in the Weddell Sea samples from the latter part of the cruise period. In the "zooplankton and Krill" containers, the results suggest that Krill only started to feed on the phytoplankton after grazing down the mesozooplankton (See § 4.2.12).

Grazing rates

In a number of experiments, Krill of three different size classes were exposed to a variety of food organisms. Food particles differed both in size and composition. The particle size ranged from <10µm (small flagellates) to >1-2mm (aggregates of *Phaeocystis* colonies and of brown-ice phytoplankton). Food composition included unialgal cultures of cryptomonads and *Phaeocystis*, natural phytoplankton assemblages, and different mixtures of cryptomonads and diatoms. The grazing rates were high for all food items tested. No obvious differences in feeding efficiency were found between the three size classes, with the exception of large Krill which did not feed effectively on the smallest food particles (<10µm). While the feeding activity of small and medium-sized Krill continued to food concentrations of less than 2 µg chlorophyll a l^{-1}, the concentration leveled off at around 8-9 µg chlorophyll a l^{-1} in beakers containing large Krill. Particles >10 µm and up to 1-2 mm, on the other hand, were grazed upon efficiently even by small Krill. The phytoplankton biomass was grazed to values well below 1 µg chlorophyll a l^{-1} by all size classes of Krill. Such concentration levels of chlorophyll were commonly encountered in situ during the cruise. Our experiments indicate that Krill is not a very selective grazer. The kinds of particles it can feed on efficiently span a wide range of particle sizes and phytoplankton composition.

Uptake and excretion of $^{32}Si(^{32}P)$ labelled phytoplankton

The ^{32}Silicon isotope offers the possibility to study the uptake and excretion of a specific type of food, notably silicon-containing diatoms and silicoflagellates. Using the filtered waste water from the ^{32}Si-uptake studies on phytoplankton collected at various stations (Van Bennekom et al.), a mixed culture was grown during several days. As a result, a considerable fraction, in the order of 10%, of the initially dissolved ^{32}Si was administered by the culture. Radioactivity measurements were carried out by Cerenkov counting of parent ^{32}P activity (L.Lindner). This culture was used for grazing by Krill. In a one day cycle much of the available labelled biomass had been grazed, as could be concluded from whole-body Cerenkov counting of live Krill. Subsequent dissection of the Krill indicated that about 50% of the ^{32}P activity had concentrated in the digestive glands with the balance of activity primarily in muscle tissue, approx. 35%, and in the cuticle plus epidermis, approx. 13%. The gut contained only a few percent and blood even less. Decay analysis of the samples will eventually reveal the actual ^{32}Si-distribution. Fecal pellets were shown to contain much ^{32}Si as could be expected; figures on the rate of excretion of ^{32}Si are not available yet.

Faeces

String-like faeces most probably produced by Krill dominated in sediment-trap samples, particularly in the "Krill" station (157). Deeper traps (150 m) usually contained broader strings than the shallower traps (50 or 75 m).

Potential settling velocities of Krill faecal strings of different size were measured at 0°C and 34‰ S in order to explain these differences. "Natural" Krill faeces were obtained from Krill collected by nets. Potential sinking rate depended on size (volume) and increased from less than 100 to over 500 m/day. Extrapolating from these data the largest faecal strings from the deeper traps might have sinking velocities of up to 1000 m/day. The smallest faecal strings could probably be degraded before reaching the 150 m trap. We also experimented with Krill faecal strings from cultures fed on different food types obtained from Sigrid Schiel. Food composition appeared to be a dominant factor influencing sinking rate: faecal strings from Krill fed on *Phaeocystis* or Cryptomonas showed a lower sinking rate than those from Krill fed on ice-algae, "natural" faecal strings having settling velocities in between. Experiments with oval faecal pellets abundant in deeper sediment traps showed these to have higher sinking rates than Krill faeces of equal volume, the higher rates were probably related to the difference in form and compaction.

Migration and schooling behaviour

Continuous observations of acoustic backscattering were made with a 30 and 150 kc echosounder in the upper 500 m of the water column. Along the 49°W transect schools present on the echograms were counted and their depth, horizontal and vertical extension were measured. In some cases a verification of the organisms responsible for the backscattering was attempted by making RMT 1+8 hauls through the depth layers where schools occurred. These catches yielded as most abundant organisms invariable Krill when dense schools were observed and salps and

siphonophores when faint more curtain like structures were present. The amount of schools, and their vertical extension and depth, increased from the end of November to the end of December, suggesting a growing biomass in the water column. A strong increase of ammonia centred at approx. 50-100 m depth was reported during this period (see § 4.1.6) and grazed down phytoplankton stocks support the suggested biomass increase.
The observed schools showed a distinct diel migration and dispersed during the "night" between 22.00 and 02.00 hours. The depth of occurrence decreased near the ice edge, while in the ice hardly any schools were observed. That Krill was present in the ice covered water was evident from observations of large numbers of Krill washed on the ice in the ships wake and large numbers of penguins and seals in this part of the section (§ 4.4). This agrees with underwater observations of Marshall, that the Krill stays directly under the ice floes, invisible for the echosounder, to graze on the ice algae. It seems that the gradual blocking of light in the water column by the increasing numbers of ice floes triggers the upward migration and subsequent dispersal of the Krill under the floes.

Preliminary results and discussion.

The EPOS studies show that the role of Krill in the pelagic ecosystem is a complicated one. The first leg of the EPOS programme, in Oktober/November, gave prove of the winter situation. Chlorophyll concentrations were low and no acoustic backscattering was observed and netcatches were very meager, hardly yielding any Krill. Under ice observations showed that dense Krill populations were activily grazing on the ice algae growing on the underside of the ice cover. During EPOS Leg 2, end November to January, the spring/summer development of the pelagic ecosystem was observed. Chlorophyll concentration were evidently raised compared to the first leg and showed a large degree of patchiness along the two transects studied, but also in time. Juvenile and sexually inmature Krill were found under the ice, while in the open water an increasing number of swarms were detected with the echosounder. Net catches yielded relatively large catches from 1 to 42 kilos wetweight of Krill per haul. ETS experiments revealed distinct differences in metabolic activity between inmature and mature Krill, suggesting that the energy and food demand goes up significantly during the sexual development. Only the relatively inactive stages were found under the ice. In the mean while (as a result of the increased metabolic activities?) maturing Krill moved out from its winter habitat to open waters, forming large and dense swarms, 'cleaning' the water from its algae bloom, causing a hail of faeces in the deeper water layers. The effect of Krill grazing on the phytoplankton stock may have been witnessed at station 157, where the chlorophyl concentration decreased by about 50% overnight. Preliminary data from the echograms seem to support this grazing theory. The observed patchiness in phytoplankton biomass may be caused for a large part by the grazing of swarms, and maybe we should speak in this context of swarms as being the 'megaherbivores' of the ocean. Grazing and uptake experiments showed that consumption by Krill can be impresively high and effective. The study of Krill faeces pointed out that its menu varies from small algae to mesozooplankton. Possibly carnivorous behaviour occurs when the searching swarms cannot find sufficient algae stocks to support their metabolic demands. More evidence of the presence

stocks to support their metabolic demands. More evidence of the presence of a large and grazing Krill stock is given by the ammonium profiles (§ 4.1.6), which showed a peak concentration in this area.

It is too early to ty exact figures to the relation between primary production and Krill abundance and grazing rate. However, the present data set is both extremely varied as well as extensive and should deliver enough evidence to compose a picture of Krill life history. After working up these datasets it will be possible to present an unique and reasonably complete balance of stocks, flows and processes in the Antarctic pelagic ecosystem and its spatial and temporal variation.

When these data sets have been processed it will be possible to present a total balance of flows through the Antarctic pelagic ecosystem due to Krill.

4.4 SEA-BIRDS, SEALS AND WHALES

J. A. van Franeker

Objectives

Sea-birds, seals and whales are the top consumers in the Antarctic ecosystem, and as such they can be useful monitors of the characteristics of the water masses below. Changes in species composition of bird and mammal fauna may be expected to reflect changing physical and biological properties of the environment. Biomass estimates of top consumers represent minimum figures for biomass/productivity in consecutive lower levels in the food chain.

The purpose of this study was to identify which are the factors that regulate distribution and abundance of species(communities) of sea-birds and mammals. This preliminary cruise report mainly serves to give an impression of the type of data collected. Factors explaining the observed patterns can only be discussed properly after comparing data from this study with the results of a wide variety of research programs on EPOS Leg 2 .

Work at Sea

During all transects of EPOS Leg 2 the distribution and densities of birds and mammals were surveyed from an outdoor observation post, installed on top of the bridge of Polarstern. Outdoor observations were preferred to observations from the bridge as a full angle of view is needed for optimal counts and identifications. Additionally, sounds are a useful help in spotting inconspicuous animals, like penguins in open water. The census method consisted of standard 10 minute counts, covering a transect 300 meters wide, usually 150 meters to each side of the moving ship. Distances were determined with a range-finder as described by Heinemann (1981). The counting method differs slightly from the one advised by the BIOMASS Working Party on Bird Ecology (1982): in contrast to BIOMASS methods, birds flying through the transect area were not counted continuously, but only at specific time points as described by Tasker et al. 1984. Continuous counts of flying birds would lead to bias in density estimates. Ship-associated individuals of any species were omitted from counts. For each ten min count, data on sea-state, precipitation, ice-cover, icebergs, etc. were noted. Furthermore, any count can be linked to the 10 min averages of all ship´s data, like position, temperatures, wind and speed. Knowing the speed of the ship, results of 10-min counts can be used to calculate densities or biomass per unit area. Calculating average density or biomass from 10 min counts is possible only for birds and seals, as they occur regularly enough to level out any incidental variations. In rare animals, such as whales, the low frequency of occurrence hampers such use of data. Species observed outside the transect area, or associated with the ship, were noted separately to obtain maximum information on species distribution (not density).

In addition to the standard counts from the moving ship, bird occurrences around the ship at stations were recorded as well. For each species the maximum number of individuals that was simultaneously observed was noted. Observations usually lasted about an hour, with a minimum of 30 min.

Binoculars (10x40) were used to scan the surroundings, because groups of birds were often resting at some distance from the ship. Station observations give a qualitative description of bird-life in an area, but cannot be used for quantitative work as there is no reference to surface area.

Preliminary Results

This preliminary report can only show results of the first transect along the 49th meridian, from 57 to 62 degrees latitude (south plus northward transect combined; 26 November to 12 December 1988). A general description of the changing sea-bird species/communities along the transect is best given by a listing of station observations (Tab. 25). Station numbers allow comparison with physical, chemical, and biological data presented in other chapters of the EPOS Leg 2 cruise report.

Albatrosses dominated the bird community in 'Scotia' waters. Further south, in 'Confluence' waters albatrosses disappeared and were replaced by smaller types of tube-nosed sea-birds; the Cape Petrel especially became highly abundant. Data collected during later transects indicate that even within the Confluence there is a zonation into separate Prion, Fulmar and Cape Petrel areas. The 'Weddell Sea' water was ice covered during the first transect, and the bird community was dominated by Adelie Penguins, Snow- and Antarctic Petrel. Chinstrap Penguins were encountered from open Confluence waters far into the more open ice areas.

The occurrence of different bird communities in the consecutive zones from north to south, is also clearly reflected when expressing data as biomass Figs. 76-79 From transect counts in between stations (geographical positions) average figures for observed biomass per unit area have been calculated. E.g. a) no observations were possible between stations 144-145 and between 149-150; b) weights of some species had to be roughly estimated and may be changed in later analyses; c) corrections from 'observed' to 'estimated' numbers may be applied during later analysis.

Results of biomass calculations are shown for albatrosses (Fig.76), for petrels (Fig.77), and for penguins (Fig.78). Apart from the shifting species communities, the figures also show an increase of bird biomass in ice-covered areas, which becomes especially apparent when combining all bird data in Fig.79. High numbers of Penguins, mostly Adelie Penguin, are responsible for this increase. The maximum average of nearly 60 kg per square kilometre represents about 15 penguins.

Tab. 25: Observations of Birds at Stations along 49°West (EPOS Leg 2, first south/north transect, 26 Nov. - 11 Dec. 1988)

	test	meso	time	meso	micr	time	bloo	micr	meso	meso	time	micr	meso
nr	142	143	159	145	146	157	158	148	149	151	156	152	153
date	2611	2611	1012	2711	2711	612	812	2811	2811	2911	412	2911	3011
lat	5628	5700	5700	5800	5830	5900	5922	5930	6000	6100	6100	6130	6200
T	4.3	1.7	2.3	0.3	-0.2	-0.1	-0.4	-0.7	-0.8	-1	-1.1	-1.1	-1.2
Ice	0	0	0	0	0	1	5	1	35	75	50	95	98
RWA			1										
BIP		1	1	1									
SPP	1		2										
GHA	1	2	12										
LMS	3		4	1									
WCP	3	2	4	1			1						
BBA	3	5	70	1	1		1						
PRI	100	150	50	3	50	75	2						
BBS	2	1	1	1	1		2		3				
FUL	1	7	7	4	2	2	5	3	5				
DAP	20	15	3	100	100	1700	330	15	20		6	1	
WSP	1	4	2	1		10	5	1	4	1	8	4	
Msp	3	5	4	3	2	10	6	1	1		2	2	
CHI			5	3		23	23	2	8	3	40		
KIP			1			1					1		
TER						1			7		4		
GUL						4			1	2	6		
SKU							2	1			1		
SNO						6	3	1	15	2	7	12	2
THA							1		1	1	3	1	1
ADE										16	20	13	32

numbers given are maximum numbers of birds simultaneously present

T = surface water temperature as recorded by ship

Ice = approximate percentage of ice cover

RWA	=ROYAL/WANDERING ALBATROSS	= *Diomedeae pomophora/vexulans*
BIP	=BLUE PETREL	= *Halobaena caerulea*
SPP	=SOFT-PLUMAGED PETREL	=*Pterodroma mollis*
GHA	=GREY-HEADED ALBATROSS	= *Diomedea chrysostoma*
LMS	=LIGHT MANTLED SOOTY ALBATROSS	=*Phoebetria palbebrata*
WCP	=WHITE CHINNED PETREL	=*Procellaria aequinoctialis*
BBA	=BLACK BROWED ALBATROSS	=*Diomedea melanophris*
PRI	=PRION (ANTARCTIC)	=*Pachyptila* sp *(vittata)*
BBS	=BLACK BELLIED STORM PETREL	=*Fregatta tropica*
FUL	=SOUTHERN FULMAR	=*Fulmarus glacialoides*
DAP	=CAPE PETREL(PIGEON)	=*Daption capense*
WSP	=WILSON'S STORM PETREL	=*Oceanites oceanicus*
Msp	=GIANT PETREL (SOUTHERN)	=*Macronectes* sp *(giganteus)*
CHI	=CHINSTRAP PENGUIN	=*Pygoscelis antarctica*
KIP	=AMERICAN SHEATHBILL	=*Chionis alba*
TER	=TERN (ARCTIC/ANTARCTIC)	=*Sterna* sp *(paradisea(vittata)*
GUL	=DOMINICAN GULL	=*Larus dominicanus*
SKU	=ANTARCTIC SKUA	=*Catharacta antarctica*
SNO	=SNOW PETREL	=*Pagodroma nivea*
THA	=ANTARCTIC PETREL	=*Thalassoica antarctica*
ADE	=ADELIE PENGUIN	=*Pygoscelis adeliae*

Fig. 76 to 79

The observed biomass of top-consumers in ice-covered areas shows a further sharp increase if seals are also considered (Fig.80). In areas with high ice-cover (>90%), 2 to 3 seals were observed per square kilometre, mostly Crabeater Seals, but also some Leopard Seals. Many Leopard Seals had rather small pups, whereas pups of Crabeaters had already reached a size not easily distinguishable from that of adults. Average seal biomass increased to ca. 400 kg in areas with over 90% ice-cover. Seal biomass was over 500 kg per km^2 in between Sta.152 and 153. Both during transect counts and during time stations, data could be collected to show that Crabeater seals tend to sleep on the ice during the day and enter the water in late afternoon to feed during the night. They are more difficult to detect when in the water, and will be strongly underestimated. Data in Fig.80 are not corrected for this, and represent minimum figures for seals only.

Fig. 80

Whales were not observed during the first transect along 49°West. Only in late December did whale sightings become common, with many observations of Minke Whales in the ice areas, and regular groups of larger fin whales (Fin and/or Sei Whale) in open water. As stated before, inclusion of whales in biomass figures as presented in this report is problematic, as the frequency of observations of whales within the counted transect is too low to result in reliable averages. The following listing summarizes observations of mammal species during EPOS Leg 2 (up to January 4).

Seals and Whales Observed

CRABEATER SEAL = *Lobodon carcinophagus* : abundant in ice areas
LEOPARD SEAL = *Hydrurga leptonyx*: common in ice areas
WEDDELL SEAL = *Leptonychotes weddellii* : one on sea ice 47°West
ELEPHANT SEAL = *Mirounga leonina* : few at ice edge off South Orkneys
ANTARCTIC FUR SEAL = *Arctocephalus gazella* : one in open water
SOUTHERN BOTTLENOSE WHALE = *Hyperoodon planifrons* : two seen north of the South Orkneys, just out of the ice edge
MINKE WHALE = *Balaenoptera acutorostrata* : common in the ice during the second half of December
SEI WHALE ? = *Balaenoptera borealis*?: two single individuals, probably of this species in open water along 49°West.
FIN WHALE ? = *Balaenoptera physalus*?: several groups, together at least 12 individuals seen along 49°West during the second half of December. (Fin and Sei Whale identification is problematic, but the large whales seen definitely belong to either one of these species).
SPERM WHALE = *Physeter catodon* : one seen along 49°West
LONGFINNED PILOT WHALE = *Globicephala melaena* : a group of at least 6 individuals seen at 57°South in Scotia water.

Discussion

The data on distribution and abundance of birds and mammals will be compared to the results of other research programmes during EPOS Leg 2. For example, bird distributions were clearly correlated to CTD profiles during

the first transect, with different communities in Scotia, Confluence, and Weddell Sea water masses. A general impression from bird counts during later transects was that such a correlation remained largely intact, though shifts with retreating ice and other factors do occur. Intensive contact will be going on between this study and zooplankton programmes, as sea-bird abundance would be expected to be largely determined by food distribution. Especially data from continuous echo-sounding (see § 4.3.3) will be important as direct reference to ten-min periods is possible. For some stretches also, continuous phytoplankton monitoring is available. An important component of the bird/mammal program is the quantification of the high biomass encountered in ice-covered areas. It seems that this high biomass does not correspond very well to any of the data collected in the deeper water layers below the ice. No high zooplankton numbers are recorded (netting/echo-sounding), and data on phytoplankton abundance, nutrients, and breakdown products show little to nothing of elevated levels of biological production. Still, the abundance of birds and seals provides evidence that the sea-ice harbours very large and reliable stocks of suitable food, presumably mainly Krill. In turn this means that algal production in, or close below the ice, must be high enough to supply at least survival energy for such large zooplankton stocks. Clearly, the ice studies conducted by AWI both during EPOS Leg 1 and EPOS Leg 2 have important interactions with the bird program, as quantitative data on ice-based food-webs are still scant (Carey, 1985).

Literature confirms that high bird biomasses in ice areas are not limited in time or space. High densities of penguins are reported from ice areas in the central Weddell Sea in late summer: from late January to late March average densities of 11 to 28 Adelies per km^2 have been reported (Cline et al 1969; Zink 1981). For the Ross Sea, Ainley et al. (1984) estimated the total bird biomass at about 40 kg per km^2, which is of the same order of magnitude as observed in ice areas during the first transect of this study (Fig.79). It seems that the tremendous importance of the sea-ice in Antarctic biological production deserves intensive further studies.

Literature Cited

Ainley, D.G., E.F. O'Connor and R.J. Boekelheide (1984). The marine ecology of birds in the Ross Sea, Antarctica.Ornithological Monographs No.32 (AOU, Washington,D.C.)

Biomass Working Party on Bird Ecology (1982).Recording observations of birds at sea. BIOMASS Handbook 18.

Carey, A.G.Jr. (1985). Marine Ice Fauna: Arctic.pp. 173-190 in: Horner, R.A.(ed) (1985). Sea Ice Biota. Boca Raton, Florida.

Cline, D.R., D.B. Siniff, and A.W. Erickson (1969).Summer birds of the pack ice in the Weddell Sea, Antarctica.Auk 86:701-716.

Heinemann, D. (1981). A range finder for pelagic bird censusing. J.Wildl.Manage.45:489-493.

Tasker, M., P.- Hope-Jones, T. Dixon & B.F. Blake (1984).Counting sea-birds from ships: a review of methods employed and a suggestion for a standardized approach. Auk 101: 567-577

Zink, R.M. (1981).Notes on birds of the Weddell Sea, Antarctica.Le Gerfaut 71:59-74.

Figures 76+77: Observed Albatross and Petrel Biomass along 49°W Section

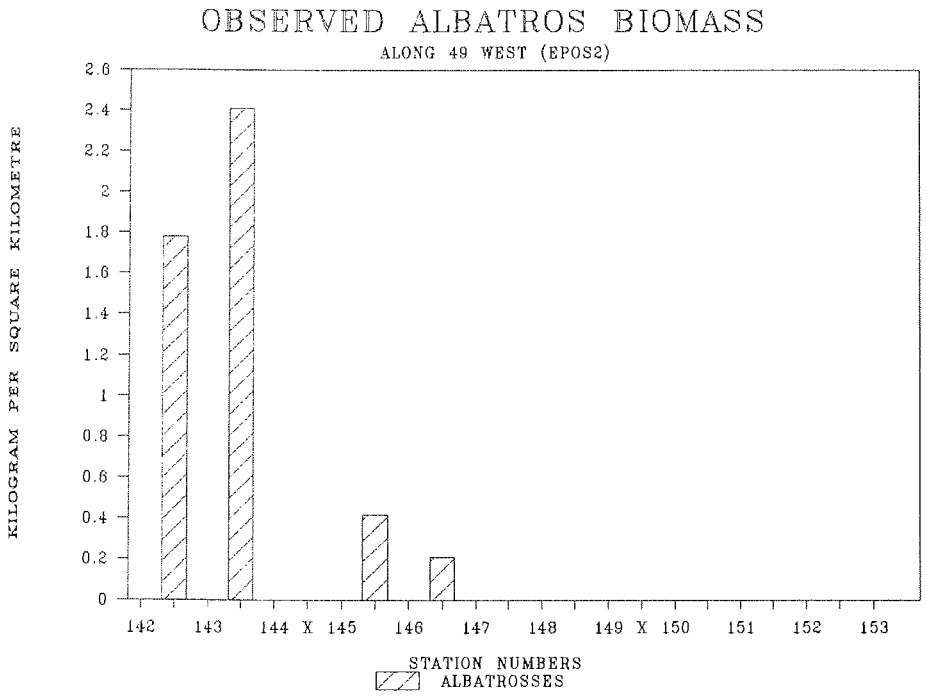

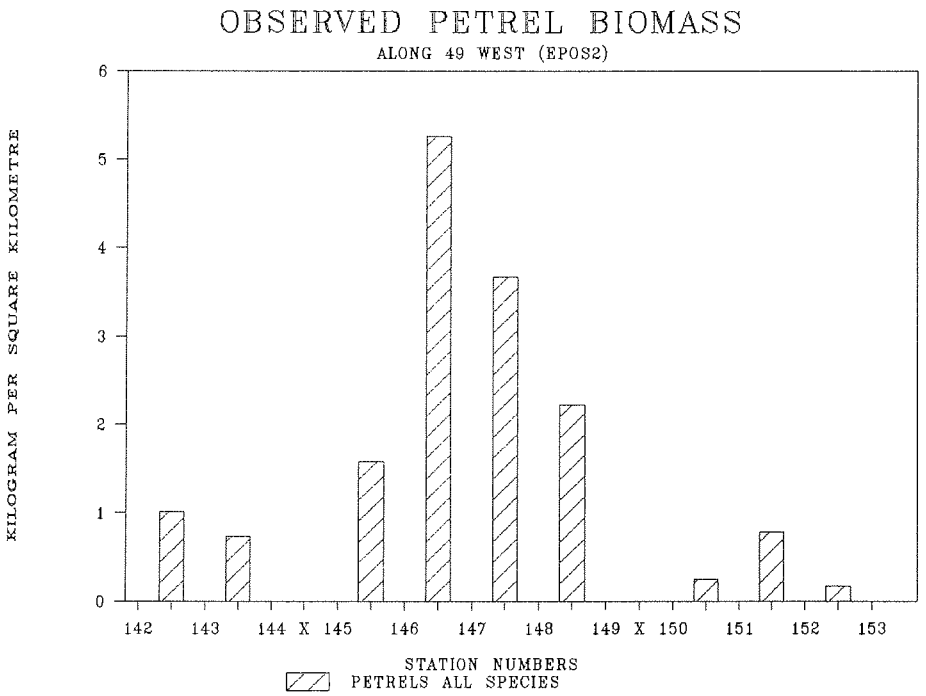

Figures 78+79: Observed Penguin and Bird Biomass along 49°W Section

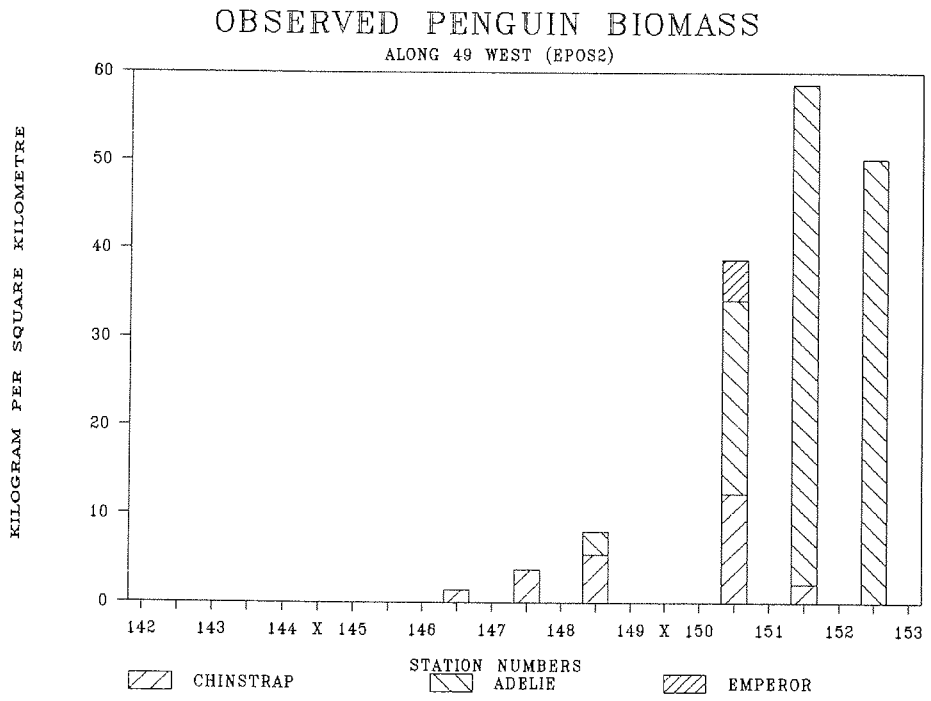

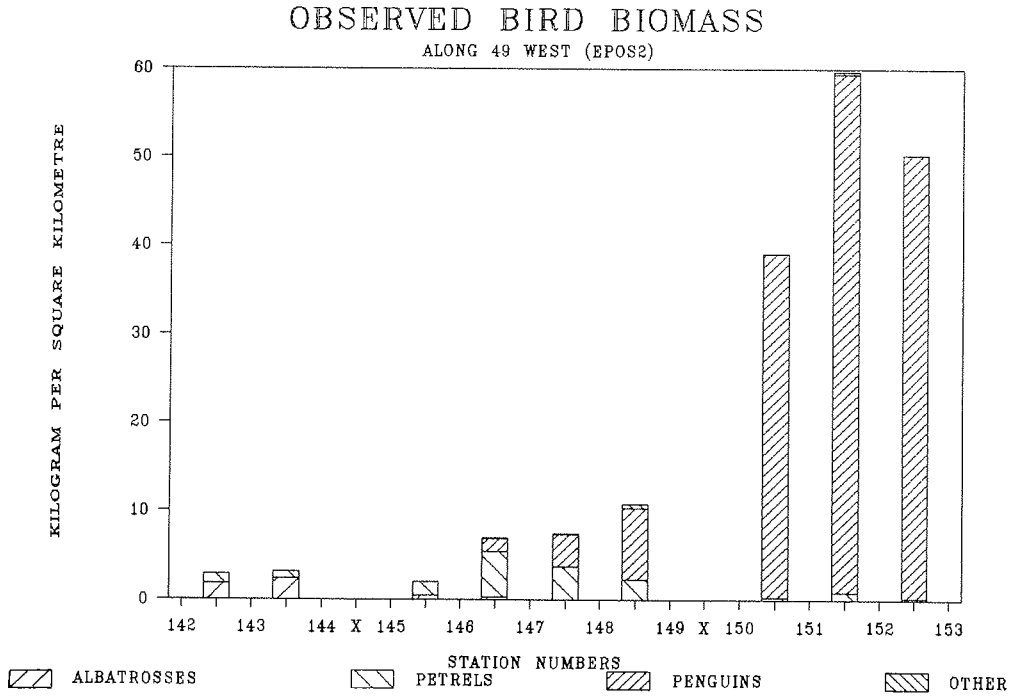

Figure 80: Observed Biomass of Seals along 49°W Section

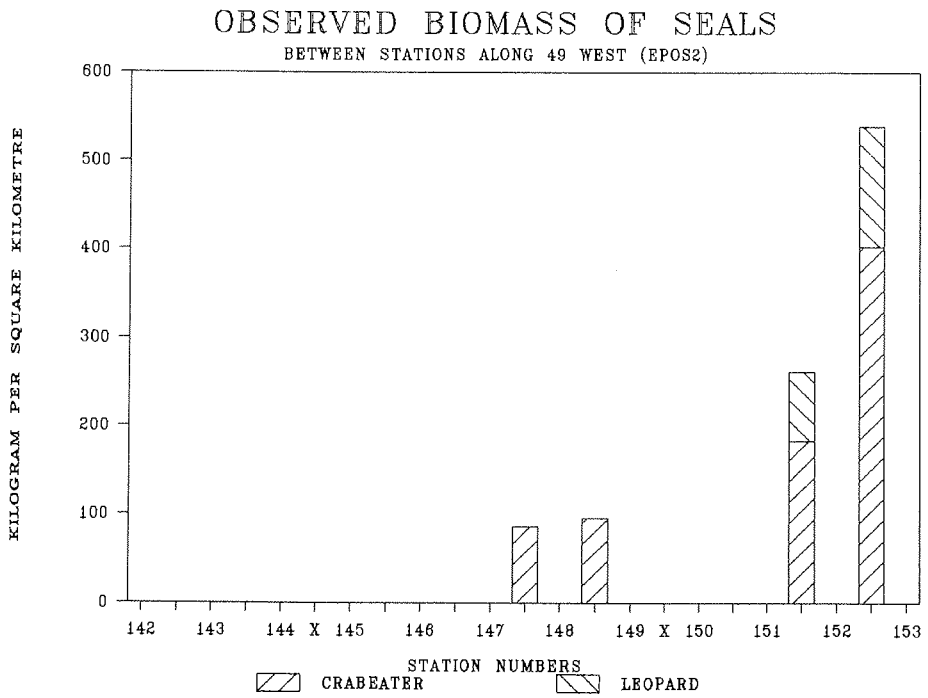

4.5 ANNEX

Station List

Used abbreviations

BO	Bongo net
COL	Colour Index Meter
CTD-RO	Conductivity Temperature Depth sonde with Rosette
FRA	Fransz net
ICE	Ice coring
MAN	Manta
MN	Multi net
NIS	Niskin Bottles
NSN	Nansen net
OM	Omori net
QUA	Quantameter
RB	Rubberboat
RMT	Rectangular Midwater Trawl (single)
RT	Ring Trawl
RO	Rosette
SD	Secchi Disc
ST	Sediment Trap
TOP	High Speed Sampler

T	Tag/ Day
M	Morgendämmerung/ Dawn
N	Nacht/ Night
A	Abenddämmerung/ Dusk

Stat. No.	Date	Position		Echo depth (m)	Gear	Haul No.	Day time	Start (GMT)	Haul dur. (min)	Depth (m)	Comment
142	26/11/88	56°28,1'S	050°47,7'W	4550	CTD-RO	1	T	09:07	55	1000	Teststation
					NIS	1	T	10:17	53	110	
					RO	1	T	11:27	11	50	
					QUA	1	T	11:48	12	65	
					CCL	1	T	12:07	5		
143	26/11/88	57°00,5'S	048°59,7'W	3935	CTD-RO	2	T	18:58	66	1500	
					NIS	2	T	20:08	85	1000	
					MN	1	T	21:42	73	1000	
					FRA	1	A	23:20	15	300	
					FRA	2	A	23:40	12	300	
					FRA	3	A	23:55	12	300	
					RO	2	N	00:11	9	30	
					RO	3	N	01:02	10	30	
					RO	4	N	01:44	9	30	
					RO	5	N	02:20	8	30	
					NSN	1	N	02:37	22	300	for experiments
144	27/11/88	57°58,4'S	049°01,6'W	3757	CTD-RO	3	N	05:40	73	1500	
145	27/11/88	57°58,4'S	048°58,7'W	4150	RMT	1	T	09:52	79	350	
					CTD-RO	4	T	11:26	26	500	
					MN	2	T	11:57	52	1000	
					FRA	4	T	12:58	12	300	
					FRA	5	T	13:11	12	300	
					FRA	6	T	13:24	13	300	
					CCL	2	T	13:51	3		
					QUA	2	T	13:58	15	70	
					SD	1	T	14:17	4		
					CTD-RO	5	T	14:23	72	1500	
					NIS	3	T	15:38	56	500	
146	27/11/88	58°30,0'S	049°01,1'W	3838	CTD-RO	6	T	20:41	71	1500	
					RMT	2	A	22:04	76	400	
					RO	6	A	23:31	9	20	
147	28/11/99	58°59,5'S	048°58,5'W	3930	NIS	4	N	03:05	75	500	
					CTD-RO	7	N	04:27	52	1500	
					MN	3	M	05:33	47	1000	
					FRA	7	M	06:30	12	300	
					FRA	8	M	06:47	10	300	
					FRA	9	M	06:57	12	300	
					CTD-RO	8	M	07:20	40	1000	
148	28/11/88	59°29,0'S	049°01,3'W	3695	RMT	3	T	11:17	70	400	
					RO	7	T	13:12	10	20	
					CCL	3	T	13:29	6		
					QUA	3	T	13:40	20	70	
					SD	2	T	14:03	3		
					CTD-RO	9	T	14:14	70	1500	
					NSN	2	T	15:28	22	300	for experiments
149	28/11/88	59°59,5'S	048°59,7'W	4034	CTD-RO	10	T	19:42	69	1500	
					NIS	5	T	20:55	60	500	
					MN	4	A	22:03	62	1000	
					FRA	10	A	23:13	12	300	
					FRA	11	A	23:27	12	300	

Stat. No.	Date	Position		Echo depth (m)	Gear	Haul No.	Day time	Start (GMT)	Haul dur. (min)	Depth (m)	Comment
					FRA	12	A	23:40	12	300	
150	29/11/88	60°29,4'S	049°01,0'W	1524	CTD-RO	11	N	05:00	60	1500	
151	29/11/88	60°58,7'S	048°59,0'W	1808	OM	1	T	11:04	27	500	
					MN	5	T	11:57	49	1000	
					FRA	13	T	12:52	12	300	
					FRA	14	T	13:06	10	300	
					FRA	15	T	13:18	12	300	
					CTD-RO	12	T	13:35	52	1500	
					NIS	6	T	14:32	58	500	
					COL	4	T	15:40	5	2	
					QUA	4	T	15:52	23	75	
					SD	3	T	16:19	3		
					RD	8	T	16:26	20	20	
					RB	1	T	16:29			
					RD	9	T	16:46	20	20	
					RD	10	T	17:06	22	20	
152	29/11/88	61°29,9'S	049°00,3'W	3208	BO	1	A	22:34	25	400	
					BO	2	A	23:05	34	400	
					CTD-RO	13	A	23:41	62	1500	
153	30/11/88	61°59,5'S	049°00,5'W	3363	OM	2	T	09:03	20	400	
					OM	3	T	09:28	18	400	
					CTD-RO	14	T	09:58	59	1500	
					NIS	7	T	11:06	47	500	
					MN	6	T	11:57	38	1000	
					FRA	16	T	12:42	12	300	
					FRA	17	T	12:56	11	300	
					FRA	18	T	13:09	11	300	
					COL	5	T	13:27	6	2	
					QUA	5	T	13:37	27	70	
					SD	4	T	14:10	5		
154	30/11/88	61°51,2'S	049°03,3'W	3352	ICE	1	T	16:09			
					CTD-RO	15	T	16:31	24	300	
					RB	2	T	17:11			
155	02/12/88	61°00,2'S	046°56,4'W	1160	ICE	2	T	08:35			
156	02/12/88	60°59,8'S	049°00,2'W	2400	ST	1	T	21:21			
					CTD-RO	16	T	21:49	24	300	
					NIS	8	T	22:29	50	300	
					CTD-RO	17	A	23:49	74	2190	
	03/12/88				CTD-RO	18	T	09:01	28	300	
					NSN	3	T	09:55	10	300	
					NSN	4	T	10:20	10	300	
					CTD-RO	19	T	10:58	22	300	
					OM	4	T	11:30	22	400	
					OM	5	T	11:56	23	400	
					CTD-RO	20	T	12:58	22	300	
					FRA	19	T	13:27	12	300	
					FRA	20	T	13:41	8	200	
					FRA	21	T	13:52	5	100	
					FRA	22	T	13:58	14	300	
					MN	7	T	14:17	34	1000	
					COL	6	T	15:28	5	2	

Stat. No.	Date	Position		Echo depth (m)	Gear	Haul No.	Day time	Start (GMT)	Haul dur. (min)	Depth (m)	Comment
					QUA	6	T	15:35	23	70	
					SD	5	T	16:04	5		
					NIS	9	T	16:07	75	1000	
					RB	3	T	17:17			
					OM	6	T	17:35	20	400	
					OM	7	T	17:58	22	400	
					CTD-RO	21	T	18:57	29	300	
					RB	4	T	19:32			
					OM	8	T	19:35	24	400	
					OM	9	T	20:00	25	400	
					ST	2	T	22:16			
					CTD-RO	22	A	22:40	23	300	
					CTD-RO	23	A	23:58	63	1800	
	04/12/88				MN	8	N	01:12	35	1000	
					FRA	23	N	01:55	11	300	
					FRA	24	N	02:08	7	200	
					FRA	25	N	02:18	4	100	
					FRA	26	N	02:30	8	300	
					FD	11	N	02:45	10	20	
					OM	10	N	03:00	25	400	
					OM	11	N	03:27	25	400	
					CTD-RO	24	T	09:00	36	300	
					OM	12	T	10:53	25	400	
					OM	13	T	11:20	25	400	
					NIS	10	T	12:45	38	300	
					RB	5	T	12:45			
					RB	6	T	13:12			
					CTD-RO	25	T	13:27	23	300	
					OM	14	T	13:55	23	400	
					OM	15	T	14:20	24	400	
					COL	7	T	15:00	3	2	
					QUA	7	T	15:03	27	75	
					SD	6	T	15:34	5		
					RB	7	T	16:15			
					NIS	11	T	16:57	113	2200	
					TOP	1	T	19:10	30	300	
					CTD-RO	26	T	19:45	20	300	
					RB	8	T	21:05			
					CTD-RO	27	A	22:03	26	300	
157	05/12/88	59°01,9'S	048°58,8'W	3850	CTD-RO	28	T	15:12	23	300	
					FRA	27	T	15:40	12	300	
					FRA	28	T	15:54	8	200	
					FRA	29	T	16:04	5	100	
					FRA	30	T	16:11	12	300	
					MN	9	T	16:27	46	1000	
					COL	8	T	17:21	2	2	
					QUA	8	T	17:26	25	75	
					SD	7	T	17:57	5		
					RMT	4	T	18:13	63	300	
					CTD-RO	29	T	19:38	22	300	
					NIS	12	T	20:05	40	300	

Stat. No.	Date	Position		Echo depth (m)	Gear	Haul No.	Day time	Start (GMT)	Haul dur. (min)	Depth (m)	Comment
					CTD-RO	30	A	21:35	114	3978	
					OM	16	A	23:37	21	400	
					OM	17	A	00:00	25	400	
	06/12/88				CTD-RO	31	N	01:24	32	300	
					OM	18	N	02:00	25	400	
					OM	19	N	02:28	23	400	
					MN	10	N	02:57	56	1000	
					FRA	31	N	04:02	12	300	
					FRA	32	N	04:16	7	200	
					FRA	33	N	04:25	5	100	
					FRA	34	N	04:25	5	300	
					CTD-RO	32	T	09:00	18	128	
					NSN	5	T	09:27	15	300	for experiments
					NSN	6	T	09:47	15	300	for experiments
					CTD-RO	33	T	12:51	30	545	
					ST	3	T	13:24			
					ST	4	T	13:24			
					CTD-RO	34	T	14:07	22	300	
					OM	20	T	14:34	16	400	
					OM	21	T	14:55	24	400	
					CCL	9	T	15:27	3	2	
					QUA	9	T	15:32	21	75	
					SD	8	T	15:58	5		
					FRA	35	T	16:00	13	300	
					FRA	36	T	16:16	9	200	
					FRA	37	T	16:27	3	100	
					FRA	38	T	16:32	12	300	
					NIS	13	T	16:48	93	1500	
					CTD-RO	35	T	18:26	41	1000	
					OM	22	T	19:12	23	400	
					OM	23	T	19:37	23	400	
					CTD-RO	36	T	21:26	37	500	
					OM	24	A	22:09	21	400	
					OM	25	A	22:32	21	400	
					CTD-RO	37	A	23:33	123	3642	
	07/12/88				CTD-RO	38	T	09:01	19	300	
					RMT	5	T	09:31	52	300	
					CTD-RO	39	T	11:03	25	400	
					SD	9	T	12:00	5		
					NIS	14	T	12:08	64	300	
					CTD-RO	40	T	14:31	21	300	
					CCL	10	T	15:05	4	2	
					QUA	10	T	15:11	23	75	
					SD	10	T	15:58	5		
					NIS	15	T	16:57	154	3600	
158	08/12/88	59°27,7'S	048°45,8'W	3911	CTD-RO	41	T	12:16	23	300	
					OM	26	T	12:43	25	400	
					OM	27	T	13:10	23	400	
					CTD-RO	42	T	13:37	23	300	
					FRA	39	T	14:05	12	300	
					RB	9	T	14:10			

Stat. No.	Date	Position		Echo depth (m)	Gear	Haul No.	Day time	Start (GMT)	Haul dur. (min)	Depth (m)	Comment
					FRA	40	T	14:20	8	200	
					FRA	41	T	14:30	5	100	
					FRA	42	T	14:37	12	300	for experiments
					CTD-RO	43	T	15:07	23	300	
					CCL	11	T	15:36	5	2	
					QUA	11	T	15:42	22	75	
					SD	11	T	16:06	3		
					RO	12	T	16:23	5	15	
					NIS	16	T	16:34	50	400	
					RB	10	T	18:00			
					CTD-RO	44	T	18:04	30	300	
					RMT	6	T	18:43	39	200	
					CTD-RO	45	T	20:05	30	300	
					NSN	7	T	20:50	5	300	for experiments
					NSN	8	T	21:08	7	300	for experiments
					NSN	9	T	21:20	6	300	for experiments
					CTD-RO	46	T	21:57	23	300	
					CTD-RO	47	A	22:59	62	1000	
	09/12/88				CTD-RO	48	N	01:25	21	300	
					FRA	43	N	01:55	15	300	
					FRA	44	N	02:11	11	200	
					FRA	45	N	02:23	6	100	
					FRA	46	N	02:30	14	300	for experiments
					OM	28	N	02:45	20	400	
					OM	29	N	03:08	34	400	
					CTD-RO	49	T	09:01	23	300	
					CTD-RO	50	T	11:01	25	300	
					NIS	17	T	11:39	40	300	
					OM	30	T	12:34	26	400	
					OM	31	T	13:02	24	400	
					FRA	47	T	13:35	12	300	
					RB	11	T	13:47			
					FRA	48	T	13:48	8	200	
					FRA	49	T	13:58	5	100	
					FRA	50	T	14:05	12	300	for experiments
					CCL	12	T	15:12	4	2	
					QUA	12	T	15:20	25	75	
					SD	12	T	15:45	5		
					CTD-RO	51	T	15:51	22	300	
					NIS	18	T	16:17	53	400	
					RB	12	T	16:45			
159	10/12/88	57°00,3'S	048°56,7'W	3850	RMT	7	T	09:35	45	300	
					CTD-RO	52	T	13:16	23	300	
					NIS	19	T	13:43	58	350	
					OM	32	T	14:41	22	400	
					OM	33	T	15:05	23	400	
					CCL	13	T	15:32	4	2	
					QUA	13	T	15:40	20	75	
					SD	13	T	16:03	5		
					MN	11	T	16:16	54	1000	
					CTD-RO	53	T	17:10	21	300	

Stat. No.	Date	Position		Echo depth (m)	Gear	Haul No.	Day time	Start (GMT)	Haul dur. (min)	Depth (m)	Comment
					CTD-RO	54	T	19:48	21	300	
					OM	34	T	20:57	25	400	
					OM	35	T	21:25	25	400	
					CTD-RO	55	A	22:33	21	300	
	11/12/88				CTD-RO	56	N	01:19	30	300	
					MN	12	N	02:24	33	1000	
					FRA	51	N	03:03	16	300	
					FRA	52	N	03:21	12	200	
					FRA	53	N	03:35	7	100	
					FRA	54	N	03:44	12	300	for experiments
					ST	5	T	09:08			
					CTD-RO	57	T	09:27	120	4060	
					CTD-RO	58	T	12:28	25	500	
					OM	36	T	12:57	26	400	
					OM	37	T	13:25	25	400	
					CCL	14	T	14:25	5	2	
					QUA	14	T	14:30	25	75	
					SD	14	T	14:55	5		
					FRA	55	T	15:27	12	300	
					FRA	56	T	15:41	9	200	
					FRA	57	T	15:52	6	100	
					FRA	58	T	16:00	12	300	for experiments
					CTD-RO	59	T	16:15	82	2519	
					CTD-RO	60	T	18:45	20	300	
					NIS	20	T	19:34	120	2100	
	12/12/88				CTD-RO	61	T	09:01	22	300	
					CTD-RO	62	T	11:07	26	250	
					NSN	10	T	11:37	7	300	
					NSN	11	T	12:06	7	300	
					NIS	21	T	12:26	38	300	
					RMT	8	T	13:14	51	300	
					QUA	15	T	15:05	25	75	
					CCL	15	T	15:05	5	2	
					SD	15	T	15:30	5		
					OM	38	T	15:40	27	400	
					OM	39	T	16:09	24	400	
					FRA	59	T	16:36	14	300	
					CTD-RO	63	T	16:53	24	300	
					NIS	22	T	17:21	55	400	
					RB	13	T	19:24			
160	13/12/88	56°59,9'S	047°01,2'W	3558	CTD-RO	64	T	09:01	39	1000	
					NIS	23	T	09:42	64	500	
					CTD-RO	65	T	10:50	18	200	
					FRA	60	T	11:14	13	300	
					FRA	61	T	11:29	15	300	
					FRA	62	T	11:46	12	300	
					MN	13	T	12:04	55	1000	
					BO	3	T	13:20	7	300	
					CCL	16	T	13:30	5	2	
					QUA	16	T	13:35	25	75	
					SD	16	T	14:00	5		

Stat. No.	Date	Position		Echo depth (m)	Gear	Haul No.	Day time	Start (GMT)	Haul dur. (min)	Depth (m)	Comment
					RMT	9	T	14:09	21	100	
161	13/12/88	57°30,1'S	047°00,2'W	3330	CTD-RO	66	T	17:10	50	1000	
162	13/12/88	58°00,5'S	046°57,7'W	3272	RMT	10	T	20:43	23	100	
					CTD-RO	67	T	21:27	51	1000	
					NIS	24	A	22:22	65	500	
					FRA	63	A	23:31	12	300	
					FRA	64	A	23:48	12	300	
					MN	14	N	00:08	58	1000	
					BO	4	N	01:26	9	300	
163	14/12/88	58°29,7'S	047°01,3'W	3386	CTD-RO	68	T	09:01	44	1000	
164	14/12/88	59°00,0'S	046°59,5'W	2726	CTD-RO	69	T	13:01	48	1000	
					NIS	25	T	13:54	57	500	
					CCL	17	T	14:54	4	2	
					QUA	17	T	15:00	20	75	
					SD	17	T	15:22	5		
					CTD-RO	70	T	15:27	28	400	
					FRA	65	T	16:00	12	300	
					FRA	66	T	16:15	12	300	
					FRA	67	T	16:30	12	300	
					BO	5	T	17:00	9	300	
					MN	15	T	17:15	41	1000	
					OM	40	T	18:01	29	400	
					OM	41	T	18:33	24	400	
					RMT	11	T	19:07	23	200	
165	14/12/88	59°29,9'S	047°00,0'W	4051	CTD-RO	71	T	22:17	38	1000	
166	15/12/88	60°00,0'S	047°00,0'W	3464	CTD-RO	72	T	09:01	39	1000	
					NIS	26	T	09:43	52	500	
					FRA	68	T	10:41	14	300	
					FRA	69	T	10:57	11	300	
					FRA	70	T	11:11	14	300	
					BO	6	T	11:38	10	300	
					MN	16	T	11:53	41	1000	
					CCL	18	T	12:45	5	2	
					QUA	18	T	12:50	25	75	
					SD	18	T	13:15	5		
					OM	42	T	13:19	21	400	
					OM	43	T	13:42	20	400	
					RMT	12	T	14:10	25	200	
167	15/12/88	60°30,2'S	046°59,7'W	237	CTD-RO	73	T	18:41	20	230	
					RD	13	T	20:05	7	20	
168	16/12/88	61°00,2'S	047°00,1'W	1237	CTD-RO	74	N	00:10	46	1000	
					NIS	27	N	01:00	65	500	
					BO	7	N	02:21	8	300	
					MN	17	N	02:35	44	1000	
169	16/12/88	61°30,3'S	047°00,1'W	498	CTD-RO	75	T	09:02	23	400	
					FRA	71	T	09:46	12	300	
					FRA	72	T	10:00	12	300	
					FRA	73	T	10:14	11	300	
					FRA	74	T	10:27	12	300	
					CTD-RO	76	T	11:05	33	500	
					NIS	28	T	11:42	59	500	

Stat. No.	Date	Position		Echo depth (m)	Gear	Haul No.	Day time	Start (GMT)	Haul dur. (min)	Depth (m)	Comment
					BO	8	T	13:20	9	300	
					RB	14	T	13:40			
					MN	18	T	13:42	20	450	
					COL	19	T	14:33	4	2	
					QUA	19	T	14:35	25	75	
					SD	19	T	15:05	5		
					OM	44	T	15:07	25	400	
					OM	45	T	15:34	21	400	
					RB	15	T	16:08			
					NIS	29	T	16:34	2	10	
					CTD-RO	77	T	16:44	33	435	
					ST	6	T	17:37			
					MAN	1	T	18:31	63		
					CTD-RO	78	T	20:20	16	300	
					CTD-RO	79	T	22:01	24	400	
					CTD-RO	80	A	23:32	16	300	
					FRA	75	N	00:25	16	300	
					FRA	76	N	00:42	13	200	
					FRA	77	N	00:57	5		
					FRA	78	N	01:03	15	300	for experiments
					FRA	79	N	01:20	17	300	for experiments
					MN	19	N	01:44	30	450	
					OM	46	N	02:20	20	400	
					OM	47	N	02:43	20	400	
					CTD-RO	81	T	09:01	21	300	
					NIS	30	T	10:02	31	300	
					NSN	12	T	11:35	7	300	
					NSN	13	T	11:50	7	300	
					CTD-RO	82	T	12:29	18	300	
					FRA	80	T	12:53	13	300	
					FRA	81	T	13:08	5	200	
					FRA	82	T	13:15	7	100	
					FRA	83	T	13:24	13	300	for experiments
					FRA	84	T	13:39	16	300	for experiments
					FRA	85	T	13:57	16	300	for experiments
					COL	20	T	14:50	9	3	
					QUA	20	T	15:00	25	75	
					SD	20	T	15:25	5		
					OM	48	T	15:30	21	400	
					OM	49	T	16:06	21	400	
					CTD-RO	83	T	17:04	21	426	
					NIS	31	T	18:25	47	400	for faecal pellets
					CTD-RO	84	T	19:20	16	400	
					RD	14	T	23:00	3	60	
					OM	50	A	23:07	23	400	
					OM	51	A	23:31	21	400	
170	18/12/88	60°42,3'S	045°34,2'W	42	RD	15	T	11:09	16	15	
					RD	16	T	11:25	14	15	
					RD	17	T	11:39	10	15	
					RD	18	T	11:49	10	15	
171	19/12/88	60°52,4'S	045°24,3'W	225	CTD-RO	85	T	11:03	20	200	

Stat. No.	Date	Position		Echo depth (m)	Gear	Haul No.	Day time	Start (GMT)	Haul dur. (min)	Depth (m)	Comment
					FRA	86	T	11:33	10	200	
					FRA	87	T	11:45	10	200	
					NIS	32	T	12:04	45	200	
					CTD-RO	86	T	12:59	24	223	
					OM	52	T	13:28	11	200	
					OM	53	T	13:41	15	200	
					SD	21	T	14:52	5		
					COL	21	T	14:54	1	2	
					QUA	21	T	14:59	18	75	
					RO	19	T	15:32	16	45	
					RMT	13	T	15:56	26	100	
172	20/12/88	59°00,1'S	048°59,7'W	3942	COL	22	T	09:00	5	2	
					CTD-RO	87	T	09:12	23	300	
					FRA	88	T	09:52	13	300	
					FRA	89	T	10:07	8	200	
					FRA	90	T	10:17	3	100	
					FRA	91	T	10:22	13	300	for experiments
					NIS	33	T	10:51	40	300	
					OM	54	T	11:58	23	400	
					OM	55	T	12:23	23	400	
					RB	16	T	12:52			
					NIS	34	T	13:00	46	300	
					RMT	14	T	13:56	27	300	
173	20/12/88	59°29,7'S	049°00,3'W	3684	COL	23	T	17:24	2	2	
					QUA	22	T	17:31	9	75	
					SD	22	T	17:40	5		
					CTD-RO	88	T	17:50	25	300	
					RB	17	T	18:18			
					FRA	92	T	18:38	12	300	
					FRA	93	T	18:52	8	200	
					FRA	94	T	19:02	5	100	
					FRA	95	T	19:07	12	300	for experiments
					OM	56	T	19:22	20	400	
					OM	57	T	19:44	26	400	
					NIS	35	T	20:21	37	300	for faecal pellets
					CTD-RO	89	T	21:12	16	100	
					NIS	36	T	21:46	46	300	
					RO	20	T	22:35	7	20	
					RO	21	T	22:51	8	20	
					BO	9	T	23:17	6	300	for experiments
					RMT	15	T	23:29	41	150	
174	21/12/88	60°00,0'S	049°00,2'W	2021	COL	24	T	09:00	5	2	
					SD	23	T	09:08	2		
					CTD-RO	90	T	09:14	20	300	
					FRA	96	T	09:37	13	300	
					FRA	97	T	09:52	7	200	
					FRA	98	T	10:01	4	100	
					FRA	99	T	10:07	12	300	for experiments
					NIS	37	T	10:24	30	300	
					NIS	38	T	11:24	9	37	
					OM	58	T	11:36	21	400	Omori lost

Stat. No.	Date	Position		Echo depth (m)	Gear	Haul No.	Day time	Start (GMT)	Haul dur. (min)	Depth (m)	Comment
					NIS	39	T	12:28	43	320	
					CTD-RO	91	T	13:19	27	300	
					RB	18	T	13:26			
					RMT	16	T	13:54	33	150	
175	21/12/88	60°29,8'S	048°59,5'W	1492	RO	22	T	17:31	2	2	
					COL	25	T	17:39	2	2	
					QUA	23	T	17:45	21	75	
					SD	24	T	18:10	1		
					FRA	100	T	18:58	13	300	
					FRA	101	T	19:13	8	200	
					FRA	102	T	19:23	5	100	
					FRA	103	T	19:30	12	300	
					RB	19	T	18:17			
					CTD-RO	92	T	18:28	25	300	
					BO	10	T	19:46	19	400	
					BO	11	T	20:08	26	400	
					NIS	40	T	20:37	26	300	for faecal pellets
					RMT	17	T	20:53	31	150	
					CTD-RO	93	T	21:27	11	100	
					NIS	41	T	21:56	46	300	
176	22/12/88	60°58,3'S	048°59,0'W	1214	COL	26	T	09:00	5	2	
					SD	25	T	09:06	3		
					FRA	104	T	09:30	17	300	
					FRA	105	T	09:49	6	200	
					FRA	106	T	09:57	4	100	
					FRA	107	T	10:03	12	300	
					CTD-RO	94	T	10:18	34	615	
					NIS	42	T	10:58	32	300	
					BO	12	T	11:36	24	400	
					BO	13	T	12:03	22	400	
					NIS	43	T	12:27	11	30	
					RT	1	T	12:47	22	400	
					RB	20	T	12:53			
					NIS	44	T	13:17	36	300	
177	22/12/88	61°30,1'S	049°00,0'W	3210	RB	21	T	18:20			
					COL	27	T	18:35	3	2	
					QUA	24	T	18:41	19	75	
					SD	26	T	19:03	1		
					CTD-RO	95	T	19:15	23	300	
					FRA	108	T	19:44	11	300	
					FRA	109	T	19:57	7	200	
					FRA	110	T	20:05	3	100	
					FRA	111	T	20:10	10	300	
					FRA	112	T	20:22	17	400	
					RB	22	T	20:10			
					BO	14	T	20:39	16	400	
					BO	15	T	21:04	23	400	
					NIS	45	T	21:28	34	300	for faecal pellets
					NIS	46	T	22:13	32	300	
					CTD-RO	96	T	22:48	14	100	
					NIS	47	A	23:11	46	300	

Stat. No.	Date	Position		Echo depth (m)	Gear	Haul No.	Day time	Start (GMT)	Haul dur. (min)	Depth (m)	Comment
					RT	2	A	00:00	19	400	
178	23/12/88	61°28,8'S	049°00,1'W	3214	ST	7	T	09:13			
					ST	8	T	09:17			
					COL	28	T	09:40	5	2	
					SD	27	T	09:50	3		
					CTD-RO	97	T	09:54	22	300	
					FRA	113	T	10:21	11	300	
					FRA	114	T	10:34	7	200	
					FRA	115	T	10:43	4	100	
					FRA	116	T	10:49	12	300	
					NIS	48	T	11:02	34	300	
					BO	16	T	11:40	18	400	
					BO	17	T	12:00	20	400	
					NIS	49	T	12:23	3	10	
					RB	23	T	13:00			
					NIS	50	T	13:07	23	300	
					COL	29	T	14:02	3	2	
					QUA	25	T	14:08	20	75	
					SD	28	T	14:34	2		
					ICE	3	T	16:58			
					RB	24	T	20:30			
179	24/12/88	62°09,2'S	048°58,9'W	3380	CTD-RO	98	T	09:02	105	3364	
					NIS	51	T	11:45	27	300	
					CTD-RO	99	T	12:35	47	800	
					BO	18	T	13:25	20	400	
					BO	19	T	13:49	21	400	
					COL	30	T	14:18	2	2	
					QUA	26	T	14:23	20	75	
					SD	29	T	14:49	1		
					FRA	117	T	14:56	6	300	
					FRA	118	T	15:04	6	200	
					FRA	119	T	15:12	4	100	
					FRA	120	T	15:18	11	300	
					FRA	121	T	15:31	5	50	
					NIS	52	T	15:35	53	500	
					RT	3	T	16:32	17	400	
180	25/12/88	61°25,7'S	049°01,8'W	3174	ICE	4	T	18:33			
181	26/12/88	59°15,2'S	049°01,0'W	3803	CTD-RO	100	T	13:36	22	400	
182	27/12/88	57°00,4'S	048°59,7'W	4040	CTD-RO	101	T	09:00	22	400	
					NIS	53	T	09:44	28	300	
					CTD-RO	102	T	11:05	68	1500	
					NSN	14	T	13:00	10	300	for experiments
					FRA	122	T	13:06	12	300	for experiments
					FRA	123	T	13:20	10	300	
					FRA	124	T	13:32	12	300	for experiments
					RB	25	T	13:44			
					CTD-RO	103	T	13:52	22	200	
					QUA	27	T	14:33	19	75	
					COL	31	T	14:27	3	2	
					SD	30	T	14:53	2		
					BO	20	T	15:00	18	400	

Stat. No.	Date	Position		Echo depth (m)	Gear	Haul No.	Day time	Start (GMT)	Haul dur. (min)	Depth (m)	Comment
					BO	21	T	15:20	25	400	
					MN	20	T	15:50	55	1000	
					NIS	54	T	16:50	55	500	
					CTD-RO	104	T	17:50	28	311	
					RMT	18	T	18:27	51	300	
183	27/12/88	57°29,9'S	049°00,0'W	3830	CTD-RO	105	T	22:00	67	1500	
184	28/12/88	57°20,0'S	049°00,0'W	3936	CTD-RO	106	N	00:30	53	1500	
185	28/12/88	57°39,9'S	049°00,1'W	3970	CTD-RO	107	N	03:34	60	1500	
186	28/12/88	58°00,0'S	048°59,0'W	3963	CTD-RO	108	T	09:04	60	1500	
					NIS	55	T	10:07	25	300	
					FRA	125	T	10:36	11	300	for experiments
					FRA	126	T	10:49	12	300	
					FRA	127	T	11:03	12	300	for experiments
					BO	22	T	11:20	22	400	
					BO	23	T	11:45	33	400	
					BO	24	T	12:12	17	400	
					MN	21	T	12:55	25	1000	
					QUA	28	T	13:26	24	75	
					COL	32	T	13:50	5	2	
					SD	31	T	13:55	3		
					NIS	56	T	14:02	53	500	
					CTD-RO	109	T	15:05	28	300	
					RMT	19	T	15:40	52	300	
187	28/12/88	58°29,9'S	048°59,8'W	3861	COL	33	T	19:50	5	2	
					SD	32	T	20:00	4		
					CTD-RO	110	T	20:11	61	1500	
188	29/12/88	58°59,9'S	048°59,7'W	3982	CTD-RO	111	A	23:57	65	1500	
					NIS	57	N	01:05	66	500	
					BO	25	N	02:13	23	400	
					BO	26	N	02:38	24	400	
					FRA	128	N	03:04	20	300	
					FRA	129	N	03:26	29	300	for experiments
					FRA	130	N	03:47	12	300	for experiments
					COL	34	T	09:00	5	2	
					SD	33	T	09:06	4		
					NIS	58	T	09:21	34	300	
					BO	27	T	09:58	16	300	
					MN	22	T	10:20	53	1000	
					NIS	59	T	11:19	42	300	
					RMT	20	T	12:08	53	300	
189	29/12/88	59°30,0'S	048°59,8'W	3642	COL	35	T	16:19	3	2	
					QUA	29	T	16:25	20	75	
					SD	34	T	16:49	1		
					CTD-RO	112	T	16:52	64	1576	
					RB	26	T	17:18			
190	29/12/88	59°57,0'S	049°01,0'W	4068	RMT	21	T	20:36	52	300	
					CTD-RO	113	T	21:44	65	1500	
					NIS	60	T	23:00	29	300	
					FRA	131	A	23:21	18	300	for experiments
					FRA	132	A	23:51	15	300	
					FRA	133	A	00:08	12	300	for experiments

Stat. No.	Date	Position		Echo depth (m)	Gear	Haul No.	Day time	Start (GMT)	Haul dur. (min)	Depth (m)	Comment
					NIS	61	N	00:26	58	500	
					MN	23	N	01:28	42	1000	
					BO	28	N	02:14	19	300	
					BO	29	N	02:36	21	400	
					BO	30	N	03:00	22	400	
					RO	23	N	03:24	9	21	
191	30/12/88	60°30,0'S	048°59,8'W	1510	CTD-RO	114	T	08:58	59	1500	
					CCL	36	T	10:00	5	2	
					SD	35	T	10:07	3		
192	30/12/88	60°51,6'S	048°59,7'W	2300	RMT	22	T	12:56	51	300	
					CCL	37	T	14:57	3	2	
					QUA	30	T	15:08	22	75	
					SD	36	T	15:32	3		
					CTD-RO	115	T	15:42	59	1500	
					RB	27	T	16:05			
					NIS	62	T	16:46	23	300	
					FRA	134	T	17:13	13	300	
					FRA	135	T	17:28	12	300	for experiments
					FRA	136	T	17:42	14	300	for experiments
					MN	24	T	17:59	40	1000	
					NIS	63	T	18:46	48	300	
					BO	31	T	19:36	21	400	
					BO	32	T	20:00	15	400	
					BO	33	T	20:17	13	300	
193	31/12/88	61°31,1'S	048°59,8'W	3218	CTD-RO	116	N	00:34	58	1500	
194	31/12/88	61°44,7'S	048°48,7'W	3302	CTD-RO	117	T	09:00	118	3312	
					NIS	64	T	11:03	28	300	
					FRA	137	T	11:35	14	300	for experiments
					FRA	138	T	11:51	13	300	
					FRA	139	T	12:06	13	300	for experiments
					MN	25	T	12:23	38	1000	
					CTD-RO	118	T	13:09	26	300	
					BO	34	T	13:38	16	400	
					BO	35	T	13:57	17	400	
					RB	28	T	14:04			
					BO	36	T	14:17	20	400	
					RT	4	T	14:36	16	400	
					CCL	38	T	15:00	3	2	
					QUA	31	T	15:05	25	75	
					SD	37	T	15:30	1		
					NIS	65	T	15:33	51	500	
195	31/12/88	61°45,7'S	048°43,4'W	3296	RB	29	T	17:18			
196	01/01/89	59°30,1'S	049°00,0'W	3647	CTD-RO	119	T	13:21	60	1500	
197	01/01/89	59°15,0'S	048°10,1'W	3862	CTD-RO	120	T	17:50	68	1500	
198	01/01/89	59°00,1'S	048°59,8'W	3975	CTD-RO	121	T	22:40	77	1500	
199	02/01/89	58°45,1'S	048°10,1'W	3866	CTD-RO	122	N	03:39	74	1500	
200	02/01/89	58°30,1'S	049°00,3'W	3864	CTD-RO	123	T	09:30	62	1500	
201	02/01/89	58°14,9'S	048°10,4'W	3101	CTD-RO	124	T	13:54	68	1500	
202	02/01/89	58°00,0'S	048°58,9'W	4146	CTD-RO	125	T	19:20	66	1500	
203	02/01/89	57°45,4'S	048°09,9'W	3396	CTD-RO	126	A	23:31	66	1500	
204	03/01/89	57°30,2'S	048°59,7'W	3820	CTD-RO	127	N	04:49	70	1500	

Stat. No.	Date	Position		Echo depth (m)	Gear	Haul No.	Day time	Start (GMT)	Haul dur. (min)	Depth (m)	Comment
205	03/01/89	57°15,2'S	048°09,7'W	3450	CTD-RO	128	T	09:41	79	1500	
					COL	39	T	11:00	5	2	
					SD	38	T	11:08	5		
					NIS	66	T	11:26	30	300	
206	03/01/89	56°59,9'S	048°59,8'W	3902	CTD-RO	129	T	16:12	58	1500	
207	03/01/89	57°22,0'S	048°40,4'W	3911	CTD-RO	130	T	20:32	44	1000	
					COL	40	T	21:20	5	2	
					SD	39	T	21:26	1		
					MN	26	T	21:33	16	300	
					NIS	67	T	21:55	25	300	
					FRA	140	T	22:22	13	300	
					FRA	141	T	22:37	9	200	
					FRA	142	T	22:49	5	100	
					FRA	143	T	23:55	12	300	for faecal pellets
					BO	37	A	23:09	16	300	
					BO	38	A	23:26	15	300	
					RMT	23	A	23:52	24	100	
					NIS	68	N	01:56	11	12	
208	04/01/89	57°34,3'S	048°25,0'W	3626	CTD-RO	131	T	09:17	50	1095	
					NIS	69	T	10:11	25	300	
					MN	27	T	10:42	20	300	
					FRA	144	T	11:14	13	300	
					FRA	145	T	11:29	11	200	
					FRA	146	T	11:42	5	100	
					FRA	147	T	11:48	12	300	for faecal pellets
					BO	39	T	12:05	18	300	
					BO	40	T	12:25	17	300	
					COL	41	T	12:54	2	2	
					QUA	32	T	12:59	18	75	
					SD	40	T	13:21	2		
					RMT	24	T	13:26	37	200	
209	04/01/89	57°45,5'S	048°23,3'W	3626	QUA	33	T	15:10	40	75	
					COL	42	T	15:27	1	2	
					SD	41	T	15:50	4		
					CTD-RO	132	T	15:57	87	3256	
					CTD-RO	133	T	17:35	78	3187	
					NIS	70	T	18:57	24	300	
					MN	28	T	19:26	15	300	
					FRA	148	T	19:58	14	300	
					FRA	149	T	20:00	7	200	
					FRA	150	T	20:09	4	100	
					FRA	151	T	20:15	12	300	for faecel pellets
					BO	41	T	20:30	15	300	
					RMT	25	T	20:53	31	200	

Participating Institutes and Scientists in ANT VII/3, EPOS Leg 2

ARGENTINE		
UBA	Univers. Buenos Aires Fac. Ciencias Exactas y Naturales	V.A.Alder
IAA	Instituto Antartico Argentino Cerrito 1248 Buenos Aires	I.Schloss
BELGIUM		
FUB	Free University of Brussels ANCH 2, Pleinlaan 2 B-1050 Brussel	F.Dehairs, L.Goeyens
GMB	Free University of Brussel Groupe de Microbiologie des Milieux Aquatiques Campus de la Plaine, CP 221 Boulevard du Triomph B-1050 Bruxelles	S.Becquevort, C.Lancelot, S.Mathot
CHILE		
PUC	BIOTECMAR Pontificia Universidad Catolica de Chile Casilla 127, Talcahuano	H.Gonzalez
UMC	Universidad de Magellanes Angamos Esq. Zenteno Casilla 113-D Punta Arenas	B.Magas
DANMARK		
BLH	Marine Biological Laboratory University of Copenhagen Strandpromenaden DK-3000 Helsingor	P.K.Björnsen
ISC	Institute for Sporeplanter University of Copenhagen Öster Farimagsgade 2D DK-1353 Copenhagen K	J.Larsen, H.Thomsen
FINLAND		
TZS	Tvärminne Zoological Station SF-10900 Tvärminne	J.Kuparinen

FRANCE

LAB	Laboratoire Arago/CNRS F-66650 Banyuls-sur-Mer	M.Eckernkemper, G.Jacques, M.Panouse
SZV	Université P et M Curie Station Zoologique, BP 28-CEROV Quai de la Darse F-06230 Villefranche-sur-Mer	J.Cuzin-Roudy
IMB	Laboratoire de Chimie des Ecosystème Marins Institut d'Etudes Marines 6 avenue Le Gorgeu F-29287 Brest Cedex F	A.Masson, P.Tréguer
ENR	Ecole Nationale Supérieure de Chimie ENSCR Avenue du Général Leclerc F-35700 Rennes-Beaulieu	J.Morvan

F. R. GERMANY

AWI	Alfred-Wegener-Institut für Polar- und Meeresforschung Columbusstraße D-2850 Bremerhaven	E.Mizdalski, M.Pamatmat, U.Riebesell, S.Schiel, V.Smetacek,

THE NETHERLANDS

NIOZ	Netherlands Institute for Sea Research P.O. Box 59 1790 AB Den Burg/Texel S.R.Gonzalez,	H.de Baar, J.Bennekom,A.Buma, G.Cadée,G.Fransz, R.F.Nolting, S.Ober, R.Schmidt, C.Veth
RIN	Research Institute for Nature Management P.O.Box 59 1790 AB Den Burg/Texel	J.van Franeker
NIKHEF	Nationaal Instituut voor Kernfysica en Hoge-Energiefysica Postbus 41882 1009 DB Amsterdam	L.Lindner
ITZ	Instituut voor Taxonomische Zöologie P.O. Box 4766 1009 AT Amsterdam	P.Schalk

PAKISTAN

NIO	National Institute of Oceanography 37K, Block 6, P.E.C.H.S. Karachi 29	M.Rabbani

SPAIN

ICMB	Institut de Ciències del Mar P. Nacional, s/n SP-08003 Barcelona	M.Estrada

SWEDEN

IOG	University of Gothenburg Inst. of Oceanography Box 4038 S-40040 Gothenburg	U. Cederlöf, A.Svansson
DMG	University of Gothenburg Dept. of Marine Microbiology Carl Skottsbergs Gata 22 S-41319 Gothenburg	F.Sörensson
DEL	University of Lund Phytoplankton Ecology Res. Group Dept. of Marine Ecology Box 124 S-22100 Lund	E.Granéli

FAHRTTEILNEHMER/PARTICIPANTS ANT VII/3, EPOS LEG 2

NAME	INSTITUTE	COUNTRY
Alder, Viviana A.	UBA	(Arg)
Baar, Hein de	NIOZ	(NL)
Becquevort, Sylvie	FUB	(B)
Bennekom, Johan van.	NIOZ	(NL)
Björnsen, Peter K.	BLH	(DK)
Buma, Anita	NIOZ	(NL)
Cadée, Gerhard	NIOZ	(NL)
Cederlöf, Ulf	IOG	(S)
Cuzin-Roudy, Janine	SZV	(F)
Dehairs, Frank	GMB	(B)
Eckernkemper, Marc	LAB	(F)
Estrada, Marta	ICMB	(SP)
Franeker, Jan A. van	RIN	(NL)
Fransz, George	NIOZ	(NL)
Goeyens, Leo	FUB	(B),
Gonzalez, Humberto E.	PUC	(Chile)
Gonzalez, Santiago.R.	NIOZ	(NL)
Granéli, Edna	DEL	(S)
Jacques, Guy	LAB	(F)
Kuparinen, Jorma	TZS	(SF)
Lancelot, Christiane	GMB	(B)
Larsen, Jacob	ISC	(DK)
Lindner, Louis	NIKHEF	(NL
Magas, Bedrich	UMC	(Chile)
Masson, Annick	IMB	(F)
Mathot, Sylvie	GMB	(B)
Mizdalski, Elke	AWI	(FRG)
Morvan, Jean	ENR	(F)
Nolting, Rob F.	NIOZ	(NL)
Ober, Sven	NIOZ	(NL)
Pamatmat, Mario	AWI	(FRG)
Panouse, Michel	LAB	(F)
Rabbani, Mohammad	NIO	(PK)
Riebesell, Ulf	AWI	(FRG)
Schalk, Peter	ITZ	(NL)
Schiel, Sigrid	AWI	(FRG)
Schloss, Irene	IAA	(ARG)
Schmidt, Rolf	NIOZ	(NL)
Smetacek, Victor	AWI	(FRG)
Sörensson, Fred	DMG	(S)
Svansson, Artur	IOG	(S)
Thomsen, Helge	ISC	(DK)
Treguer, Paul	IMB	(F)
Veth, Cornelis	NIOZ	(NL)

SHIP'S CREW ANT VII/3 EPOS II

Kapitän	Greve
1. Offizier	Allers
Naut. Offizier	Schiel
Naut. Offizier	Fahje
Arzt	Dr. Berg
Ltd. Ingenieur	Müller
1. Ingenieur	Schulz
2. Ingenieur	Delff
2. Ingenieur	Simon
Elektriker	Erdmann
Elektroniker	Elvers
Elektroniker	Husmann
Elektroniker	Hoops
Funkoffizier	Geiger
Funkoffizier	Raeder
Koch	Tanger
Kochsmaat/Bäcker	Kubicka
Kochsmaat/Koch	Bender
1. Steward	Scheel
Stewardess/Nurse	Pötzsch
Stewardess	Friedrich
Stewardess	Gollmann
2. Steward	Lai
Wäscher	Yang
Bootsmann	Schwarz
Zimmermann	Marowsky
Matrose	Suarez Peisal
Matrose	Bermudes B.
Matrose	Soage C.
Matrose	Gil.I.
Matrose	Abreu Dios
Matrose	Rousada M.
zusätzl. Matrose	Hopp
Lagerhalter	Schierl
Masch-Wart	Wittfoth
Masch-Wart	Dufne
Masch-Wart	Carstens
Masch-Wart	Husun
Masch-Wart	Ulbricht

Folgende Hefte der Reihe „Berichte zur Polarforschung" sind bisher erschienen:

Verkaufspreis/DM

* **Sonderheft Nr. 1/1981** – „Die Antarktis und ihr Lebensraum"
Eine Einführung für Besucher – Herausgegeben im Auftrag von SCAR

Heft Nr. 1/1982 – „Die Filchner-Schelfeis-Expedition 1980/81" 11,50
zusammengestellt von Heinz Kohnen

Heft Nr. 2/1982 – „Deutsche Antarktis-Expedition 1980/81 mit FS ‚Meteor'" 10,—
First International BIOMASS Experiment (FIBEX) – Liste der Zooplankton- und Mikronektonnetzfänge
zusammengestellt von Norbert Klages

Heft Nr. 3/1982 – „Digitale und analoge Krill-Echolot-Rohdatenerfassung an Bord des Forschungsschiffes ‚Meteor'" (im Rahmen von FIBEX 1980/81, Fahrtabschnitt ANT III), von Bodo Morgenstern 19,50

Heft Nr. 4/1982 – „Filchner-Schelfeis-Expedition 1980/81" 12,50
Liste der Planktonfänge und Lichtstärkemessungen
zusammengestellt von Gerd Hubold und H. Eberhard Drescher

* **Heft Nr. 5/1982** – "Joint Biological Expedition on RRS 'John Biscoe', February 1982"
by G. Hempel and R. B. Heywood

* **Heft Nr. 6/1982** – „Antarktis-Expedition 1981/82 (Unternehmen ‚Eiswarte')"
zusammengestellt von Gode Gravenhorst

Heft Nr. 7/1982 – „Marin-Biologisches Begleitprogramm zur Standorterkundung 1979/80 mit MS ‚Polarsirkel' (Pre-Site Survey)" – Stationslisten der Mikronekton- und Zooplanktonfänge sowie der Bodenfischerei 13,—
zusammengestellt von R. Schneppenheim

Heft Nr. 8/1983 – "The Post-Fibex Data Interpretation Workshop" 10,—
by D. L. Cram and J.-C. Freytag with the collaboration of J. W. Schmidt, M. Mall, R. Kresse, T. Schwinghammer

Heft Nr. 9/1983 – "Distribution of some groups of zooplankton in the inner Weddell Sea in summer 1979/80" 15,—
by I. Hempel, G. Hubold, B. Kaczmaruk, R. Keller, R. Weigmann-Haass

Heft Nr. 10/1983 – „Fluor im antarktischen Ökosystem" – DFG-Symposium November 1982 23,—
zusammengestellt von Dieter Adelung

Heft Nr. 11/1983 – "Joint Biological Expedition on RRS 'John Biscoe', February 1982 (II)" 16,—
Data of micronecton and zooplankton hauls, by Uwe Piatkowski

Heft Nr. 12/1983 – „Das biologische Programm der ANTARKTIS-I-Expedition 1983 mit FS ‚Polarstern'" 14,—
Stationslisten der Plankton-, Benthos- und Grundschleppnetzfänge und Liste der Probennahme an Robben und Vögeln, von H. E. Drescher, G. Hubold, U. Piatkowski, J. Plötz und J. Voß

* **Heft Nr. 13/1983** – „Die Antarktis-Expedition von MS ‚Polarbjörn' 1982/83" (Sommerkampagne zur Atka-Bucht und zu den Kraul-Bergen), zusammengestellt von Heinz Kohnen

* **Sonderheft Nr. 2/1983** – „Die erste Antarktis-Expedition von FS ‚Polarstern' (Kapstadt, 20. Januar 1983 – Rio de Janeiro, 25. März 1983)", Bericht des Fahrtleiters Prof. Dr. Gotthilf Hempel

Sonderheft Nr. 3/1983 – „Sicherheit und Überleben bei Polarexpeditionen"
zusammengestellt von Heinz Kohnen

Heft Nr. 14/1983 – „Die erste Antarktis-Expedition (ANTARKTIS I) von FS ‚Polarstern' 1982/83" 40,—
herausgegeben von Gotthilf Hempel

Sonderheft Nr. 4/1983 – "On the Biology of Krill *Euphausia superba*" – Proceedings of the Seminar and Report of the Krill Ecology Group, Bremerhaven 12.–16. May 1983, edited by S. B. Schnack 75,—

Heft Nr. 15/1983 – "German Antarctic Expedition 1980/81 with FRV 'Walther Herwig' and RV 'Meteor'" – First International BIOMASS Experiment (FIBEX) – Data of micronekton and zooplankton hauls 22,50
by Uwe Piatkowski and Norbert Klages

Sonderheft Nr. 5/1984 – "The observatories of the Georg von Neumayer Station", by Ernst Augstein 8,—

Heft Nr. 16/1984 – "FIBEX cruise zooplankton data" 19,—
by U. Piatkowski, I. Hempel and S. Rakusa-Suszczewski

Heft Nr. 17/1984 – „Fahrtbericht (cruise report) der ‚Polarstern'-Reise ARKTIS I, 1983" 29,—
von E. Augstein, G. Hempel und J. Thiede

Heft Nr. 18/1984 – „Die Expedition ANTARKTIS II mit FS ‚Polarstern' 1983/84", 25,—
Bericht von den Fahrtabschnitten 1, 2 und 3, herausgegeben von D. Fütterer

Heft Nr. 19/1984 – „Die Expedition ANTARKTIS II mit FS ‚Polarstern' 1983/84", 41,—
Bericht vom Fahrtabschnitt 4, Punta Arenas–Kapstadt (Ant-II/4), herausgegeben von H. Kohnen

Heft Nr. 20/1984 – „Die Expedition ARKTIS II des FS ‚Polarstern' 1984, mit Beiträgen des FS ‚Valdivia' und des Forschungsflugzeuges ‚Falcon 20' zum Marginal Ice Zone Experiment 1984 (MIZEX)" 42,—
von E. Augstein, G. Hempel, J. Schwarz, J. Thiede und W. Weigel